Effects of glucose and fatty acids interactions on glucose metabolism pathways in human trophoblasts

Carina Bertoldi Franco

MD, MPhil

A thesis submitted for the degree of Doctor of Philosophy of the Australian National University

July 2015

Statement

This thesis contains no material which has been accepted for the award of any other degree or diploma in any university, and is less than 100,000 words in length exclusive of tables, figures and bibliographies. To the best of my knowledge and belief, this thesis contains no material previously published or written by another person, except where due reference has been made.

Carina Bertoldi Franco

Acknowledgements

I would like to acknowledge all who contributed to this work in many ways. I am sincerely thankful to my supervisor Prof Christopher Nolan for all support, technical advice, guidance and valuable scientific discussions throughout this degree. I am also very grateful to my co-supervisor Prof Jane Dahlstrom for her advice, feed-back, orientation and support. I am indebted with Dr Viviane Delghingaro-Augusto who taught and supported me providing technical expertise in all stages of my laboratory work. I am deeply grateful to Prof Jeff Keelan from the University of Western Australia for his invaluable assistance and discussions for the change and improvement of the trophoblast isolation protocol. In addition, I greatly appreciated the generosity of Prof Yoel Sadovsky from Magee-Women's Research Institute for his contributions to the establishment of this updated protocol.

I am very grateful to the mothers who kindly donated their placentas for this research, and for the excellent help provided by the midwives, obstetricians and nurses of the Canberra Hospital (TCH) Day Surgery unit and surgical theatre. I also would like to thank the staff of Department of Anatomical Pathology of TCH, especially the Senior Scientist Jacqueline Simmonds.

Many thanks to my lab friends and colleagues Tenzin Dagpo, Hana Kaori Hanamoto, Cameron Kos, Ainy Khan Hussain, Ayumi Hosaka, Erandi Batagoda and Stephanie Cheung, who shared good experiences and fun moments inside and outside the lab.

My greatest love goes to my family in Brazil, in special to my parents Antonio Carlos Franco and Elisabet Bertoldi Franco, who crossed twice the globe spending wonderful days with me.

Finally, I would like to thank my adorable husband Everton Santos Muniz. Without his support and care, the completion of this degree would be much harder and almost impossible.

To the love of my life, Everton Santos Muniz.

Abstract

Introduction: Obesity, with its associated co-morbidities of diabetes, hyperlipidaemia and low-grade inflammation, has high prevalence in women of child-bearing age. Of further concern, it is associated with increased risk of adverse pregnancy outcomes. Considering the key role of the placenta in fetal development, alterations to its structure and function in response to the adverse metabolic milieu of maternal obesity must be important. The trophoblast is a key cell within the placental maternal-fetal barrier. The research aims were to evaluate the effects of elevated glucose supply, in the absence and presence of non-esterified fatty acids (NEFA), on pathways of glucose metabolism and trophoblast morphology in human trophoblasts in primary culture.

Methods: Trophoblasts were established in primary culture from human term placentas of normal pregnancies. The isolation protocol was optimised to improve trophoblast yield and purity. Experiments were performed at both 36 h (short-term) and 5 days (long-term) after trophoblast isolation, when most cells were, respectively, cytotrophoblasts and syncytiotropblasts. Syncytialisation was promoted by adding epidermal growth factor (EGF; 10 ng/ml) to the media. Metabolism experiments were performed over 2 h at diverse glucose concentrations in the absence or presence of NEFA (0.25 mM, palmitate: oleate ratio; 1:1). Pathways of glucose uptake, glycolysis, glucose oxidation, total and partial palmitate oxidation and glycogen synthesis were assessed using radio-labelled tracers. Lactate production and glycogen content were measured enzymatically. The effects of EGF and NEFA on trophoblast morphology, lipid droplet formation and triacylglycerol (TG) content were also assessed.

Results: The improved protocol increased the mean (± SD) trophoblast yield to 266 ± 141 x 10^6 cells, and purity to 98%. In short-term cultures, rates of trophoblast glucose

uptake and glycogen synthesis increased linearly with increasing glucose concentrations; whereas, rates of glycolysis, lactate release and glucose oxidation did not increase with glucose concentrations above 5 mM. NEFA enhanced glycogen synthesis, but did not affect other glucose metabolism pathways. Total trophoblast glycogen content increased minimally with increasing glucose supply, which was not altered by NEFA. In long-term compared to short-term culture experiments, glycogen synthesis was lower and the trophoblasts were able to increase glycolysis and glucose oxidation rates with media glucose concentrations above 5 mM. NEFA increased glucose oxidation at the media glucose concentration of 1 mM. Palmitate complete oxidation to CO_2 and partial oxidation to acid soluble products were significant metabolic pathways in both the short and long-term cultured cells. EGF promoted syncytialisation with a lesser effect of NEFA. Neither EGF nor NEFA affected trophoblast lipid droplet or TG accumulation.

Conclusion: During acute exposure to high glucose media, human trophoblasts divert glucose uptake to glycogen synthesis rather than glycolysis and glucose oxidation. This diversion, however, is less evident in more differentiated trophoblasts. NEFA have minimal effects on glucose metabolism pathways, but are a significant source of cellular metabolic energy via oxidation to CO_2, but also by partial oxidation to acid soluble products (e.g. ketone bodies, short-chain fatty acids and tricarboxylic acid cycle intermediates). Further analysis of these pathways, particularly in placentas of obese women, are warranted.

Presentations and publications

Refereed abstracts related to the thesis

- Effects of elevated fatty acids and/or glucose on glucose metabolism pathways in human trophoblasts. Annual Human Placenta Workshop, Queen's University. Kingston, Canada; July 2012.
- Effects of elevated fatty acids and/or glucose on glucose metabolism pathways in human trophoblasts. The Australian Society for Medical Research (ASMR) New Investigator Forum. Canberra, Australia; June 2013.
- Effects of elevated fatty acids and/or glucose on glucose metabolism pathways in human trophoblasts. Canberra Health Annual Research Meeting, TCH. Canberra, Australia; August 2013.
- Effects of elevated fatty acids and/or glucose on glucose metabolism pathways in human trophoblasts. Australasian Diabetes in Pregnancy Society Joint Scientific Meeting. Sydney, Australia; August 2013.
- Effects of elevated fatty acids and/or glucose on glucose metabolism pathways in human trophoblasts. Australasian Diabetes Society Joint Scientific Meeting. Melbourne, Australia; August 2014.
- Effects of elevated fatty acids and/or glucose on glucose metabolism pathways in human trophoblasts. Canberra Health Annual Research Meeting, TCH. Canberra, Australia; August 2014.

Manuscripts in preparation related to the thesis

- Effects of glucose and fatty acids interactions on glucose metabolism pathways in human trophoblasts**.**
- Placental adaptations to obesity and implications for the fetus. A review.

Other manuscripts published during the PhD candidature

- **Bertoldi Franco C.** Osteoporosis in gastrointestinal diseases. Translational Gastrointestinal Cancer. 2015; 4 (1):57.

- Paz-Filho G, Mastronardi C, **Bertoldi Franco C,** Wong M-L, Licinio J. Leptin: Molecular mechanisms, systemic pro-inflammatory effects, and clinical implications. Arquivos Brasileiros de Endocrinologia e Metabologia. 2012; 56 (9): 597.

Table of Contents

Statement.....ii

Acknowledgements.....iii

Dedication.....iv

Abstract.....v

Presentations and publications.....vii

Abbreviations.....xv

Chapter 1: Introduction.....1

1.1 Obesity overview.....2

1.2 Epidemiology of obesity during pregnancy.....3

1.3 Maternal metabolism in normal pregnancy.....4

1.3.1 Glucose metabolism.....4

1.3.2 Lipid metabolism.....6

1.3.3 Other physiological alterations.....8

1.4 Gestational complications associated with obesity and its co-morbidities.....10

1.5 Overview of glucose and fatty acid metabolism pathways.....19

1.5.1 Glucose metabolism overview.....19

1.5.2 Glycolysis.....22

1.5.3 Lactate production.....26

1.5.4 Tricarboxylic acid cycle and oxidative metabolism of glucose.....28

1.5.5 Glycogen synthesis.....32

1.5.6 β-oxidation of saturated fatty acids.....34

1.5.7 Ketone bodies production.....37

1.6 Normal structure of the placenta 40
1.6.1 Macroscopic anatomy of the placenta 40
1.6.2 Microscopic anatomy of the placenta 45
1.7 Placental nutrient transport and metabolism 49
1.7.1 Glucose transport and metabolism 50
1.7.1.1 Effects of NEFA on placental glucose metabolism 57
1.7.2 Lipid transport and metabolism 57
1.7.3 Amino acid transport and metabolism 64
1.8 Rationale of this thesis research 69
1.8.1 Hypotheses 69
1.8.2 Thesis research aims 70
Chapter 2: Primary human trophoblast isolation and culture 71
2.1 Introduction 72
2.2 Study participants 73
2.3 Primary human trophoblast isolation–protocol 1 73
2.3.1 Preparation of solutions and media 73
2.3.2 Tissue harvesting and digestion 73
2.3.3 Trophoblast purification 74
2.3.4 Cell counting and plating 75
2.4 Primary human trophoblast isolation-protocol 2 75
2.4.1 Tissue harvesting and digestion 75
2.4.2 Trophoblast purification 77
2.4.3 Cell counting 79
2.4.4 Cell plating 79
2.5 Cytological assessment 79

2.5.1 Purity of trophoblast cultures 79
2.5.2 Light microscopy 81
2.6 Results 81
2.7 Discussion 91
2.8 Conclusion 94
Chapter 3: General methods 95
3.1 Methods for assessment of glucose and lipid metabolism in primary trophoblast cultures 96
3.1.1 Introduction 96
3.1.1.1 Principles of metabolic tracer-tracee methodology 98
3.1.2 Metabolism studies 100
3.1.2.1 Preparation of primary trophoblasts for metabolic assessments 100
3.1.2.2 Total glucose uptake 102
3.1.2.3 Glycolysis 107
3.1.2.4 Total lactate release into the media 111
3.1.2.5 Glucose and palmitate oxidation 115
3.1.2.6 Glycogen synthesis measured with tracer 122
3.1.2.7 Total glycogen content 127
3.1.3 Trophoblast protein content 129
3.2 Cellular morphology and triacylglycerol quantification in long-term cultures 129
3.2.1 Oil red O staining 129
3.2.2 Triacylglycerol quantification 132
3.3 Statistical analysis 136

Chapter 4: Results for glucose metabolism studies in short-term trophoblast cultures 137

4.1 Introduction 138

4.2 Total glucose uptake 141

4.3 Glycolysis 144

4.4 Total lactate release into the media 146

4.5 Glucose oxidation 148

4.6 Palmitate oxidation and acid soluble product formation 150

4.7 Glycogen synthesis measured with tracer 153

4.8 Total glycogen content 155

4.9 Discussion 157

4.9.1 Effects of increasing media glucose concentration on glucose metabolism pathways in primary human trophoblast cultures 158

4.9.1.1 Glucose uptake 158

4.9.1.2 Glycolysis 159

4.9.1.3 Glucose and palmitate oxidation 161

4.9.1.4 Glycogen 164

4.9.2 NEFA effects on glucose metabolism pathways in primary human trophoblast cultures 167

4.10 Limitations in the methods for the assessment of glucose metabolism 173

4.11 Conclusions 177

Chapter 5: Results for metabolism and morphology studies in long-term primary human trophoblast 178

5.1 Metabolism studies 179

5.1.1 Introduction 179

5.1.2 Results 181

5.1.2.1 Total glucose uptake 181

5.1.2.2 Glycolysis 183

5.1.2.3 Glucose oxidation 185

5.1.2.4 Palmitate oxidation and acid soluble product formation 187

5.1.2.5 Glycogen synthesis with tracer 190

5.2 Cellular morphology and triacylglycerol quantification in long-term primary human trophoblast cultures 192

5.2.1 Introduction 192

5.2.2 Results 194

5.2.2.1 Oil red O staining 194

5.2.2.2 Triacylglycerol quantification 199

5.3 Discussion 201

5.3.1 The effects of increasing the media glucose concentration on glucose metabolism pathways in primary human trophoblasts in long compared to short-term cultures 202

5.4 Limitations 208

5.5 Conclusions 208

Chapter 6: Summary of results and final conclusions 210

6.1 Summary of results 211

6.2 Discussion 213

6.3 Future directions 220

6.4 Final conclusions 221

Appendix 1: Material, reagents and solutions..... 223

Appendix 2: Material, reagents and solutions..... 232

References..... 238

Abbreviations

µ	Micro
AAP	Aminoantipyrine
Ab	Antibody
ACT	Australian Capital Territory
ADP	Adenosine diphosphate
AKT/PKB	Protein kinase B
ATGL	Adipose triglyceride lipase
ATP	Adenosine triphosphate
BAEE	Na–benzoyl–L–arginine ethyl ester
BMI	Body mass index
BSA	Bovine serum albumin
BSA-FA free	Bovine serum albumin-fatty acid free
C	Celsius
CC1	Cell conditioning 1
Ci	Curie
CI	Confidence interval
cm	Centimetres
CMRL	Connaught Medical Research Laboratories
CPM	Counts per minute
CPT	Carnitine palmitoyltransferase
CRP	C-reactive protein
DAB	3, 3′-Diaminobenzidine
DBD	Digestion buffer with dispase II
ddH_2O	Distillated water

DHA	Docosahexaenoic acid
DMEM	Dulbecco's Modified Eagle Medium
DNA	Deoxyribonucleic acid
DPM	Disintegrations per minute
EC	Endothelial cell
EDTA	Ethylenediaminetetraacetic acid
EGF	Epidermal growth factor
EL	Endothelial lipase
ELB	Erythrocyte lysis buffer
EPA	Eicosapentaenoic acid
ESPA	N-Ethyl-N-(3-sulfopropyl)-m-anisidine
FABP	Fatty acid binding protein
FABPpm	Fatty acid binding protein plasma membrane
FAD	Flavin adenine dinucleotide
FAT/CD36	Fatty acid translocase
FATP	Fatty acid transport protein
FC	Fetal capillary
g	Gram
g	Gravity (for relative centrifugal force-RCF-in centrifuges)
GDM	Gestational diabetes mellitus
Gluc	Glucose
GLUT	Glucose transporter
G6P	Glucose 6-phosphatase
G6PC	Glucose 6-phosphatase catalytic subunit
h	Hour

HAPO	Hyperglycemia and Adverse Pregnancy Outcomes
HBSS	Hank's Balanced Salt Solution
HDL-C	High density lipoprotein cholesterol
HEPES	4-(2-hydroxyethyl)-1-piperazineethanesulfonic acid
HGF	Hepatocyte growth factor
HIER	Heat induced epitope retrieval
HMG-CoA	β-hydroxy-β-methylglutaryl-CoA
HODE	Hydroxyoctadecadienoic acid
hPL	Human placental lactogen
HREC	Human Research Ethics Committee
HSL	Hormone sensitive lipase
ICAM	Intracellular adhesion molecule
IHC	Immunohistochemistry
IL	Interleukin
IRR	Incidence relative risk
IU	International units
IVS	Intervillous space
JNK	c-Jun NH_2 terminal kinase
kBq	Kilobecquerel
kg	Kilogram
K*m*	Michaelis constant
KRBH	Krebs-Ringer Bicarbonate HEPES
KU	Kunitz units
l	Litre
LCAD	Long-chain acyl-CoA dehydrogenase

LCHAD	Long-chain L-3-hydroxyacyl-CoA dehydrogenase
LDH	Lactate dehydrogenase
LDL-C	Low density lipoprotein cholesterol
LGA	Large for gestational age
LKAT	Long-chain 3-ketoacyl-CoA thiolase
LPL	Lipoprotein lipase
m	Milli
m^2	Meter square
M	Molar
MCAD	Medium-chain acyl-CoA dehydrogenase
MCP	Monocyte chemoattractant protein
mol	Molar
mTOR	Mammalian target of rapamycin
n	Nano
NAD	Nicotinamide adenine dinucleotide
NADH	Reduced nicotinamide adenine dinucleotide
NADPH	Reduced nicotinamide adenine dinucleotide phosphate
NEFA	Non-esterified fatty acids
NF	Nuclear factor
ns	Non-significant
OR	Odds ratio
PBS	Phosphate buffered saline
PCA	Perchloric acid
p-FABPpm	Placental membrane fatty acid binding protein
PPAR	Peroxisome proliferator-activated receptor

PSN	Penicillin-Streptomycin-Neomycin
PUFA	Polyunsaturated fatty acids
RNA	Ribonucleic acid
SA	Specific activity
SCHAD	Short-chain L-3-hydroxyacyl-CoA dehydrogenase
SD	Standard deviation
sec	Second
SEM	Standard error
SNAT	Na^+-coupled neutral amino acid transporter
SYN TR	Syncytiotrophoblast
TauT	Taurine transporter
TCA	Tricarboxylic acid
TCH	The Canberra Hospital
T1DM	Type 1 diabetes mellitus
T2DM	Type 2 diabetes mellitus
TNF	Tumour necrosis factor
TG	Triacylglycerol
UDP	Uridine diphosphate
UTP	Uridine triphosphate
VLCAD	Very-long-chain acyl-CoA dehydrogenase
VLDL-C	Very low density lipoprotein cholesterol
Vmax	Maximal velocity
vol	Volume
VSM	Vasculo-syncytial membrane
wt	Weight

Chapter 1

Introduction

1.1 Obesity overview

Obesity prevalence has doubled from 1980 to 2008 worldwide and reached epidemic levels in both developing and developed countries (1). About 1.7 billion adults have overweight or obesity making excess body fat the sixth most relevant risk factor to the overall burden of disease worldwide (2).

Obesity is a complex disease that occurs owing to a disruption between energy intake and expenditure and it is characterized by an increased amount of body fat mass (2). The aetiology of obesity is multifactorial, involving genetic and environmental factors. The neuro-endocrine system is affected and the physiologic regulatory mechanisms that signal caloric storage and control hunger, satiety and basal energy expenditure are impaired (2).

Obesity diagnosis is made by calculating the body mass index (BMI) that is calculated as the body weight (in kg) divided by the square of the height (in meter) (3). Thus, obesity is defined as the BMI $\geq$ 30 kg/m^2 according to the World Health Organization (3).

Obesity is closely related to the metabolic syndrome. The National Cholesterol Education Program's Adult Treatment Panel III report (ATP III) has identified the metabolic syndrome as a multiplex risk factor for cardiovascular disease (4). According to the ATP III, the metabolic syndrome diagnostic criteria include at least 3 of the following components: abdominal obesity, hypertriglyceridaemia, decreased high density lipoprotein cholesterol (HDL-C), systemic arterial hypertension and/or hyperglycaemia (4). Besides dyslipidaemia and glucose intolerance, the most common pathophysiologic alterations observed in obesity associated with the metabolic syndrome are hypersinsulinaemia, cellular lipotoxicity, disturbed adipokine levels (i.e. hyperleptinaemia, leptin resistance, hypoadiponectinaemia, elevated levels of resistin and others), impairment of endothelial function, higher levels of pro-coagulant factors, a pro-inflammatory status [e.g elevated levels of interleukin (IL)-6 and IL-18, C-reactive protein (CRP), tumour necrosis factor (TNF)-α] and elevated oxidative stress (4). These

chronic pathophysiological factors lead to obesity-related diseases including type 2 diabetes mellitus (T2DM), psychiatric disorders, asthma, sleep disorders, renal diseases, cardiac, cerebral and peripheral vascular diseases, non-alcoholic steato-hepatitis, osteoarthritis, cancer and many gestational complications (4).

1.2 Epidemiology of obesity during pregnancy

As for the general population, the prevalence of overweight and obesity in childbearing age women (20-49 years) is increasing globally, not only in developed countries, but also in low-income countries in the past decades (5-7). The highest proportion of these women is in the Americas, where the prevalence reaches 70%, Europe and Oceania. Africa and Asia also exhibit a high prevalence of overweight and obese women, being more than 40% in Africa (5).

In Australia, about 45% of women aged 18-44 are overweight or obese (8). However, the prevalence of overweight and obesity in pregnant women has indicated a trend of plateau and these conditions may have become endemic in this country (6). Data from a study with an Australian population of 75,000 women, who had a singleton pregnancy and gave birth between 1995 and 2008, showed that, overall, pre-pregnancy BMI has been stable for women with BMI < 35 kg/m^2 (6). The percentage of women with pre-pregnancy BMI between 30 and 35 kg/m^2 reduced from 7.7% to 7.5% and the percentage of those with BMI between 25-30 kg/m^2 remained unchanged (20%). Nevertheless, a small but significant increase was observed in the prevalence of women with BMI $\geq$ 35 kg/m^2 (from 2.5% to 3.2%) and $\geq$ 40 kg/m^2 (from 1.2% to 2.0%) over the years (6). These data indicate that obesity is still a major burden for maternity services and the most severe cases are becoming more frequent.

Gestational diabetes mellitus (GDM), defined as a degree of glucose intolerance with onset or recognition during pregnancy, has a prevalence of 1-14% depending on the

diagnostic cut-off used and the population evaluated (9, 10). GDM prevalence increases in overweight/obese mothers (11), especially in those with higher weight gain during the first half of pregnancy (12, 13). The prevalence of hypertensive disorders of pregnancy also increases with high BMI, reaching 1.4-13.5% in obese women in comparison with 0.7-4.7% in normal BMI pregnant women (14).

While some of the adverse pregnancy outcomes related to obesity can be attributed to hyperglycaemia, maternal obesity has been identified as an independent risk factor for complications, in particular for macrosomia, preeclampsia, stillbirth and excess fetal adiposity (15-17). Other components present in obesity such as low grade inflammation, dyslipidaemia, sleep apnoea, hormonal and adipokine alterations (4) may also contribute to adverse gestational outcomes. The detrimental roles of non-glycaemic factors contributing to obesity related diseases are well known, but their effects in pregnancy are not completely elucidated. In addition, there are not many studies that have investigated the possible synergistic effect of hyperglycaemia in association with these factors, particularly dyslipidaemia, in the pathogenesis of pregnancy complications.

Before discussing the pathophysiological processes involved in gestational complications related to obesity in this chapter, maternal metabolism in normal pregnancy is presented in the following section.

1.3 Maternal metabolism in normal pregnancy

1.3.1 Glucose metabolism

Glucose is the major nutrient during pregnancy and maternal glucose metabolism has been extensively studied. Basal glucose and insulin metabolism in healthy lean women do not show major differences in the first trimester of gestation in comparison with the non-gravid state (18-20). In early pregnancy, post-prandial glucose is normal or a little lower than in non-pregnant women (18, 19), and endogenous insulin secretion is

increased in response to oral or intravenous glucose (18). A study that evaluated healthy lean pregnant women pre- and during pregnancy showed that at 12-14 weeks of gestation insulin levels raised by 120% during the first phase of insulin secretion (i.e. 0-5 minutes after intravenous glucose injection, an estimate of β cell function), but the second phase of insulin secretion (i.e. 5-60 minutes after intravenous glucose injection) did not significantly increase in relation to pre-pregnancy (21). Another alteration observed was a higher insulin clearance in early pregnancy in comparison with before the conception (22), which may occur due to a rise in glomerular filtration that starts in the beginning of the gestation and peaks in mid-pregnancy (23).

In the second trimester of pregnancy, a progressive physiological resistance to insulin initiates secondary to placental production of insulin counter-regulatory hormones [e.g. progesterone, human placental lactogen (hPL) and cortisol releasing hormone] (24), alterations in the growth hormone axis and increased leptin synthesis from both adipose tissue and the placenta (25). Thus, as the gestation advances, insulin sensitivity decreases by 45 to 70% in comparison with the non-pregnant state (20, 21, 26). Consequently, both basal and post-prandial insulin levels progressively enhance to compensate the insulin resistance. It was reported a significant increase by 65% in basal insulin and basal C-peptide (22), and a 3.0 to 3.5-fold higher response in the first and second-phase of insulin release during the intravenous glucose tolerance test in the last trimester of pregnancy in comparison to pre-pregnancy (21). Also, the metabolic clearance of insulin is increased in the last trimester in relation to early pregnancy, possibly owing to placental action (22). The insulin resistance of pregnancy is more marked in peripheral tissues (i.e. muscles) (21), while, insulin sensitivity is preserved in the liver, where insulin infusion supresses more than 90% endogenous glucose production (18, 20). Moreover, late in gestation hepatic gluconeogenesis rises mostly from lipid sources (glycerol from lipolysis) than from pyruvate (27) since insulin resistance promotes lipolysis.

1.3.2 Lipid metabolism

Pregnancy is characterized by maternal metabolic adaptations to provide adequate nutrients to support fetal growth. The first two trimesters of pregnancy are marked by anabolism and an increase in maternal fat depots (28). The maternal fat accumulation follows a rise in the appetite and food ingestion from early pregnancy possibly owing to enhanced levels of the orexigenic hormone progesterone and a relative lack of the anorectic effect of estradiol (29). At least in rats, this hyperphagic effect is perpetuated from mid-pregnancy through a transitory hypothalamic resistance to leptin, which is a potent inhibitor of food intake (29). Prolactin, progesterone and hPL decrease leptin actions in the brain by inducing leptin receptor mRNA down-regulation and suppression of leptin signal transduction (29). Hyperphagia associated with changes in insulin metabolism such as higher insulin secretion in response to glucose with maintenance of tissue sensitivity to insulin (20, 21) contributes to maternal gain of fat (30). Insulin induces maternal fat deposition through stimulation of glucose uptake, increase of adipose tissue lipoprotein lipase (LPL) activity (31) and suppression of adipocyte lipolysis (32). LPL is found in the capillary endothelium and, when activated, promotes hydrolysis of plasma triacylglycerol (TG) rich lipoproteins [e.g. very low density lipoprotein cholesterol (VLDL-C) and chylomicrons] (31). Non-esterified fatty acids (NEFA) and glycerol are then released and taken up by maternal adipocytes (33). Concomitantly, maternal adipocyte lipolysis is inhibited by stimulated Akt activity, which down-regulates protein kinase A, the key enzyme during lipolysis (34). A decrease in maternal lipid concentrations is therefore observed in the first 8 weeks of pregnancy (27). Subsequently, other lipid alterations are observed mostly due to the actions of estrogen (27). TG levels begin to rise from 10 weeks of pregnancy (35), whereas low density lipoprotein cholesterol (LDL-C) and total cholesterol levels progressively rise from the second

trimester (35, 36). HDL-C concentration shows a peak in mid-pregnancy decreasing afterwards (35, 36).

As the gestation progresses and peripheral tissues become insulin resistant, maternal metabolism shifts from a predominant anabolic to a catabolic status. Adipose tissue lipolysis is increased and, consequently, higher levels of circulating maternal lipids are observed in the third trimester of pregnancy (35-37). Insulin resistance contributes to amplify the rise in maternal plasma levels of amino acids, glucose and lipids during the post-prandial state to nourish the fetus (27). Insulin resistance also decreases the activity of adipose tissue LPL in the third trimester of pregnancy (36). Thus, less NEFA is taken up by maternal adipocytes from circulating TG favouring the breaking down of the maternal adipose tissue. Moreover, hepatic lipase activity reduces after meals and increases during fasting to provide NEFA and other lipid products to the fetus when maternal glucose is scarce (27). As a result, the hepatic synthesis of VLDL-C is stimulated and the VLDL-C/TG clearance is decreased (36). Thus, maternal TG levels are 2 to 3-fold higher at term (38, 39) in comparison with early pregnancy. Maternal NEFA levels increase later than the other lipids (40, 41) and are 2-fold higher at term than in non-pregnant controls (42). NEFA enhancement, in turn, contributes to insulin resistance in healthy pregnancy (43). As a consequence of increased lipolysis, notably in the state of fasting, NEFA and glycerol production are enhanced as well as hepatic ketone synthesis from the NEFA (44). High NEFA and ketones can provide energy to maternal tissues and spare glucose and amino acids to the fetus (28, 44). In addition, total cholesterol and LDL-C are increased by about 60% in the last trimester in comparison with early pregnancy (35, 36).

In addition to changes in lipid concentrations late in pregnancy, lipoprotein qualitative alterations are also observed (36). Lipoproteins not usually rich in TG in the non-gravid condition (i.e. HDL-C and LDL-C) start to assemble higher amounts of TG

(TG/cholesterol ratio) owing to increased activity of cholesteryl ester transfer protein and inhibition of hepatic lipase (36).

1.3.3 Other physiological alterations

Maternal plasma levels of amino acids are usually lower during fasting and the post-prandial state during pregnancy (24). This is mainly caused by maternal and fetal amino acids utilisation for anabolic needs than amino acid metabolism for energy production, since the nitrogen balance is usually positive during gestation (24). Even though, amino acids such as serine, threonine and alanine may be used for gluconeogenesis in the maternal liver after prolonged fasting (24).

In addition to the metabolic alterations previously discussed, healthy pregnancy displays changes in adipokines and cytokines leading to a pro-inflammatory status especially late in gestation (45, 46). The placenta expresses leptin, resistin, IL-6, IL-10, TNF-α, monocyte chemoattractant protein (MCP)-1 among others inflammatory molecules which act locally and systemically (46). Leptin is highly synthesized by the syncytiotrophoblast (the main source), amnion cells and the fetal endothelial cell (47, 48) and is distributed to both maternal and fetal circulations (49) with functions not yet fully understood. Leptin is directly related to insulin resistance (45) and serum leptin correlates with lipid oxidation during both early and late gestation (50). Adiponectin is synthesized by maternal adipose tissue but not by the placenta (51) and its levels show progressive decrease with gestation age with the lowest levels in late pregnancy (52-55). Studies have also described higher resistin levels in pregnant women than in non-pregnant controls, although with divergent longitudinal results (53, 56, 57). Low adiponectinaemia and raised resistin levels are similarly observed in non-pregnant women with central obesity and the metabolic syndrome (58, 59). In healthy pregnancies, decreased adiponectin concentrations have been implicated in insulin resistance development but not in alterations in maternal lipid oxidation or lipolysis (52). Fasting insulin has been negatively correlated to adiponectin

levels throughout gestation ($r=-0.66$, $p < 0.0001$), and adiponectin concentrations were associated with peripheral ($r=0.55$, $p=0.001$) but not with hepatic insulin sensitivity (52). Supporting this findings, lower adiponectin levels have been described in GDM women (60, 61) and in non-diabetic overweight/obese gravidas (51, 54). Resistin has been also correlated to insulin sensitivity in healthy pregnancies (62). However resistin role in GDM is uncertain since studies have reported lower (62), similar (53) or higher (57, 63, 64) resistin concentrations in GDM women. In addition, resistin has not been independently related to insulin resistance in GDM pregnancies (62).

Healthy pregnancy also increases CRP (65) and pro-inflammatory circulating cytokine levels (45, 66). In non-gravid conditions, TNF-α is secreted by immune cells, fibroblasts and adipocytes, and is associated with BMI and insulin resistance (67) as well as insulinaemia (68). In pregnancy, TNF-α levels gradually increase from early to term pregnancy, mainly from placental sources, and this has been an important contributing factor in the induction of insulin resistance of pregnancy, since it is inversely related to maternal insulin sensitivity (66).

Besides, healthy pregnant women seem to have higher oxidative stress rates (69). A study has shown that rates of DNA damage, which is an indication of oxidative stress, were increased in the third trimester of pregnancy and that these rates were positively associated to maternal total body fat, TG, total cholesterol and LDL-C (69).

Therefore, major physiological alterations affect maternal metabolism, hormones and adipokines/cytokines in healthy pregnancy. The normal pregnancy profile resembles the pathologic features observed in obesity and the metabolic syndrome. Hence, pregnancy represents a metabolic “overload test” adding extra demands to susceptible women with overweight/obesity and/or the metabolic syndrome before the conception. These conditions highly enhance the likelihood of adverse outcomes to the feto-placental-maternal unit (70). For instance, even though obese pregnant women have a reduction in

insulin sensitivity late in pregnancy similar to that which is observed in lean pregnant women (71, 72), the insulin response stimulated by glucose infusion appears to be lower in obese women with normal glucose tolerance than in the healthy lean controls (21). Glucose and insulin metabolism changes are also even more pronounced in women with GDM (20, 72). Both lean and obese women with GDM have lowered whole body insulin sensitivity and reduced suppression of endogenous glucose production by insulin compared to controls matched for BMI (20, 72). In addition, insulin secretion is impaired in GDM and, as insulin requirement is physiologically increased late in gestation, even minor reductions in pancreatic β cells can lead to hyperglycaemia (26, 72, 73). Women with GDM in comparison with controls can have higher glycerol levels (74), a more atherogenic lipid profile (75, 76) and an earlier (76) and more intense hypertriglyceridaemia (76, 77).

1.4 Gestational complications associated with obesity and its co-morbidities

Obesity is not only associated with factors that cause gestational complications (e.g. diabetes, dyslipidaemia and other components of the metabolic syndrome), but it is also an independent predictor of pregnancy adverse outcomes. Higher BMI is a well-established predictor of GDM (10, 13, 78). The increment of 1 kg per m^2 in the first trimester maternal BMI is associated with a 1.12-fold [95% confidence interval (CI) 1.10–1.14)] higher risk of GDM (79). In an Australian study, the adjusted odds ratio (OR) for GDM was 3.99 (95% CI 3.47–4.59) for mothers with self-reported pre-pregnancy BMI of ≥ 30 kg/m^2 and 6.45 (95% CI 5.01–8.28) for the subgroup with BMI ≥ 40 kg/m^2 (6). GDM is usually associated with impairment of pancreatic β cell function in women with an already pre-conception dysfunctional β cell secretion and insulin resistance (20, 72, 80, 81), explaining why obesity is strongly associated with GDM. Thus, the physiological

reduction of insulin sensitivity that occurs in pregnancy overloads the chronically impaired β cells of overweight/obese women, which become unable to secrete enough insulin to cope with the high metabolic demands, and consequently hyperglycaemia ensues.

Besides GDM, there is evidence that elevated maternal BMI increases the chance of large for gestational age (LGA) babies, higher fetal adiposity, fetal hyperinsulinaemia, neonatal hypoglycaemia, and congenital malformations (16, 17, 82). A large study has shown that a BMI of $\geq$ 25 kg/m^2 in the first trimester of gestation is an independent predictor of infant mortality, particularly of neonatal deaths (83). The magnitude of this association was modest for overweight mothers, but doubled the risk of infant mortality for women with a BMI of $\geq$ 35 kg/m^2 in comparison to those with normal BMI (83). Most deaths were due to congenital anomalies and birth asphyxia in both term pregnancies and preterm deliveries (83). Moreover, obesity was the most significant modifiable risk factor for stillbirth in developed countries (15).

In addition, maternal obesity is a relevant risk factor for hypertensive gestational disorders and pre-eclampsia (14), which is a pregnancy-specific disease defined as new hypertension and proteinuria with onset at $\geq$ 20 weeks of gestation (84). In the "Hyperglycemia and Adverse Pregnancy Outcome (HAPO)" study, maternal obesity was the strongest independent predictor of pre-eclampsia, with the OR increasing in parallel with the BMI, being as high as 8.35 (95% CI 5.22-13.36) for women with BMI > 44 kg/m^2 (85). Interestingly, many characteristics observed in patients with the metabolic syndrome are shared by women with a pre-eclampsia history (86), with both groups being susceptible to future cardio- and cerebrovascular disease as is further discussed.

There is also evidence that maternal obesity raises the risk for caesarean section (78, 87), induction of labour, postpartum bleeding (87), and birth trauma (88). Data from a large Chinese cohort study showed that pre-conception BMI is a more important predictor of

pregnancy complications than excessive weight gain during pregnancy (89). In comparison with women with normal pre-pregnancy BMI and an adequate weight gain during pregnancy according to the Institute of Medicine guidelines (90), the highest risks for caesarean section (OR: 3.69), pregnancy specific hypertension (OR: 7.08) and GDM (OR: 3.57) were observed in women with obesity and appropriate weight gain (89). However, the highest likelihood of preterm delivery (OR: 1.49), LGA (OR: 3.99) and macrosomia (OR: 4.1) was found in women who were both obese and had excessive weight gain during pregnancy (89). On the other hand, the increased risk of complications was not as great for women with a normal BMI who had an excessive weight gain during pregnancy, being significant increased for LGA (OR: 1.91), macrosomia (OR: 1.9), pregnancy specific hypertension (OR: 1.35) and caesarean section (OR: 1.34) (89). These findings suggest that women with pre-existing obesity have a more deleterious metabolic milieu during pregnancy that lean women who gain excess weight in pregnancy, although both scenarios add risk. Finally, a recent large Swedish study reported that obese women who have undergone bariatric surgery exhibited a lower risk of LGA neonates and GDM. However, there was an increased risk of small for gestational age neonates and a trend towards the increase of stillbirth or neonatal death (91).

Regarding obesity co-morbidities, GDM notably if undiagnosed and untreated, contributes to adverse gestational outcomes (92, 93). Nevertheless, even relatively mild maternal glycaemic levels are important independent determinants of pregnancy complications (94). The HAPO study showed that, after adjustment for BMI, maternal glucose levels are associated with increased risks of macrosomia and LGA babies, caesarean section, neonatal hypoglycaemia and higher cord blood C-peptide concentrations (94). Moreover, the treatment of GDM reduces the risk of hypertensive disorders, macrosomia, birth trauma, caesarean delivery (93) and perinatal death (95).

Treatment of GDM is also an effective treatment for the prevention or attenuation of pre-eclampsia (92, 93).

As expected, pre-existing diabetes also increases the risk of gestational complications and more than triplicates the pre-eclampsia likelihood (OR: 3.56; 95% CI 2.54-4.99) (96). Severe complications such as intrauterine growth restriction, congenital malformations, perinatal death and maternal mortality are more prevalent in pregnancies complicated by pre-pregnancy diabetes, especially with inadequate glycemic control (15, 97). In developed countries, overt diabetes is among the most important maternal risk factor for stillbirth, which was 3 times more likely to occur in women with pre-gestational diabetes (15). In this meta-analysis, more than 2000 stillbirths per year could be attributed to pre-existent diabetes (15). In a population without congenital defects, fetal and infant death were, respectively, 4.6-fold and 1.9-fold more frequent in women with pre-existent diabetes than in healthy mothers (98). The risk of fetal and infant death were similar between type 1 diabetes mellitus (T1DM) and T2DM women (98). In this study, the increment of each 1 mmol/mol in a periconceptional HBA1C > 49 mmol/mol increased the relative risk of stillbirth by 2% and of infant deaths by 3%. (98). Of relevance, recurrent miscarriage has been reported to be associated with increased measures of insulin resistance in the first trimester of pregnancy (99). Moreover, over six intervals of maternal first trimester glycated protein levels, the miscarriage risk for T1DM women was highest in those women in the highest extreme (100). Surprisingly, the frequency of miscarriage was also increased in normal women with the highest glycated protein levels, even though this level was 2-5 times lower that in diabetic pregnancies with the highest glycated protein levels, i.e. in pregnancies with the worst first trimester diabetes control (100). These data reinforce the detrimental effects that intrauterine hyperglycaemia exerts on the fetus.

As mentioned before, pregnancy is a hyperlipidaemic state with marked physiological increases especially in TG levels (28). Pathological hyperlipidaemia, with lipid levels beyond those of healthy gestation, is observed in pregnancies affected by obesity, in which it is common to have abnormally high serum concentrations of TG, VLDL-C and low levels of HDL-C (101). Maternal dyslipidaemia years before (102), or during pregnancy (103), has been associated with pre-eclampsia (102, 103). Pre-eclampsia is a disease characterised by poor placentation, placental oxidative and endoplasmic reticulum stress, followed by the development of maternal systemic illness involving endothelial dysfunction and systemic inflammation (84). Women with pre-eclampsia, in comparison with heathy gravidas, present higher lipid levels and a more atherogenic lipid profile including increased concentrations of small and dense LDL-C particles (35, 104, 105). The association between lipid alterations and pre-eclampsia reported in clinical studies may be explained by dyslipidaemia causing the endothelial dysfunction, such that the dyslipidaemia is implicated in the pathogenesis of pre-eclampsia (106). Endothelial cells take up NEFA, when abnormally increased in the maternal circulation, leading to endothelial dysfunction with reduction of vasodilator synthesis (e.g. prostacyclin) and contributing to pre-eclampsia (107). Moreover, women with pre-pregnancy dyslipidaemia may have established chronic endothelial dysfunction, which can be aggravated by the pregnancy metabolic overload also increasing the risk of pre-eclampsia development (106). Alternatively, the endothelial dysfunction in pre-eclampsia could disrupt lipid metabolism and favour the dyslipidaemia. In the long-term, women with a history of pre-eclampsia have a higher predisposition to dyslipidaemia, abnormal lipid oxidation (108) and chronic hypertension (109). Consequently, these women have increased rates of atherosclerotic cardiac disease, stroke, renal morbidity and mortality (110-112). Also, oxidized lipids can impair trophoblast invasion contributing to the poor placentation noticed in preeclampsia (107)

In addition to pre-eclampsia, maternal hyperlipidaemia has been associated with preterm birth. The risk of preterm delivery was higher in pregnant women with hyperlipidaemia measured early in pregnancy, defined as total cholesterol or TG more than 1 standard deviation (SD) above the mean (113). Also, the highest concentrations of total cholesterol and LDL-C were found in overweight women with preterm delivery < 34 weeks (113). In the long prospective "Coronary Artery Risk Development in Young Adults" study, pre-pregnancy total cholesterol levels in the highest quartile was also related to an increased risk of preterm delivery (OR: 3.80; 95% CI 1.07-7.57) (114). Moreover, in research that aimed to develop a predictive model for preterm birth, the addition of the combination of first trimester total cholesterol and change in total cholesterol between trimesters to other maternal characteristics and biochemical analyses proved to be the best model (115). Besides, women with higher non-fasting NEFA in the first trimester of pregnancy had twice the risk of preterm delivery comparing with women with lower levels (116). This association was worse for preterm birth < 34 weeks, in which higher levels of NEFA increased preterm birth by almost 4-fold (116). Similarly, women with NEFA levels in the highest tertile measured at 30 weeks of gestation had higher risk of preterm delivery (OR: 3.49, 95% CI 1.73-7.03), a risk that persisted after excluding GDM and pre-eclampsia cases from the analysis (OR: 3.30, 95% CI 1.38-7.87) (117). Of note, a study in which maternal lipids were measured in the second trimester of pregnancy showed that the relationship between total cholesterol, HDL-C and LDL-C levels and preterm birth follows a U shape curve; whereas the relation between TG and preterm birth is linear (118). Women with extremely low total cholesterol, HDL-C and LDL-C levels were twice more likely to have preterm birth related to a medical indication (118). This association of low cholesterol levels and preterm birth may be due to (i) the presence of an underlying maternal disease, (ii) the usual increases in cholesterol is not achieved due to poor placental function, or (iii) a subnormal increase in maternal lipids is inadequate

for optimal fetal nutrition and development (118). Conversely, those with higher LDL-C and total cholesterol had a 1.5-fold increased risk of spontaneous preterm birth. TG in the third and fourth quartile nearly doubled the spontaneous preterm birth risk (118). This result was maintained even after excluding patients with placental vascular pathology, pre-eclampsia and gestational hypertension (118).

Moreover, maternal lipids seem to be strongly associated with fetal growth and may explain why the prevalence of macrosomic neonates is higher in maternal obesity or GDM with excellent glycaemic control. In a study that included healthy and GDM women, maternal TG levels measured early in pregnancy showed a weak correlation with neonatal birth weight independently of maternal BMI ($r=0.12$, $p=0.02$) (39). However, this association was much stronger when the subgroup of women with GDM was analysed ($r=0.60$, $p < 0.001$) (39), suggesting that TG, which is also a marker of insulin resistance and the metabolic syndrome, may be exerting a synergistic effect along with GDM in the pathogenesis of abnormal fetal growth. The association of higher TG levels and LGA was also demonstrated in women with an abnormal GDM screening test but normal glucose tolerance test (119). Fasting TG > 75^{th} percentile (> 2.9 mmol/l) measured in the second trimester of pregnancy increased the risk of delivering LGA babies by 11.6-fold independent of maternal pre-pregnant BMI, rate of weight gain and fasting glucose (119). Accordingly, levels of NEFA and TG at 36 weeks and near the delivery in well-controlled GDM mothers were independently associated with LGA birth (120). Besides, third trimester maternal levels of NEFA and TG showed a modest but significant correlation with intrauterine fetal growth measured by abdominal circumference at 28, 32 and 36 weeks; whilst maternal glycaemia was not related to fetal growth at any assessed time point (120). Conversely, there was a lack of correlation between maternal lipids and neonatal weight in the babies healthy women (74). In this study, women with normal pregnancies gave birth to a similar proportion of LGA neonates as women with well-

controlled GDM women and there were no differences in the maternal lipid levels between the two groups (74). Nonetheless, in the pregnancies of the GDM mothers, placental weight, neonatal adiposity, cord NEFA, insulin and glucose concentrations were all increased compared to pregnancies of normal mothers (74). These results may reflect differences in the placental lipid transport (discussed in more details in section 1.7.2) and the fetal insulin response in an environment of more marked maternal insulin resistance such as in GDM.

Whether elevated lipid levels have a pathogenic role in adverse pregnancy outcomes, or simply correlate with other metabolic syndrome pathogenic factors, is unknown. As discussed before, in hypertriglyceridaemic states such as pregnancy, HDL-C and LDL-C turn into TG richer particles, whilst VLDL-C contains higher fractions of cholesteryl esters. Consequently, the ratio of total cholesterol/apoB in LDL-C decreases, LDL-C particles become smaller and are more prone to oxidation and likely to cause inflammation and atherogenesis (121). Also, lipolysis of TG-rich lipoproteins yields NEFA, oxidised lipids and hydroxyoctadecadienoic acid (HODE) molecules, particularly 9- and 13-HODE (122). These lipolysis products promote the endothelial synthesis of reactive oxygen species, TNF-α and intracellular adhesion molecule (ICAM) expression contributing to inflammation (122). In the adipose tissue, liver and skeletal muscle, increases in NEFA levels can stimulate the activity of c-Jun NH_2 terminal kinase (JNK) (123) and nuclear factor (NF) κB (124) pathways, raising the concentrations of pro-inflammatory chemo- and cytokines (MCP-1, TNF-α , IL-1β) (125). Thus, because of fatty acids pro-inflammatory, pro-oxidative and atherogenic properties (126-128), maternal high fatty acid concentrations may contribute to alterations in the implantation process, endothelial microvascular injuries and a dysfunctional placenta leading to poor outcomes such as pre-eclampsia, preterm labor or premature rupture of membranes.

Finally, the effects of obesity and its comorbidities during pregnancy can increase the likelihood of long-term adverse consequences for both the mother and the offspring. GDM rises maternal long-term risks of T2DM (129-132), the metabolic syndrome and consequent cardiovascular disease (133). The risk of T2DM in a meta-analysis was 7-fold higher for women with GDM history in comparison with women with normoglycaemia during pregnancy (132). This association was even higher in a recent study, which reported a 26-fold increased risk of future T2DM for women with previous GDM in comparison with those without GDM, and a future T2DM incidence rate per 1000 person-years of 115 for women whose GDM ended in a stillbirth (133). Women with GDM history have been demonstrated to be twice as likely to develop any cardiovascular disease, especially ischemic heart disease [incidence relative risk (IRR) 4.54; 95% CI 1.88-10.96)] and peripheral vascular disease (IRR=5.84; 95% CI 2.26-15.06) (133). For GDM women with stillbirth, the risk of cardiovascular events was 17-fold higher (133). Besides, women with pre-eclampsia history have a higher predisposition to dyslipidaemia, abnormal lipid oxidation (108) and chronic hypertension (109). Consequently, they have increased rates of atherosclerotic cardiac disease, stroke, renal morbidity and overall mortality (109-112).

Regarding the consequences for the offspring, abnormal hyperlipidaemia, even temporarily during pregnancy, can induce pathological changes in the fetus such as fatty streak formation in fetal arteries (134), which may contribute to atherosclerosis in adulthood. Maternal obesity is also associated with increased risk of obesity in the offspring (135, 136). Maternal obesity in the first trimester of pregnancy led to a 2-fold increase in obesity rates in children aged 2-4 years (135). In addition, T2DM was more prevalent in youths (aged 10-22 years) who were exposed to maternal overweight (OR: 2.6; 95% CI 1.2-5.5), obesity (OR: 4.6; 2.2-9.5) or diabetes (OR: 5.7; 95% CI 2.4-13.4) in pregnancy (137). Furthermore, pre-conception obesity was the strongest predictor of

obesity in children in another study (136). Pre-conception maternal obesity was associated with a 4.0-fold (95% CI: 1.23, 13.22) higher risk of having an obese child (at age 8.8 ± 1.8 years), which was independent of maternal glycaemia (136). Maternal diabetes, on the other hand, was associated with an increased likelihood of pre-diabetes or T2DM in the offspring (at age 18–27 years) (138). Maternal GDM raised this risk by 7.8 times (95% CI 2.6-23.4), whereas exposure to maternal T1DM enhanced the risk by 4 times (95% CI 1.31-12.3) (138). These studies outline the strong associations between maternal obesity and/or hyperglycaemia during pregnancy and the transgenerational risk of obesity and diabetes suggesting that not only genetic predisposition and lifestyle are involved in the pathogenesis of these conditions. Long-term implications of an altered intrauterine environment of maternal obesity and obesity related disorders in the offspring may be due to fetal or neonatal programming via epigenetic inheritance (139), which contributes to the obesity and T2DM epidemics perpetuation (140).

1.5 Overview of glucose and fatty acid metabolism pathways

In this section, general aspects of glucose metabolic pathways and lipid oxidation are presented. Specific characteristics of glucose and fatty acid metabolism in the placenta are discussed in section 1.7.

1.5.1 Glucose metabolism overview

The majority of human cells take up glucose via sodium-independent facilitated diffusion with exception of cell in the gastrointestinal tract and renal tubules where glucose is absorbed through an active transport (sodium-glucose symporter) (141, 142). Facilitated diffusion is mediated by glycoproteins of the glucose transporter (GLUT) family. So far 14 GLUT isoforms have been described in humans (143). Among them, GLUT1-4 are the most relevant and studied. GLUT1 (ubiquitous expression), GLUT2 (expression in hepatocytes, enterocytes and pancreatic islets) and GLUT3 (mainly found in neurons) are

insulin-independent and always expressed in the plasma membrane. GLUT1 and 3 are responsible for basal glucose uptake, whilst GLUT2 has a major role in the regulation of insulin secretion and glucose homeostasis. GLUT4 is found inside cytoplasmic vesicles in myocytes, adipocytes and cardiomyocytes and needs insulin signalling for these vesicles to translocate and fuse with the plasma membrane (144, 145). The main glucose transporter in trophoblasts is GLUT1 (146), which is coupled with hexokinase 1. Once glucose enters the cell through GLUT1, glucose is phosphorylated to glucose 6-phosphate in an irreversible reaction catalysed by hexokinase 1 preventing glucose efflux to the extracellular compartment. In the cytoplasm, glucose 6-phosphate can be metabolise via the glycolytic pathway to pyruvate from which it can (i) be converted to lactate (anaerobic glycolysis); (ii) enter the tricarboxylic acid (TCA) cycle to be oxidised (oxidative glucose metabolism); (iii) or go to the fatty acid synthesis pathway via the anaplerosis pathway (147). Alternatively, glucose 6-phosphate can be incorporated into glycogen storage or directed to the pentose phosphate pathway to form precursors for RNA and DNA synthesis (148) (Figure 1.1).

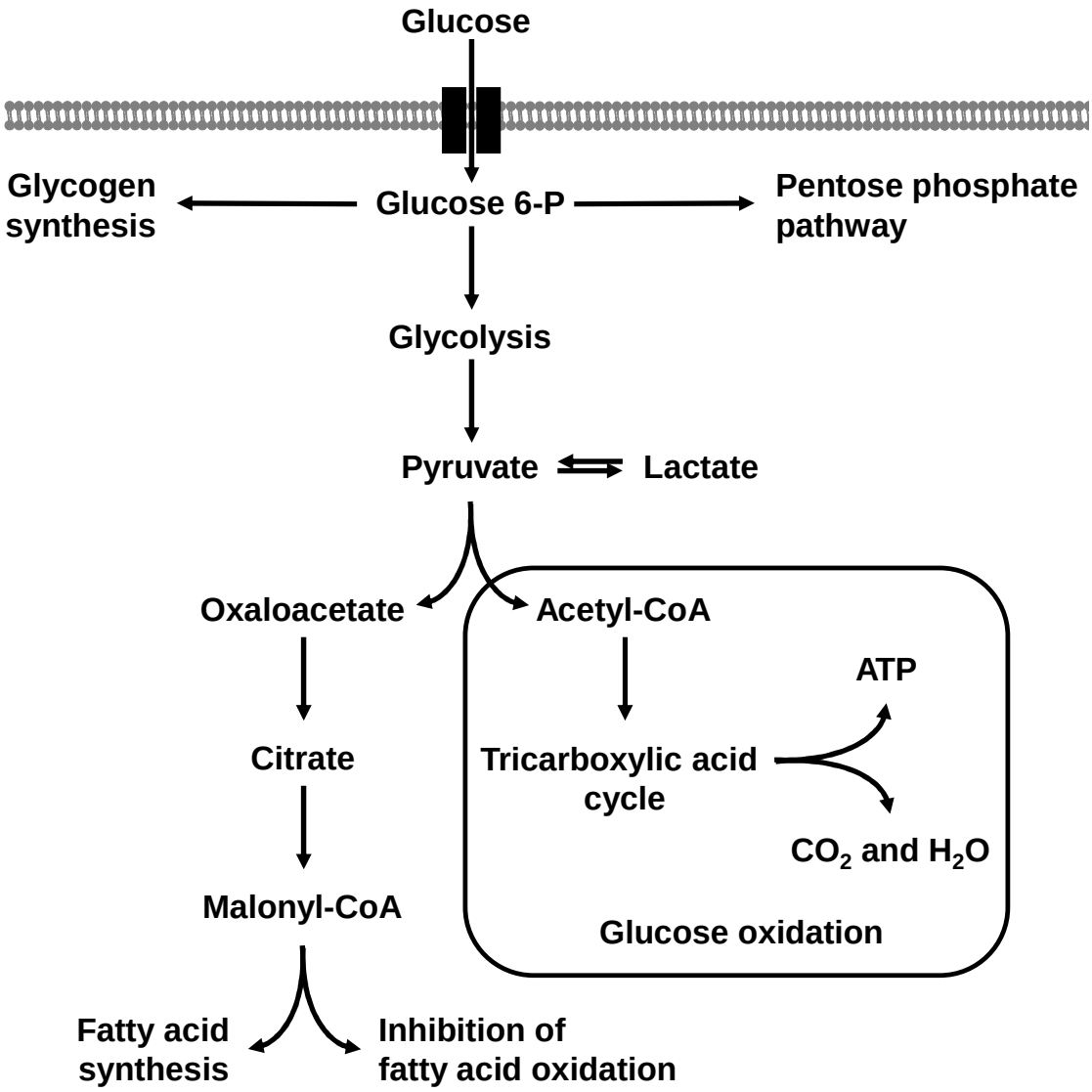

Figure 1.1. Glucose metabolism overview. Glucose can have different metabolic fates once taken up into a cell. Glycolysis is the main pathway of glucose metabolism, generating ATP and pyruvate which can be further metabolised to (i) lactate in conditions of limited oxygen supply (anaerobic glycolysis); (ii) acetyl-CoA and oxidative metabolism in the TCA cycle to produce ATP, CO_2 and H_2O (aerobic glycolysis); or to (iii) oxaloacetate to provide substrate for fatty acid synthesis. Malonyl-CoA, an important anaplerotic intermediate, inhibits the oxidation of fatty acids in situations of high glucose supply. Alternative pathways for glucose 6-phosphate are into the pentose phosphate pathway or to glycogen synthesis.

TCA: tricarboxylic acid.

1.5.2 Glycolysis

During glycolysis, the six-carbon glucose molecule is cleaved into 2 three-carbon pyruvate molecules. The yield of this reaction is two ATP, two NADH and two H^+ (Figures 1.2 and 1.3 summarise all glycolysis steps). Glycolysis is regulated by enzymes (hexokinase, phosphofructokinase-1, pyruvate kinase), metabolites (NADH and ATP concentrations) and hormones (e.g. glucagon and insulin) to maintain a steady ATP supply for cellular needs (149, 150).

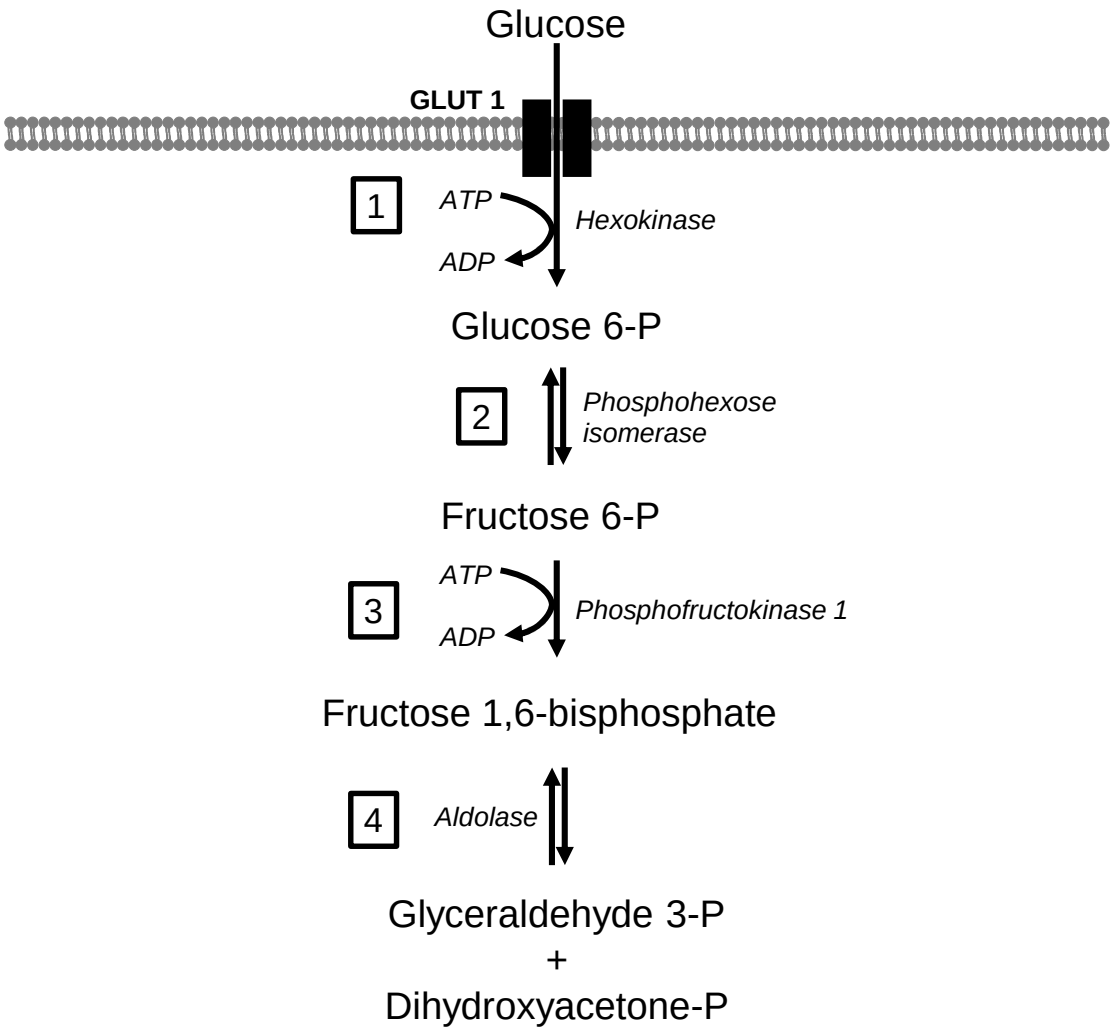

Figure 1.2. First phase of glycolysis. 1. Glucose enters the cells and is irreversibly phosphorylated to glucose 6-phosphate. 2. Glucose 6-phosphate is converted to fructose 6-phosphate by isomerization. 3. Fructose 6-phosphate receives an inorganic phosphate donated by ATP and is converted to fructose 1,6-bisphosphate. 4. Fructose 1,6-bisphosphate is cleaved into glyceraldehyde 3-phosphate and dihydroxyacetone-phosphate catalysed by aldolase with release of water. This first phase of glycolysis uses 2 molecules of ATP (149, 150).

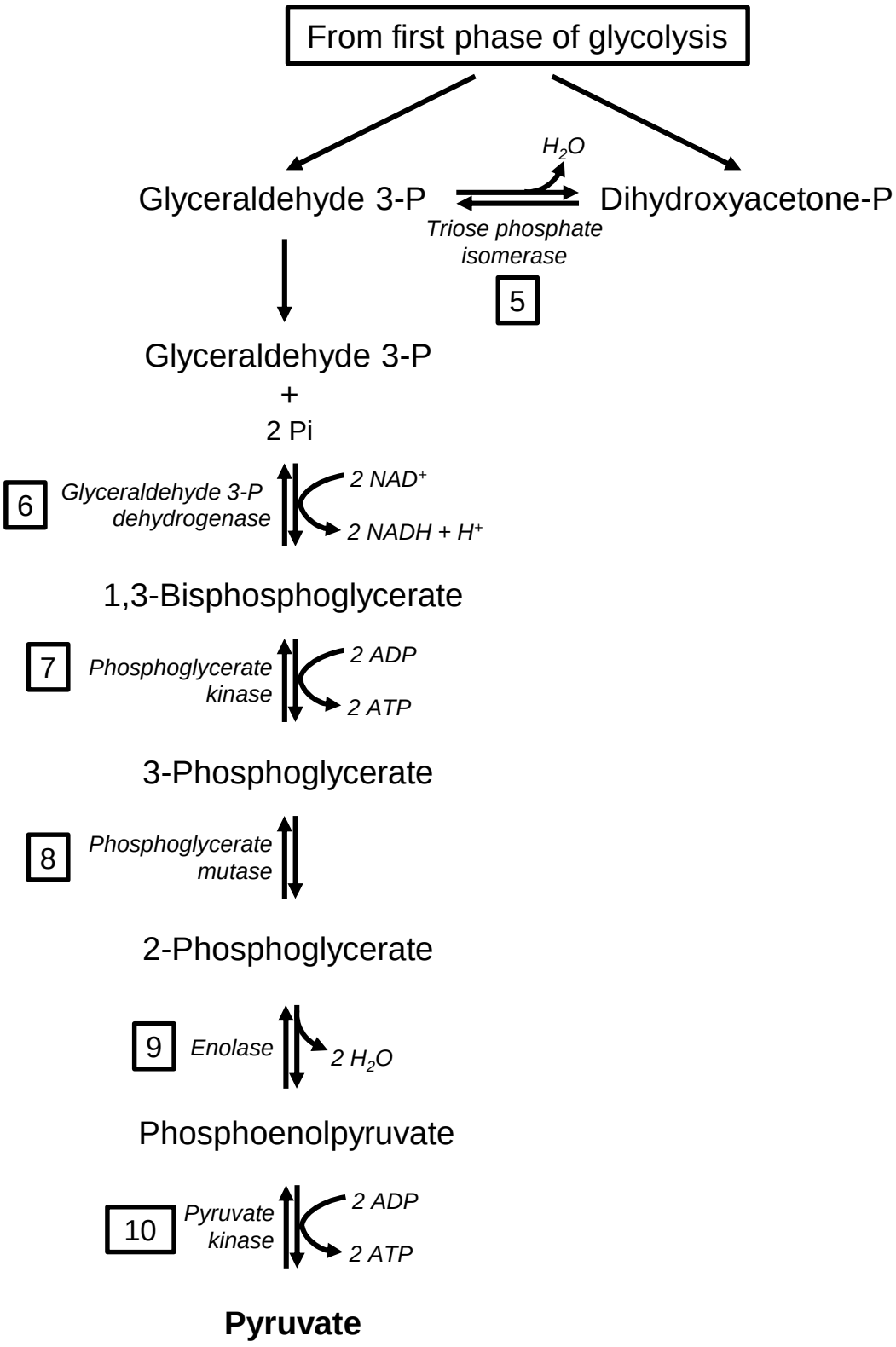

Figure 1.3. Second phase of glycolysis. 5. Contrary to glyceraldehyde 3-phosphate, dihydroxyacetone cannot be further metabolised. Thus, it needs to be converted into glyceraldehyde 3-phosphate by triose-phosphate isomerase. 6. Glyceraldehyde 3-phosphate then donates a H^+ to NAD^+ and is phosphorylated producing 1,3-bisphosphoglycerate and NADH. 7. The phosphoryl group from 1,3-bisphosphoglycerate

is transferred to ADP producing ATP and 3-phosphoglycerate. 8. The enzyme phosphoglycerate mutate transfers the phosphoryl group from the carbon in the position 3 to the carbon in the position 2, converting 3-phosphoglycerate into 2-phosphoglycerate. 9. 2-Phosphoglycerate is dehydrated to phosphoenolpyruvate releasing a molecule of water. 10. Phosphoenolpyruvate donates the phosphoryl group to ADP producing ATP and pyruvate. The second phase of glycolysis produces 4 molecules of ATP from one 6-carbon glucose, such that the net ATP production is 2 ATP molecules (149, 150).

NAD^+: oxidised nicotinamide adenine dinucleotide; NADH: reduced nicotinamide adenine dinucleotide.

1.5.3 Lactate production

In oxygen depletion or in cells devoid of mitochondria, pyruvate molecules produced at the end of glycolysis cannot be oxidised to acetyl-CoA and enter the TCA cycle. In this case, NADH produced during glycolysis cannot be oxidised again and recycle NAD^+ to accept new electrons. Thus, pyruvate must be reduced to lactate to allow NAD^+ regeneration from NADH. Lactate dehydrogenase (LDH) catalysis the transfer of H^+ from NADH to pyruvate, producing NAD^+ and lactate (Figure 1.4). Lactate can be utilised as a fuel and transformed into glucose via gluconeogenesis in the liver and kidneys (147, 151). Interestingly, some tissues including the placenta, retina and working skeletal and cardiac muscle produce high levels of lactate in spite of adequate oxygen supply (148).

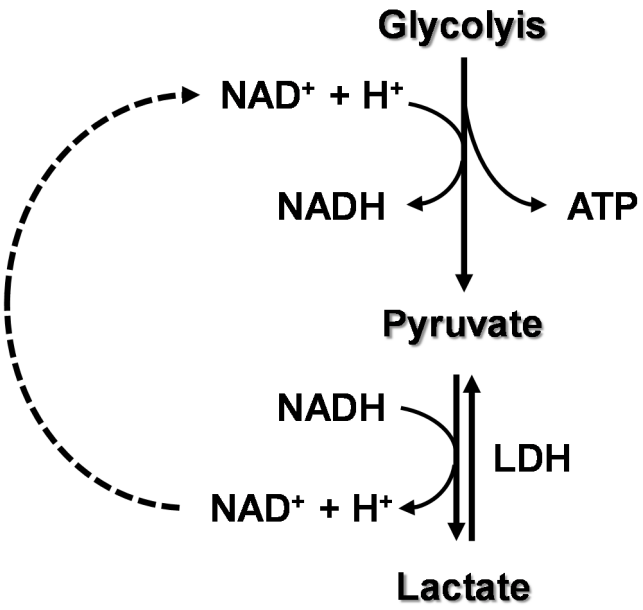

Figure 1.4. Lactate production. 1. In the end of glycolysis, 2 molecules of pyruvate are produced per glucose molecule. 2. In the absence of oxygen, pyruvate can be reduced by LDH and converted to lactate**.** NAD^+ depletion from glycolysis can be recovered by the conversion of pyruvate to lactate.
LDH: lactate dehydrogenase.

1.5.4 Tricarboxylic acid cycle and oxidative metabolism of glucose

The TCA cycle, which is also called citric acid cycle and the Krebs cycle, is a key pathway for the production of ATP from carbohydrate, lipid and protein nutrients with the fundamental key entry point being acetyl-CoA. With respect to glucose metabolism, acetyl-CoA coming from glycolysis is formed through the conversion of pyruvate (3 carbons) to acetyl-CoA (2 carbons) via the pyruvate dehydrogenase complex. Acetyl-CoA is then oxidised by the TCA cycle producing CO_2, electrons and reduced NADH and $FADH_2$. NADH and $FADH_2$ carry the electrons to the respiratory chain which releases H^+ and electrons. O_2 is reduced to H_2O and the electrons flow leads to ATP production (149) (Figure 1.5).

As previously described, pyruvate is produced at the end of glycolysis. Under aerobic conditions, pyruvate follows an oxidative decarboxylation by pyruvate dehydrogenase complex. In this process a carboxyl group from pyruvate is released as a CO_2 molecule and the remaining carbons are converted into acetyl group of acetyl-CoA which will feed the TCA cycle (Figure 1.6).

The TCA cycle is complex and extensive regulated by compounds and intermediates from both glucose and fatty acid metabolic pathways. Pyruvate conversion to acetyl-CoA is inhibited by fatty acids, ATP, NADH and acetyl-CoA; citrate synthase activity is inhibited by ATP, NADH, citrate and succinyl-CoA; α-ketoglutarate synthesis from isocitrate is down-regulated by ATP; and finally, succinyl-CoA and NADH inhibit succinyl-CoA production from α-ketoglutarate (149).

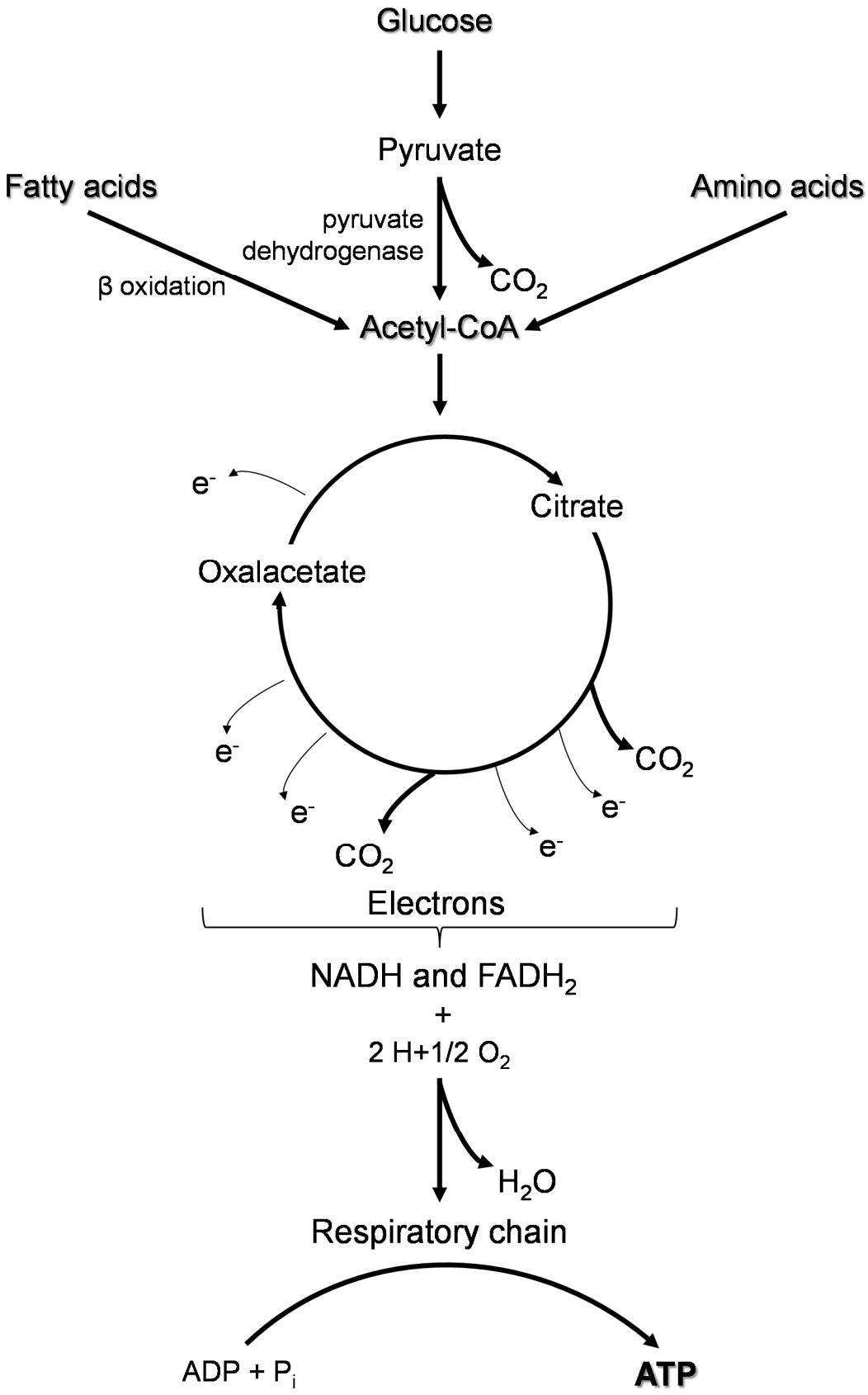
Glucose
Pyruvate
Fatty acids
Amino acids
pyruvate
dehydrogenase
β oxidation
CO_2
Acetyl-CoA
e^-
Citrate
Oxalacetate
e^-
e^-
CO_2
e^-
e^-
CO_2
Electrons
$NADH$ and $FADH_2$
+
2 H+1/2 O_2
H_2O
Respiratory chain
ADP + P_i
ATP

Figure 1.5. Cellular respiration. Nutrient oxidation yields acetyl-CoA, which enters the TCA cycle. At the end of a cycle, electrons are released and carried by NADH and $FADH_2$ to the respiratory chain. ATP is produced following electron transfer.
TCA: tricarboxylic acid; NADH: reduced nicotinamide adenine dinucleotide; FAD: flavin adenine dinucleotide.

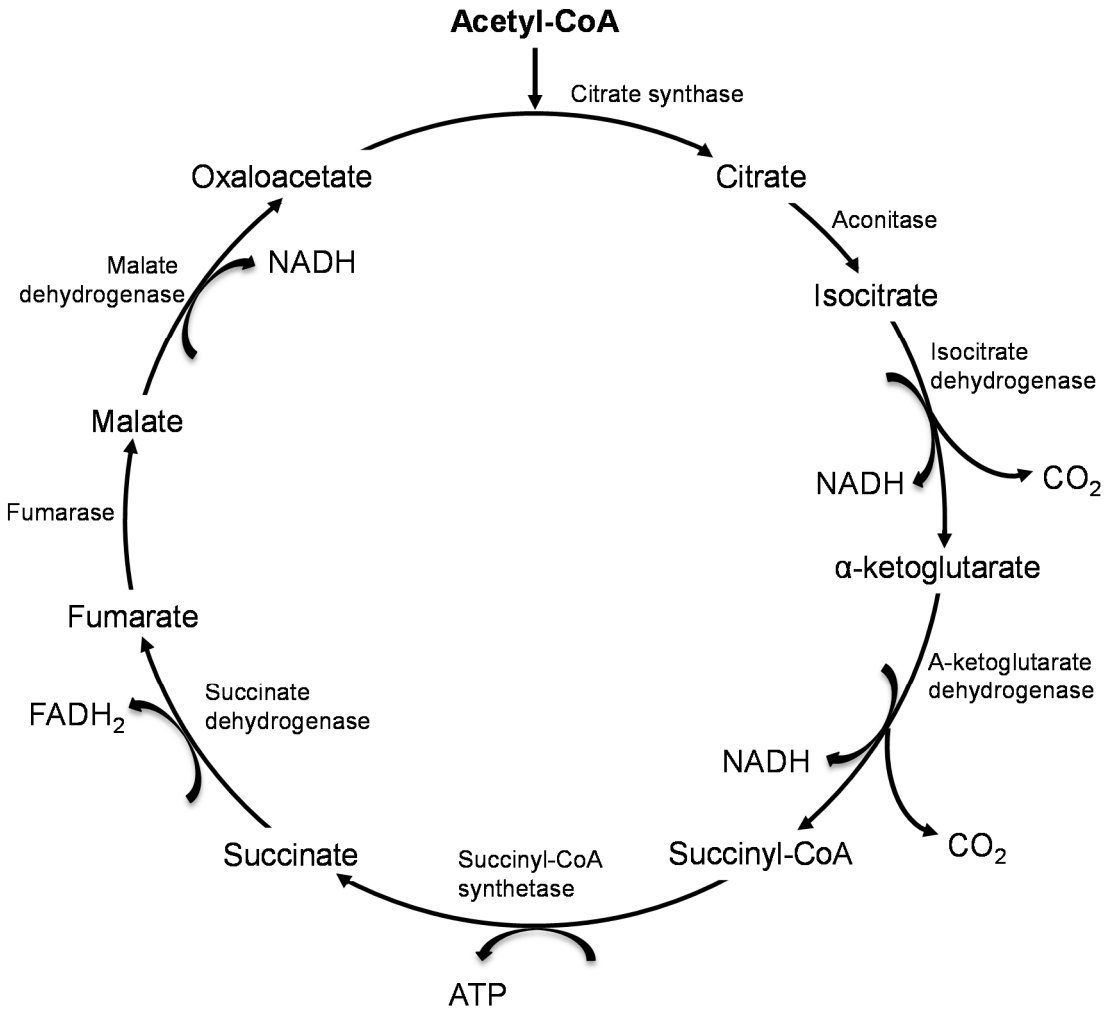

Figure 1.6. S**ummary of the TCA cycle.** Acetyl-CoA produced from glucose or fatty acids enters the cycle and is condensed to citrate by citrate synthase. Citrate is successively dehydrated and hydrated by aconitase enzyme and isocitrate is formed. Isocitrate undergoes an oxidative decarboxylation by isocitrate dehydrogenase, releases CO_2 and α-ketoglutarate is formed. Another oxidative decarboxylation occurs generating succinyl-CoA, which is converted to succinate by the action of succinyl-CoA synthetase. This latter reaction breaks a strong succinyl-CoA thioester bond releasing energy that is used for ATP production. Succinate is then dehydrogenated, donating 2 H^+ to FAD with fumarate and $FADH_2$ production. Fumarate is hydrated forming malate, which donates 1 H^+ to NAD^+ and is converted to oxaloacetate. In the presence of acetyl-CoA, oxaloacetate can re-start the cycle. At the end of a complete oxidation, a molecule of glucose (via glycolysis) yields a total of 30-32 ATP, whilst a molecule of palmitate produces a total of 108 ATP (149).

TCA: tricarboxylic acid; FAD: flavin adenine dinucleotide; NAD^+: oxidised nicotinamide adenine dinucleotide.

The TCA cycle is not only involved in catabolic but also in anabolic reactions, which produce biosynthesis precursors for many other pathways. Anaplerotic processes refill TCA intermediates to keep their concentrations stable. Pyruvate carboxylase reversibly catalysis the most relevant anaplerotic reaction, in which pyruvate receives a carbon from CO_2 and is converted into oxaloacetate at the expense of an ATP. Pyruvate carboxylase is tightly regulated by acetyl-CoA, being stimulated in the presence of acetyl-CoA surplus and inhibited in acetyl-CoA depletion. Concerning lipid metabolism, anaplerotic pathways provide precursors to *de novo* fatty acid synthesis (152). Thus, citrate produced from oxaloacetate and acetyl-CoA can be transformed in malonyl-CoA by action of citrate lyase and acetyl-CoA carboxylase. Malonyl-CoA is an important signalling of glucose and other nutrient oversupply being utilised for fatty acid synthesis or fatty acid elongation, and inhibiting fatty acid oxidation. Therefore, malonyl-CoA levels increase in conditions of high glucose supply, hyperinsulinaemia and physical inactivity and decrease in glucose depletion and physical activity. Hence, malonyl-CoA participates in the cross talk between glucose and fatty acid metabolism (153).

1.5.5 Glycogen synthesis

Excess glucose can be polymerised and stored as glycogen in nearly all animal tissues but it is particularly produced in skeletal muscles and the liver. Glycogen is a big branched polymer, with thousands of glucose molecules and one reducing end. Glycogen is packed in granules that contain the enzymes necessary to its metabolism (Figure 1.7 shows the reactions and enzymes involved in glycogen synthesis). When glucose blood levels are low, glycogen non-reducing end can be phosphorylated yielding glucose 1-phosphate that is transformed in glucose 6-phosphate and utilised in other metabolic pathways. The branches can also be cleaved by the debranching enzyme releasing free glucose. Glycogen synthesis is stimulated by insulin, whereas epinephrine and glucagon promote glycogen phosphorylation (154).

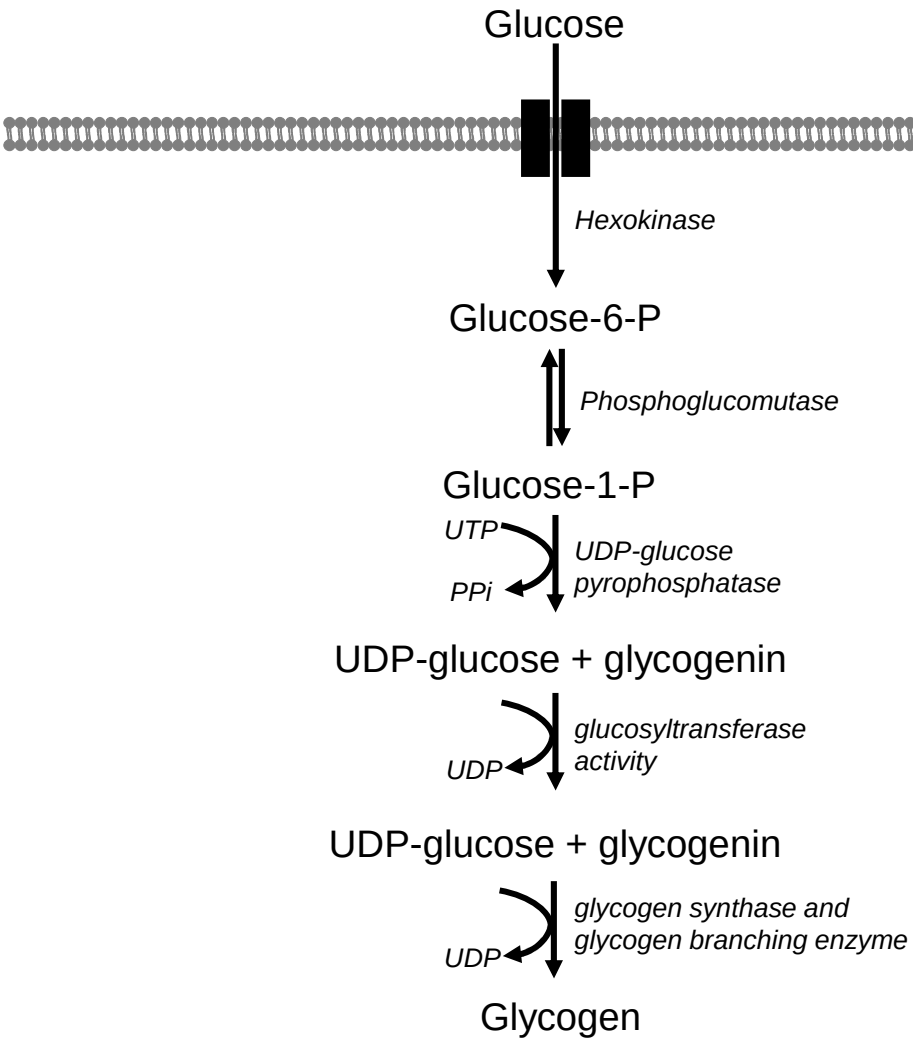

Figure 1.7. Glycogen synthesis. Glycogen synthesis begins with the conversion of glucose 6-phosphate to glucose 1- phosphate by phosphoglucomutase action. Glucose 1-phosphate is linked to an UDP molecule, which is a sugar nucleotide constituted by uridine and a glucosyl group. UDP-glucose then provides glucose residues to elongate the non-reducing end of a glycogen molecule, a transfer that is catalysed by glycogen synthase. However, the glycogen-branching enzyme is necessary to bind new glucose molecules to the branch points of glycogen. To initiate a glycogen molecule *de novo* the protein glycogenin acts as a primer and an enzyme, binding UDP-glucose to glycogenin itself. Subsequently, glycogen synthase will add new glucose molecules to lengthen the glycogen molecule (154, 155).

UDP: uridine diphosphate.

1.5.6 β-oxidation of saturated fatty acids

β-oxidation is the first step of fatty acid catabolism. In this pathway long-chain fatty acids are oxidised into acetyl-CoA that will enter the TCA cycle. Lipids such as TG are hydrolysed into free fatty acids and glycerol by the action of lipases such as LPL. Long free fatty acids (≥ 14 carbons) entering the cell must initially be activated to an acyl-CoA by the action of fatty acyl-CoA synthetase at the expense of ATP within the cytosol. The fatty acyl-CoA, however, need to be imported into the mitochondrial matrix for β-oxidation and this is via carnitine transport cycle. Fatty acyl-CoA is converted to fatty acyl carnitine by carnitine acyl-transferase 1 at the external mitochondrial membrane, is transported across the membrane by the carnitine translocating protein, and is converted back to fatty acyl-CoA at the inner mitochondrial membrane by carnitine acyl transferase 2. Subsequently, carnitine acyltransferase 2 moves the fatty acid acyl group from carnitine to an intramitochondrial coenzyme A, releasing free carnitine. Fatty acids are catabolized by consecutive losses of acetyl-CoA (2 carbons) during β-oxidation such that a 16-carbon palmitate molecule, for instance, will yield 8 acetyl-CoA molecules. Four reactions occur in each β-oxidation loop: (i) dehydrogenation of fatty acyl-CoA producing $FADH_2$ and enoyl-CoA; (ii) hydration of enoyl-CoA into β-hydroxyacyl-CoA; (iii) dehydrogenation of β-hydroxyacyl-CoA with production of NADH and β-ketoacyl-CoA; (iv) cleavage of the carboxy-terminal portion (with 2 carbons) from the fatty acid forming an acetyl-CoA molecule plus a thioester of fatty acid in a reaction catalysed by acyl-CoA acetyltransferase (thiolase) (156) (Figure 1.8).

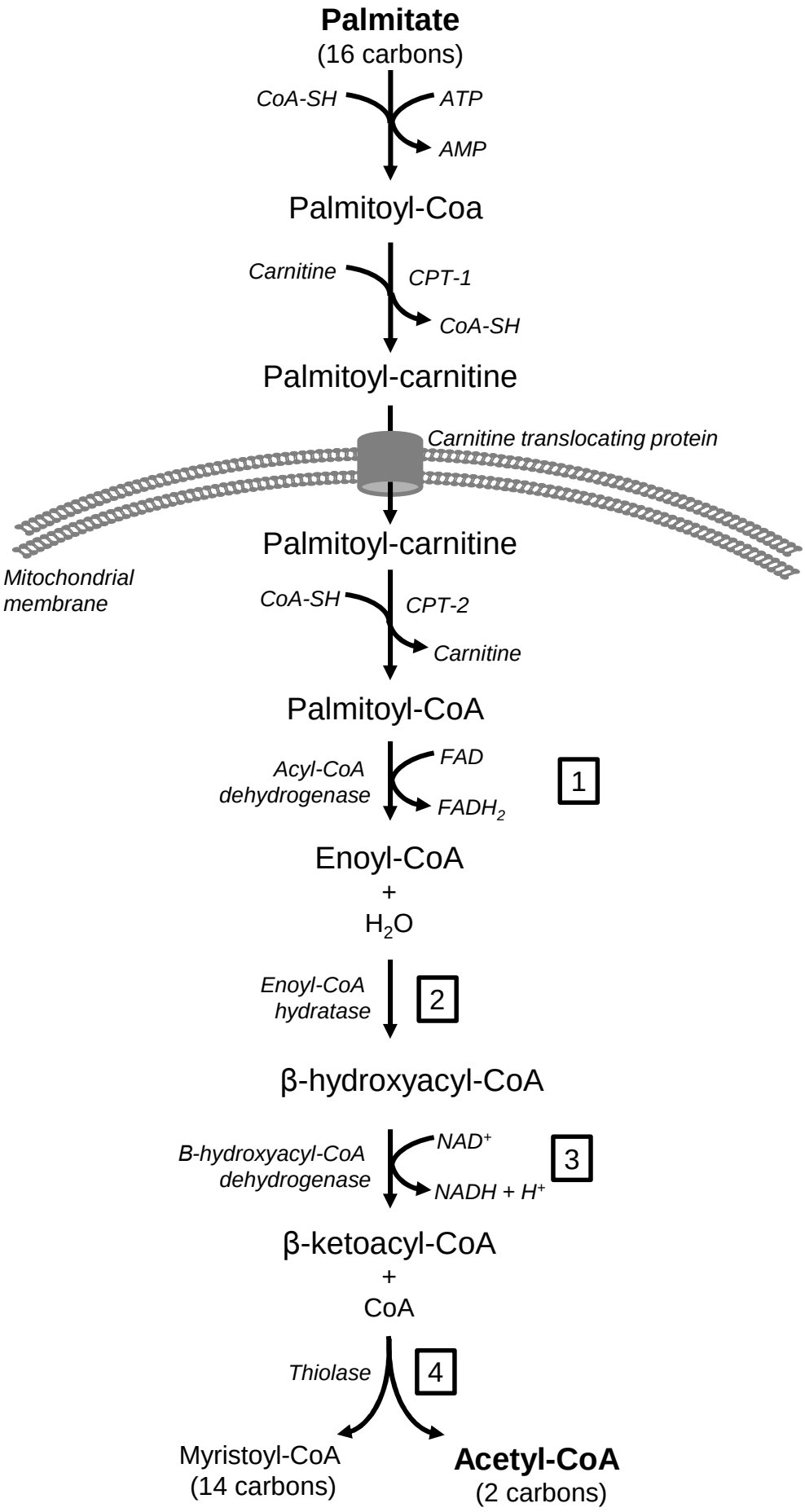
Palmitate
(16 carbons)
CoA-SH
ATP
AMP
Palmitoyl-Coa
Carnitine
CPT-1
CoA-SH
Palmitoyl-carnitine
Carnitine translocating protein
Palmitoyl-carnitine
Mitochondrial membrane
CoA-SH
CPT-2
Carnitine
Palmitoyl-CoA
Acyl-CoA dehydrogenase
FAD
FADH2
1
Enoyl-CoA
+
H2O
Enoyl-CoA hydratase
2
β-hydroxyacyl-CoA
B-hydroxyacyl-CoA dehydrogenase
NAD+
NADH + H+
3
β-ketoacyl-CoA
+
CoA
Thiolase
4
Myristoyl-CoA
(14 carbons)
Acetyl-CoA
(2 carbons)

Figure 1.8. β-oxidation of saturated fatty acid (e.g. palmitate). Following access to the mitochondrial matrix via the carnitine transport cycle, β-oxidation involves the repetition of 4 enzymatic reactions. The aim of each passage is to remove 2 carbons from the fatty acid producing an acetyl-CoA group. Complete β-oxidation of palmitate yields 8 acetyl-CoA groups. 1. Fatty acyl-CoA is dehydrogenated producing $FADH_2$ and enoyl-CoA. 2. Enoyl-CoA is converted to β-hydroxyacyl-CoA through hydration. 3. β-hydroxyacyl-CoA loses 2 H^+ producing NADH and β-ketoacyl-CoA. 4. Acyl-CoA acetyltransferase (thiolase) catalyses the reaction between β-ketoacyl-CoA and a CoA group. As a result, the fatty acid carboxy-terminal portion with 2 carbons is cleaved forming an acetyl-CoA molecule plus a thioester of fatty acid with 14 carbons (156).
CPT: carnitine palmitoyltransferase 1; FAD: flavin adenine dinucleotide.

1.5.7 Ketone bodies production

Ketone bodies, i.e. β-hydroxybutyrate, acetone and acetoacetate, are synthesized in the liver. β-hydroxybutyrate and acetoacetate can be used as an energy source by extra-hepatic tissues. The rate of ketone body production is low in metabolic healthy and well-nourished people. However, in decompensated diabetes or starvation, ketone body production is increased due to the accumulation of acetyl-CoA secondary to the depletion of TCA cycle intermediates by exaggerate gluconeogenesis. Thus, acetyl-CoA is redirected from β-oxidation to ketone body production (Figure 1.9). After hepatic synthesis, β-hydroxybutyrate is released into the blood circulation and can be oxidised to acetoacetate in other tissues (157) (Figure 1.10).

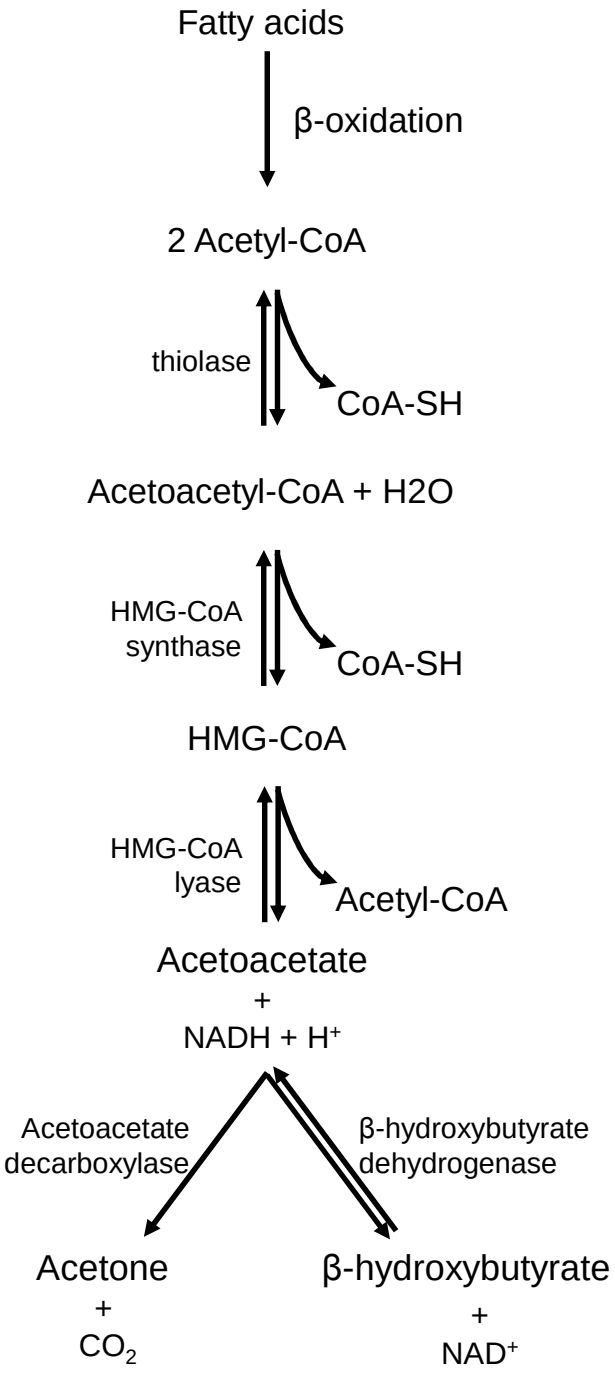

Figure 1.9. Ketone body formation. The linkage of two molecules of acetyl-CoA catalysed by a thiolase is the first step in ketone body synthesis. Acetoacetyl is formed and condensed to a β-hydroxy-β-methylglutaryl-CoA (HMG-CoA) through the action of the enzyme HMG-CoA synthase. HMG-CoA lyase, which is present in the mitochondrial matrix, cleaves HMG-CoA molecule generating acetyl-CoA and free acetoacetate. The latter is reduced to β-hydroxybutyrate by a β-hydroxybutyrate dehydrogenase in a reversible reaction. Acetoacetate can also lose a CO_2 molecule and produce acetone, a reaction catalysed by an acetoacetate decarboxylase (157).

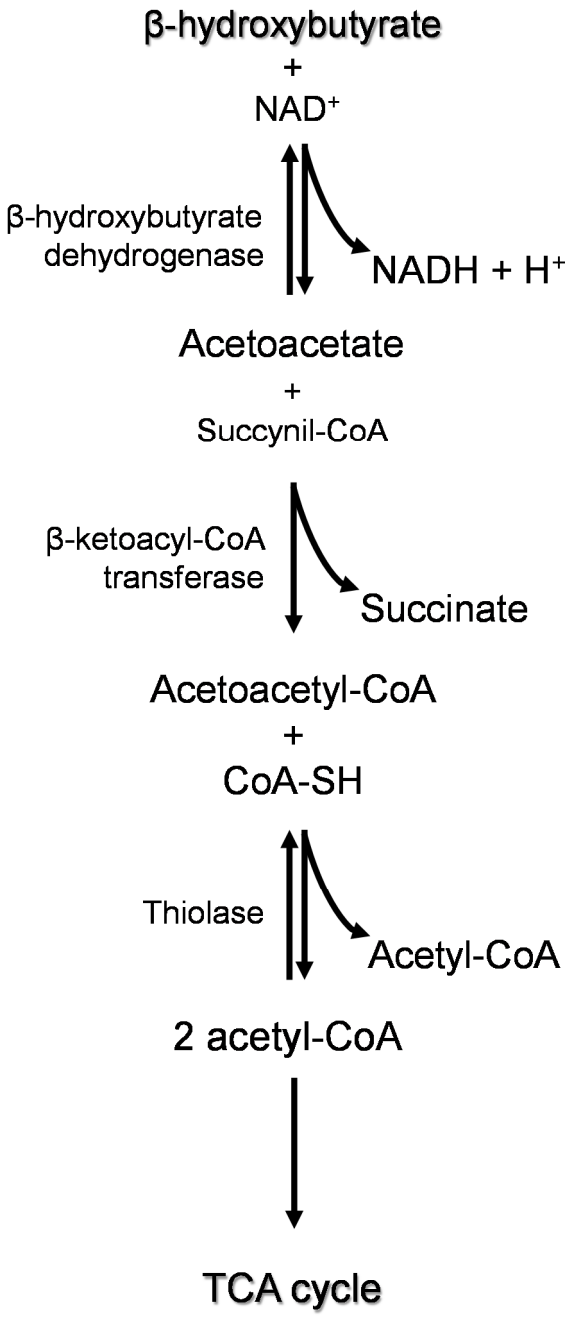

Figure 1.10. **Ketone body utilisation as energy.** β-hydroxybutyrate produced in the liver is released into the blood circulation and oxidised to acetoacetate in other tissues. Succinyl-CoA donates a CoA to acetoacetate, which is transformed in acetoacetyl-CoA by a β-ketoacyl-CoA transferase. Then, acetoacetyl-CoA is cleaved by a thiolase in 2 molecules of acetyl-CoA restarting the TCA cycle.

TCA: tricarboxylic acid.

1.6 Normal structure of the placenta

1.6.1 Macroscopic anatomy of the placenta

A normal term placenta has a discoid shape that can be symmetrically or eccentrically round. It measures between 2 to 4 cm in thickness, around 20 to 22 cm in diameter and weighs a mean of 470 g (158).

The basal plate represents the maternal surface of the placenta, which is attached to the uterus during the gestation (Figure 1.11). The parenchyma has a spongy and soft consistency. The basal plate is usually maroon or deep red and is divided into 10 to 40 lobes (cotyledons). The outer surface of the basal plate is occupied by the decidua that is the pregnancy endometrium. The decidua that underlies the basal plate, being also the implantation site of the embryo in the uterus, is called the decidua basalis. The decidua parietalis covers the remainder of the uterine cavity, and the decidua capsularis extends around the chorion in the first trimester. After 16 weeks of gestation, the growing fetus drives the decidua capsularis in contact with the decidua parietalis. In consequence, both deciduae fuse and the uterine cavity disappears (158-160).

The fetal side of the placenta-the chorionic plate-is covered by the translucent, slightly grey and smooth amnion membrane (Figure 1.12). At the edge of the placental disc, the chorionic and basal plates converge and form the chorioamniotic membrane, constituted by the amnion attached to the smooth chorion or chorion laeve. The umbilical cord inserts into the chorionic plate, usually centrally or slightly eccentrically, and contains 2 arteries and 1 vein. Rising from the fetus, the umbilical arteries progressively branch and reduce their diameter until they form the terminal villi. The role of the terminal villi is to deliver fetal blood to the villous trees. The umbilical vein, in turn, is formed from the junction of veins of the villous trees and runs underneath the umbilical arteries (Figure 1.12). Each cotyledon is supplied by one to four villous trees emerging from the chorionic plate.

Cotyledon villous trees are immersed in maternal blood delivered inside the intervillous space by spiral arteries. This contact between the villous trees and maternal blood allows for the exchange of gases, hormones and nutrients between mother and the fetus. Maternal blood in the intervillous space is drained through the utero-placental veins, the openings of which are on the floor of the intervillous space (158, 159, 161) (Figure 1.13).

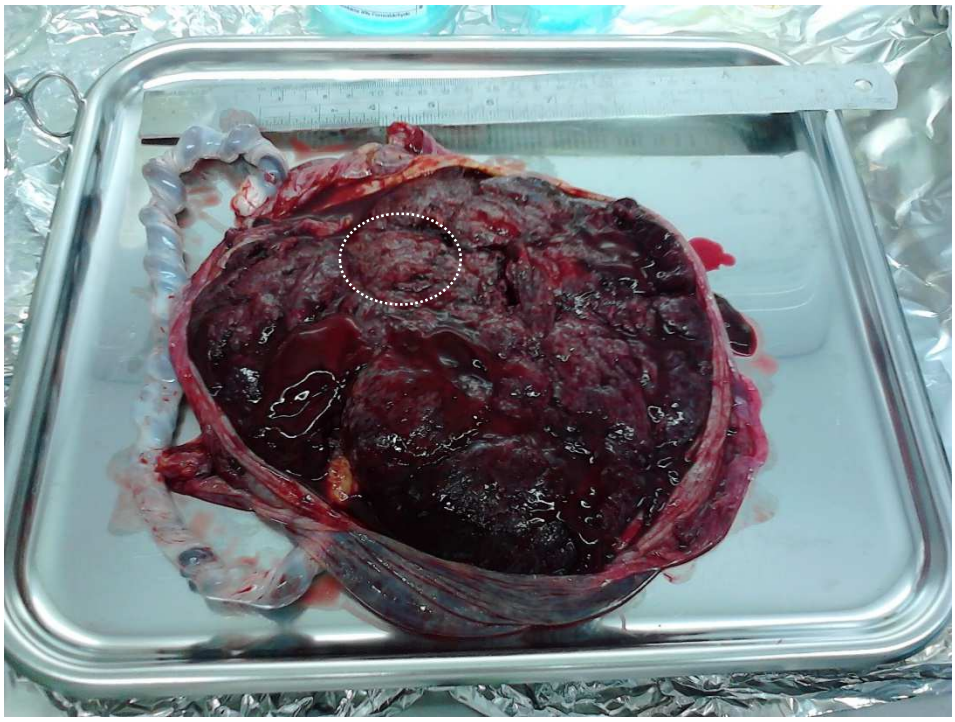

Figure 1.11. Photograph of a delivered placenta showing the maternal side. The basal plate of the placenta is a maroon/reddish, soft and spongelike structure. It has the cotyledons, which are supplied by vessels from the villous trees and represent the fetal lobules. The cotyledons cause irregular invaginations in the maternal decidua. The dotted line surrounds a cotyledon.

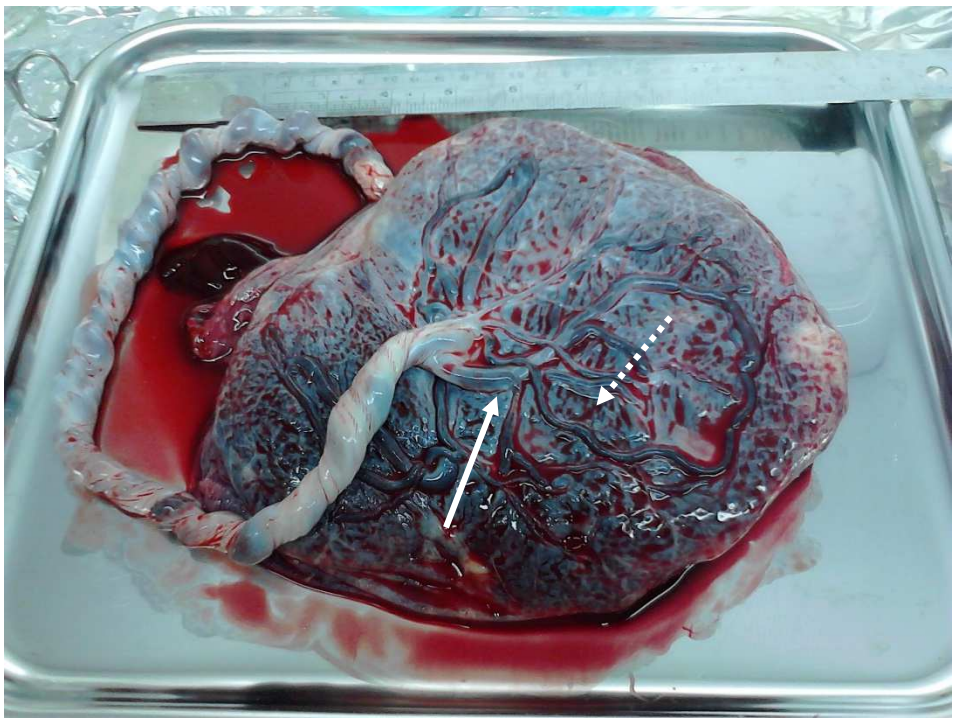

Figure 1.12. Photograph of a delivered placenta showing the fetal side. The chorionic plate of the placenta is covered by the amnion and chorion. The umbilical cord usually centrally or eccentrically inserts into the chorionic plate. Solid arrow: umbilical vein branch; dashed arrow: umbilical artery branch.

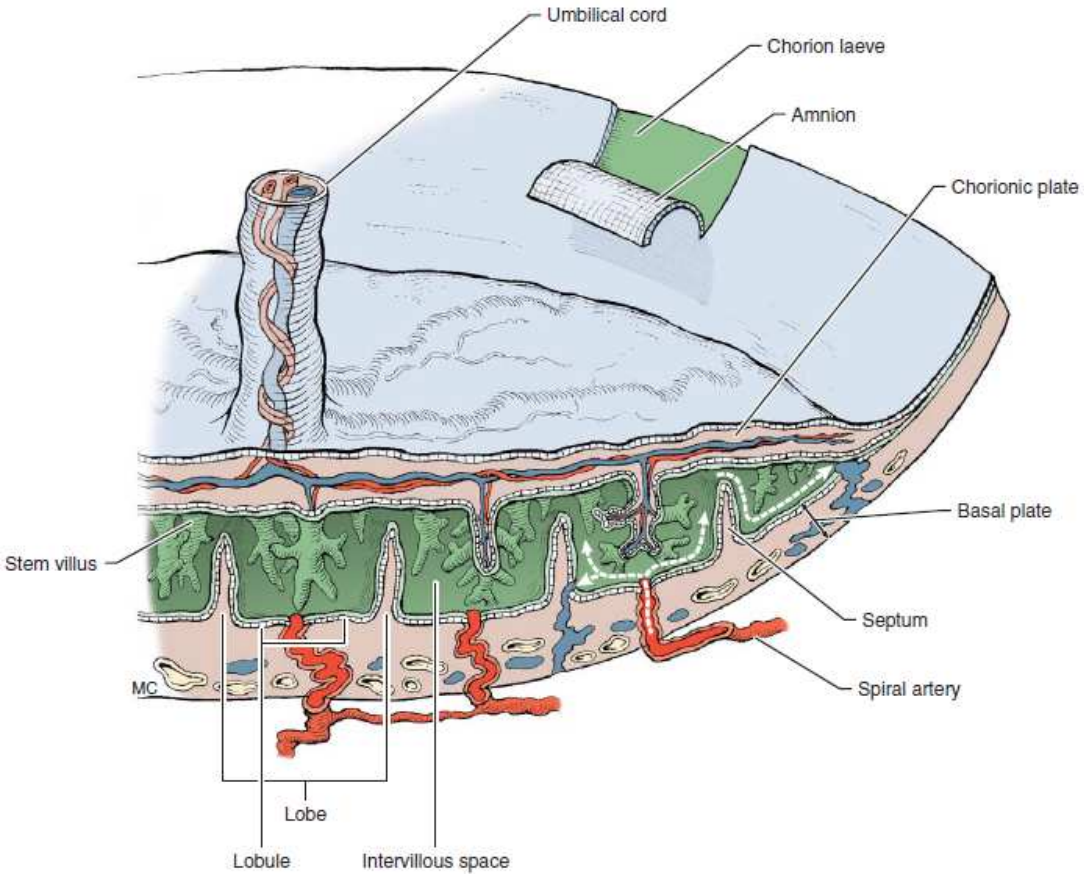

Figure 1.13. Cross section of a term placental. From the uterus, the spiral arteries deliver maternal blood into the intervillous space. Blood from the intervillous space, in turn, is collected by the utero-placental veins. The umbilical cord, which is covered by the chorion and the amnion, has 2 arteries and 1 vein. The umbilical arteries successively branch and reduce in diameter up to the terminal villi, where fetal blood is delivered to the chorionic villi. Conversely, the umbilical vein is constituted by the union of chorionic veins into larger vessels and supply the fetus with blood after exchanges with maternal blood. This figure was taken from Burton *et al.* (162) with kind permission of Elsevier Health Sciences.

1.6.2 Microscopic anatomy of the placenta

The basal plate is constituted by decidual stromal cells, immune cells (e.g. macrophages, T-lymphocytes and natural killer cells), extravillous trophoblasts, blood clots, extracellular matrix and fibrinoid. On the chorionic plate, the fetal membranes possess the amnion, which is composed by (i) a single layer of epithelium with a subjacent basement membrane attached to an avascular connective tissue layer of amniotic mesenchyme; (ii) a layer of extravillous trophoblast; and (iii) the decidua capsularis. In the villi, the basement membrane separates the villous trophoblast epithelium from the mesenchymal core, which contains fibroblasts, myofibroblasts, endothelial cells, erythrocytes, smooth muscle cells and macrophages (158, 160).

As described, the vessels arising from the chorionic plate progressively branch until they supply the capillaries of the villi. A minority of villi contact the basal plate forming anchoring villi, in which trophoblastic cell columns are found. The remaining villi containing the fetal vessels float within the maternal blood of the intervillous space. These free villi are classified as mesenchymal villi, immature intermediate villi, stem villi, mature intermediate villi and terminal villi depending on stromal and vessel features, the diameter and the time during gestation that they are established. Because mesenchymal villi and immature intermediate villi are scarce in the term placenta and stem villi are mostly involved in the mechanical support to the villous (160), only mature intermediate villi and terminal villi are discussed here.

From around 20 weeks of gestational age, the placenta starts forming mature intermediate villi that are abundant at term. Mature intermediate villi are long and composed by a loose stroma with small vessels and capillaries. Terminal villi emerge from mature intermediate villi and are at the end of the villous tree with vast participation in the exchanges between mother and fetus. Because of this important function, terminal villi show numerous capillaries and capillary-derived sinusoids that enlarge the exchange surface. The

structure established by the basement membrane, the syncytiotrophoblast and the fetal endothelium is called the vasculo-syncytial membrane (Figure 1.14). The exchanges between mother blood in the intervillous space and fetal blood in the small vessels of villi are optimised by the abundance of capillaries together with the very thin maternal-fetal barrier in terminal villi (160, 162).

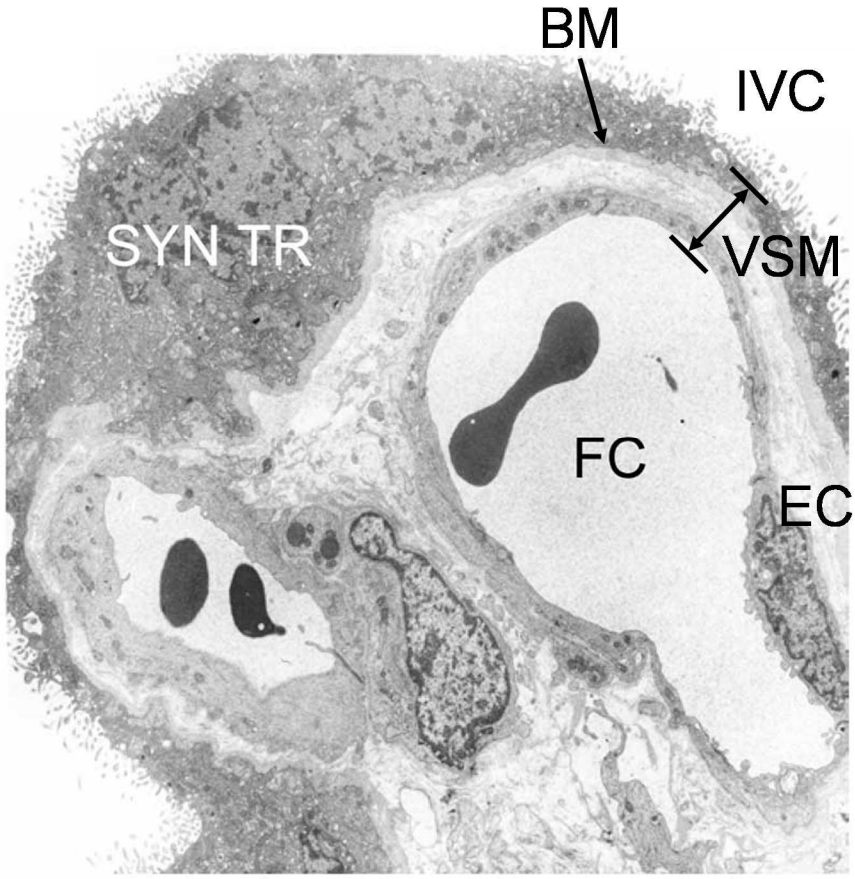

Figure 1.14 Electron microscopy of a placental terminal villous showing the maternal-fetal barrier. Terminal villi are at the end of the villous tree and participate in the placental exchanges between mother and the fetus. They are composed by capillaries, sinusoids, cyto and syncytiotrophoblasts, stroma, mesenchymal cells and the basement membrane. The vasculo-syncytial membrane (VSM) is a thin structure formed by the basement membrane (BM), the syncytiotrophoblast (SYN TR) and the fetal endothelial cell (EC). The exchanges between maternal blood from the intervillous space (IVS) and blood from the fetal capillary (FC) occur across the VSM. This figure was taken from Carter *et al.* (163).

Among the cells present in terminal villi, cytotrophoblasts and the syncytiotrophoblast are the focus of interest in this thesis. In term placenta terminal villi, single cytotrophoblasts are found under the syncytiotrophoblast layer and both cyto and syncytiotrophoblasts rest on the trophoblast basement membrane. The main function of villous cytotrophoblasts, which are mononucleated epithelial cells, is to divide and differentiate to fuse into the syncytiotrophoblast. Hence, villous cytotrophoblasts act as a pool of immature cells that renew the syncytiotrophoblast. In addition, villous cytotrophoblasts can also be converted into extravillous cytotrophoblasts if the contact with the syncytiotrophoblast or with the basement membrane is lost. Undifferentiated cytotrophoblasts are simple and cuboid cells, with few organelles and a low metabolic activity. To fuse with the syncytiotrophoblast, undifferentiated cytotrophoblasts have to be transformed into intermediate cytotrophoblasts, which have a very active metabolism and possess more organelles, in particular mitochondria, ribosomes and rough endoplasmic reticulum. The intermediate cytotrophoblasts are then converted into differentiated cytotrophoblasts that have an even higher quantity of organelles, proteins and nucleic material. Finally, the differentiated cytotrophoblasts fuse with the syncytiotrophoblast becoming part of this large layer (160, 162).

The syncytiotrophoblast is a multinucleated and uninterrupted layer that covers all villous tree surfaces. This layer has an apical microvillous membrane with a brush border bathed into maternal blood and a basal membrane in contact with the cytotrophoblasts or the basement membrane. In contrast with the cytotrophoblasts, the syncytiotrophoblast layer is a completely differentiated cellular structure without mitotic activity. Because the syncytiotrophoblast is responsible for many functions (e.g. synthesis of hormones, cytokines and adipokines, and the transport and metabolism of nutrients), it displays various organelles such as mitochondria, golgi bodies, pinocytotic vesicles, phagosomes, lysosomes, and secretory droplets. The syncytiotrophoblast is renewed by the

incorporation of cytotrophoblasts, as explained before, whilst the senescent nuclei are packed, surrounded by cellular membrane and released into the maternal circulation as syncytial knots (159, 162).

1.7 Placental nutrient transport and metabolism

The placenta transports and metabolises glucose, fatty acids, and amino acids. Glucose is the main source of energy for the placenta and the fetus, and it is readily transported across the placenta via facilitated transport (164) mostly dependent on the maternal-fetal gradient (165, 166). Lipids cross the placenta with more difficulty than glucose involving complex transport processes. In addition to their function as source of energy, they are essential for the synthesis of cellular membranes and hormones by the placenta and fetus, especially for the fetal nervous system, adipose tissue and feto-placental steroid production (33, 166, 167). Amino acids are transported by the placenta to the fetus via active and facilitated transport and are utilized for protein synthesis, metabolism into other substrates and production of energy (168).

It is also worthy of note that the fetus is not a passive agent in its intrauterine growth, as it seems to regulate the delivery of nutrients by signalling the placenta. For example insulin, a potent stimulant of anabolism and cellular growth (169), is produced by the fetal pancreas in response to the maternal supply of nutrients, in particular glucose, but also fatty acids and amino acids (169). While in early pregnancy, maternal insulin may have a role in placental growth from the maternal side of the placenta, fetal insulin, acting on the fetal side (endothelial cells) of the placenta, is thought to be more dominant later in pregnancy (170). Therefore, both the maternal metabolic milieu and nutrient supply, prominently in early pregnancy, and fetal production of metabolic hormones such as insulin, insulin growth factors, and leptin later in pregnancy, can affect placental nutrient transport and metabolism (171, 172). Thus, in response to the maternal metabolic

environment, the fetus can also respond modulating its own growth by regulation of placental function and nutrient delivery among other mechanisms (171, 172). In the presence of obesity and/or diabetes during the pregnancy, nutrient oversupply can stimulate fetal hyperinsulinaemia leading to increased fetal aerobic metabolism, higher glucose uptake into fetal tissues and stimulated adipogenesis (169).

1.7.1 Glucose transport and metabolism

Both the placenta and the fetus largely consume glucose for energy. Although the fetal liver contains most enzymes necessary for gluconeogenesis, this pathway is insignificant during intrauterine life (173). Consequently, the fetus relies on placental glucose transfer from the maternal circulation across the syncytiotrophoblast and endothelial cells. Glucose flux through the placenta is determined by the maternal-to-fetal glucose gradient, density and kinetics of glucose carriers, glucose use by the placenta, uterine-placental and umbilical-placental blood flow and the thickness of the maternal-fetal barrier (166). Non-carrier mediated diffusion is responsible for just a small fraction of glucose transport across the syncytiotrophoblast microvillous membrane (174, 175). Nevertheless, considerable rates of glucose diffusion have been demonstrated in placental perfusion studies (165, 176, 177).

Of the facilitative glucose transporters, GLUT1(146), 3 (178), 4 (179), 9 (143), 10 (180), 11 (181) and 12 (144) have been detected in human placentas. Among them, the most widespread glucose transporter is GLUT1. As previously discussed, GLUT1 is coupled with a hexokinase, which is highly active in the placenta (182). The function of GLUT1 and hexokinase 1 is independent of insulin (183), but GLUT1 expression in the placenta can be modulated by insulin and/or hyperglycaemia (184-186). GLUT1 is expressed in cytotrophoblasts, stromal cells, vascular smooth muscle, fetal endothelial cells (174), with the most dense expression in the syncytiotrophoblasts (146, 187). GLUT1 protein expression and transport activity increase in the second trimester of pregnancy (187)

probably in response to a much higher fetal glucose requirement associated with fast intrauterine growth. Accordingly, term trophoblast homogenates present much higher abundance of GLUT1 protein than first trimester trophoblast homogenates (179). In the syncytiotrophoblasts, both basal and microvillous membranes show GLUT1 expression. In term trophoblasts, GLUT1 is asymmetrically expressed with higher expression in the syncytiotrophoblast microvillous membrane than in the basal membrane, leading to greater glucose transport rates through the apical membrane (187, 188), although there are also descriptions of symmetric glucose transport across the syncytiotrophoblast membranes (189). GLUT3 is a high affinity glucose transporter protein that is expressed in the extravillous trophoblast, villous cytotrophoblast, endothelial and stromal cells (178), and absent in the syncytiotrophoblast (178). In term placentas, endothelial cells present the highest expression of GLUT3 (178). GLUT4, which is insulin-responsive, has been identified in the syncytiotrophoblast cytosol from early pregnancy placentas (179), although not by all authors (190). At term, GLUT4 has a weaker expression (179) and is particularly found in villous stromal cells (191). GLUT4 function in pregnancy is not completely clear yet, and it may be implicated in insulin-stimulated glucose uptake that has been observed in first trimester, but not term, placental villous fragments (179). Overall, GLUT3 and GLUT4 are biologically more relevant in early pregnancy than GLUT1, whilst GLUT1 and GLUT3 seem to be the most important glucose transporters of the maternal-fetal barrier at term, in syncytiotrophoblasts and endothelial cells, respectively. However, glucose transport through GLUT1 and GLUT3 has also been implicated in placental angiogenesis and implantation processes and in the metabolism of decidual leukocytes (190).

Placental glucose uptake shows a strong positive relation with the available glucose supply (176, 192), and appears to be saturable at supra-physiological maternal glucose levels (165, 193, 194), which shows the high capacity of the placental glucose transport

system. This efficient glucose uptake has been demonstrated in multiple studies over the past decades. Using microvillous preparations, the K*m* for 3-O-methylglucose transport was 31 ± 13 mM with a *Vmax* of 7.2 μmol/minute/mg protein (175). Also, the maximal placental glucose uptake rate in perfused placentas, assessed over a maternal perfusate glucose range from 3 to 53 mM, corrected for simple glucose diffusion, was 1.6 μmol/minute/g (165). This rate of uptake was measured at maternal perfusate glucose concentrations of 20 mM and higher (165).

Glucose utilisation by placental metabolism (total glucose uptake minus glucose transfer to the fetus), as measured in placental perfusion studies, also was shown to correlate with the maternal perfusate glucose levels up to 17-22 mM (165). Under normal circumstances, about 50% of glucose taken up from the maternal circulation by the placenta has been estimated to be transferred to the fetus (165). From the remaining 50% of glucose uptake, about 40% has been estimated to be metabolised by the placenta and released as lactate, about 20-25% undergoes oxidative metabolism with the other 35-40% assumed to be metabolised in other pathways (165, 195). Considering that glycolysis into lactate yields about 16 times less ATP than complete glucose oxidation (refer to section 1.5.1 of this chapter), the low rates of placental glucose oxidation possible necessitates, for energy requirements, the high rates of glucose uptake and lactate production. However, against this is the finding that both placental glucose oxidation (165) and lactate release have not been shown to relate to placental glucose utilisation (196). In placental perfusion studies, glucose oxidation and lactate production have been shown to be maximal at relatively low maternal glucose perfusate concentrations (165, 176).

Lactate has also been the main glucose metabolic product in other placental experimental models, corresponding to around 70% of glucose metabolism in placental fragments (197) and in isolated trophoblasts (148). Nonetheless, in comparison with placental perfusion studies, much lower fractions of glucose metabolism into glucose oxidation have been

reported in both early pregnancy (2.4%) and term placental fragment cultures (<2%) (197), as well as in primary trophoblast cultures from term placenta (1.8-3%) (148).

Interestingly, total glucose uptake was reduced in placentas from GDM mothers (176) and the transplacental glucose flux into the fetal circulation was similar (198) or reduced (176) in comparison with placentas from healthy mothers. Also, maternal GDM independent of insulin therapy led to a lower placental glucose utilisation than in normal controls (198). In addition, early studies found that pyruvate kinase activity, which is insulin-responsive, was increased in GDM placentas in comparison with controls (199). As neonates born to those GDM mothers were significantly heavier (199), increases in pyruvate kinase function could lead to higher fetal supply of pyruvate derived products including lactate and fatty acids. Nevertheless, in placental perfusion experiments in which the newborns' weights were matched, the lactate release into maternal and fetal circulations was reduced in placentas from GDM pregnancies on diet in comparison with normal controls (176). Whether these differences in placental glucose metabolism participate in a placental adaptation to prevent fetal excessive growth is undetermined.

There is less known about glucose utilisation in isolated trophoblasts in response to increasing culture glucose concentrations. A previous study from our group showed that glycolysis measured by a radioactive tracer method, as described in Chapter 3, did not increase with increasing media glucose concentrations above physiological levels (200). Indeed, glycolysis rates were near maximal at 4 mM glucose and maximum at media glucose concentrations of 8 mM (200). Thus, it is probable that isolated trophoblasts will not increase glucose oxidation or lactate synthesis at high glucose media concentrations, but this still needs confirmation.

As discussed in section 1.5.1, glucose 6-phosphate can be oxidised via the pentose phosphate pathway, which produces precursors for the synthesis of coenzymes, nucleotides, RNA and DNA (ribose 5-phosphate) and NADPH for reducing reactions

especially involved in the biosynthesis of fatty acids and cholesterol (149). Hence, the shift of glucose to this pathway occurs in organs with intense growth or with high biosynthesis demands (149). Ultimately, the NADPH supply also participates in anti-oxidative processes protecting the cells against excess free oxygen radicals (201). Only a few authors have investigated the pentose phosphate pathway in the human placenta. Glucose oxidation via the TCA cycle and pentose phosphate pathway, measured through the ratio of $^{14}CO_2$ production from [1-^{14}C]-glucose and [6-^{14}C]-glucose, have suggested that oxidation via the TCA cycle is higher than via the pentose phosphate pathway in term placental slices, whereas in younger placentas (6-20 weeks) oxidation by the pentose phosphate pathway is greater (202). Different proportions of glucose utilisation via glycolysis and the TCA cycle or the pentose phosphate pathway were found in another research study, but the pentose phosphate pathway also accounted for higher portions of glucose utilisation (10%) in early pregnancy (6-10 weeks) compared to term placentas (5%) (197). In human trophoblast cultures from term placentas, the oxidative pentose phosphate pathway represented less than 1% of the total glucose metabolised (148). Furthermore, the activity of this pathway was greater soon after trophoblast isolation than in trophoblasts established in culture for one to three days with increasing differentiation into syncytiotrophoblasts (148). It is unknown whether glucose partitioning into the pentose phosphate glucose pathway increases with increasing glucose supply.

Although the placenta expresses enzymes implicated in gluconeogenesis (e.g. phosphoenolpyruvate carboxykinase, alanine and aspartate aminotransferase) (203), the key gluconeogenic enzyme glucose 6-phosphatase (G6Pase) found in the placenta has more kinetic similarities with the brain G6Pase isoform than with the hepatic isoform (203). Whether the human placenta is capable of gluconeogenesis and the precise function of placental G6Pase are unclear.

The placenta expresses many enzymes and proteins involved in glycogen turn-over including glycogen synthase (204), glycogenin (178), glycogen branching enzyme, glycogen debranching enzyme (205) and glycogen phosphorylase (206). Nonetheless, placental glycogen metabolism does not seem to be regulated by insulin as observed in other tissues such as the liver and skeletal muscle (207). In these latter tissues, insulin stimulates glycogen deposition and inhibits glycogen hydrolysis (207). In the placenta, glycogen turn-over is mostly controlled by intracellular substrate availability, therefore the levels of intracellular glucose and glucose 6-phosphate can modulate the enzymes implicated in placental glycogen synthesis and degradation (182, 207). Placental glycogen can be stored in fetal endothelial cells, pericytes, cyto- and syncytiotrophoblasts, stromal cells, smooth myocytes (208) and in the amnion epithelium (207). It is speculated that glucose produced from placental glycogenolysis is mostly used by the placenta for its own metabolic needs, although some could be metabolised into other products such as lactate or be transferred to the fetus with requirement of glucose 6-phosphatase (207). In addition, in the presence of maternal hyperglycaemia, excess glucose could be buffered by the placenta as a "defensive reaction" against fetal glucotoxicity.

In normal pregnancies, the amount of placental glycogen reduces as the pregnancy progresses (207). Glycogen accumulation represented 4.8% and 1.3% of glucose metabolism in placental slices from early pregnancy and term placentas, respectively (197). Glucose flux into glycogen synthesis measured by ^{14}C incorporation from [1-^{14}C]-glucose or [6-^{14}C]-glucose corresponded to < 1% of total glucose metabolism in isolated human cytotrophoblasts in short-term incubations (148). Also, ^{14}C incorporation into glycogen halved in 1-3 days in comparison to freshly isolated trophoblasts, suggesting that glycogenesis is higher in more undifferentiated cells (148).

Contrary to what occurs in normal pregnancies, glycogen levels increase in term placentas affected by diabetes (182), although this finding is not universal and seems to depend on diabetes type or therapy (208, 209). Furthermore, gene expression profiles in GDM have indicated an increased placental glycogen turn-over, as protein and enzymes implicated in both glycogenesis (glycogenin and glycogen branching enzyme) and glycogenolysis (glycogen debranching enzyme) were overexpressed in GDM placentas (205).

Primary human trophoblasts raised glycogen accumulation in cultures in media at 10 mM glucose in comparison with 1 mM glucose concentrations assessed by electron microscopy (200). However, total glycogen content was unchanged when cytotrophoblasts were cultured in glucose concentrations ranging from 5.5 to 28 mM in another study (210). Of note, trophoblast glycogen content increased for 2 h after replacing the culture media and was 1.5-fold higher from 2 to 5 h following the media replacement (210). It would be helpful to know more about the dynamics of this glycogen increase post-media refreshment, according to the media glucose concentration and whether the cells are from normal or diabetic pregnancies. Moreover, Desoye has proposed that fetal hyperinsulinaemia, in response to maternal obesity and/or diabetes, is the major factor driving the excess glycogen accumulation in the affected placenta (169). This explanation is supported by the lack of relationship between placental insulin receptors and serum plasma insulin from mothers with or without diabetes (209), the absence of glycogen content increment in cells from the maternal side of the placenta (trophoblasts) in the presence of high concentrations of glucose and insulin (210), the evidences of a preferential glycogen accumulation in the placental cells in contact with fetal blood (endothelial fetal cells and pericytes) as well as the primary location of glycogenin and GLUT3 in the endothelial cells at term (178).

1.7.1.1 Effects of NEFA on placental glucose metabolism

Interactions between fatty acid and glucose metabolism have for long been described to occur in muscle and adipose tissue and particular reference is often made with respect to this interaction to the pathogenesis of insulin resistance in T2DM (211). Glucose and fatty acid compete for their oxidation in muscle and the utilisation of one nutrient directly inhibits the use of the other even without hormonal action, according to the Randle cycle hypothesis (212). Fatty acids can affect glucose metabolism at many points: (i) inhibition of glucose transport and hexokinase action; (ii) inhibition of phosphofructokinase-1 (a regulatory enzyme of glycolysis-refer to section 1.5.2 of this chapter); and (iii) inhibition of pyruvate dehydrogenase, which catalyses the conversion of pyruvate into acetyl-CoA to be oxidised in the TCA cycle (212). There are scarce data on the effects of fatty acids on human placental glucose metabolism. In placental rat slices, oleate at high dose (0.8 mM) did not change glucose uptake, oxidation nor lactate release, but it slightly increased (by 0.8%) glucose incorporation into glycogen (182). The effects of NEFA on glucose metabolism is still not defined in human placenta, notably the effects of different types of NEFA such as the saturated NEFAs palmitate and stearate. Thus, the study of NEFA effects on glucose metabolism in the placenta, particularly in trophoblast and endothelial cell cultures, could help to clarify the pathophysiology of the gestational complications that increase more frequently in obesity/diabetes.

1.7.2 Lipid transport and metabolism

Maternal TG are the primary lipid source to the fetus, but it must be hydrolyzed by placental LPL into NEFA and glycerol to be taken up by the placenta and transferred to the fetus (213). LPL protein has been identified in the syncytiotrophoblast and villous cytotrophoblasts in early pregnancy and only in smooth muscle cells of vascular vessels in term placentas. In addition, LPL mRNA greatly increased at term (214). The placenta

also expresses endothelial lipases (EL), which contain a predominant phospholipase function with preferably hydrolysis of HDL-C-derived phospholipids, and a minor role in TG hydrolysis (215). Comparing with LPL, EL mRNA expression was higher in both term and first trimester placentas (214). At term, EL mRNA expression in trophoblasts decreased, whereas EL mRNA of whole placenta increased being mostly expressed in endothelial cells from fetal vessels (214). This indicates a rearrangement of EL from the trophoblast early in pregnancy to the endothelial fetal cells as gestation advances possibly to better supply the fetal developmental demands (214).

The placenta transports NEFA via passive diffusion or through saturable transport processes dependent on trophoblast proteins (216, 217). Hence, trophoblasts can take up fatty acids using plasma membrane proteins, including fatty acid transport proteins (FATPs), fatty acid binding protein plasma membrane (FABPpm), placental membrane fatty acid binding protein (p-FABPpm) and fatty acid translocase (FAT/CD36) (216, 217). Into the cytoplasm, fatty acids bind to FABP which facilitate the use of fatty acids for biological functions in the trophoblast intracellular compartment (216, 217). From the syncytiotrophoblast basal membrane, the fetal circulation receives NEFA via FAT/CD36 and FATP or via passive diffusion (217). Fatty acids are then carried by fetal albumin to the liver to be metabolised into TG which is transported back into fetal plasma (217). The placenta also expresses adipophilin and perilipin (218, 219), proteins implicated in intracellular lipid droplet formation and essential for the action of intracellular lipases (219, 220).

Cholesterol is also transferred to the fetus by the placenta and is particularly important for steroid hormone synthesis, cellular membranes and as a bile precursor (221). Cholesterol and TG containing lipoproteins can be taken up by the trophoblast via specific membrane receptors, e.g. scavenger receptor class B (HDL-C); LDL-receptor related protein 1 (VLDL-C); lipoprotein-related protein 2 (HDL-C and LDL-C); and ATP-

binding cassette transporters (efflux of cholesterol through cellular membranes) (222, 223). Besides, trophoblasts also contain membrane lipoprotein receptors that, once bound to LDL-C and VLDL-C, internalize the lipoprotein particles (166). In the cytosol, the lipoproteins are carried into endosomes and lysosomes where cholesterol is freed, the TG fractions of LDL-C and VLDL-C are hydrolyzed by intracellular lipases, and the placental membrane lipoprotein receptors are then recycled (166).

In addition to lipid transporters and proteins linked to fatty acid storage, the placenta contains enzymes for fatty acid oxidation. The expression of enzymes that act in the first, third and fourth steps of β-oxidation of fatty acids (see Figure 1.8 in this chapter), i.e. acyl-CoA dehydrogenase complex [medium-chain acyl-CoA dehydrogenase (MCAD), long-chain acyl-CoA dehydrogenase (LCAD), very-long-chain acyl-CoA dehydrogenase (VLCAD)]; β-hydroxyacyl-CoA dehydrogenase complex [short-chain L-3-hydroxyacyl-CoA dehydrogenase (SCHAD) and long-chain L-3-hydroxyacyl-CoA dehydrogenase (LCHAD)], and acyl-CoA acetyltransferase (thiolase) [long-chain 3-ketoacyl-CoA thiolase (LKAT)]; respectively, have been described in human placenta (224). In term placentas, all cited enzymes were found to be expressed in the syncytiotrophoblast, where the expression was the highest, and in cytotrophoblasts. However, no expression was detected in chorionic villous vessels nor mesenchymal tissue (224). Moreover, all these enzymes were expressed from 12 weeks of pregnancy towards term, but the expression and activity of LCHAD, SCHAD and LKAT decreased with pregnancy progression, especially after 28 weeks (224). Therefore, there is remarkable evidence that the placenta is capable of lipid uptake, transport and metabolism, including fatty acid recycling, oxidation and storage.

The fetus may synthesise some fatty acids (225, 226), but obtains about 50% of its body fat from the maternal circulation (166) and it is totally dependent on maternal nutrition and placental transfer to acquire essential fatty acids (EFA) [i.e. the polyunsaturated fatty

acids (PUFA) α-linoleic (n-3; 18:3) and linoleic (n-6; 18:2) acids] (217). The longer chain products of α-linoleic and linoleic acids are crucial for kidney, liver, retina, brain, gonads and adrenals development (227), which may be reflected by the placenta preference in transferring the n-3 derived docosahexaenoic acid (DHA) to the fetus in comparison with palmitic acid, oleic acid and linoleic acid (228), and also by findings of higher proportions of long-chain PUFAs in fetal than maternal plasma (226).

It has been demonstrated that the transport and metabolism of fatty acids can be altered in pregnancies affected by obesity and diabetes. Nevertheless, the results are not homogeneous, possibly due to differences in study design, type of diabetes assessed (GDM, T1DM or T2DM), GDM severity and therapy (diet alone or insulin therapy), the occurrence of adverse outcomes such as macrosomia and, in particular, maternal BMI. Furthermore, it appears that the combination of GDM and obesity is a major determinant of changes in placental lipid metabolism. mRNA expression of adipose TG lipase (ATGL) was up-regulated and hormone sensitive lipase (HSL) was down-regulated in placentas from women with well-controlled GDM compared with healthy controls matched for BMI and gestational age of delivery (218). Even so, there were no differences in the protein expression of placental ATGL, HSL, LPL and EL between women with and without GDM (218). In addition, IL-6, which is commonly increased in obesity and GDM, led to fatty acid accumulation in primary human trophoblast cultures (229). Nonetheless, this was not associated with alterations in genes involved in placental fatty acid transport (FATP1 and FATP4), adipophilin or LPL activity (229). A study that investigated the expression of genes implicated in glucose and lipid metabolism in placentas from T1DM and GDM mothers, both with macrosomic neonates, compared to those from normal pregnancies, showed that 67% of up-regulated genes were involved in lipid metabolism and only 9% of up-regulated genes were related to glucose metabolism (205). Genes associated with the synthesis of TG, cholesterol and steroids were, however,

preferably overexpressed in placentas of GDM obese mothers with minor or no alterations in the placentas of T1DM women (205). This supports the importance of the combination of obesity and diabetes in the origin of gestational complications related to placental lipid metabolism dysfunction (205).

Another study that evaluated (i) normal BMI healthy mothers, (ii) obese mothers, and (iii) obese mothers with well-controlled T2DM or GDM, showed increased placental villous NEFA accumulation and increased expression of FABP4 only in the group with obesity and diabetes (230). The obese and GDM group also had higher circulating TG levels in both maternal and cord blood and heavier neonates than normal BMI and non-diabetic obese mothers (230). Surprisingly though, villous TG quantities were higher in the control group than in the obese or obese/diabetic groups (230). In primary trophoblast cultures, incubation with 10 nM insulin, 0.8 mM linoleate and 0.4 mM oleate highly induced FABP4 expression and led to increased intracellular TG content; whereas siRNA knockdown of FABP4 reduced the TG content (230). The authors concluded that up-regulation of FABP4 in trophoblasts induced by lipid is a key factor in determining the accumulation of fatty acids in these cells (230). They also suggested that increased concentrations of maternal lipids in the presence of diabetes and obesity drive placental fatty acid transport to the fetus through FABP4. As a result, the fetus exhibits higher circulating TG with greater fat mass, however without a rise in placental TG content (230).

Furthermore, EL mRNA expression was increased in placentas from obese-GDM women in comparison with lean controls, which was not seen in placentas from only obese or only GDM women (231). Treatment of normal placental villus primary endothelial cells with TNF-α or leptin caused a dose-dependent up-regulation of EL expression from normal pregnancies and these effects were further increased when cells were incubated with both TNF-α and leptin (231). These results implicate TNF-α and leptin in altering

lipid metabolism within the placenta. In this research, as placental EL function is not fully understood, the authors have discussed the hypothesis that increased EL activity in endothelial cells of the fetus might increase the hydrolysis of phospholipids and TG, leading to higher NEFA availability for fetal uptake (231). However, no relationship between EL expression and fetal growth assessment was seen in this study and EL activity was not measured (231). These data also indicate that the combination of obesity and diabetes, which precipitates a more dysfunctional metabolic profile, has a synergistic role in the pathogenesis of pregnancy complications, associations that have been demonstrated in clinical studies, and that the fetus seems to actively participate in these processes.

Changes in placental lipid metabolism in cultures appears to be more strongly driven by exposure to high levels of lipids than to high glucose concentrations. In primary human trophoblast cultures, 0.4 mM oleate induced expression of genes related to cholesterol and TG synthesis, an effect that was not observed in the presence of 10 mM glucose concentration (205). The combination of 0.4 mM oleate and 10 mM glucose did not increase the effect of 0.4 mM oleate alone (205). Moreover, in primary human trophoblasts in culture, treatment with 0.25 mM NEFA (palmitate plus oleate) increased NEFA esterification into diacylglycerol and TG, adipophilin expression and lipid droplet formation (200). Conversely, NEFA treatment decreased fatty acid oxidation and lipolysis (200). These results are consonant with an increased lipid storage in trophoblasts induced by NEFA (200). Exposure to high compared to low glucose levels (10 vs 1 mM) did not impact on lipid pathways, other than down-regulated mRNA adipophilin expression (200). In addition, the presence of NEFA, but not high glucose media, increased trophoblast syncytialisation indicating that high levels of NEFA may precipitate changes in placental structure (200). At variance with these results, human term placental explants exposed to higher levels of media glucose (11 mM *vs* 5 mM) decreased fatty acid oxidation, increased NEFA esterification into total lipids and increased placental TG

content, demonstrating that glucose can also affect placental lipid metabolism (232). These discrepancies may be secondary to methodological differences such as incubation conditions and tissue culture of isolated trophoblast cultures in one study (200) and villous explants in the other, as the latter included mixed cell population of metabolically active cells (e.g. fibroblasts and endothelial cells together with trophoblasts) in a model that maintains the histological structure (232).

Few studies have addressed the roles of altered cholesterol metabolism in the placenta in obesity and diabetes, despite the alterations in cholesterol metabolism that happens in normal pregnancy (33). Placentas from women with plasma total cholesterol concentration > 8 mM late in pregnancy have demonstrated decreased LDL-receptor protein expression in relation to women with cholesterol < 7 mM (233). Likewise, LDL-receptor protein expression was inversely correlated with term maternal plasma LDL concentrations (r=-0.53), maternal plasma total cholesterol concentration (r=-0.49), and maternal plasma apoB-100 levels (r=-0.44) (233). LDL-receptor expression was also associated with maternal pre-pregnancy BMI (233). For women with cholesterol > 8 mM, LDL-receptor expression was lower in placentas from women in the highest BMI group in comparison with those in the lowest BMI group (233). Interestingly, cord plasma cholesterol was the same in neonates born to high and low cholesterol women (233) suggesting that these cholesterol transport alterations in the placenta may spare the fetus from abnormal maternal circulating lipids. Moreover, high levels of oxysterols may take part in the pathogenesis of structural and functional alterations in the placenta since there is evidence that these cholesterol oxidation products impair differentiation and syncytialisation of term human trophoblasts *in vitro* (234).

As mentioned in section 1.3.2 of this chapter, plasma maternal glycerol levels are increased during the catabolic phase of pregnancy mainly in the last trimester. However, it is unlikely that substantial glycerol transport from the mother to the fetus exists in

humans. The intense use of glycerol as a substrate for maternal hepatic and renal gluconeogenesis possibly precludes glycerol placental transport (235). Ketone bodies cannot be produced by the fetus and are usually at low concentrations in maternal blood, but can be increased due to maternal fasting or uncontrolled diabetes (235). The placenta is able to metabolise ketone bodies for energy production and to deliver them to the fetus, which may also utilise ketone bodies as a nutritional source (236). Ketone bodies are transported by the placenta via passive diffusion or, at least in rat, via a carrier-mediated transport system (237).

Data on other factors linking obesity and placental lipid metabolism have been emerging. A recent study with term placental explants have demonstrated that hepatocyte growth factor (HGF) can reduce CPT-1 activity and fatty acid oxidation, stimulate NEFA esterification and *de novo* fatty acid synthesis with rise in TG content (238). HGF, which is a pro-inflammatory cytokine synthesized by the adipose tissue and thereupon augmented in obesity, was increased in the amniotic fluid in the second trimester of obese gravidas (238).

1.7.3 Amino acid transport and metabolism

Contrary to proteins that have a high molecular size and do not cross the placenta (e.g. insulin), amino acids are transported through the placenta by active transport or facilitated diffusion (239). The amino acid transport across the syncytiotrophoblast microvillous and basal membranes is a controlled process, whereas amino acids have free passage through the fetal endothelium (240). Amino acid transporters, also sub-classified in isoforms, are not evenly distributed in the microvillous and the basal membranes of the syncytiotrophoblast. About 20 amino acid transporter types have been identified in the human placenta and only the main groups are described here. Systems A, ASC, β, X^-_{AG} are sodium-dependent transporters, while systems L, T, y^+ and y^+L are sodium-independent (240). System A or Na^+-coupled neutral amino acid transporters (SNAT) are

mostly responsible for the uptake of small neutral non-essential amino acids such as glycine and alanine into the trophoblast (241). System A transporters are found in both the syncytiotrophoblast microvillous and basal membranes, but are much more active at the microvillous membrane (241, 242). System L carries essential amino acids, specially branched chain amino acids (e.g. leucine) (241), through the syncytiotrophoblast microvillous membrane (241) and the basal membrane (243). In addition, system L mediates the transport of the aromatic amino acids tyrosine and tryptophan across the microvillous membrane (243). System T transports tyrosine, tryptophan, alanine, phenylalanine and leucine through the basal membrane (243, 244), whereas system ASC (alanine, serine and cysteine), which is part of a superfamily of non-polar and some anionic amino acid transporters, has also been found in the basal (242) and microvillous membranes (245). The β-amino acid transport system [e.g. taurine transporter (TauT)] is much more active in the microvillous membrane than in the basal membrane maintaining an elevated trophoblast intracellular concentration of taurine (246, 247). Cationic amino acids (e.g. arginine) are mainly transported through the microvillous membrane by the system y^+ and through the basement membrane by the system y^+L (248). The anionic amino acids (e.g. aspartate and glutamate) are transported by X^-_{AG} system, which has been described in both the microvillous and basal membrane (249).

The three main mechanisms of amino acid transport are (i) the uptake from maternal circulation with intracellular accumulation in the syncytiotrophoblast (e.g. system A)(239); (ii) the exchange of syncytiotrophoblast amino acids with the maternal or fetal circulation amino acid pools which results in qualitative but not quantitative changes in amino acids (e.g. system ASC and some isoforms of systems L and y^+L) (250); and (iii) the efflux of amino acid from the syncytiotrophoblast cytosol through the basal membrane into the fetal circulation (e.g. some isoforms of systems T and L) (244).

An adequate amino acid supply is crucial for a normal fetal growth, and a fetus with adequate growth usually has higher circulating amino acid concentrations than the mother (251, 252). Amino acids can be converted to other metabolic substrates (e.g. into glucose through gluconeogenesis); be oxidised by the fetus and the placenta to produce energy; and/or be used as a source of nitrogen and carbon by the fetus (168). The placenta is also able to synthesise amino acids, such as alanine, from protein catabolism or pyruvate transamination (168). Different amino acids are selectively transported in healthy pregnancies and a study has demonstrated that phenylalanine, leucine, methionine, and isoleucine cross the placenta faster than tryptophan, lysine, threonine, and histidine (253). Moreover, the combination of amino acid types and the amino acid concentrations in maternal plasma seems to determine the umbilical cord amino acid uptake, i.e. some specific amino acids present in maternal circulation may inhibit the placental transfer of amino acids to the fetus (254).

Disturbances in placental transport and fetal uptake of amino acids have been identified in fetal growth restriction (245, 246, 255), a condition in which the fetal-to-maternal plasma amino acid ratio is decreased in comparison with pregnancies with normally grown fetuses (256). Less studies have investigated the role of placental amino acid transport in fetal aberrant growth in pregnancies affected by obesity and/or diabetes, nevertheless some evidences suggest that amino acid transport can be altered in these conditions. Some amino acids were found to be increased in cord plasma from well-controlled GDM, but normal in maternal plasma (257), suggesting a selective increase in the placental amino acid transport in GDM (257). The activity of the system A and protein expression of the SNAT2 isoform were raised in the placental microvillous membranes from obese mothers with LGA neonates (258). According to this study, placental amino acid transporters may have been stimulated by the activation of insulin and mammalian target of rapamycin (mTOR) signalling pathways (258). In addition, the system A activity

in the microvillous membrane was increased in T1DM and GDM pregnancies, but leucine transport across the microvillous membrane was up-regulated only in GDM pregnancies associated with LGA babies (259). Conversely, the activity of system A transporter was down-regulated in the microvillous membranes of placentas from GDM/T1DM pregnancies with LGA neonates probably due to a reduced number of transporters in comparison with healthy pregnancies with appropriate for gestational age babies (260). Besides, the activity of placental TauT was lower in women with obesity early in pregnancy in comparison with women with normal BMI, even though the TauT protein expression was normal (261). As in this study neonates born to obese mothers presented normal growth, the authors suggested that this is possibly a post-translational down-regulation of amino acid transport in response to maternal obesity preventing fetal overgrowth (261). It is unknown whether a specific amino acid transporter decrease in one system can be overcome by a compensatory rise in a transporter for the same amino acid in another system, which could explain the disparities between these studies.

Leptin has been implicated in modulation of placental amino acid transport. Acute exposure to supra-physiological doses of leptin promoted the activity of system A amino acid transport in villous explant cultures from healthy mothers via the JAK-STAT pathway (262). However, the activity of system A reduced with a more prolonged incubation with leptin (262). This may be a placental modulation in response to an adipokine that signals maternal adipose tissue and therefore nutritional plenty (262). Supporting this hypothesis, system A activity was decreased in placental fragments from obese women with normal neonates in comparison with normal BMI mothers (263). Also, maternal plasma leptin was negatively correlated to system A activity and the syncytiotrophoblast leptin receptor density was reduced in the obese compared to the normal BMI mothers (263). Moreover, adiponectin decreased SNAT2 expression (protein and mRNA) and system A activity insulin-stimulated in primary human trophoblast cells

(264). Adiponectin inhibited insulin action through down-regulation of the insulin signalling pathways, as indicated by decreased insulin receptor substrate 1 and protein kinase B (AKT/PKB) phosphorylation, and possibly via PPAR-α activation (264), but the latter requires further investigation.

In addition to adipokines, there are evidences that pro-inflammatory cytokines are involved in the regulation of placental amino acid transport. In human primary trophoblast cultures from term placentas, physiological levels of TNF-α and IL-6 increased the activity of system A and the protein expression of both SNAT1 and SNAT2 (265).

Besides, the fetus may contribute to placental delivery of amino acids. In a mouse model of genetic intrauterine growth restriction, the knock-out of the insulin growth factor II transcript in the trophoblast firstly led to a reduction in the placental size which was followed by fetal growth restriction (266). Initially, placental transport of amino acids was increased presumably in an attempt to compensate for the delayed fetal growth (266). More studies concomitantly investigating amino acid concentrations in maternal plasma and umbilical cord together with amino acid placental transport are needed to elucidate the regulation and dynamics of amino acid in obesity and diabetes.

1.8 Rationale of this thesis research

Due to the high prevalence and well-known detrimental consequences of obesity and/or diabetes during pregnancy, studies that investigate the pathophysiology of these conditions in the feto-placental-maternal unit are invaluable. Previous studies in our laboratory have shown the effects of high levels of glucose and NEFA on lipid metabolism and morphology in primary human trophoblasts, which are the placental cells in contact with maternal blood during pregnancy (200). In continuation of this line of research, the current series of experiments were designed to assess the effects of high concentrations of NEFA and/or glucose on glucose metabolism pathways in primary human trophoblasts in culture in addition to the effects of NEFA on trophoblast morphology. Moreover, the studies were conducted in cells at different stages of differentiation to investigate whether glucose metabolism diverges in cultures richer in cytotrophoblasts or syncytiotrophoblasts.

1.8.1 Hypotheses

a. In the presence of higher glucose concentrations, total glucose uptake will be increased in human trophoblasts. However, glycolysis and glucose oxidation will not be augmented. Excess glucose will be stored as glycogen.
b. In the presence of NEFA, glucose uptake and metabolism will be inhibited in human trophoblasts.
c. Glucose metabolism will be different between cytotrophoblast and syncytiotrophoblast cultures since they present diverse cellular structure.
d. Chronic exposure to NEFA will change cellular morphology of human trophoblasts in primary cultures.

1.8.2 Thesis research aims

a. To investigate the metabolic flux of glucose through major pathways of metabolism in primary human trophoblast cultures exposed to increasing glucose concentrations.
b. To assess the acute effects of NEFA on glucose metabolism in human trophoblast cultures.
c. To evaluate glucose metabolism differences in human cytotrophoblast and syncytiotrophoblast cultures.
d. To study the chronic effects of NEFA on human trophoblast culture morphology.

Chapter 2

Primary human trophoblast isolation and culture

2.1 Introduction

This chapter describes the protocols used for human trophoblast isolation and culture. Placental perfusion, explant cultures, trophoblast cell lines and primary cell cultures are models to study human placental metabolism. Each method has advantages and limitations. Primary trophoblast culture, however, is a commonly used technique to address trophoblast metabolism in spite of its artificial *in vitro* environment and lack of modulation by other cells from the placenta. It allows for assessment of trophoblast metabolism alone, as other cell types are not present. Primary cultures have the advantage over cell lines that the cells are not malignant or transformed and are therefore more closely related to the trophoblasts of *in vivo* human placenta.

The first 11 trophoblast isolation experiments of this work were performed with a protocol established in the laboratory during a previous trophoblast study (200). The results however obtained were inconsistent, with variable cell yield and trophoblast purity. In addition, the protocol length demanded complex logistics and the cells were usually obtained and seeded overnight. Thus, a new method based on protocols from two well established trophoblast research centres (234, 267) was developed and tested. The main differences between the previous and the new protocol were the villous tissue harvesting procedure, the enzymatic digestion, a better control of the experimental variables and the logistics. The new protocol produced a higher trophoblast yield and higher trophoblast purity. This enhanced the reproducibility of the experiments performed with these trophoblasts.

For this thesis, the first used protocol is named "primary trophoblast isolation-protocol 1." The new (current) protocol is described as "primary trophoblast isolation-protocol 2." Only protocol 2 derived trophoblasts are included in the metabolism and morphology studies of this thesis.

2.2 Study participants

This study was approved by the Australian Capital Territory (ACT) Health Human Research Ethics Committee (HREC) and HREC Calvary Health Care ACT. Informed written consent was obtained from all mothers providing the placentas. The participants were recruited at TCH and Calvary John James Maternity, between March of 2012 and March of 2015. Only the placentas from women undergoing elective caesarean section for obstetric indications (e.g. breech), with singleton pregnancies, at term (> 37-41 weeks of gestation), without obstetric complications in the current or past pregnancies (e.g. GDM, abnormal fetal growth) and without medical diseases (e.g. obesity, diabetes mellitus, systemic hypertension, current smoking) were included.

2.3 Primary human trophoblast isolation–protocol 1

2.3.1 Preparation of solutions and media

Refer to Appendix 1-Material, reagents and solutions.

2.3.2 Tissue harvesting and digestion

Digestion buffer was prepared using calcium and magnesium free Hank's Balanced Salt Solution (HBSS) and 4-(2-hydroxyethyl)-1-piperazineethanesulfonic acid (HEPES) (refer to Appendix 1) and divided into two Erlenmeyer flasks. The flasks containing the digestion buffer were kept at 37ºC. The placentas were collected from the surgical theatre and brought to the laboratory within 30 minutes of the newborn delivery. Five cotyledons were dissected and finely chopped. The remaining placenta, with cord and membranes, was sent to the Department of Anatomical Pathology at TCH for macroscopic and histological analysis to confirm normality. The harvested tissue was rinsed with warm (37ºC) saline solution to remove blood under sterile conditions. The tissue was evenly divided in two parts and placed into the flasks containing the digestion buffer. DNase 1

and trypsin were added to each flask. DNase 1 final concentration was 0.13 KU/ml and trypsin final concentration was 0.25%. After capping the flasks with aluminum foil, they were placed in a water bath (Ratek, Melbourne, VIC, Australia) at 37ºC, with gentle shaking for 30 minutes (shaking set=4). After digestion, the flasks were placed under the tissue culture hood, tilted to allow undigested tissue pieces to settle down for about 1 minute. The supernatant was collected into 50 ml Falcon tubes with 3 ml of fetal bovine serum (FBS) to inhibit trypsin action. Falcon tubes with supernatant were kept under sterile conditions at room temperature. A new volume of digestion buffer, trypsin and DNase 1 (refer to Appendix 1) was added to the remaining tissue fragments and incubated in the shaking water bath (30 minutes, 37ºC) for the second digestion. The same procedure was used to collect the supernatant from the second digestion into 50 ml Falcon tubes containing 3 ml of FBS. Then, the digestion buffer, trypsin and DNase 1 were added into the flasks and the remaining tissue submitted to a third digestion in the shaking water bath (30 minutes, 37ºC). The supernatant was collected as for the previous digestions. The supernatants from all digestions were centrifuged (1000 *g*, 20 minutes, 25ºC) in an Allegra X-15R centrifuge (Beckman Coulter, Lane Cove, NSW, Australia). After centrifugation, the supernatants were discarded and each cell pellet was resuspended in 5 ml Connaught Medical Research Laboratories (CMRL) supplemented with 25 mM HEPES, Penicillin-Streptomycin-Neomycin (PSN) Antibiotic Mixture (100X) and 10% FBS (vol/vol) (complete CMRL medium-refer to Appendix 1). The cell suspensions were poured through sterile 100 µm nylon mesh strainers into a single 50 ml Falcon tube to separate the undigested tissue. The cell suspension was centrifuged again (1000 *g*, 10 minutes, 25ºC) to completely remove trypsin.

2.3.3 Trophoblast purification

The supernatant was discarded and the cell pellet was resuspended in 24 ml of calcium and magnesium free HBSS with 1% PSN (vol/vol). Aliquots of this cell suspension (4 ml

each) were carefully layered onto Percoll density discontinuous gradients (5%-70%) prepared in six 50 ml Falcon tubes (refer to Appendix 1). The gradients were centrifuged (1200 *g*, 20 minutes, 25ºC, brake off). Percoll gradient separates villous fragments and mesenchymal cells on the top, trophoblasts in the middle (around the 20 ml tube mark) and blood cells on the bottom (268). Trophoblasts from all gradients were collected using a 5 ml pipette into a new 50 ml Falcon tube. Serum-free CMRL medium at room temperature was added and the cell suspension was centrifuged (1000 g, 10 minutes, 25ºC) to remove the Percoll. This wash procedure was repeated once and the cell pellet was then resuspended with 10 ml of complete CMRL medium.

2.3.4 Cell counting and plating

Twenty-five µl of cell mix and 25 µl of 0.4% trypan blue was mixed and the viable cell number was counted using a haemocytometer.

Cells were seeded in a density of 1 x 10^6 live cells per well (12 well culture plates) and in a concentration of 1 x 10^6 cells per ml of complete CMRL medium. Rat tail collagen was used to coat microplate wells to increase the trophoblast adhesion (refer to Appendix 1 for collagen preparation). Collagen coated plates were prepared no more than 15 days before cell seeding. Plated cells were kept in a humidified incubator (37ºC, 5% CO_2) and daily observed under light microscopy.

2.4 Primary human trophoblast isolation-protocol 2

2.4.1 Tissue harvesting and digestion

Each of the placentas were collected into a sterile bucket at room temperature within 30 minutes of newborn delivery and weighed. For further examination, the placentas were placed on a sterile metallic tray. The placentas were measured and examined macroscopically for any abnormalities. One section of the umbilical cord, one roll of

extra-placental membranes (including the rupture site), two full sections of the placental plate (paraumbilical and lateral), a decidual shave and any abnormal areas were placed in 10% buffered formalin for later microscopic assessment by the staff of the Department of Anatomical Pathology at TCH.

Membranes and the decidua basalis were removed. Blocks of 5 cm x 3 cm x full thickness were cut and placed into a bowl full of cold 0.9% sterile saline solution. The blocks were then briefly dried on sterile cheese cloth sheets covering a 1,000 ml beaker and then transferred to a sterile metallic tray. The villous tissue was scraped leaving vessels and connective tissue behind. The scraped tissue was placed in a beaker filled with 250 ml of cold sterile saline solution and strained using cheesecloth covering a new beaker. The tissue was rinsed thoroughly with sterile cold saline solution to remove blood. The strained tissue was placed inside a sterile plastic culture bottle and weighed. Two-hundred ml of Dulbecco's Modified Eagle Medium [DMEM-5.5 mM glucose, 3.97 mM L-alanyl-L-glutamine (GlutaMAX ™), 1mM sodium pyruvate] and 5 ml of HEPES (1 M, pH 7.4) were added to the bottle. The tissue was kept at 4°C overnight.

Next morning, 500 to 750 ml of digestion buffer was prepared mixing HBSS (10X), HEPES (250 mM, pH 7.4) and Milli-Q water (refer to Appendix 1 for details of reagents, volumes and concentration of solutions). The total volume of digestion buffer to be used was determined by the harvested placenta tissue weight, being 500 ml for < 120 g and 750 ml for > 120g of tissue. Dispase II was added according to the final volume of digestion buffer, being 20 ml of dispase II for a total of 500 ml and 30 ml for a total of 750 ml of digestion buffer. The final dispase II concentration in the digestion buffer was 2 caseinolytic units/ml. Digestion buffer with dispase II (DBD) was then filtered using a 0.22 µm filter and kept at 37°C until use. Two ml of the DBD was added to each of two bottles of 100 mg DNase 1 (lyophilized powder) and 10 ml of DBD were added to each of two bottles of 100 mg trypsin (lyophilized powder). The remaining DBD volume was

evenly divided into two or three Erlenmeyer flasks (Pirex, borosilicate, 500 ml capacity, graduated, with screw caps, Brisbane, QLD, Australia). The harvested villous tissue, which had been kept at 4°C overnight, was strained on 2 unfolded and straight sheets of cheesecloth (total of 4 layers) held by 4 sterile clamps covering a 3,000 ml beaker. The tissue was then thoroughly rinsed with warm saline solution to completely remove the media. The villous tissue was divided into 3 equal parts and placed into the Erlenmeyer flasks containing DBD. Five ml of trypsin and 1 ml of DNase 1 were added to each Erlenmeyer flask. The flasks were closed with caps, swirled and placed into a 37°C water bath with moderate shaking for 30 minutes. The oscillation was set at 6.5 (the water bath oscillates–left to right–132 times per minute). The temperature was checked and the flasks were swirled every 10 minutes. Seven ml of sterile warm calcium and magnesium free phosphate buffered saline (PBS) was added to the remaining trypsin and 2 ml of PBS to the remaining DNase 1. After the incubation time, 4 ml of diluted trypsin and 1 ml of diluted DNase 1 were added to each Erlenmeyer flask. The final trypsin concentration was 3,520 Na–benzoyl–L–arginine ethyl ester (BAEE) units/ml and the final DNase 1 concentration was 533.3 KU/ml. The flasks were placed into the shaking water bath for an additional 15 minutes at 37°C. Two 1,000 ml beakers, which contained 50 ml of FBS each, were covered with 2 unfolded cheesecloth sheets held by 2 sterile clamps per beaker. The digested tissue was filtered through the 2 cheesecloth “pockets”, which were squeezed using sterile gloves to optimise the yield of trophoblasts into the filtrate.

2.4.2 Trophoblast purification

The cellular filtrate was transferred to ten to sixteen 50 ml Falcon tubes and centrifuged (350 *g*, 20 minutes, 20°C). After discarding the supernatants, each pellet was resuspended in 5 ml of DMEM complete media. The cell suspensions were placed into two 50 ml Falcon tubes and centrifuged (350 *g*, 20 minutes, 20°C) to remove the trypsin. After centrifugation, the supernatants were discarded and the pellets from each tube were

thoroughly resuspended in 40 ml of erythrocyte lysis buffer (ELB) (refer to Appendix 1). Cells were exposed to ELB for approximately 5 minutes at room temperature. Five ml of FBS was slowly pipetted into the bottom of each tube to inactivate the ELB and cells were then centrifuged (290 *g*, 7 minutes, 20°C) to completely remove the ELB. The supernatants were discarded and 25 ml of complete media was added to each tube for a second wash. Cells were thoroughly resuspended as before and centrifuged (290 *g*, 7 minutes, 20°C). The supernatants were discarded and 7.5 ml of 5% Percoll were added to each of the two Falcon tubes (a total of 15 ml of cells/Percoll). The pellets were resuspended using a sterile glass Pasteur pipette, followed by passage twice through an 18 gauge needle using a 10 ml syringe. The cell suspensions were filtered through a 100 µm cell strainer into a single new Falcon tube. Five ml aliquots of the cell suspension was carefully overlaid onto each of three 35 ml Percoll gradient tubes (prepared within 24 h prior to trophoblast isolation) with a 5 ml pipette (refer to Appendix 1 for Percoll gradients/layering preparation). The tubes were centrifuged with "slow" acceleration and without break (1200 *g*, 20 minutes, 20°C). Trophoblasts appeared as a thick layer around the 25 ml mark on the 50 ml Falcon tube (between the 30 and 35% Percoll concentration layers). Trophoblasts (about 5-10 ml per tube) were collected with a sterile glass Pasteur pipette pre-rinsed with regular DMEM and placed into two new 50 ml Falcon tubes. Each tube containing the cells was topped up to 50 ml with regular DMEM and centrifuged (290 *g*, 7 minutes, 20°C) to wash out the Percoll. The two cell pellets were each resuspended in 7.5 ml of 5% Percoll and three aliquots of 5 ml of the cell suspension were applied to a second series of Percoll gradients as previously described. After centrifugation, trophoblasts were collected and placed into two new 50 ml Falcon tubes. The tubes were topped up to 50 ml with regular DMEM and centrifuged (290 *g*, 7 minutes, 20°C). The supernatant was removed and the cell pellets were resuspended in complete

DMEM (refer to Appendix 1). Cells were pooled into one tube and complete DMEM was added to total volume of 10 ml.

2.4.3 Cell counting

Twenty µl of the cell suspension was transferred into a 1.5 ml microtube and mixed well with 180 µl of 0.4% trypan blue. Ten µl of cell/trypan blue mixture was transferred into a haemocytometer. Viable cells (trypan blue excluded) in all 5 big squares (which contains 25 smaller squares) were counted twice (each side of the slide). The average cells/µl on the haemocytometer obtained was multiplied by trypan blue dilution (x 10), by conversion of µl into ml (x 10,000) and by total volume 10 ml (x 10).

2.4.4 Cell plating

Cells were plated in a density of 300,000 to 350,000 cells per cm^2 and in a concentration of 1.4×10^6 cells/ml in complete DMEM. The complete DMEM was refreshed in all wells on the following day, and every 24 hours (h) afterwards (except on day 4 of culture when the media was not changed). Plate size was selected according to the experiment (refer to Chapter 3). Microplates without collagen coating were used in all *in vitro* experiments performed in trophoblasts obtained from protocol 2.

Epidermal growth factor (EGF) was added to complete media (EGF concentration: 10 ng/ml) from the cell seeding day, for cultures maintained for more than 3 days. For short-term cultures, in which the experiments were performed within 36 h of culture, EGF was not used.

2.5 Cytological assessment

2.5.1 Purity of trophoblast cultures

Trophoblasts were established in culture for 36 h prior to short-term culture metabolism experiments (refer to Chapter 3). At this time point, a sample of cells from 4 to 6 wells

(12 well plates) was collected to be assessed for purity using immunohistochemistry (IHC). Culture media was removed from the wells and the cells were washed in warm PBS. Then the cells were covered with 350 µl of warm 0.1% trypsin. Trypsin excess was removed and the plate was incubated for 5 minutes (37ºC, 5% CO_2). Trypsin was inactivated by adding 500 µl of ice cold DMEM containing 10% of FBS (vol/vol) to each well. Cells were collected into a single 15 ml tube and then centrifuged (290 *g*, 7 minutes, 4ºC). The supernatant was discarded and the cell pellet was resuspended with 250 µl of DMEM plus 10% FBS (vol/vol). To prepare a cell clot, 250 µl of human plasma was added to the cells with up and down pipetting, followed by the addition of 250 µl of thrombin. The cell mixture was incubated at room temperature for 3 minutes to allow clot formation. Five ml of 10% buffered formalin was added and left for at least 2 h for cell fixation. The cell clot was placed on a filter paper in a cassette and further fixed in 10% buffered formalin for 6 h. Then, the cell block was processed into a wax block. The wax block was cut in 4 µm thick sections for haematoxylin and eosin staining and in 3 µm thickness for IHC staining. The sections were mounted on positively-charged slides and IHC was performed on a Ventana Benchmark NexES machine (Roche, Castle Hill, NSW, Australia). Cytokeratin antibody (Ab) monoclonal-mouse-clone AE1/AE3 was used to stain trophoblasts. Firstly, heat induced epitope retrieval (HIER) with Cell Conditioning 1 (CC1) buffer (pH 8-8.5) was performed for 36 minutes at 95ºC. Then, cytokeratin Ab was added at 1:150 concentration and incubated for 24 minutes. CD68 Ab monoclonal-mouse-clone KP1 was used to stain macrophages. Antigen retrieval was performed with protease 1 for 12 minutes at room temperature. CD68 Ab was added at 1:150 concentration and incubated for 36 minutes. Vimentin was used as a marker for mesenchymal cells, such as fibroblasts. HIER using CC1 pH 8-8.5 was performed for 36 minutes at 95ºC. Vimentin Ab was added at 1:150 dilution and incubated for 32 minutes. *ultra*View Multimer Ig contained the secondary Ab goat anti-Mouse IgG, goat anti-

Mouse IgM and goat anti-rabbit IgG. The secondary antibodies were part of the "*ultra*View Universal DAB Detection Kit". Photomicrographs of IHC slides (40x) were taken. Percentage of trophoblasts was calculated based on five random pictures (40x) per culture.

2.5.2 Light microscopy

Cell cultures were regularly examined under light microscope. Photomicrographs of cell cultures (40x) were obtained at specific culture time points (36 h for protocol 1) and (36 h, 3 d and 5 d for protocol 2). Trophoblast photomicrographs taken on days 3 and 5 of culture in the presence or absence of EGF were analysed by 2 independent viewers and scored according to Table 2.1.

Table 2.1

Score for fresh trophoblast culture morphology analysis

Score	Cellular aggregation	Syncytia
1	Single cells	None
2	Loose small cellular groups	< 20% cell area
3	Tight small cellular groups	20-50% cell area
4	Tight large cellular groups	> 50% cell area

Photomicrographs of trophoblast cultures in complete DMEM in the presence or absence of EGF (10 ng/ml) taken on days 3 and 5 of culture were analysed and scored by two independent viewers.

2.6 Results

Eleven trophoblast isolations were performed with protocol 1 and 48 isolations with protocol 2. The mean (± SD) yield was 42.6 ± 36.5 x 10^6cells for protocol 1 and 266.1 ±

141.3 x 10^6 cells for protocol 2 (Table 2.2). The mean harvested tissue weight was 133 ± 35 g for protocol 2. Tissue weight was not measured in protocol 1.

Cells were plated in a density of 1 x 10^6 cells for protocol 1 on collagen coated 12 well plates (Figure 2.1) and 300,000-350,000 cells/cm^2 (1.4 x 10^6 cells for 12 well plates) on plin plates for protocol 2 (Figure 2.2). No marked morphology differences between cells obtained from protocol 1 and 2 (cultured without EGF) were observed up to 36 h in culture (Figures 2.1 and 2.2). However, trophoblasts cultured with EGF showed earlier cellular aggregation and higher syncytialisation than cultures without EGF (Figures 2.3 and 2.4), particularly after 3 days of culture.

Samples from 4 independent trophoblast isolations were immunostained for cytokeratin and CD68 (protocol 1) and 13 samples were stained for cytokeratin, CD68 and vimentin markers for protocol 2. Trophoblast purity was only 65% for protocol 1 with macrophages contamination (Figure 2.5) and was 98% for protocol 2 (Figure 2.6). The same degree of trophoblast purity was observed in cultures maintained in the presence of EGF (Figure 2.7).

Table 2.2

Human trophoblast isolations

Summary of trophoblast isolations performed in this research		
	Protocol 1	**Protocol 2**
Experiment total number	11	48
Mean cell number isolated per placenta ± SD (range)	42.6 ± 36.5 x 10^6 (0-107.7 x 10^6)	266.1 ± 141.3 x 10^6 (63.8 x 10^6-621.5 x 10^6)
Trophoblasts (range)	66% (52-78%)	98% (96-99%)
CD68 positive cells (range)	34% (21-47%)	1% (0-3%)
Mesenchymal cells (vimentin positive) (range)	Not performed	1% (1-4%)

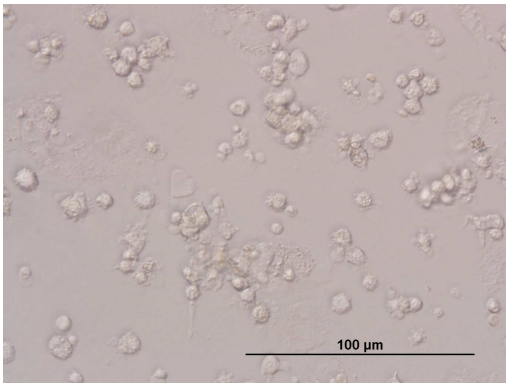

Figure 2.1. Representative photomicrograph from trophoblast primary cultures after 36 h in culture (protocol 1derived cells). Cells were cultured in complete DMEM without EGF.

DMEM: Dulbecco's Modified Eagle Medium; EGF: epidermal growth factor.

No EGF	Plus EGF
24 h	
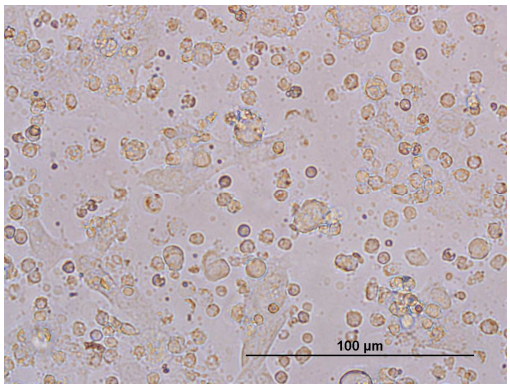	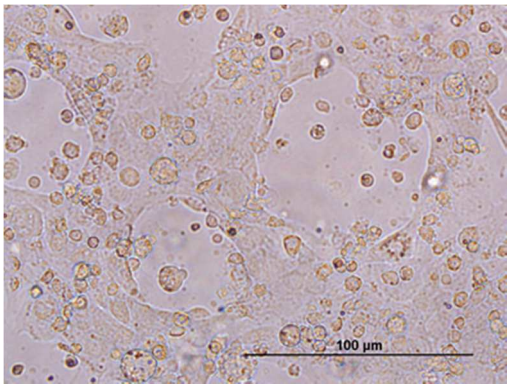
A	**G**
36 h	
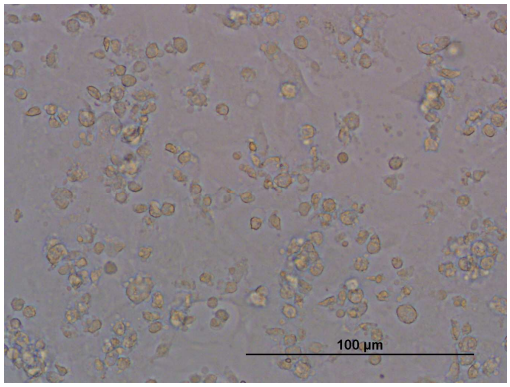	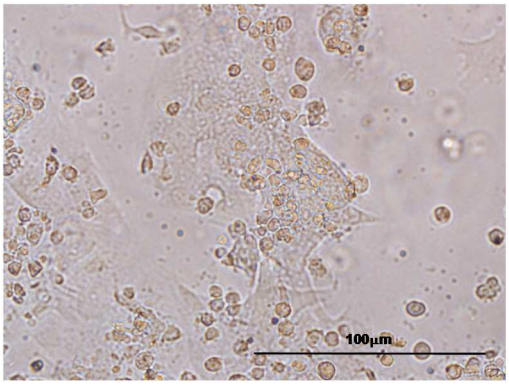
B	**H**
3 days	
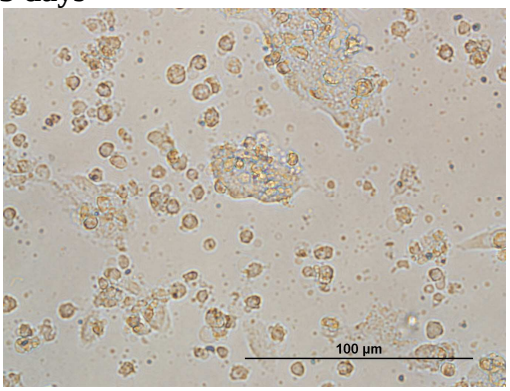	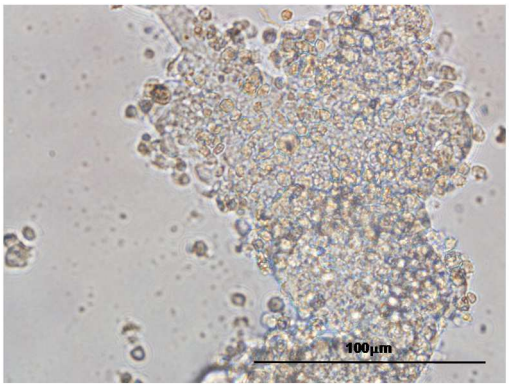
C	**I**

5 days

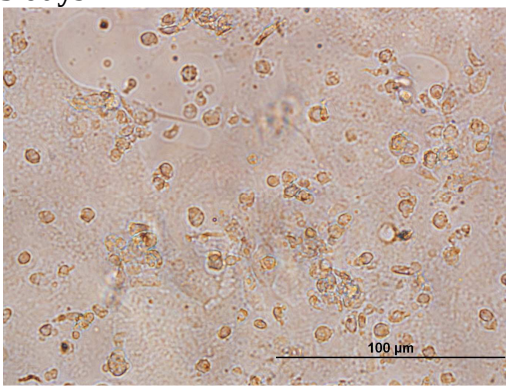

D

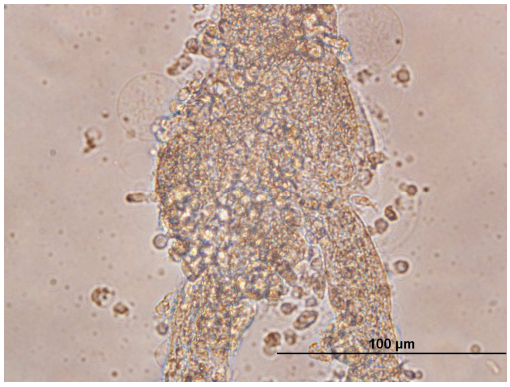

J

6 days

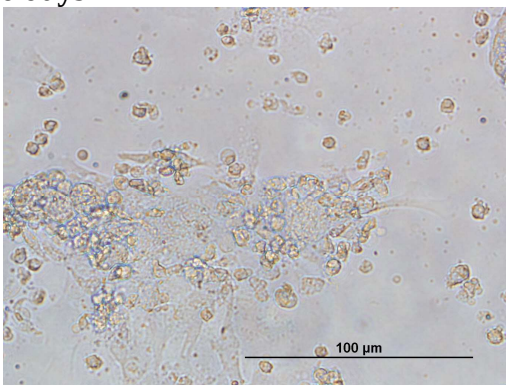

E

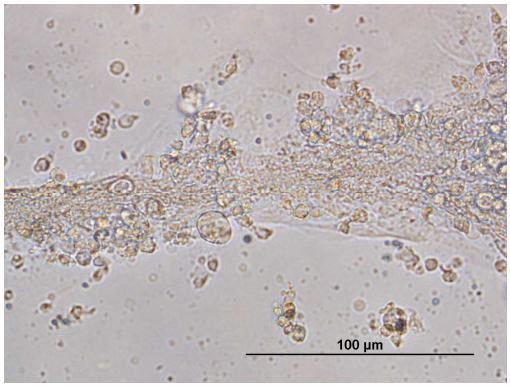

K

7 days

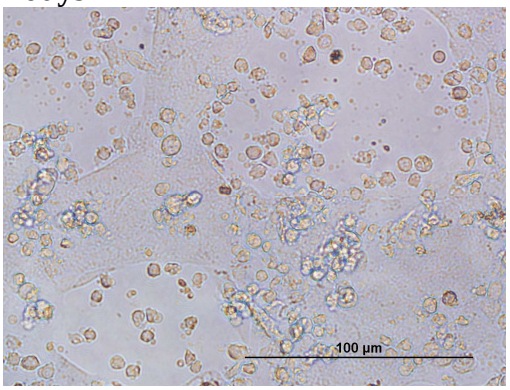

F

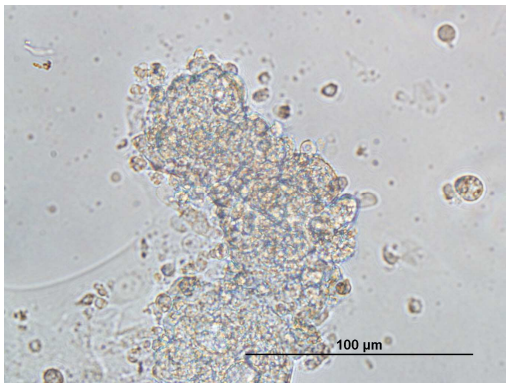

L

Figure 2.2. Representative photomicrographs from trophoblast primary cultures (protocol 2 derived cells) after 24 h, 36 h, 3 days, 5 days and 7 days of the isolation. A-F. Trophoblast cultures in complete DMEM without EGF showed large numbers of single cells. G-L. Cells cultured in complete DMEM with EGF more commonly promoted syncytialisation evident in the longer duration culture time points (I-L).

DMEM: Dulbecco's Modified Eagle Medium; EGF: epidermal growth factor.

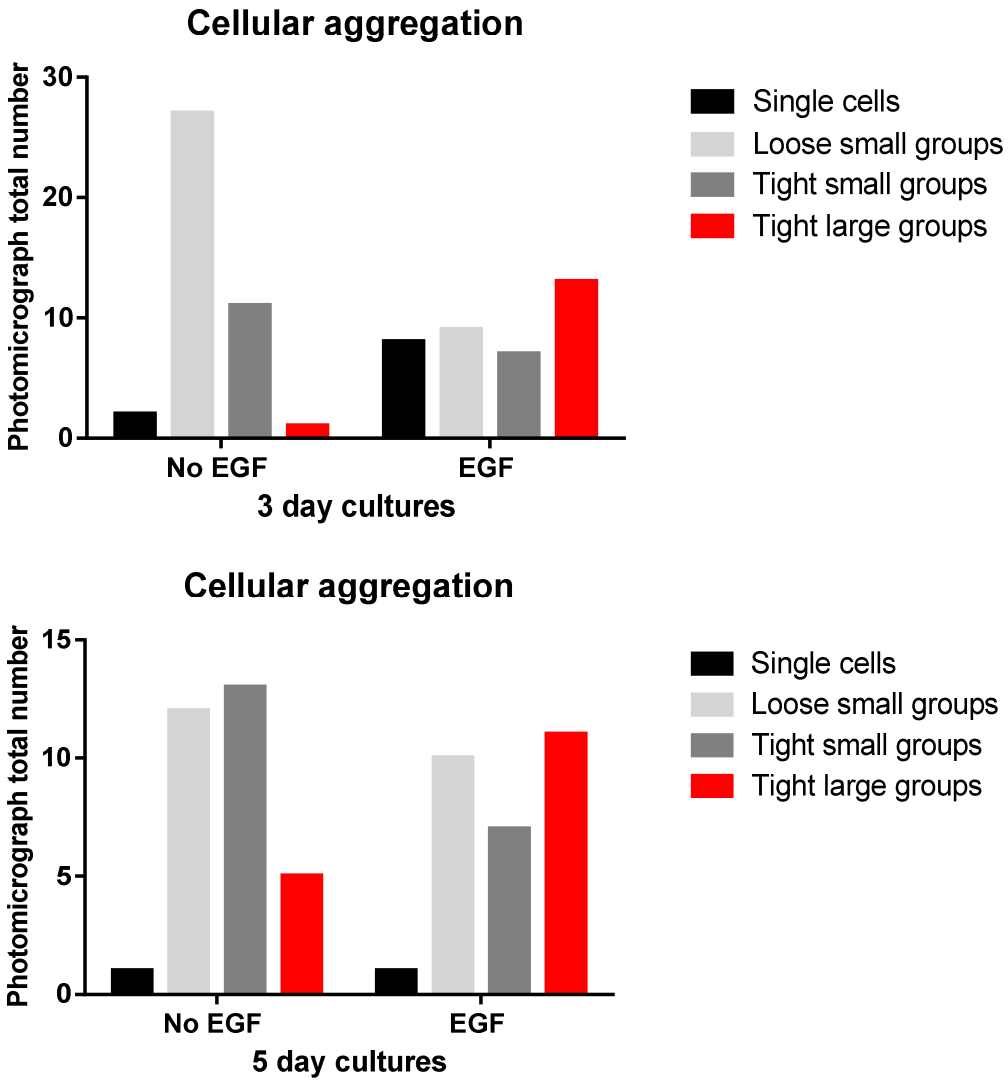

Figure 2.3. Complete DMEM supplemented with EGF led to earlier trophoblast aggregation than complete DMEM without EGF. Trophoblast culture photomicrographs taken on days 3 and 5 of culture in the presence or absence of EGF were analysed by 2 independent viewers and scored for cellular aggregation. Cellular aggregation (as described in Table 2.1) induced by EGF was evident on day 3 of culture. However, cellular aggregation was not significantly different in the presence or absence of EGF in older cultures. Chi-square (EGF effect): 3 day cultures, $p < 0.0001$; 5 day cultures, non-significant (ns). A total of 78 pictures (3 days) and 60 pictures (5 days) from12 independent trophoblast isolations were analysed. At least 5 photomicrographs were randomly taken from each trophoblast isolation.

DMEM: Dulbecco's Modified Eagle Medium; EGF: epidermal growth factor.

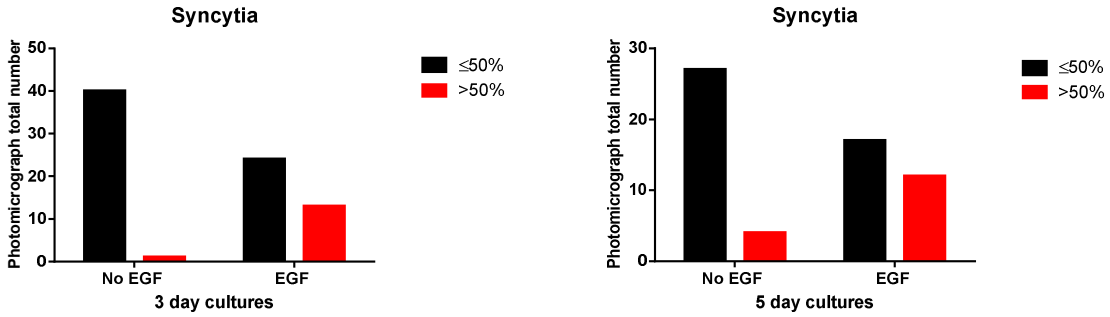

Figure 2.4. EGF clearly induced syncytialisation in trophoblast cultures. Trophoblast culture photomicrographs taken on days 3 and 5 of culture in the presence or absence of EGF were analysed by 2 independent viewers and scored for syncytialisation. Graphs represent total number of photomicrographs analysed showing ≤ 50% or > 50% of trophoblast areas being syncytialised (as described in Table 2.1). EGF led to syncytialisation from the 3rd culture day. The difference was maintained on culture day 5.

Fisher's exact test (EGF effect): 3 day cultures, p=0.0002; 5 day cultures, p=0.019. A total of 78 pictures (3 days) and 60 pictures (5 days) from 12 independent trophoblast isolations were analysed. At least 5 photomicrographs were randomly taken from each trophoblast isolation.

EGF: epidermal growth factor.

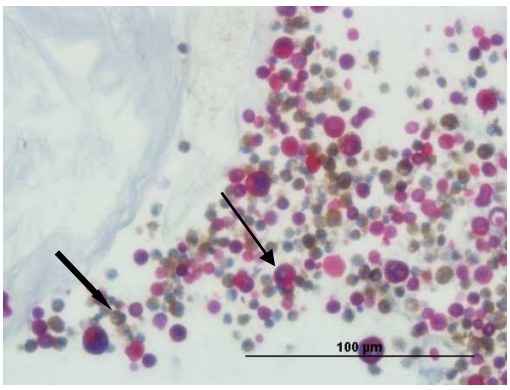

Figure 2.5. Primary human trophoblast isolation-protocol 1. Representative photomicrographs of cell isolates cultured for 36 h. Slides were stained for cytokeratin AE1/AE3 (pink-IHC marker for trophoblasts) and CD68 (brown-IHC marker for macrophages). It shows trophoblasts mixed with a large number of macrophages. Thin arrows are indicative of cytotrophoblasts and thick arrows of CD68 positive cells.
IHC: immunohistochemistry.

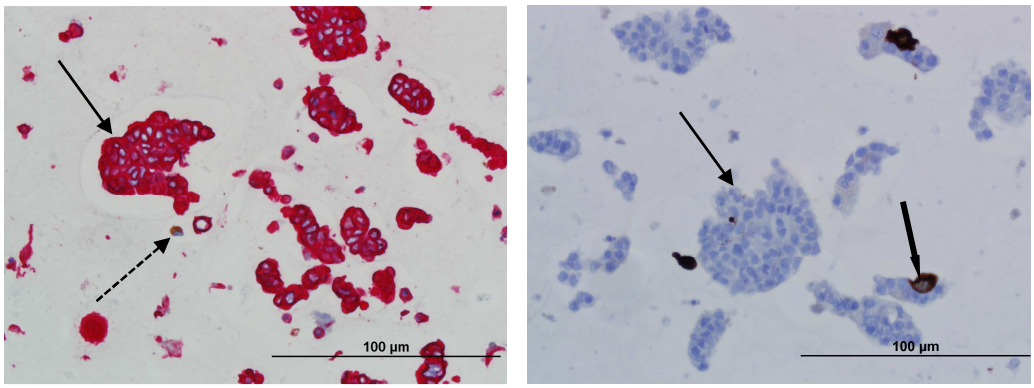

A **B**

Figure 2.6. Primary human trophoblast isolation-protocol 2. Representative photomicrographs of cell isolates cultured for 36 h. A. Photomicrograph of cells stained for cytokeratin AE1/AE3 (pink-IHC marker for trophoblasts) and CD68 (brown-IHC marker for macrophages). B. Photomicrograph of cells stained for vimentin (brown-IHC marker for mesenchymal cells). Trophoblasts are stained in blue (vimentin negative). Thin arrows are indicative of cytotrophoblasts, dashed arrows of macrophages and thick arrows of vimentin positive cells.

IHC: immunohistochemistry.

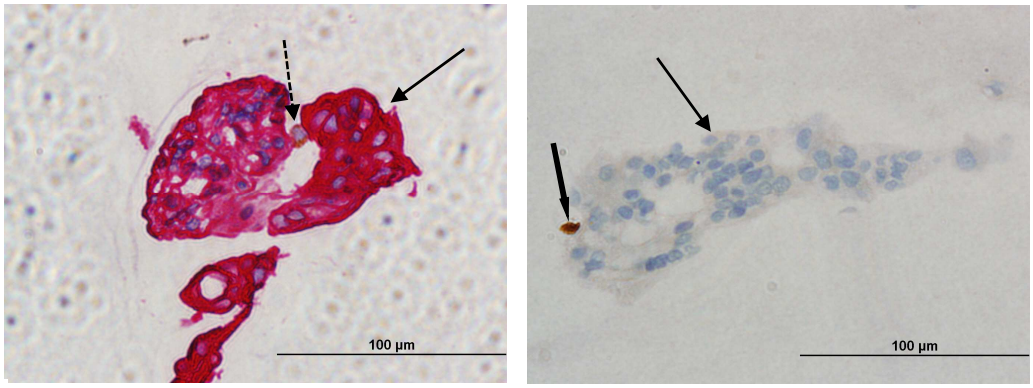

A **B**

Figure 2.7. Primary human trophoblast isolation-protocol 2. Representative photomicrographs of cell isolates cultured for 10 days with EGF. A. Photomicrograph of cells stained for cytokeratin AE1/AE3 (pink-IHC marker for trophoblasts) and CD68 (brown-IHC marker for macrophages). B. Photomicrograph of cells stained for vimentin (brown-IHC marker for mesenchymal cells). Trophoblasts are stained in blue (vimentin negative). Thin arrows are indicative of cytotrophoblasts, dashed arrows of macrophages and thick arrows of vimentin positive cells.

EGF: epidermal growth factor; IHC: immunohistochemistry.

2.7 Discussion

Placental function and metabolism can be studied through animal models, human placental perfusion, placenta explants culture, cell lines or primary cell cultures. Animal models are suitable for placental studies *in vivo* with the advantage that maternal and fetal assessments can be conducted together. This is the only real way to examine placental function under very complex *in vivo* physiological conditions. On the other hand, there are usually many confounding factors which are difficult to control. Also, extrapolation of results from animals to humans is limited due to differences in placental anatomy and physiology between species. Placental cotyledon perfusion is a procedure in which the placenta complex structure is maintained. However, functionality of the placental tissue is preserved for a few hours only, which restricts this methodology to short-term assessment studies (269, 270). Placental explant or cell cultures are more appropriate methods for longer term metabolic studies. Trophoblast function and metabolism can be studied in term villous explant cultures for up to 10 days if the tissue is carefully assessed for structural integrity since the syncytiotrophoblast may detach or undergo fibrinoid necrosis (271). Placental explant cultures have the advantage of tissue and cellular architecture maintenance, with preservation of cell to cell contact and modulation between placental cell types, such as cyto- and syncytiotrophoblasts, endothelial cells, mesenchymal stromal cells and immune cells (271). This modulation is particularly important when cytotrophoblast proliferative activity has to be analysed since cytotrophoblasts, which lose their mitotic activity *in vitro*, are able to divide even in term placentas if in contact with syncytiotrophoblasts (272). Conversely, metabolic studies of specific cellular groups cannot be individualised in this co-culture technique. When a specific type of cells has to be analysed, isolated cell culture is a suitable method. Cells can be obtained from primary cell isolations or from cell lines derived from normal or choriocarcinoma cells.

Cytotrophoblasts are epithelial cells that fuse during the differentiation process becoming a multinucleated syncytial structure named the syncytiotrophoblast. Syncytiotrophoblasts are not able to divide (273). *In vivo*, villous cytotrophoblasts are highly proliferative and are a pool for constant rehnewal of the syncytial tissue. Early in pregnancy, during blastocyst adhesion, cytotrophoblasts have the ability to fuse together, i.e. 2 mononucleated cells can fuse their membranes (272). Nevertheless, throughout pregnancy, they will only fuse with the syncytiotrophoblast layer, losing their capacity to fuse with other cytotrophoblasts (272). In culture, these natural events change. Cytotrophoblasts lose their mitotic capacity and are able to fuse with each other (274).

Cell lines have to be able to multiply and to have an extended lifespan with a stable phenotype compatible with the mother cell. Cell lifespan extension may be increased through spontaneous immortalization or be induced by transfection. Nonetheless, these techniques alter mitosis regulation which may change cellular function and gene expression producing cells different from normal cytotrophoblasts (275).

Finally, cytotrophoblasts, macrophages or endothelial cells can be obtained through primary cultures from human placentas. Several human cytotrophoblast isolation protocols have been developed. Most of these protocols are variations of 3 mains steps: (i) villous tissue harvesting; (ii) enzymatic digestion with trypsin and/or dispase and DNase 1; (iii) trophoblast purification with Percoll gradients (276). Cytotrophoblast primary cultures are usually time consuming and expensive, but they are particularly valuable if the research aims are to investigate trophoblast function and metabolism.

In this study, the trophoblast isolation-protocol 1 produced an inconsistent cell number such that the cell yield from some experiments was not enough to perform the planned experiments (Table 2.2). Moreover, many cell isolates were contaminated with immune cells, especially macrophages as observed by IHC for cytokeratin (an epithelial marker for trophoblasts) and for CD68 (a macrophage marker) (Figure 2.5). Based on the results

from these experiments (Table 2.2), a new protocol was introduced following protocols described by Nelson *et al.* (267) and Aye *et al.* (234) with modifications.

In the new protocol, the harvesting technique was changed resulting in more volume of villous tissue collected; trypsin was substituted by trypsin XII-S, which has a higher degree of purity; DNase 1 concentration was increased; and dispase II, which promotes a gentle cellular dissociation, was introduced. Percoll gradient number was reduced from 14 to 7 (Appendix 1) making its preparation faster without compromising the results. The cell yield was significantly increased and the average cell number was more consistent (Table 2.2). Trophoblast purity was highly enhanced, with almost no other placental cell contamination (Figure 2.6). Furthermore, red blood cells were almost totally excluded from the fresh trophoblast cultures (Figures 2.2). Erythrocytes were visualised in some protocol 1 derived cultures (photomicrographs are not shown). Erythrocytes may interfere in glucose metabolism experiments and so should be removed (277).

Cytotrophoblasts can differentiate and fuse into syncytiotrophoblasts after 3-5 days in culture containing serum (274). However, morphology changes were not observed in cultures followed for up 7 days in this research. Thus, EGF was added to cells plated for long-term culture from the isolation day to induce cytotrophoblast differentiation and fusion into syncytiotrophoblasts (274). With EGF addition, marked morphologic differences were observed from 3 days of culture (Figure 2.2).

Cells were plated on collagen coated plates in protocol 1. Interestingly, this procedure caused very strong cellular attachment to the microplates, making difficult cell detachment by scraping or following trypsin treatment. For that reason, cells were seeded in plain culture plates for protocol 2. A good cell attachment was observed after 4 h of culture with an improved cellular collection from the wells. Based on these observations, collagen coating was eliminated from the established protocol.

2.8 Conclusion

Placental metabolism can be studied by diverse methods. Each method has its own applications and limitations and so researchers have to be aware of these particularities when analysing results. Primary human trophoblast culture is a reasonable technique to address trophoblast metabolism although it is expensive, requires a significant time to perform and is an artificial environment without the complex placental tissue architecture of placental perfusion or explant cultures.

Through the work of this thesis, the laboratory established a new high-quality protocol with reproducible, elevated yield and highly pure results. Following this step, trophoblast metabolism studies were performed as described in Chapter 3.

Chapter 3

General methods

3.1 Methods for assessment of glucose and lipid metabolism in primary trophoblast cultures

3.1.1 Introduction

This chapter describes the methods by which various pathways of glucose metabolism, as well as fatty acid oxidation, were measured in human trophoblasts after their establishment in primary culture. Experiments were divided according to trophoblast culture age (refer to Chapter 2 for culture details). Experiments performed after 36 h of culture in complete DMEM at 5.5 mM glucose, when most cells are cytotrophoblasts, were classified as short-term culture studies. The results of these studies are given in Chapter 4. Experiments performed after 5 days of culture in complete DMEM at 5.5 mM glucose with EGF (final concentration: 10 ng/ml), when many trophoblasts have differentiated into syncytiotrophoblasts, were classified as long-term culture studies. The results of these studies are presented in Chapter 5. In order to assess the effects of EGF, with and without NEFA, on lipid droplet formation, trophoblast TG content, and syncytialisation, trophoblasts were cultured in one set of experiments from the isolation day, with and without EGF (10 ng/ml), and additionally from day 2 to day 5 in the presence and absence of NEFA (0.1 mM, palmitate: oleate ratio; 1:1). The results of these experiments are also shown in Chapter 5.

The metabolism pathways that were assessed in this research are presented in Figure 3.1.

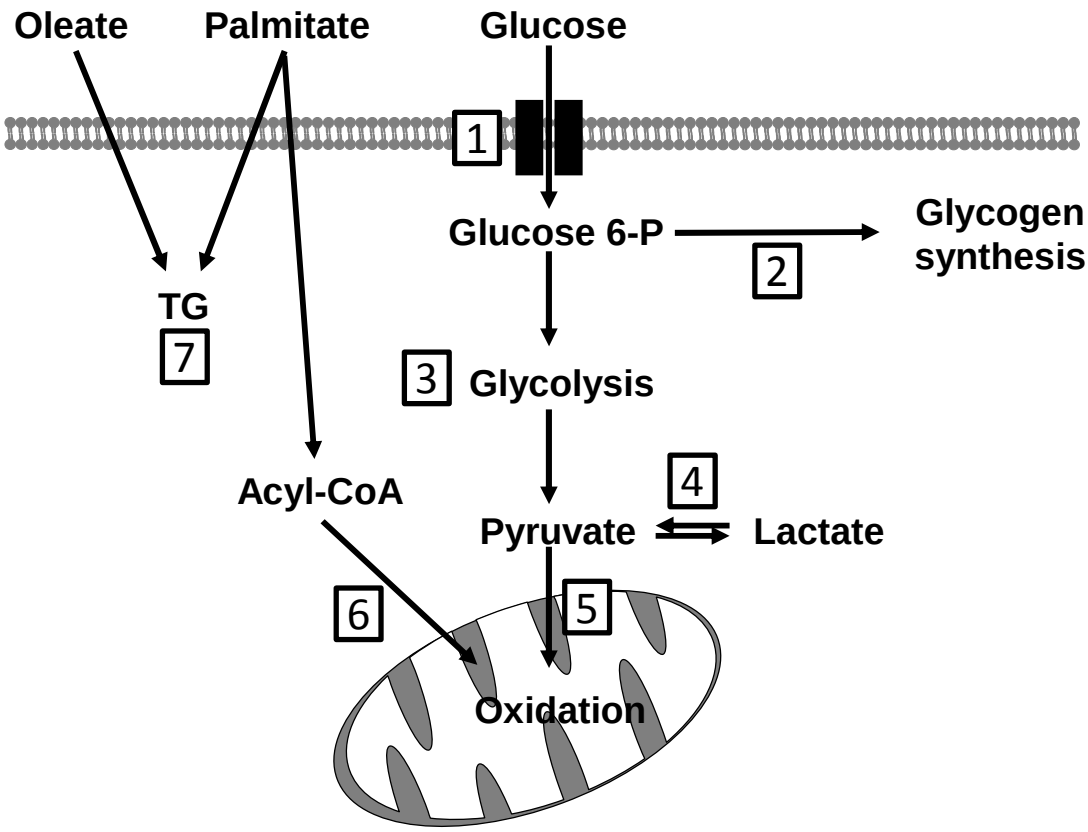

Figure 3.1. Metabolism pathways studied in human trophoblasts in primary culture.

1. Total glucose uptake; 2. Glycogen synthesis; 3. Glycolysis; 4. Lactate production; 5. Glucose oxidation; 6. Fatty acid oxidation; 7. TG synthesis.

TG: triacylglycerol.

3.1.1.1 Principles of metabolic tracer-tracee methodology

In the current research, most metabolic fluxes were studied through radioactive tracer-tracee methodology, as discussed below and in the results of Chapters 4 and 5.

Isotopes of an element have the same number of protons, but differing numbers of neutrons, such that their atomic mass differ (278). These chemical similarities and physical differences permit the use of the isotope-labelled molecules, as tracers, to track and measure the metabolic reactions of the naturally existing molecules, the tracees (278, 279). For instance, a naturally existing ^{12}C-D-glucose molecule (a tracee) demonstrates the same chemical structure but different physical properties to ^{13}C-labelled D-glucose or ^{14}C-labelled D-glucose (tracers) (278). Isotopes can be divided into stable (e.g. ^{1}H, ^{2}H, ^{12}C and ^{13}C) and radioactive (e.g. ^{3}H and ^{14}C) (279). Contrary to stable isotopes, radioactive isotopes disintegrate with the emission of sub-atomic particles, such that they do not maintain a permanent atomic mass. Although stable isotope-labelled molecules are safer and optimal for *in vivo* human studies because they are not a source of ionizing radiation, their use in research has disadvantages. Stable isotope studies need a larger tracer mass due to high natural background causing lower sensitivity, and they require complex and expensive equipment such as mass spectrometry for measurement. For these reasons, the use of stable isotopes results in much higher research costs. Radioactive isotope-labelled metabolites are not present in biological systems, and therefore, only very small tracer amounts are necessary to map a metabolic reaction (280). Moreover, radioactive metabolic tracers are relatively cheaper and can be measured more easily than stable tracers. Hence, radioactive isotopes are more attractive for *ex-vivo* metabolism studies (278).

Radioactive isotopes that release electrons (β radiation), once mixed with scintillation cocktail, emit flashes of light. Betacounters contain a photomultiplier tube that can read and quantify the absolute radioactive emissions with high sensitivity (278). Thus,

radioactive tracers are quantified as disintegrations per minute (DPM) or counts per minute (CPM) (280).

The analysis of metabolism using radioactive isotope labelled metabolic tracers is based on the dilution principle, in which a known amount of tracer is added to a biological system, such as a cell culture system, diluting a known concentration of tracee. As the detection of the fate of the tracer is easier to follow than the tracee, but the metabolism of the tracer and tracee are presumed to be identical, the fate of the naturally occurring metabolite can be determined. Therefore, following the cellular uptake and accumulation of a metabolic tracer within a cell culture system, together with its conversion into other substances, which might remain within the cells or be released out of the cells, provides a means by which the cellular handling of the corresponding tracee through a metabolic pathway of interest can be determined (278, 279). For example, to measure glucose flux into glycogen in cell cultures, an isotope-labelled glucose (e.g. [(U)^{14}C]-glucose) is added in tracer amounts to the media containing a known concentration of the tracee [(U)^{12}C]-glucose (such that the dilution of tracee by tracer can be determined) and the system is incubated for a determinate period after that the accumulation of the tracer into the product glycogen is determined (279). The specific activity (SA) of the media is the measure of tracee dilution by tracer, which is the DPM or CPM (due to the presence of the tracer) measured per amount of tracee (280) (SA calculation is showed below). Hence, if the SA of the glucose in the media is *x* CPM (glucose tracer) per nmol of glucose (tracee), and *y* CPM accumulates into the glycogen pool per h, the accumulation of glucose into glycogen per h will be *y*/*x* nmol/h. However, although it is assumed that tracers behave exactly in the same way as the natural occurring molecule, it is important to be aware of the possibility of the existence of radioactive impurity that may lead to fractions of the tracer behaving in different ways (280). In this case, this “impure” tracer

portion may be quantified as the result of a chemical reaction without reflecting the truth (280).

3.1.2 Metabolism studies

3.1.2.1 Preparation of primary trophoblasts for metabolic assessments

Trophoblasts were established in primary culture (refer to Chapter 2 for trophoblast isolation and culture details) in complete DMEM (refer to Appendix 1 for media preparation) at a glucose concentration of 5.5 mM and, for long-term experiments only, EGF at 10 ng/ml. Cells were seeded in flasks or microplates according to the experiment at a density of 300,000 to 350,000 cells per cm^2 (Table 3.1). After 36 h or 5 days of culture, respectively, short and long-term culture glucose metabolism and fatty acid oxidation studies were performed. Metabolism was generally measured in Krebs-Ringer Bicarbonate HEPES (KRBH) buffer (Appendix 2) with 0.5% fatty acid free bovine serum albumin (BSA-FA free), in the presence or absence of a moderately high concentration of a NEFA saturated and monounsaturated mix (0.25 mM, palmitate: oleate ratio; 1:1). For NEFA stock preparation, refer to Appendix 2. Briefly, on the experimental day, trophoblasts were checked and culture medium was removed. Cells were washed twice in warm washing solution (KRBH, 1 mM glucose, 0.1% BSA-FA free). Warm (all warm solutions described in this chapter were heated up to 37ºC) incubation solution (KRBH with additives, as described for each experimental protocol) was added to plates or flasks, which were incubated at 37ºC, 5% CO_2 for 2 h. After incubation, cellular metabolism was stopped [e.g. by placing microplates on ice or injecting perchloric acid (PCA)] and the cells or supernatant were processed according to the specific experiment. All results were normalised by protein content (method is described below). Refer to Appendix 2 for reagents, suppliers and solution preparation cited in this chapter.

Table 3.1

Cell density seeded according to experiments

Short-term culture experiments		
Experiment	**Plastic ware**	**Cell density**
Total glucose uptake, glycolysis, lactate release into the media and glycogen synthesis	12 well plates	1.4 x 10^6 cells per well
Total glycogen content	6 well plates	3.5 x 10^6 cells per well
Glucose and palmitate oxidation	T25 flasks	7.5 x 10^6 to 8.75 x 10^6 cells per flask*
Long-term culture experiments		
Experiment	**Plastic ware**	**Cell density**
Glycolysis	12 well plates	1.4 x 10^6 cells per well
Glucose and palmitate oxidation	T25 flasks	7.5 x 10^6 to 8.75 x 10^6 cells per flask*
Oil red O	Chamber slide	2.45 x 10^5 cells per well
Total glucose uptake, glycogen synthesis and triacylglycerol quantification	6 well plates	3.5 x 10^6 cells per well

*The aim was to plate 350,000 cells per cm^2. However, if the cell yield from trophoblast isolation was not enough, cultures were established in a cell density of 300,000 cells per cm^2.

3.1.2.2 Total glucose uptake

Labelled 2-deoxyglucose, a glucose analogue, is a suitable tracer to assess total glucose uptake in trophoblast cultures because 2-deoxyglucose is a poor Na-dependent glucose transport substrate and it is mainly transported by the facilitative GLUT transporters (281). In addition, 2-deoxyglucose is phosphorylated by a hexokinase to 2-deoxyglucose 6-phosphate as would a D-glucose molecule. This phosphorylation maintains the hexose gradient, delays the time to achieve an equilibrium and prevents 2-deoxyglycose from being further metabolised (282). It is believed that the placenta presents a very low glucose 6-phosphatase activity with a negligible 2-deoxyglucose-6-phosphate to unphosphorylated 2-deoxyglucose (283). Therefore, total glucose uptake can be calculated through the measurement of intracellular labelled 2-deoxyglucose-6-phosphate metabolised from labelled 2-deoxyglucose (Figure 3.2). Other glucose tracers are less appropriate for glucose uptake studies. For instance, labelled 3-O-methyl glucose is not phosphorylated and reaches equilibrium across the cell membrane very quickly, whilst labelled D-glucose will be further metabolised through other metabolic pathways (282).

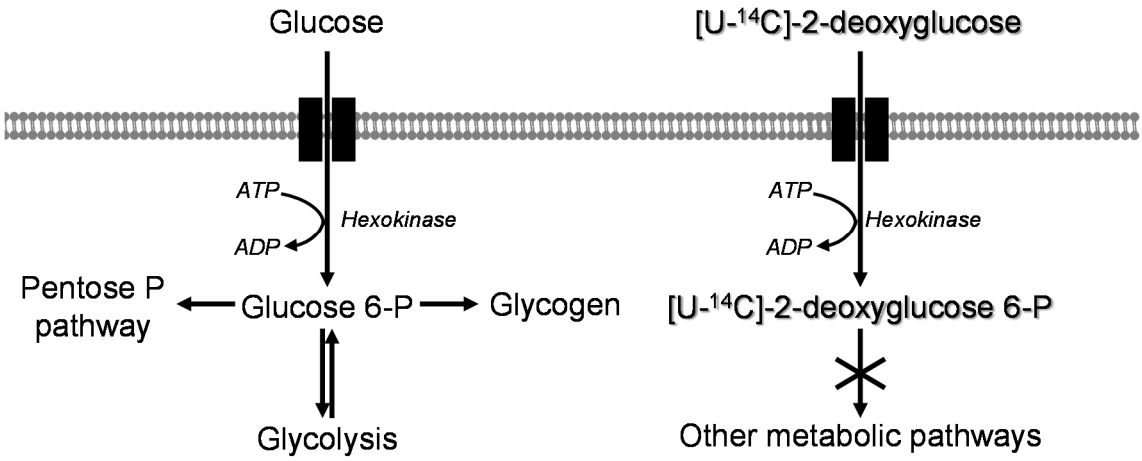

Figure 3.2. Glucose uptake and phosphorylation by trophoblasts. As for a D-glucose molecule, [(U)^{14}C]-2-deoxyglucose is taken up by trophoblasts through a GLUT. However, in contrast to a glucose molecule, which is phosphorylated to glucose-6-phophate and follows through diverse metabolic fates, a [(U)^{14}C]-2-deoxyglucose molecule is inactivated by phosphorylation and trapped inside the cells. It is assumed that [(U)^{14}C]-2-deoxyglucose tracer is representative of glucose tracee allowing for total glucose uptake calculation, since [(U)^{14}C]-2-deoxyglucose is transported into the cells to the same extent as D-glucose, and that both molecules present similar uptake kinetics. In addition, intracellular [(U)^{14}C]-2-deoxyglucose 6-phosphate intracellular accumulation is considered stable since its hydrolysis is believed to be negligible.

For short-term culture studies, trophoblasts were established in culture for 36 h as described in Section 3.1.2.1. Culture medium was removed and cells were washed twice in 1 ml of warm KRBH, 0.1% BSA-FA free, at 1 mM glucose. Then, 1 ml of warm KRBH containing 0.5% BSA-FA free, [(U)^{14}C]-2-deoxyglucose (refer to Table 3.2 for amount) and 1, 5, 15, 25 or 35 mM glucose, plus or minus 0.25 mM NEFA, was added to each well.

Table 3.2

[(U)^{14}C]-2-deoxyglucose specific activity for total glucose uptake protocol

[(U)^{14}C]-2-deoxyglucose kBq/ml (µCi/ml)	Cold glucose (mmol/l)	Cold glucose per 100 µl of media (nmol)	CPM in 100 µl of media	SA of the media (CPM/nmol glucose)
3.7 (0.1)	1	100	*a*	*a*/100
7.4 (0.2)	5	500	*b*	*b*/500
11.1 (0.3)	15	1500	*c*	*c*/1500
14.8 (0.4)	25	2500	*d*	*d*/2500
14.8 (0.4)	35	3500	*d*	*d*/3500

SA: specific activity; CPM: counts per minute.

Trophoblasts were incubated in a humidified incubator at 37ºC, 5% CO_2 for 2 h. Immediately after incubation, plates were placed on ice to stop metabolism. Trophoblasts were washed twice in 500 µl cold PBS to remove unmetabolised [(U)^{14}C]-2-deoxyglucose. Trophoblasts, which contained intracellular phosphorylated tracer, were then scrapped twice in cold 500 µl PBS on ice and collected into scintillation vials. Ten ml of scintillation liquid was added to the vials and intracellular accumulation of [(U)^{14}C]-2-deoxyglucose-6-phosphate was counted in a betacounter (Tri-Carb B3110TR Liquid Scintillation Analyzer, Perkin Elmer, Waltham, MA, USA) (Figure 3.3). Negative controls (wells without cells) were included in all experiments. Each condition was measured in triplicate (3 wells) for samples and blanks in each individual experiment.

The same procedures were followed for glucose uptake in long-term cultures, however the studies were carried out after 5 days of culture in DMEM 5.5 mM plus EGF (10 ng/ml), as described in Section 3.1.2.1, and the cells were plated in 6 well plates. Also, less conditions were assessed (5 or 25 mM glucose plus or minus 0.25 mM NEFA).

[(U)^{14}C]-2-deoxyglucose concentrations were selected according to the cold glucose concentrations (Table 3.2). For total glucose uptake calculation, the radiation in 100 µl of [(U)^{14}C]-2-deoxyglucose media for each glucose concentration was counted in triplicates and SA in CPM per nmol was calculated (Table 3.2) (refer to section 3.1.1.1). Total glucose uptake was calculated subtracting the background CPM from the sample CPM and dividing the result by the SA. Results were normalised by mg of protein and expressed as total glucose uptake in nmol/h/mg protein.

$$\text{Total glucose uptake (nmol gluc/h/mg protein)} = \frac{(\text{cpm samples} - \text{cpm background})/\text{specific activity}}{\text{mg protein x 2 h (incubation period)}}$$

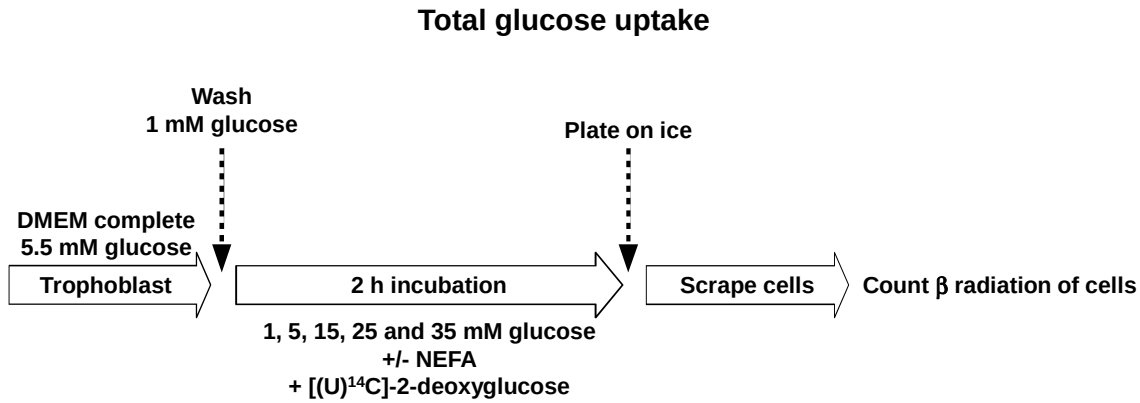

Figure 3.3. Total glucose uptake by trophoblast-protocol scheme. For short-term culture studies, trophoblasts were established in culture for 36 h in complete DMEM at 5.5 mM glucose in 12 well plates. Cells were washed twice in KRBH, 0.1% BSA-FA free and 1 mM glucose. Cells were then incubated in 1 ml of KRBH containing 0.5% BSA-FA free, $[(U)^{14}C]$-2-deoxyglucose (amount according to Table 3.2), 1, 5, 15, 25 or 35 mM glucose, plus or minus 0.25 mM NEFA. After 2 h incubation (37ºC, 5% CO_2), plates were placed on ice to stop the metabolism. Cells were washed twice in cold PBS. Trophoblasts were scrapped twice in 500 µl cold PBS and collected into scintillation vials. Ten ml of scintillation liquid was added to each vial. Intracellular radiation was counted in a betacounter and total glucose uptake by trophoblasts was calculated.

For long-term culture experiments, trophoblasts were established in culture for 5 days in complete DMEM at 5.5 mM glucose supplemented with EGF (10 ng/ml) in 6 well plates. Incubations were performed in 2 ml KRBH, 0.5% BSA-FA free, $[(U)^{14}C]$-2-deoxyglucose (see Table 3.2), 5 or 25 mM glucose, plus or minus 0.25 mM NEFA. All other procedures were the same as for short-term culture total glucose uptake experiments.

DMEM: Dulbecco's Modified Eagle Medium; KRBH: Krebs-Ringer Bicarbonate HEPES; BSA: bovine serum albumin; FA: fatty acid; NEFA: non-esterified fatty acids; PBS: phosphate buffered saline; EGF: epidermal growth factor.

3.1.2.3 Glycolysis

Glucose utilisation rate via glycolysis by trophoblasts was measured with [5-^{3}H]-glucose tracer. [5-^{3}H]-glucose loses its ^{3}H into ^3H_2O at the reaction catalysed by aldolase, in which fructose 1,6-bisphosphate is cleaved into glyceraldehyde 3-phosphate and dihydroxyacetone-phosphate (refer to Chapter 1 section 1.5.2). If this reaction is not complete, ^3H_2O is produced at the enolase reaction, when 2-phosphoglycerate is dehydrated to phosphoenolpyruvate (284). Therefore, glycolysis can be measured by determining the amount of ^3H_2O production (Figure 3.4). In theory, other glucose metabolic pathways, such as the pentose phosphate or glycogen synthesis, cannot be measured using this method, making [5-^{3}H]-glucose a suitable tracer for glycolysis estimation. For short-term culture studies, trophoblasts were cultured for 36 h in complete DMEM (5.5 mM glucose) in 12 well plates in a density of 1.4 x 10^6 cells per well as described in Section 3.1.2.1. Trophoblasts were washed twice in 1 ml of warm KRBH, 0.1% BSA-FA free at 1 mM glucose. Because ^3H_2O can be formed inside [5-^{3}H]-glucose storage bottles due to radiolysis (285), for all experiments [5-^{3}H]-glucose tracer was evaporated under nitrogen gas prior to the media preparation so as to avoid ^3H_2O contamination. One ml of KRBH incubation containing 0.5% BSA-FA free, [5-^{3}H]-glucose (see Table 3.3 for amount) at 1, 5 or 15 mM glucose, plus or minus 0.25 mM NEFA, was added to each well. As blank controls, wells with media, but no cells, were treated like samples (background). After 2 h incubation in a humidified cell culture incubator at 37ºC, 5% CO_2, the supernatant with ^3H_2O from metabolised glucose was transferred to 1.5 ml microtubes. Microtubes were then centrifuged (2095 *g*, 5 minutes, 4ºC) to precipitate cell debris. Following the centrifugation, 300 µl of the supernatant from each tube was transferred to new 1.5 ml microtubes without caps. These tubes were carefully placed with tweezers into scintillation vials containing 500 µl of sterile cold Milli-Q water at the bottom. Vials were tightly closed and kept at 55ºC for 24 h. ^3H_2O

produced by trophoblasts was recovered through evaporation and equilibrium with the cold water in the bottom of each scintillation vial. After incubation, scintillation vials were placed at room temperature for 2 h to reduce water drops on vial walls. Microtubes with unmetabolised tracer were discarded and 10 ml of scintillation liquid was added to each sample, which was counted in a betacounter. Recovered $^{3}H_2O$ counts represent metabolised glucose tracer via glycolysis by trophoblasts. Recovery efficiency was estimated through evaporation and equilibrium of a known quantity of $^{3}H_2O$. Thus, 300 µl of $^{3}H_2O$ (1:160 dilution in Milli-Q water) was equilibrated with 500 µl cold water through evaporation under the same conditions as the control blank and experimental samples to measure recovery efficiency (Figure 3.4). Equilibrated $^{3}H_2O$ at the bottom of the scintillation vial and 300 µl of unequilibrated $^{3}H_2O$ solution were counted in a betacounter and the percentage recovery was calculated. Samples, blanks and efficiency of $^{3}H_2O$ recovery tubes were measured in triplicates and results for the samples were normalised by mg of protein.

For long-term culture experiments, the same procedures were performed with the exception of that trophoblasts were established in complete DMEM at 5.5 mM glucose plus EGF (10 ng/ml) for 5 days after the isolation, as described in Section 3.1.2.1, and glycolysis was measured at media cold glucose concentrations of 1, 5 and 25 mM.

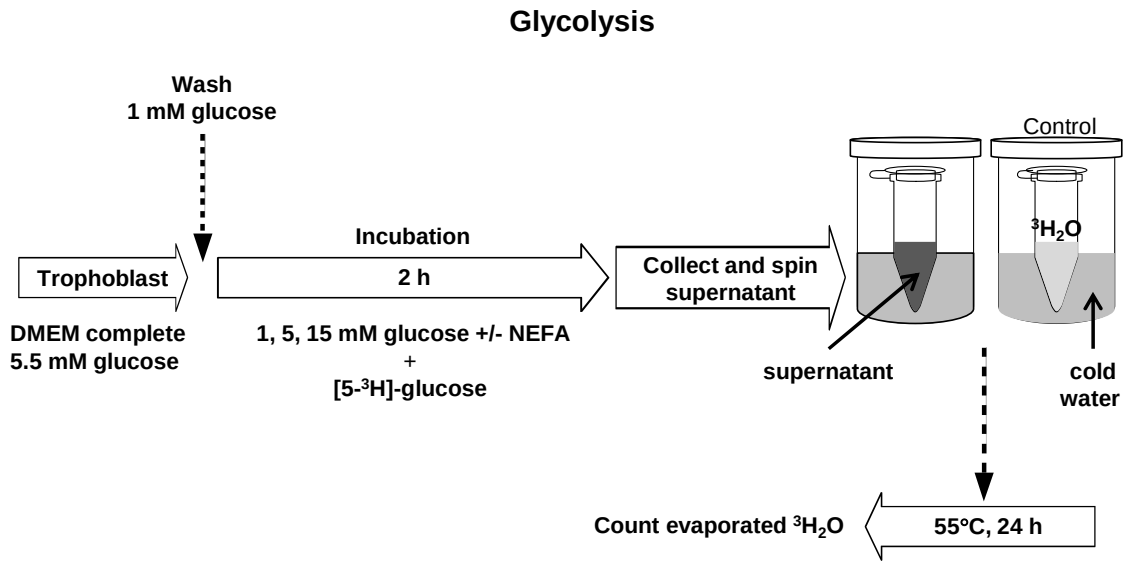

Figure 3.4. Glycolysis-protocol scheme. Trophoblasts were established in culture for 36 h in complete DMEM at 5.5 mM glucose for short-term culture studies; and for 5 days in complete DMEM at 5.5 mM glucose plus EGF (10 ng/ml) for long-term culture studies. Cells were washed twice in KRBH, 0.1% BSA-FA free and 1 mM glucose. Trophoblasts were then incubated for 2 h (37ºC, 5% CO_2) in 1 ml of KRBH containing 0.5% BSA-FA free, [5-^{3}H]-glucose (see Table 3.3 for amount), plus or minus 0.25 mM NEFA and 1, 5 or 15 mM glucose (for short-term culture studies) or 1, 5 or 25 mM glucose (for long-term culture studies). After incubation, the media was collected and centrifuged. Produced tritiated water in the supernatants was recovered into cold water through evaporation and equilibration at 55ºC for 24 h. Equilibrated tritiated water was counted in a betacounter with 10 ml of scintillation cocktail. Efficiency of ^3H_2O recovery was calculated by measuring the amount of known tritiated water (in triplicate) recovered by the equilibration procedure at the same time as the experimental samples and blanks were analysed. This method was adapted from Pathmaperuma *et al.* (200) with modifications. DMEM: Dulbecco's Modified Eagle Medium.; KRBH: Krebs-Ringer Bicarbonate HEPES; BSA: bovine serum albumin; FA: fatty acid; NEFA: non-esterified fatty acids; EGF: epidermal growth factor.

The amounts of [5-^{3}H]-glucose used in preparation of the media according to the cold glucose concentrations are described in Table 3.3. For the glycolysis rate calculations, the radiation in 100 µl of [5-^{3}H]-glucose containing media for each glucose concentration was counted in triplicates and SA in CPM per nmol was calculated (Table 3.3). Total ^3H_2O produced was calculated subtracting the background CPM from the sample CPM, multiplying by 100% divided by percentage of recovery (equilibration efficiency). Since, from 1 ml of [5-^{3}H]-glucose media added to each well and metabolised, only 300 µl was placed to be equilibrated, total ^3H_2O produced was corrected multiplying by 1000/300.

$$\text{Total } ^3\text{H2O production} = (\text{cpm sample} - \text{cpm blank}) \times \frac{1000}{300} \times \frac{100\%}{\text{recovery efficiency}}$$

$$\text{Glucose metabolism via glycolysis(nmol gluc/h/mg protein)} = \frac{\text{total } ^3\text{H2O production/specific activity}}{\text{mg protein x 2 h (incubation period)}}$$

Table 3.3

[5-^{3}H]-glucose specific activity for glycolysis protocol

[5-^{3}H]-glucose kBq/ml (µCi/ml)	Cold glucose (mmol/l)	Cold glucose per 100 µl of media (nmol)	CPM in 100 µl of media	SA of the media (CPM/nmol glucose)
18.5 (0.5)	1.0	100	*a*	*a*/100
37 (1.0)	5.0	500	*b*	*b*/500
55.5 (1.5)	15.0	1500	*c*	*c*/1500
55.5 (1.5)	25.0	2500	*d*	*d*/2500

SA: specific activity; CPM: counts per minute.

3.1.2.4 Total lactate release into the media

At the end of glycolysis, 2 pyruvate molecules are generated per glucose molecule. In anaerobic conditions or in tissues such as the placenta, which can produce high levels of lactate in spite of adequate oxygen supply (148), pyruvate can be reduced by LDH and converted to lactate (refer to Chapter 1 section 1.5.3) **(**Figure 3.5).

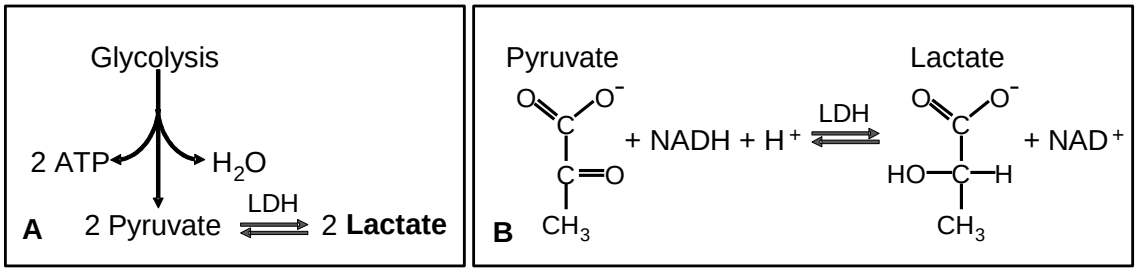

Figure 3.5. Pyruvate and lactate production. A. At the end of glycolysis, 2 molecules of pyruvate are produced per glucose molecule. B. Pyruvate can be reduced by lactate dehydrogenase (LDH) and converted to lactate.

Trophoblasts were established in culture for 36 h in complete DMEM (5.5 mM glucose) in 12 well plates in a density of 1.4 x 10^6 cells per well after the isolation, as described in Section 3.1.2.1. Cells were washed twice in 1 ml of warm KRBH, 0.1% BSA-FA free and 1 mM glucose. Trophoblasts were then incubated for 2 h (37ºC, 5% CO_2) in 400 µl of KRBH containing 0.5% BSA-FA free, 1, 5 or 15 mM glucose, plus or minus 0.25 mM NEFA, in triplicate. At the end of the incubation, supernatant was quickly collected, centrifuged (2095 *g*, 5 minutes, 4ºC) to remove cell debris and frozen at -80ºC (Figure 3.6). An enzymatic colorimetric kit (BioVision, Milpitas, CA, USA) was used to measure the total amount of lactate released by trophoblasts. The principle of this method is to oxidise the lactate present in the samples and standards by a reaction catalyzed by LDH (Figure 3.5). NADH, a co-product of this reaction, interacts with a probe producing a colour that can be read. The assay was performed according to the manufacturer instructions as follow: "lactate subtract mix" was dissolved in 220 µl of "lactate assay buffer"; "lactate enzyme mix" was also resuspended in 220 µl of "lactate assay buffer". For the standard curve preparation, 10 µl of lactate standard was diluted into 990 µl "lactate assay buffer" and serial dilutions were then prepared by adding "lactate assay buffer" to the diluted lactate standard to produce 0, 2, 4, 6, 8 and 10 nM of lactate. "Lactate assay buffer", "lactate subtract mix" and "lactate enzyme mix" were mixed to prepare the "reaction mix" in the proportion 46 µl: 2 µl: 2 µl, respectively. "Reaction mix" total volume was determined by the number of samples and standards of each assay. Fifty µl of undiluted samples and 50 µl of the standards were added to a 96 well microplates. Both samples and standards were added to the wells in duplicates. Fifty µl of the "reaction mix" was added to wells loaded with samples and standards and the plate was incubated for 30 minutes at room temperature. After colour development, standards and samples were placed in a microplate reader at absorbance 450 nm (Fluostar Optima BMG, LabTech, Offenburg, Germany). Results were normalised by mg of protein.

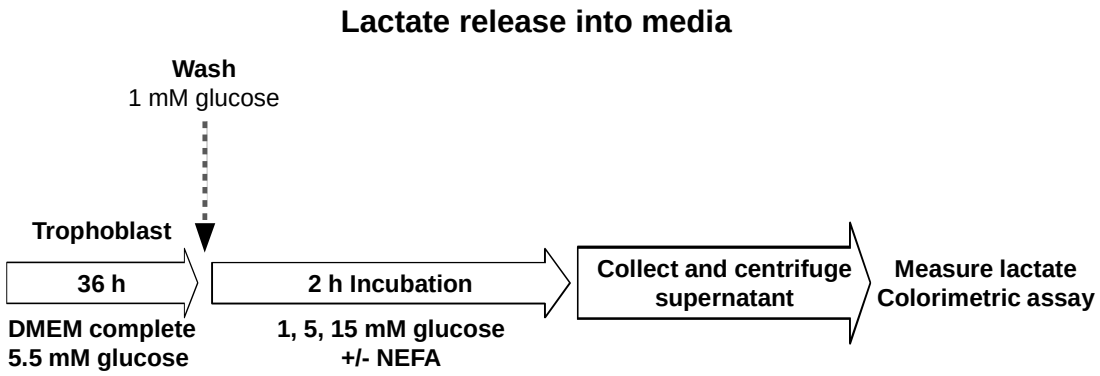

Figure 3.6. Lactate release into media-protocol scheme. Trophoblasts were established in culture for 36 h in DMEM at 5.5 mM glucose. Cells were washed twice in 1 ml KRBH, 0.1% BSA-FA free at 1 mM glucose. Trophoblasts were then incubated for 2 h (37ºC, 5% CO_2) in 400 µl of KRBH containing 0.5% BSA-FA free, 1, 5 or 15 mM glucose, plus or minus 0.25 mM NEFA. At the end of incubation, the media was collected, centrifuged and the supernatant was transferred to new microtubes. Lactate release was quantified using an enzymatic colorimetric assay.

DMEM: Dulbecco's Modified Eagle Medium.; KRBH: Krebs-Ringer Bicarbonate HEPES; BSA: bovine serum albumin; FA: fatty acid; NEFA: non-esterified fatty acids.

3.1.2.5 Glucose and palmitate oxidation

Glucose oxidation was measured through $^{14}CO_2$ production from [(U)^{14}C]-glucose during the TCA cycle (Figure 3.7).

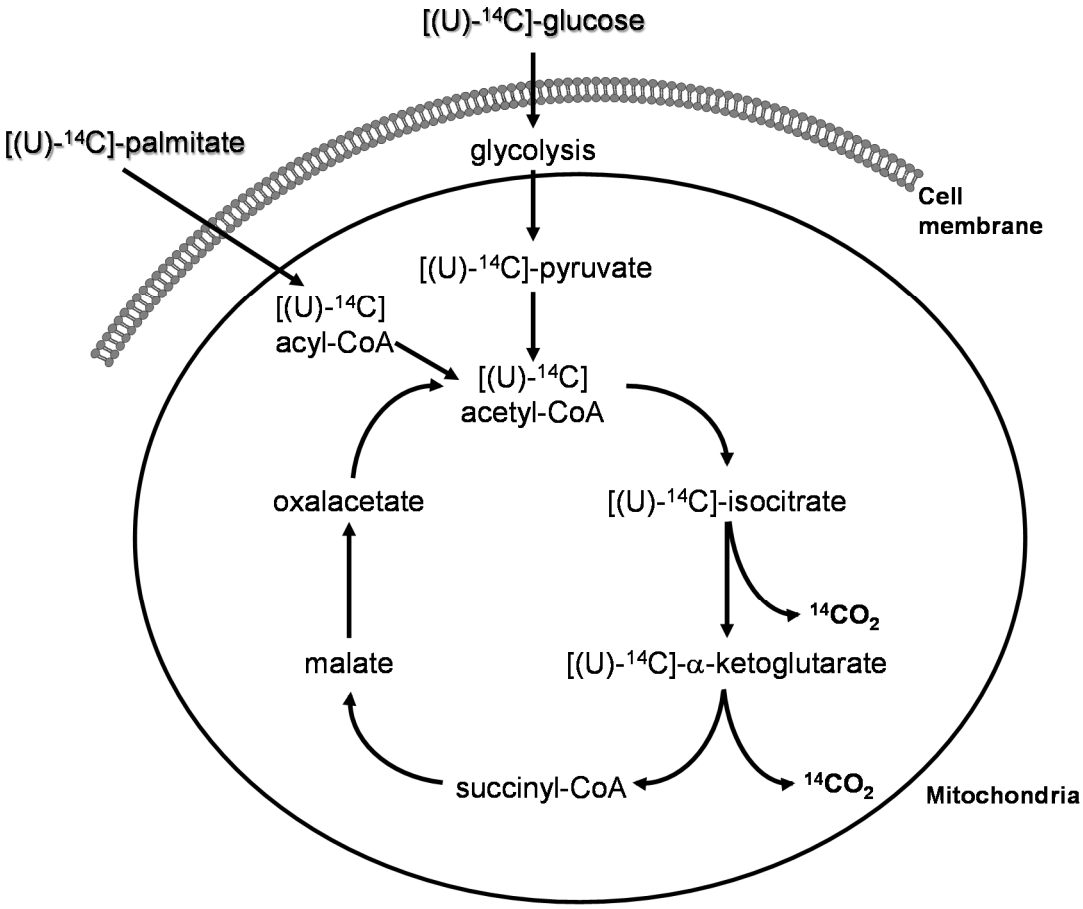

Figure 3.7. Glucose and palmitate oxidation. Glucose and palmitate carbons are changed to the acetyl group of acetyl-CoA, which will enter the mitochondria to be oxidised in the tricarboxylic acid cycle. At one turn of this cycle, 2 CO_2 molecules are produced in oxidative decarboxylation steps.

For short-term cultures, trophoblasts were established in culture for 36 h in complete DMEM at 5.5 mM glucose, as described in Section 3.1.2.1. On the experimental day, media was removed and trophoblasts were washed twice in 2 ml of warm KHBH, 0.1% BSA-FA free at 1 mM glucose. Then, 2 ml of incubation solution containing KRBH, 0.5% BSA-FA free, 1, 5 or 25 mM glucose, [(U)^{14}C]-glucose, plus or minus 0.25 mM NEFA was added to assess glucose oxidation (refer to Table 3.4 for [(U)^{14}C]-glucose concentration according to cold glucose).

Table 3.4

[(U)^{14}C]-glucose specific activity for glucose oxidation protocol

[(U)^{14}C]-glucose kBq/ml (μCi/ml)	Cold glucose (mmol/l)	Cold glucose per 100 μl of media (nmol)	CPM in 100 μl of media	SA of the media (CPM/nmol glucose)
3.7 (0.1)	1	100	*a*	*a*/100
7.4 (0.2)	5	500	*b*	*b*/500
14.8 (0.4)	25	2500	*d*	*d*/2500

SA: specific activity; CPM: counts per minute.

After adding incubation solution to cells, the flasks were caped with rubber stoppers to avoid gas leakage. Those stoppers were prepared in advance with tubing containing filter paper soaked in 5% KOH to trap $^{14}CO_2$ expelled by the cells (refer to Appendix 2 for all preparation details). At the end of the incubation, 200 μl of 40% (vol/vol) PCA was injected into the flasks with a syringe (1 ml, Tuberculin syringe, BD, Singapore) and a needle (25 gauge, Precision Glide Needle, BD, Singapore) through the cap to acidify the medium and liberate the CO_2. Flasks with PCA were left overnight at room temperature. Next morning, filters were removed from the end of tubing with tweezers and placed into scintillation vials. Ten ml of scintillation liquid was added in the vials and left for at least 12 h to allow CO_2 to leach out of the filter. Then, the samples were counted in a betacounter. As a direct comparison, palmitate oxidation was performed at the same time using a similar method. For palmitate oxidation, 2 ml of a solution containing 5 or 25 mM

glucose, 0.1 mM L-carnitine, 0.1 mM palmitate and [(U)^{14}C]-palmitate (final concentration: 0.1 μC/ml) was added to each flask (Figure 3.8). Only for palmitate oxidation, the incubation solution with PCA and dead cells was collected into 2 ml microtubes after the paper filter (with $^{14}CO_2$) removal. The solution was centrifuged (2095 *g*, 5 minutes, 4ºC) to precipitate the debris. The supernatant containing acid soluble fatty acid oxidation intermediates, such as ketone bodies, short-chain fatty acids and TCA cycle intermediates (Figure 3.9), was transferred into scintillation vials with scintillation liquid and counted in a betacounter. All samples and controls (flasks without cells) were performed at least in duplicates (if the trophoblast yield from isolation was enough, samples were performed in triplicates).

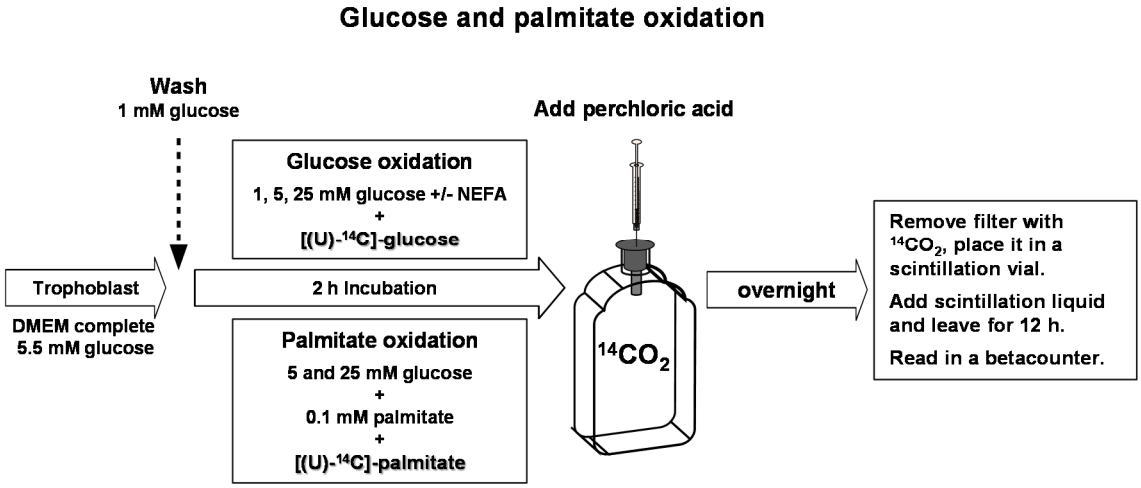

Figure 3.8. Glucose and palmitate oxidation in short-term cultures. For short-term culture studies, trophoblasts were established in culture in T25 flasks for 36 h in complete DMEM (5.5 mM glucose). Cells were washed twice in 2 ml of KHBH, 0.1% BSA-FA free and 1 mM glucose. Then, 2 ml of KRBH, 0.5% BSA-FA free, 1, 5 and 25 mM glucose plus or minus 0.25 mM NEFA and [(U)^{14}C]-glucose (for amount refer to table 3.4) were added to assess glucose oxidation. For palmitate oxidation, 2 ml of a solution containing 5 or 25 mM glucose, 0.1 mM L-carnitine, 0.1 mM palmitate and [(U)^{14}C]-palmitate (final concentration: 0.1 μC/ml) (for amount refer to table 3.5) were added. After 2 h incubation in a humidified incubator at 37ºC and 5% CO_2, 200 μl of 40% PCA was injected into the flasks and left overnight. Next morning, filters containing $^{14}CO_2$ were removed and transferred to scintillation vials. Ten ml of scintillation cocktail was added and after 12 h, samples were read in a betacounter. For palmitate oxidation, after filter removal, the solution containing cellular debris, PCA and incubation solution from each sample was transferred to 2 ml microtubes and centrifuged. Supernatant was placed in scintillation vials. Ten ml of scintillation cocktail were added and acid soluble products were read in a betacounter.

For long-term culture studies, trophoblasts were established in culture in T25 flasks for 5 days in complete DMEM (5.5 mM glucose) with EGF (10 ng/ml). All procedures were performed as for short-term cultures, except that the cells were incubated only at 5 and 25 mM for glucose oxidation experiments. This method was adapted from (152) with modifications.

DMEM: Dulbecco's Modified Eagle Medium; KHBH: Krebs-Ringer Bicarbonate HEPES; BSA: bovine serum albumin; FA: fatty acid; NEFA: non-esterified fatty acids; PCA: perchloric acid; EGF: epidermal growth factor.

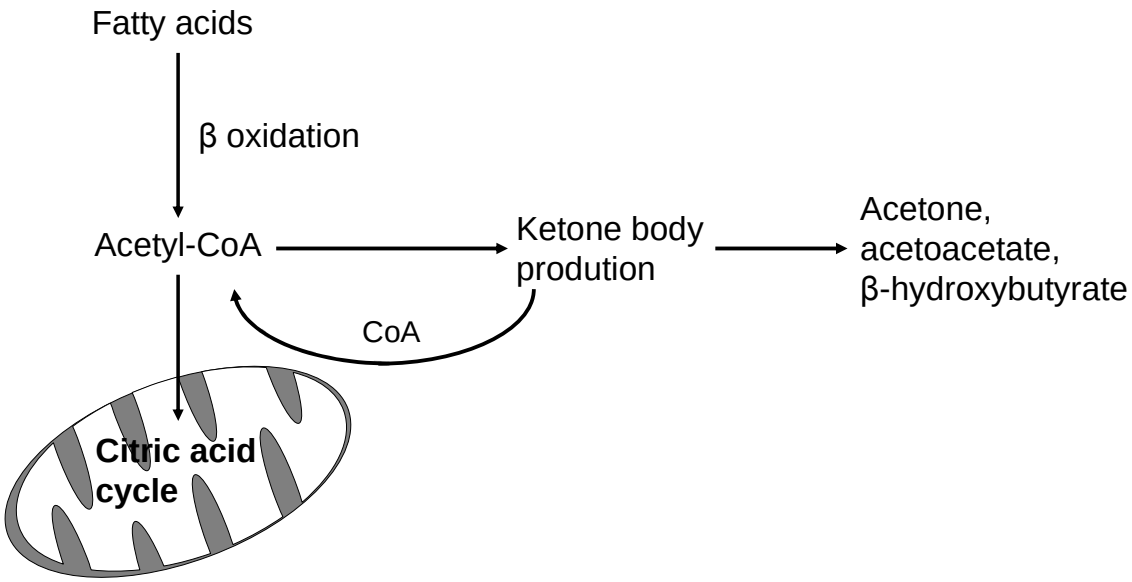

Figure 3.9. Fatty acid oxidation, ketone body production and acid soluble products. Fatty acids can be metabolised to acetyl-CoA and skip the TCA cycle especially in conditions which deplete oxaloacetate. In this situation, the TCA cycle activity will be reduced and acetyl-CoA conversion will be shifted to ketone body production. Ketone bodies as well as short-chain fatty acids and metabolites such as citrate can together be measured as acid soluble products of fatty acid metabolism.

TCA: tricarboxylic acid.

To calculate glucose and palmitate oxidation, the radiation in 100 µl of [(U)^{14}C]-glucose containing media and in 100 µl of [(U)^{14}C]-palmitate containing media was counted in triplicates and SA in CPM per nmol for each was calculated (Tables 3.4 and 3.5). Oxidation was calculated subtracting the background CPM from the sample CPM and dividing the result by SA. Also, soluble acid products were calculated subtracting the background CPM from the sample CPM and dividing the result by SA. Results were normalised by mg of protein and expressed nmol/h/mg protein.

$$\text{Glucose oxidation (nmol gluc/h/mg protein)} = \frac{(\text{cpm samples} - \text{cpm background})/\text{specific activity}}{\text{mg protein x 2 h (incubation period)}}$$

$$\text{Palmitate oxidation (nmol palm/h/mg protein)} = \frac{(\text{cpm samples} - \text{cpm background})/\text{specific activity}}{\text{mg protein x 2 h (incubation period)}}$$

$$\text{Acid soluble products (nmol palm/h/mg protein)} = \frac{(\text{cpm samples} - \text{cpm background})/\text{specific activity}}{\text{mg protein x 2 h (incubation period)}}$$

Table 3.5

[(U)^{14}C]-palmitate specific activity for palmitate oxidation protocol.

[(U)^{14}C]-2-deoxyglucose kBq/ml (µCi/ml)	Cold palmitate (mmol/l)	Cold glucose per 100 µl of media (nmol)	CPM in 100 µl of media	SA of the media (CPM/nmol glucose)
3.7 (0.1)	1	10	*A*	*A*/10

SA: specific activity; CPM: counts per minute.

3.1.2.6 Glycogen synthesis measured with tracer

[(U)^{14}C]-glucose tracer was used to measure glucose flux into glycogen. It is assumed that a glucose molecule with all carbons labelled is metabolised as a glucose molecule (Figure 3.10). The amount of [(U)^{14}C]-glucose tracer stored as glycogen can be assessed through precipitation of glycogen.

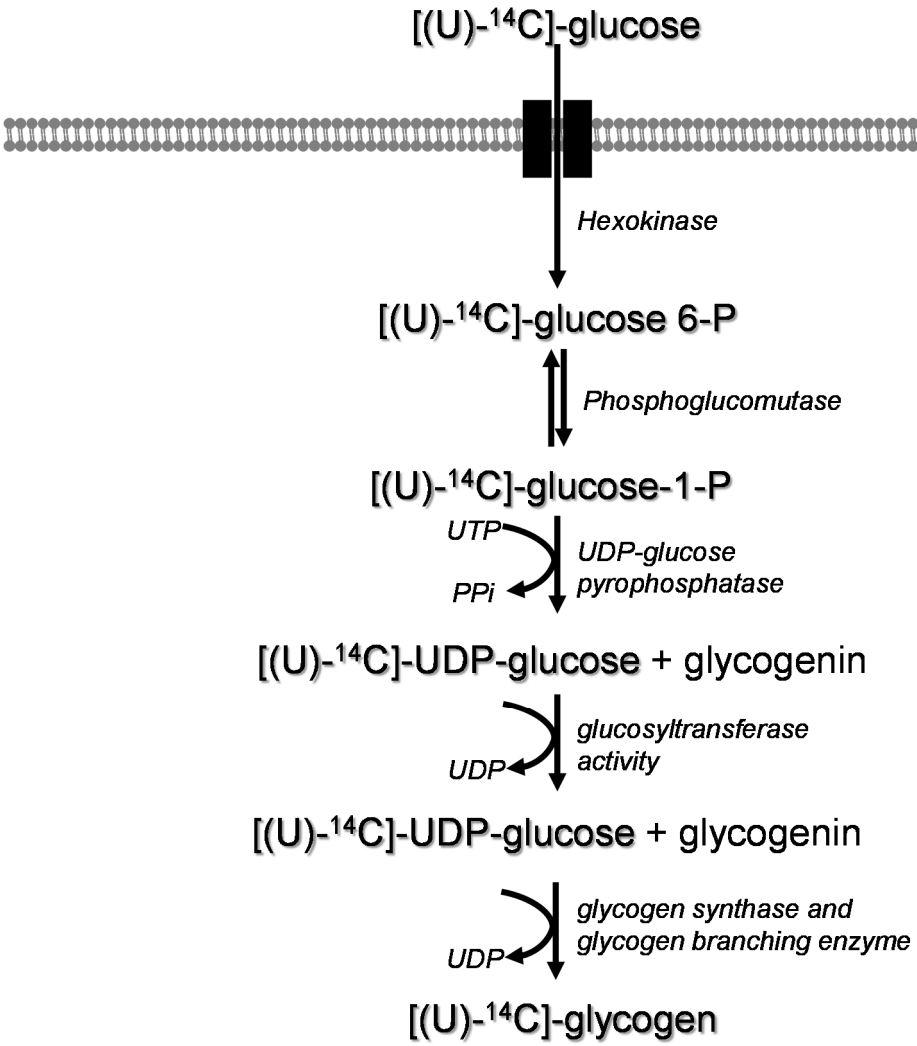

Figure 3.10. Glycogen synthesis with tracer. Glucose can be stored into trophoblasts as glycogen. It is assumed that the [(U)^{14}C]-glucose tracer is metabolised into glycogen the same way that cold glucose tracee is metabolised. [(U)^{14}C]-glucose tracer is taken up by trophoblasts, phosphorylated and then converted to [(U)^{14}C]-glucose-1-phosphate by phosphoglucomutase. UDP-glucose pyrophosphatase adds an UDP to [(U)^{14}C]-glucose-1-phosphate and a [(U)^{14}C]-UDP-glucose molecule is formed. Finally, glycogen synthase adds UDP-glucose molecules to elongate the glycogen chain.
UTP: uridine triphosphate; UDP: uridine diphosphate.

For short-term culture experiments, trophoblasts were cultured for 36 h in complete DMEM at 5.5 mM glucose in 12 well plates, as described in Section 3.1.2.1. Cells were washed twice in 1 ml of warm washing solution. One ml of incubation KRBH solution containing [(U)^{14}C]-glucose (for amount see Table 3.6), 0.5% BSA-FA free, at glucose concentrations of 1, 5, 15, 25 or 35 mM, in the presence or absence of 0.25 mM NEFA was added to the cultured cells. Wells with media, but no cells, were treated like samples to measure the background. After 2 h incubation in a humidified incubator 37ºC, 5% CO_2, microplates were placed on ice to avoid glycogen hydrolysis. Cells were washed twice in 500 µl cold PBS to remove the background. Trophoblasts were then scraped twice on ice in 500 µl cold PBS, collected into 1.5 ml microtubes and centrifuged (335 *g*, 10 minutes, 4ºC). After centrifugation, supernatant was discarded and samples were quickly placed on dry ice and stored at -80ºC (Figure 3.11).

Table 3.6

[(U)^{14}C]-glucose specific activity for glycogen protocol

[(U)^{14}C]-glucose kBq/ml (µCi/ml)	Cold glucose (mmol/l)	Cold glucose per 100 µl of media (nmol)	CPM in 100 µl of media	SA of the media (CPM/nmol glucose)
3.7 (0.1)	1	100	*a*	*a*/100
7.4 (0.2)	5	500	*b*	*b*/500
11.1 (0.3)	15	1500	*c*	*c*/1500
14.8 (0.4)	25	2500	*d*	*d*/2500
14.8 (0.4)	35	3500	*d*	*d*/3500

SA: specific activity; CPM: counts per minute.

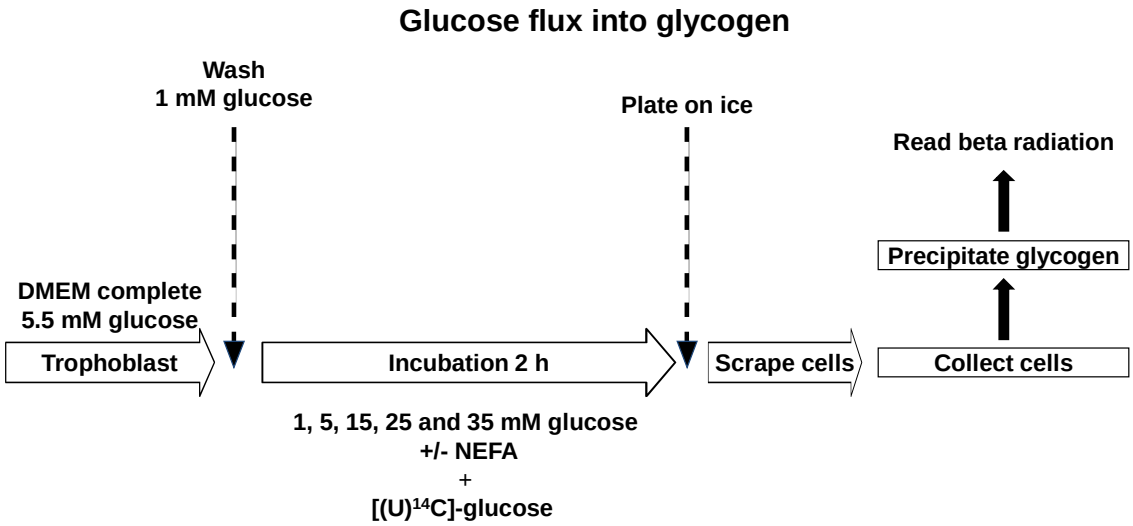

Figure 3.11. Glucose flux into glycogen-protocol scheme. For short-term culture studies, trophoblasts were established in culture for 36 h in complete DMEM at 5.5 mM glucose in 12 well plates. Cells were washed twice in KRBH, 0.1% BSA-FA free and 1 mM glucose. Cells were then incubated in 1 ml of KRBH containing 0.5% BSA-FA free, $[(U)^{14}C]$-glucose (see Table 3.6 for amount), at 1, 5, 15, 25 or 35 mM cold glucose concentrations, plus or minus 0.25 mM NEFA. After 2 h incubation (37ºC, 5% CO_2), plates were placed on ice to stop the metabolism. Cells were washed twice in cold PBS. Trophoblasts were then scrapped twice in ice 500 µl cold PBS, collected into 1.5 ml microtubes and centrifuged. After centrifugation, the supernatants were discarded and samples were quickly placed on dry ice and stored at -80ºC into microtubes. Later, glycogen was precipitated (see text for procedure description). Samples were diluted in water and collected into scintillation vials. Scintillation liquid was added to the samples and radiation was counted in a betacounter.

For long-term culture experiments, trophoblasts were established in culture for 5 days in complete DMEM at 5.5 mM glucose supplemented with EGF (10 ng/ml) in 6 well plates, as described in Section 3.1.2.1. Incubations were performed in 2 ml KRBH containing 0.5% BSA-FA free, $[(U)^{14}C]$-glucose (refer to Table 3.6) at 5 or 25 mM cold glucose, plus or minus 0.25 mM NEFA. All other procedures were done as for short-term culture experiment.

DMEM: Dulbecco's Modified Eagle Medium.; KRBH: Krebs-Ringer Bicarbonate HEPES; BSA: bovine serum albumin; FA: fatty acid; NEFA: non-esterified fatty acids; EGF: epidermal growth factor.

Later, 30 µl of 30% KOH (Appendix 2) was added to the pellets, which were heated at 70ºC for 30 minutes until the pellets were digested. Fifteen µl of 6% Na_2SO_4 was added to the samples and thoroughly mixed with up and down pipetting plus vortexing for glycogen digestion. To make a final methanol concentration of 70%, 105 µl of 100% methanol was added to each of the samples, which were placed overnight at -20ºC to allow glycogen precipitation. On the next day, samples were centrifuged (1000 *g*, 30 sec, 4ºC) and supernatants were discarded. Pellets were then washed twice by adding 1 ml of 100% methanol, vortexing, centrifuging (1000 *g*, 30 seconds, 4ºC) and discarding the supernatant. After pellet washing, tubes were placed on a heating block at 50ºC to completely evaporate methanol. When dry, pellets were resuspended in 400 µl of Milli-Q water and collected into scintillation vials. Ten ml of scintillation cocktail was added to each vial and the samples were counted in a betacounter.

For long-term culture experiments, trophoblasts were cultured for 5 days from the isolation in complete DMEM (5.5 mM glucose) with EGF (10 ng/ml) in 6 well plates. All procedures were the same as for the short-term cultures, except that the cells were incubated in 5 or 25 mM glucose and all the reagent volumes were adjusted according to the well size. Well size was changed because the signal obtained from glucose flux into glycogen experiments in long-term trophoblasts cultured in 12 well plates (1.4×10^6 cells per well) was low. Thus, cells were plated in 6 well plates (3.5×10^6 cells per well) to enable higher readings. The glycogen precipitation method was adapted from Walaas *et al.* (286) with modifications.

For glycogen calculation, the radiation in 100 µl of [(U)^{14}C]-glucose media for each glucose concentration was counted in triplicates and SA in CPM per nmol was calculated (Table 3.6). Glycogenesis was calculated subtracting the background CPM from the sample CPM and dividing the result by SA. Results were normalised by mg of protein and expressed as nmol glucose incorporated into glycogen/h/mg protein.

$$\text{Glycogen (nmol glucose incorporated/h/mg protein)} = \frac{(\text{cpm samples} - \text{cpm background})/\text{specific activity}}{\text{mg protein x 2 h (incubation period)}}$$

3.1.2.7 Total glycogen content

In parallel to glycogen synthesis with tracer, total glycogen content was measured in experiments performed without [$U^{14}C$]-glucose tracer. Trophoblasts were cultured for 36 h in complete DMEM at 5.5 mM glucose. To deplete glycogen immediately prior to the experiment, however, cells were pre-incubated for 2 h in complete DMEM at 1 mM glucose concentration (Appendix 2). After the pre-incubation, trophoblasts were washed twice in 2 ml of warm washing solution and 2 ml of incubation solution containing glucose at 1, 5, 15, 25 and 35 mM glucose concentration in the presence or absence of NEFA mix was added to the cells. After 2 h incubation (37ºC, 5%, CO_2), plates were placed on ice and cells were washed twice in 2 ml of cold PBS. Trophoblasts were then scraped twice on ice in 1 ml cold PBS, collected into 2 ml microtubes and centrifuged (335 *g*, 10 minutes, 4ºC). After centrifugation, supernatant was discarded and samples were placed on dry ice and stored at -80ºC. Later, glycogen precipitation was performed as for the glycogen synthesis with tracer method. Following methanol evaporation on a heating block, the pellets were resuspended in 50 µl amyloglucosidase (2 mg/ml) solution (Appendix 2) and placed into a water bath at 40ºC for 90 minutes to hydrolyze glycogen to glucose. Glucose was then measured using an enzymatic colorimetric kit (Appendix 2). Glycogen was also measured from samples cultured in complete DMEM at 5.5 mM glucose concentration to determine the "basal glycogen". Glycogen from bovine liver was used as a control (Appendix 2). Figure 3.12 shows the scheme for assessment of trophoblast glycogen content according to incubation conditions.

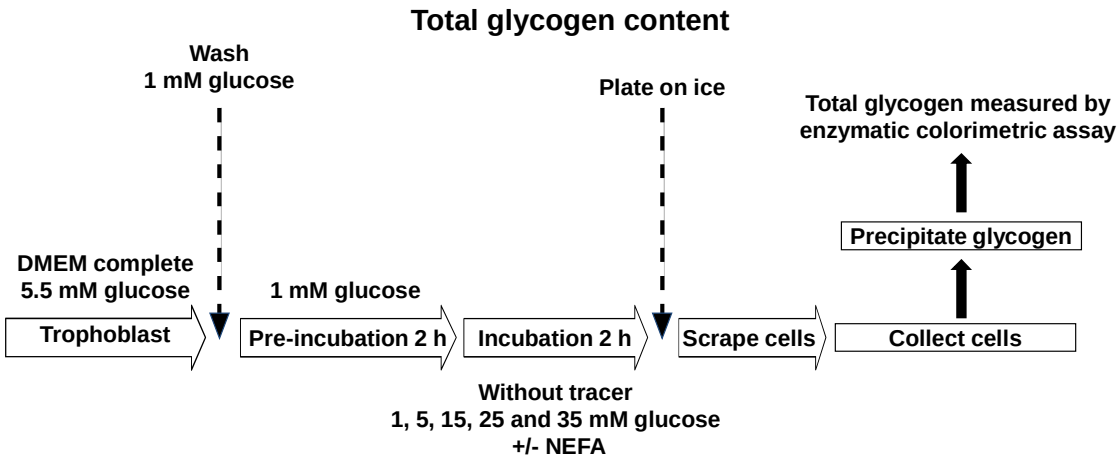

Figure 3.12. Total glycogen content-protocol scheme. Trophoblasts were established in culture for 36 h in complete DMEM at 5.5 mM glucose in 6 well plates. Cells were washed twice in KRBH, 0.1% BSA-FA free and 1 mM glucose, pre-incubated for 2 h in 400 µl KRBH, 0.1% BSA-FA free and 1 mM glucose. After removal of the pre-incubation media, cells were incubated for 2 h (37ºC, 5% CO_2) in 400 µl of KRBH, 0.5% BSA-FA free, at 1, 5, 15, 25 and 35 mM glucose concentrations plus or minus 0.25 mM NEFA. The plates were then placed on ice to stop the metabolism and cells were washed twice in cold PBS. Trophoblasts were then scrapped twice in 500 µl of ice cold PBS, collected into 1.5 ml microtubes and centrifuged. Following centrifugation, supernatant was discarded and samples were quickly placed on dry ice and stored at -80ºC. Later, glycogen was precipitated (see text for procedure description). After glycogen precipitation, pellets were resuspended in amyloglucosidase (2 mg/ml) solution and incubated into a water bath at 40ºC for 90 minutes to hydrolyze glycogen into glucose. Glucose was then measured using an enzymatic colorimetric kit. Glycogen basal was defined as glycogen from samples cultured in complete DMEM at 5.5 mM glucose concentration without incubations in KRBH. Refer to Appendix 2 for reagents and solutions.

DMEM: Dulbecco's Modified Eagle Medium.; KRBH: Krebs-Ringer Bicarbonate HEPES; BSA: bovine serum albumin; FA: fatty acid; NEFA: non-esterified fatty acids.

3.1.3 Trophoblast protein content

Trophoblast protein content was used to normalise the results to take in account any variation in cell number per well or flask in each experiment. At the same time point as for the metabolism studies, the cells were washed twice in cold PBS and scraped twice on ice (in 500 µl of PBS for 12 well plates and in 1 ml of PBS for 6 well plates). For cells seeded on T25 flasks, cells were extracted by trypsinisation (method is described in section 2.5.1 of Chapter 2). Cell mix was collected from wells and centrifuged (335 *g*, 4°C, 10 minutes). Supernatant was discarded and pellets were frozen after the addition of 100 µl of protein lysis buffer (Appendix 2) per 1.4 x 10^6 seeded cells. On the protein assay day, the samples were sonicated 10 times (Sonicator Omni-Ruptor 250, Omni International, Kennesaw, GA, USA) on ice and 10 µl of samples and standards were placed on a 96 well plate in duplicate. BSA was used as the standard. Two-hundred µl of the bicinchoninic acid (BCA) method colour solution (Pierce BCA protein kit) was added to the samples and standards and incubated at 37°C for 30 minutes. Following colour development, microplates were read in a microplate reader at an absorbance 540 nm.

3.2 Cellular morphology and triacylglycerol quantification in long-term cultures

3.2.1 Oil red O staining

Trophoblasts were seeded in chamber slides (245 x10^3 trophoblasts per chamber) in 200 µl of complete DMEM at 5.5 mM glucose in the presence or absence of EGF (10 ng/ml) and kept for 5 days (see Appendix 1 for reagents and material suppliers). From day 2 to day 5 of culture, trophoblasts were grown in 400 µl of complete DMEM (5.5 mM glucose; ± 10 ng/ml EGF) in the presence or absence of NEFA mix (0.1 mM, palmitate: oleate ratio; 1:1) according to Figure 3.13.

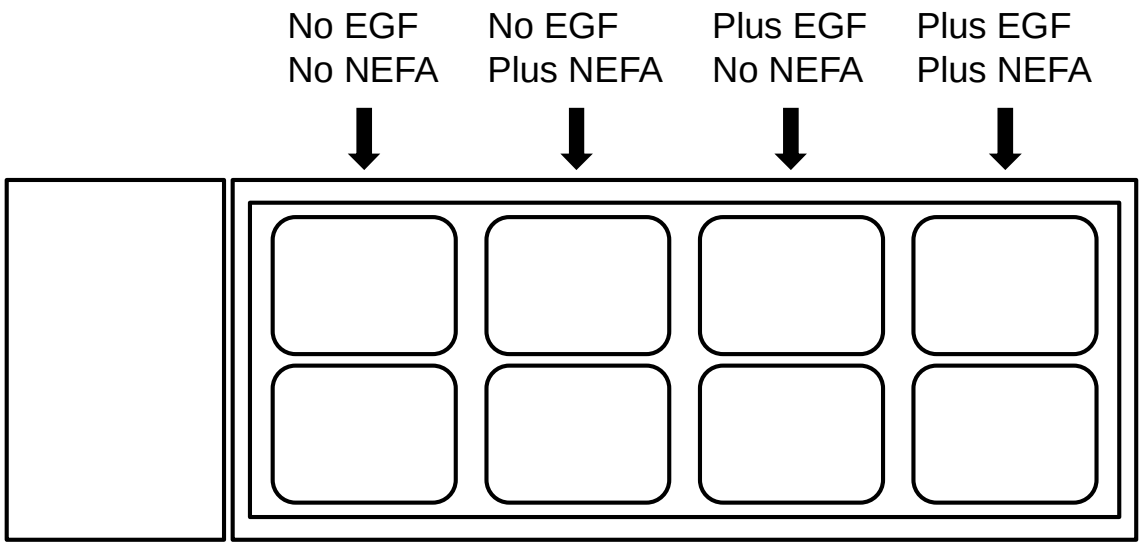

Figure 3.13. Trophoblast culture in chamber slides for assessment of cell morphology and lipid droplet accumulation. Trophoblast were cultured in complete DMEM at 5.5 mM glucose in the presence or absence of EGF (10 ng/ml) from the isolation day. From day 2 to day 5 of culture, NEFA mix (0.1 mM, palmitate: oleate ratio; 1:1) was added to 2 chambers in which cells had been maintained in the presence of complete DMEM supplemented with EGF and to 2 chambers in which cells were grown in complete DMEM without EGF. On day 5 of culture, slides were stained for Oil red O and counterstained for haematoxylin.

On day 5 of culture, cells were stained with Oil Red O, a neutral lipid droplets stain that is specific for TG and cholesteryl esters, in particular cholesteryl oleate (287), and counterstained with haematoxylin. For the staining, culture media was removed and trophoblasts were gently washed twice with 300 µl of PBS for 2 minutes each wash. PBS was removed and 300 µl of 10% buffered formalin was added to each well, and the slides were incubated at room temperature for 10 minutes. Formalin was removed and 300 µl of fresh 10% buffered formalin was then added to the wells and left for 30 minutes for fixation. Formalin was removed and the chamber framing was detached from the slide using the lever from the chamber slide kit. Slides were gently washed by dipping 10 times into a 50 ml Falcon tube filled with distillated water (ddH_2O). This washing (10 dips) was repeated once again into a new 50 ml Falcon tube with fresh ddH_2O. Cells were then gently rinsed by dipping the slide in 60% isopropanol for 1 minute at room temperature. Trophoblasts were stained with freshly prepared Oil Red O working solution (refer to Appendix 2 for preparation of solutions) for 15 minutes at room temperature. The staining was performed in a slide tray using a transfer pipette to cover the sections with Oil Red O, making sure the slide tray was covered to prevent evaporation of the isopropanol. After incubation, slides were again washed by dipping 10 times in ddH_2O. On the staining day, Harris haematoxylin was diluted in ddH_2O (1:2) and filtered with a 0.22 µm filter. Nuclei were then stained by dipping the slides in 50 % Harris haematoxylin 4 times. Slides were gently washed in ddH_2O and dipped in warm tap water 5 times to intensify the colour blue of haematoxylin. Finally, slides were gently washed 3 times with ddH_2O for 2 minutes each. Chamber slides were cover slipped using PermaFluor aqueous mounting media (Appendix 2) and coverslip edges were sealed off with nail polish. Slides stained for Oil red O were analysed by 2 independent viewers and scored according to Table 3.6. Lipid droplets were classified according to whether the globules size were small or large and scored according to the percentage of cells containing them in each slide. In addition,

percentages of cell area forming cellular aggregation and syncytia were also analysed (Table 3.6).

Table 3.6

Score for morphology of trophoblasts Oil red O stained

Morphology analysis	Score				
Percentage of cells with large lipid droplets	<10%	10-25%	25-50%	50-80%	>80%
Percentage of cells with small lipid droplets	<20%	20-80%	>80%		
Percentage of cell area forming cellular aggregation	< 10%	10-25%	25-50%	50-80%	> 80%
Percentage of cell area forming syncytia	<5%	5-10%	10-25%	>25%	

3.2.2 Triacylglycerol quantification

Primary human trophoblast cultures were established in 6 well plates in a density of 3.5 x 10^6 cells over 2 days post isolation in complete DMEM (5.5 mM glucose) with or without EGF (10 ng/ml). For a further 3 days, trophoblasts were also cultured in complete DMEM (5.5 mM glucose; with and without EGF) in the presence or absence of NEFA (0.1 mM, palmitate: oleate ratio; 1:1). At the same time point as for Oil Red O staining, culture media was removed and cells were detached using trypsinisation (method is given in Chapter 2, section 2.5.1). Cells from 2 wells (a total of 7 x 10^6 trophoblasts per sample) were collected in 1.5 ml microtubes and centrifuged (290 *g*, 7 minutes, 4ºC). Supernatants were discarded and the pellets were resuspended in 1 ml of cold PBS. Cell suspensions were mixed well and 100 µl was taken from each sample and stored in 1.5 ml microtubes for later protein measurement. Samples for TG extraction were centrifuged again (290 *g*,

7 minutes, 4ºC). Supernatants were discarded and 25 µl of 0.5 M alcoholic KOH was added to each pellet to promote lipid saponification. Samples were sonicated on ice for 10 times. Cell homogenates were incubated in a water bath at 70˚C for 20 minutes. Following incubation, samples were placed at room temperature for 10 minutes to cool down. Then, 50 µl of 0.15 M $MgSO_4$ was added to each microtube to precipitate insoluble debris. Negative controls without cells were prepared mixing 25 µl of 0.5 M KOH and 50 µl of 0.15 M $MgSO_4$ to measure the background. All microtubes were vortexed well and centrifuged (5,250 *g*, 5 minutes, 4˚C) to precipitate insoluble substances. Supernatant was transferred into a new set of microtubes and pellet was discarded. Samples were then measured with an enzymatic colorimetric kit (Appendix 2). The principle of this method is to measure the glycerol concentration following TG hydrolysis by a LPL enzyme. The glycerol is phosphorylated to glycerol 3-phosphate by glycerol kinase. Glycerol 3-phosphate is converted to dihydroxyacetone phosphate and hydrogen peroxide by the enzyme glycerol phosphate oxidase. Hydrogen peroxide, N-Ethyl-N-(3-sulfopropyl)-m-anisidine (ESPA) and 4-aminoantipyrine (4-AAP) are converted to quinoneimine dye and water in a redox-coupled reaction catalysed by a peroxidase. The dye produces a colour in which the absorbance is directly correlated with the glycerol concentration in the sample (Figure 3.14). The assay was performed following the manufacturer's instructions: free glycerol reagent was reconstituted in 40 ml of Milli-Q water and TG reagent was dissolved in 10 ml of Milli-Q water. Glycerol was used as a standard. Ten µl of samples, standards (0.5, 1, 2, 4, 6, 8 and 10 µl glycerol standard and completed volume with water up to 10 µl final volume) and negative controls were added to 96 well plates. A hundred and sixty µl of free glycerol reagent solution was distributed to the wells. Plates were gently shaken and incubated at room temperature for 15 minutes. Then, 40 µl of TG reagent solution was added to the wells. Plates were carefully mixed and incubated for 15 minutes at room temperature. Absorbance was read in a microplate reader at 540

nm. Results were normalised by trophoblast protein content. TG extraction method was adapted from Salmon *et al.* (288) with modifications.

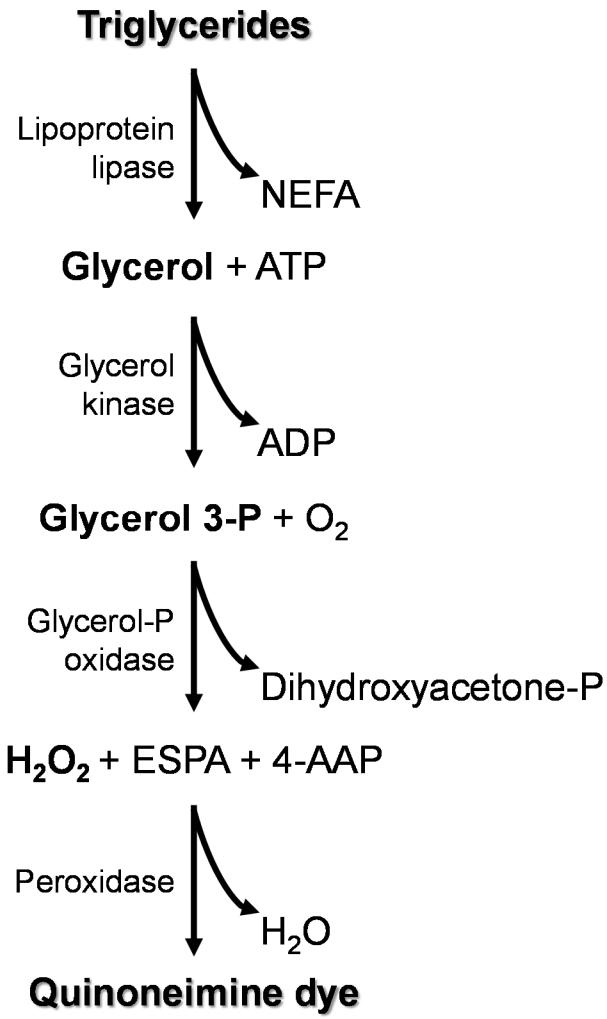

Figure 3.14. TG determination assay principle. TG is hydrolysed by LPL to release glycerol, which is phosphorylated to glycerol 3-phosphate by glycerol kinase. Glycerol 3-phosphate is converted to dihydroxyacetone phosphate and hydrogen peroxide by the enzyme glycerol phosphate oxidase. Hydrogen peroxide, N-Ethyl-N-(3-sulfopropyl)-m-anisidine (ESPA) and 4-aminoantipyrine (4-AAP) are converted to quinoneimine dye and water in a redox-coupled reaction catalysed by a peroxidase. The dye produces a colour in which the absorbance is directly correlated with the glycerol concentration in the sample.

LPL: lipoprotein lipase; TG: triacylglycerol.

3.3 Statistical analysis

The statistical analyses in this thesis were performed using the software GraphPad Prism 6 (GraphPad Software, Inc., La Jolla, CA, USA). Variable distribution (normality) was tested with the Shapiro-Wilk test and the Kolmogorov-Smirnov test. Results were given as means ± standard error of the mean (SEM) in graphic descriptions or SD for normally distributed data in which the description of dispersion from the mean was appropriate. Student *t* test was used to compare means of 2 groups of continuous variables that were normally distributed and the Mann-Whitney test was used for non-parametric comparisons. ANOVA with Bonferroni's *post-hoc* testing was used for comparisons between the mean of more than 2 continuous variables. Chi-square and Fisher's exact test were used to compare categorical data. Statistical significance was considered for a p value of < 0.05.

Chapter 4

Results for glucose metabolism studies in short-term trophoblast cultures

4.1 Introduction

Previous research has shown that glucose metabolism by glycolysis in trophoblasts is near maximal at the glucose concentration of 4 mM (200). Human placental perfusion studies, however, suggest that glucose utilisation of placenta is not maximal until the perfusate glucose concentration reaches about 17 mM (165, 176). The purpose of the following metabolism experiments in short-term cultures was to evaluate trophoblast glucose uptake and metabolism in more detail to elucidate the reasons for the discrepancy between the previous placental glucose utilisation and trophoblast glycolysis findings. In addition, because of interest in the effects of elevated lipids on placental function, the experiments were also designed to determine the effects of fatty acids on glucose uptake and metabolism. Pathways of glucose uptake, glycolysis, lactate production, glucose oxidation and glycogen synthesis were assessed in trophoblasts established in culture for 36 h (Figure 4.1). The experiments were performed over 2 h at diverse glucose concentrations in the presence or absence of NEFA (0.25 mM, palmitate: oleate ratio; 1:1). Palmitate oxidation and acid soluble products from palmitate were also measured to allow comparison between rates of glucose and fatty acid oxidation.

A combination of radio-labelled metabolic tracer methods and metabolite assay methods were used, as described in Chapter 3. All tracer methods were performed taking into account the SA of the tracers within the incubation media. Total glucose uptake in trophoblasts was assessed by measuring intracellular ^{14}C labelled 2-deoxyglucose 6-phosphate accumulation. Glycolysis was analysed through ^{3}H labelled water production from [5-^{3}H]-glucose, whilst lactate release into the media was measured using an enzymatic metabolite colorimetric assay. Glucose and palmitate oxidation were assessed through the production of ^{14}C labelled CO_2 from [(U)^{14}C]-glucose and [(U)^{14}C]-palmitate, respectively. Glucose flux into glycogen synthesis was quantified using a [(U)^{14}C]-

glucose tracer and the total intracellular glycogen content was measured with an enzymatic colorimetric method.

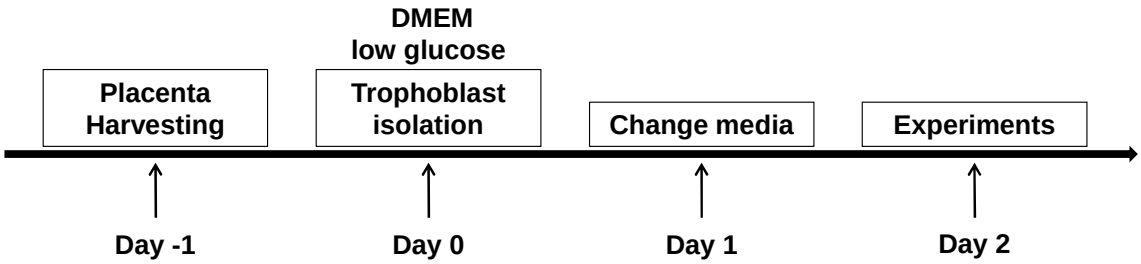

Figure 4.1. Experimental design scheme for metabolism studies in short-term primary human trophoblast cultures. Human placental villous tissue was harvested (day -1) and trophoblasts were isolated and seeded on the following day (day 0). Human trophoblasts were established in complete DMEM at 5.5 mM glucose (refer to Chapter 2 for culture details and Appendix 1 for media preparation). Short-term trophoblast culture metabolism experiments were performed 36 h post isolation, when most cells were cytotrophoblasts.

DMEM: Dulbecco's Modified Eagle Medium.

4.2 Total glucose uptake

In primary human trophoblast cultures established over 36 h post isolation, the rate of glucose uptake as measured by the ^{14}C labelled 2-deoxyglucose 6-phosphate method during 2 h incubations, as described in Chapter 3, increased through all cold glucose concentrations from 1 to 15 mM without reaching plateau. There were no differences in the presence or absence of NEFA. Total glucose uptake, as assessed by this method, was strongly correlated with the medium glucose concentration [r^2=0.71, $p < 0.0001$ (no NEFA); r^2=0.88, $p < 0.0001$ (plus NEFA)] (Figure 4.2). After this preliminary result, the total glucose uptake protocol was revised. Cold glucose concentrations of 25 to 35 mM were then added to the experiment in an attempt to determine the level at which total glucose uptake reaches a maximum and plateau. Using the same tracer method, the rates of total glucose uptake increased through all media glucose concentrations from 1 to 35 mM without reaching plateau in the absence of NEFA in the media. For trophoblasts incubated with NEFA, the relationship between increasing glucose concentration and glucose uptake was not different from that observed in the absence of NEFA. The strong linear correlations between total glucose uptake rates and cold glucose concentrations were maintained [r^2=0.82, $p < 0.0001$ (no NEFA); r^2=0.64, $p < 0.0001$ (plus NEFA)] (Figure 4.3).

Figure 4.2. Total glucose uptake by trophoblasts in short-term cultures progressively increased with increasing glucose availability without effect of NEFA. Total glucose uptake in trophoblasts established in culture for 36 h, as measured by the ^{14}C labelled 2-deoxyglucose 6-phosphate method during 2 h incubations as described in Chapter 3, increased through all cold glucose concentrations from 1 to 15 mM. Total glucose uptake was similar in the presence or absence of 0.25 mM NEFA.

Two-way ANOVA: NEFA effect ns; glucose effect $p < 0.0001$; NEFA-glucose interaction ns. Data are means ± SEM of 8 independent experiments in which each point was the average of triplicate wells.

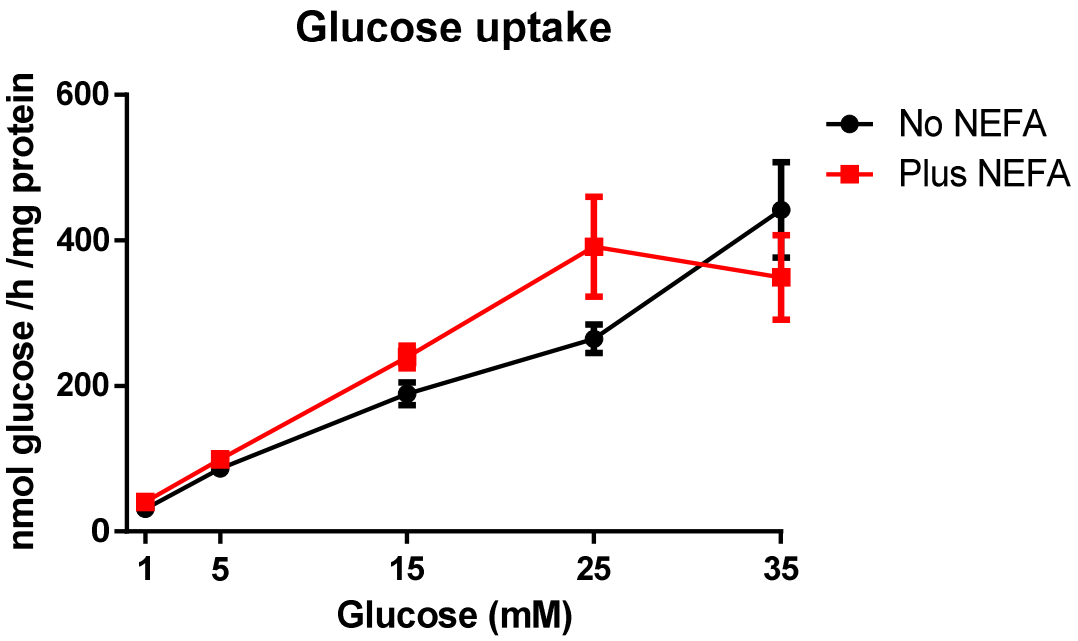

Figure 4.3. Total glucose uptake by trophoblasts in short-term cultures progressively increased with media glucose concentrations up to 35 mM without evidence of plateau. Total glucose uptake in trophoblasts established in culture for 36 h, as measured by the ^{14}C labelled 2-deoxyglucose 6-phosphate method during 2 h incubations as previously described (Chapter 3), increased through all cold glucose concentrations from 1 to 35 mM. Total glucose uptake was similar in the presence or absence of 0.25 mM NEFA.

Two-way ANOVA: NEFA effect ns; glucose effect $p < 0.0001$; NEFA-glucose interaction ns. Data are means ± SEM of 5 independent experiments in which each point was the average of triplicate wells.

4.3 Glycolysis

The rate of glucose utilisation via glycolysis by primary human trophoblasts cultures established over 36 h post isolation was measured by the [5-^{3}H]-glucose tracer method, as described in Chapter 3. Glycolysis rate was almost maximum at the lowest cold glucose concentration of 1 mM glucose in the media. There was a minimal increase in the rate of glycolysis with rising cold glucose concentrations from 1 to 15 mM, statistically significant only in the presence of NEFA (57.1 % increase). However, the rates of glycolysis at the different glucose concentrations overall were not statistically different according to the absence or presence of NEFA (Figure 4.4).

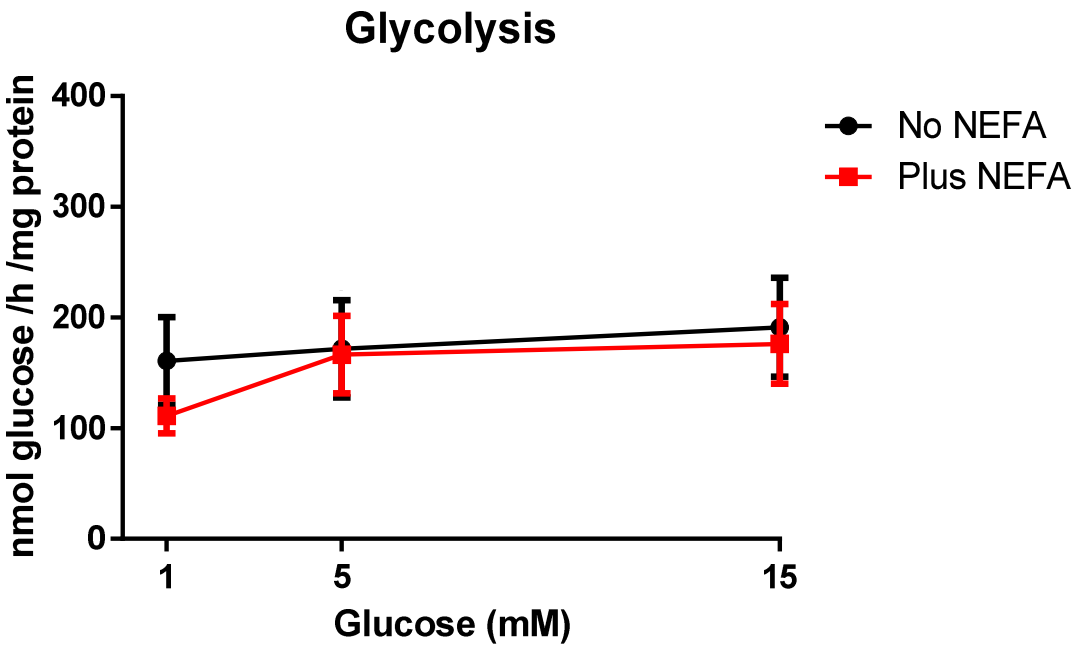

Figure 4.4. Glucose utilisation via the glycolysis pathway in short-term human trophoblast cultures was maximal at low media glucose concentrations without effect of NEFA. Glycolysis rate over 2 h incubations, as estimated by the [5-^{3}H]-glucose tracer method (refer to Chapter 3), showed a limited increase with increasing media glucose concentrations from 1 to 15 mM in trophoblasts established in culture for 36 h. Glycolysis rates were similar in the presence or absence of 0.25 mM NEFA.

Two-way ANOVA: NEFA effect ns; glucose effect p=0.002; NEFA-glucose interaction ns. Bonferroni *post-hoc* test: 1 mM glucose *vs* 5 mM glucose (plus NEFA) p=0.044; 1 mM glucose *vs* 15 mM glucose (plus NEFA) p=0.018. Data are means ± SEM of 8 independent experiments in which each point was the average of triplicate wells.

4.4 Total lactate release into the media

Lactate released into the media by human trophoblasts established in cultures over 36 h after isolation was measured by an enzymatic colorimetric assay as described in Chapter 3. Lactate release was maximum at the media glucose concentration of 5 mM. The lactate release rate was similar in the absence or presence of NEFA. Lactate release increased by 22.5% (in the absence of NEFA) and by 20.8 % (in the presence of NEFA) when glucose concentration in the media rose from 1 to 15 mM (Figure 4.5).

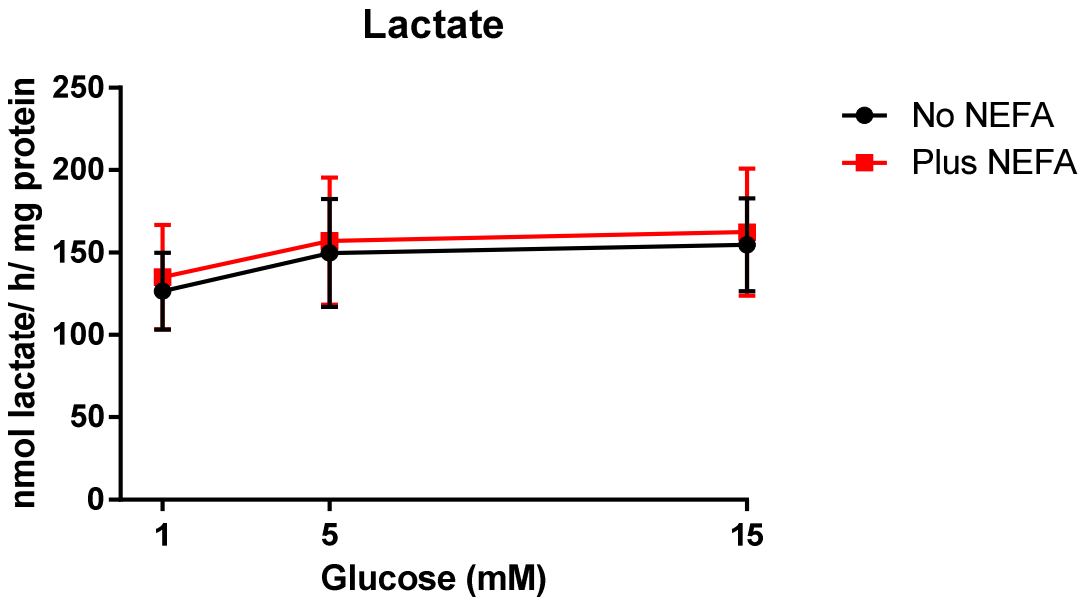

Figure 4.5. Lactate release into the media in short-term primary human trophoblast cultures plateaued at the media glucose concentration of 5 mM without NEFA effect. Lactate release in primary human trophoblasts established in culture over 36 h post isolation, as measured by the enzymatic colorimetric assay described in Chapter 3, reached the maximum concentration at 5 mM glucose in the media. Lactate release was similar in the presence or absence of 0.25 mM NEFA.

Two-way ANOVA: NEFA effect ns; glucose effect p=0.012; NEFA-glucose interaction ns. Bonferroni *post-hoc* test: 1 mM glucose *vs* 5 mM glucose (no NEFA) p=0.009; 1 mM glucose *vs* 15 mM glucose (no NEFA) p=0.003; 1 mM glucose *vs* 5 mM glucose (plus NEFA) p=0.011; 1 mM glucose *vs* 15 mM glucose (plus NEFA) p=0.004. Data are means ± SEM of 4 independent experiments in which each point was the average of triplicate wells.

4.5 Glucose oxidation

Glucose oxidation in primary human trophoblasts established in culture over 36 h after isolation was assessed through [(U)^{14}C]-glucose metabolism into ^{14}C labelled CO_2 as described in Chapter 3. Glucose oxidation was significantly higher in the absence of NEFA at the lowest glucose concentration in the media (1 mM) than in the presence of NEFA, and there was a non-significant trend for it to be lower in the presence of NEFA at glucose concentrations of 5 and 25 mM. With rising glucose concentrations in the media, trophoblast glucose oxidation increased in both the absence and presence of NEFA, with the majority of this increase occurring for media glucose concentration rises from 1 to 5 mM. (Figure 4.6).

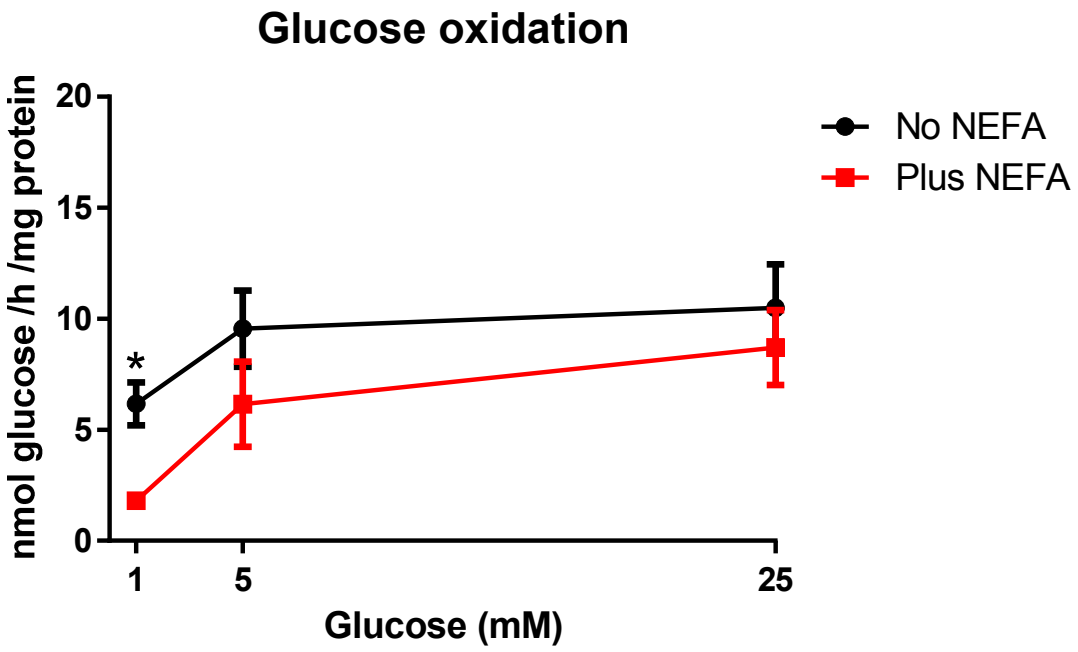

Figure 4.6. Glucose oxidation in short-term trophoblast cultures was near maximum at a cold glucose concentration of 5 mM in the media. Overall, NEFA did not affect this metabolic pathway. Glucose oxidation in human trophoblasts established in culture over 36 h after isolation was measured by the [(U)^{14}C]-glucose tracer metabolism method in which ^{14}C labelled CO_2 is captured and quantified (refer to Chapter 3). Glucose oxidation was almost maximum at the media glucose concentration of 5 mM. The presence of NEFA significantly reduced glucose oxidation rate only at 1 mM cold glucose concentration.

Two-way ANOVA: NEFA effect p=0.025; glucose effect p=0.003; NEFA-glucose interaction ns. Bonferroni *post-hoc* test: *1 mM glucose (no NEFA) *vs* 1 mM glucose (plus NEFA) p=0.025; 1 mM glucose *vs* 5 mM glucose (no NEFA) ns; 1 mM glucose *vs* 25 mM glucose (no NEFA) p=0.018; 5 mM glucose *vs* 25 mM glucose (no NEFA) ns; 1 mM glucose *vs* 5 mM glucose (plus NEFA) p=0.017; 1 mM glucose *vs* 25 mM glucose (plus NEFA) p=0.0009; 5 mM glucose *vs* 25 mM glucose (plus NEFA) ns.

Data are means ± SEM of 6 independent experiments in which each point was the average of duplicate or triplicate T25 flasks.

4.6 Palmitate oxidation and acid soluble product formation

In primary human trophoblasts established in culture over 36 h after isolation, the rate of palmitate oxidation was measured during 2 h incubations by the [(U)^{14}C]-palmitate tracer method in which ^{14}C labelled CO_2, as well as ^{14}C labelled acid soluble products, are captured and quantified (refer to Chapter 3). Palmitate oxidation showed a trend towards reduction with the increase in the media glucose concentration from 5 to 25 mM (Figure 4.7). The levels of acid soluble products accumulation from palmitate oxidation, as described in Chapter 3, were similar at media glucose concentrations of 5 and 25 mM. (Figure 4.8).

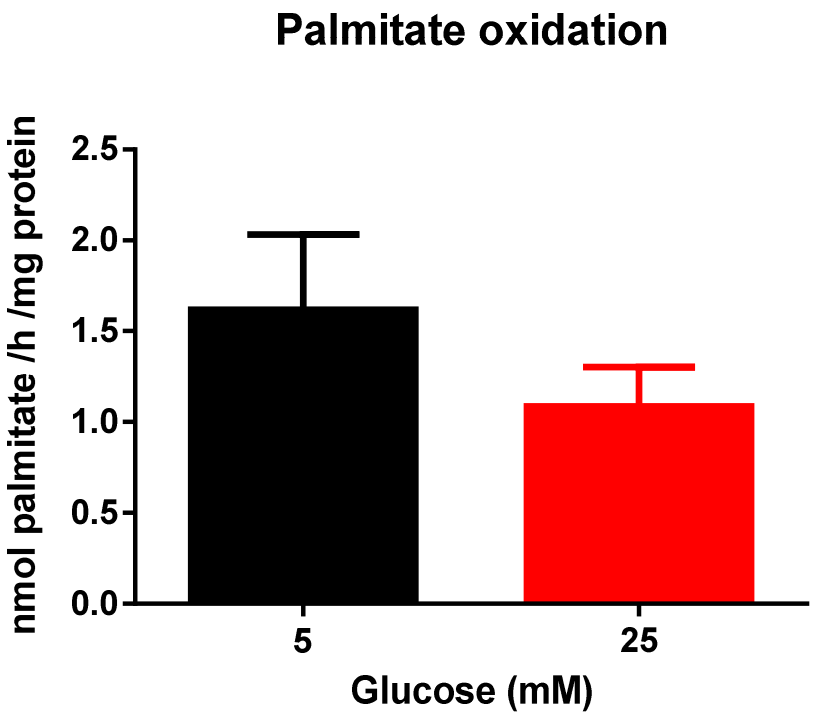

Figure 4.7. Palmitate oxidation in short-term trophoblast cultures showed a trend towards reduction in the presence of a high level of glucose in the media. Palmitate oxidation in human trophoblasts established in culture over 36 h after isolation and measured by [(U)^{14}C]-palmitate tracer metabolism into ^{14}C labelled CO_2 (described in Chapter 3) presented a downward trend at 25 mM glucose concentration in the media. Data are means ± SEM of 6 independent experiments in which each value was the average of duplicate or triplicate T25 flasks.

Figure 4.8. Acid soluble product generation during palmitate oxidation in short-term human trophoblast cultures were similar at lower and higher glucose levels in the media. Palmitate oxidation into acid soluble products in human trophoblasts established in culture over 36 h after isolation, as measured by [(U)^{14}C]-palmitate tracer metabolism into ^{14}C acid soluble products according to the method described in Chapter 3, exhibited similar values at 5 and 25 mM glucose concentrations in the media. Data are means ± SEM of 4 independent experiments in which each value was the average of duplicate or triplicate T25 flasks.

4.7 Glycogen synthesis measured with tracer

The acute glucose flux into glycogen in human trophoblasts established in culture over 36 h post isolation was quantified using the [(U)^{14}C]-glucose tracer method, as explained before (Chapter 3). Glycogen synthesis increase was linearly correlated with all media glucose concentrations from 1 to 35 mM [r^2=0.70, $p < 0.0001$ (no NEFA); r^2=0.75, $p < 0.0001$ (plus NEFA)]. Trophoblast cultures in the presence of 0.25 mM NEFA showed significantly higher glycogen synthesis as quantified by this tracer method (Figure 4.9).

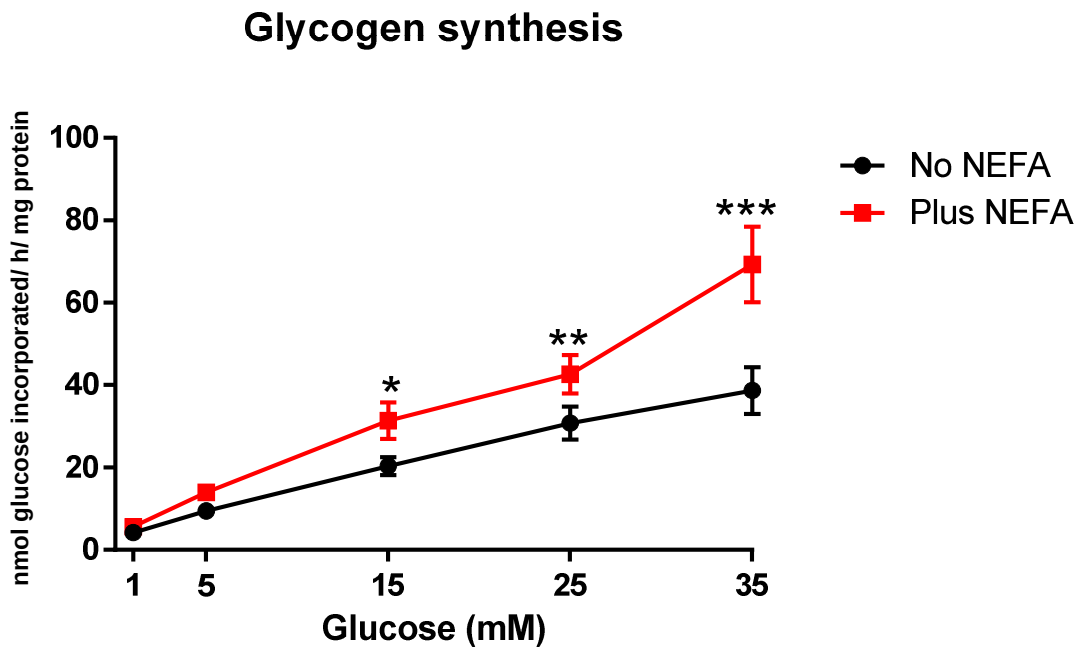

Figure 4.9. The acute glucose flux into glycogen synthesis in short-term primary human trophoblast cultures increased with rising cold glucose concentrations in the media. **Glycogen synthesis was further increased in the presence of NEFA.** The acute glucose flux into glycogen in human trophoblasts established in culture over 36 h after isolation, as quantified with [(U)^{14}C]-glucose tracer method described in Chapter 3, progressively increased through all glucose concentrations in the media from 1 to 35 mM. Glycogen synthesis was significantly higher in the presence of 0.25 mM NEFA.

Two-way ANOVA: NEFA effect p=0.006; glucose effect p < 0.0001; NEFA-glucose interaction p < 0.0001. Bonferroni *post-hoc* test: *15 mM glucose (no NEFA) *vs* 15 mM glucose (plus NEFA) p=0.006; **25 mM glucose (no NEFA) *vs* 25 mM glucose (plus NEFA) p=0.003; ***35 mM glucose (no NEFA) *vs* 35 mM glucose (plus NEFA) p < 0.0001. Data are means ± SEM of 7 independent experiments in which each point was the average of triplicate wells.

4.8 Total glycogen content

Total intracellular glycogen content in human trophoblasts established in culture over 36 h post isolation was measured using an enzymatic colorimetric assay as described in Chapter 3. Total glycogen content quantified in trophoblasts grown for 36 h in complete media at 5.5 mM glucose concentration without further incubation was considered the "basal" glycogen concentration. Total glycogen content measured after acute incubations (2 h pre-incubation in complete DMEM at 1 mM glucose followed by 2 h incubation in KRBH, 0.5% BSA-FA free, at glucose concentrations of 1, 5, 15, 25 and 35 mM in presence or absence of NEFA), as described in Chapter 3, showed a minimal increase in glycogen content with increasing media glucose according to ANOVA (Figure 4.10). However, with *post-hoc* testing, total glycogen content quantified after incubations was not different from basal glycogen content and was similar in the presence or absence of NEFA. The glycogen content (nmol glucose equivalent as glycogen ± SD) after 2 h incubation at the indicated glucose concentration in the absence and presence of NEFA was, respectively, 225.67 (± 59.61) and 235.37 (± 66.78) nmol/mg protein at 1 mM glucose, 253.11 (± 41.70) and 257.14 (± 52.63) nmol/mg protein at 15 mM glucose, and 244.61 (± 51.39) and 278.09 (± 79.00) nmol/mg protein at 35 mM glucose. This is comparable to the basal glycogen content of 215.88 (± 30.90) nmol/mg protein.

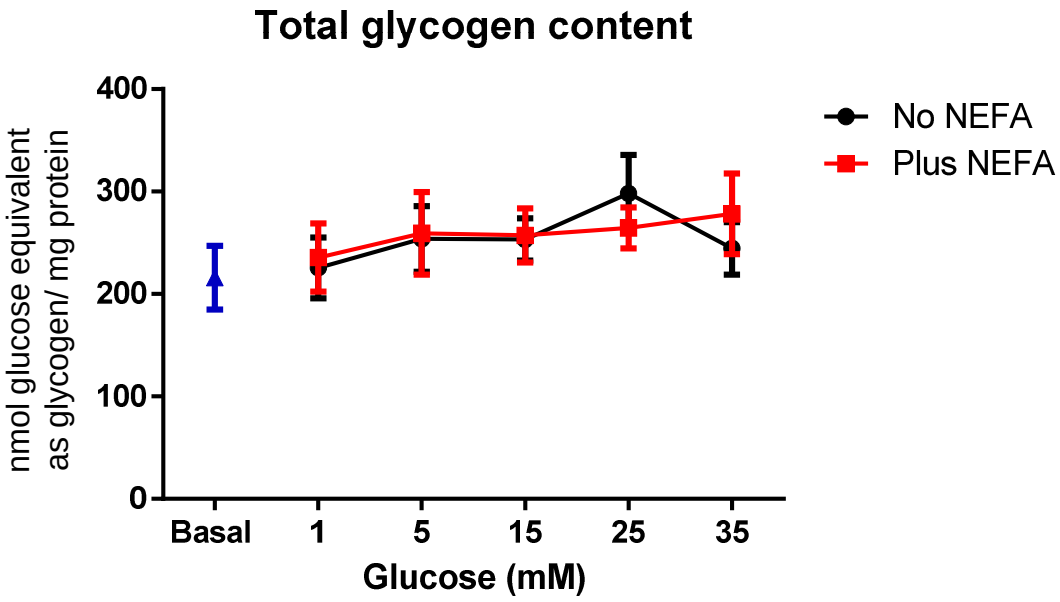

Figure 4.10. Total glycogen content in short-term human trophoblast cultures increased minimally with rising media glucose concentration and was not affected by the presence of NEFA. Total glycogen content in trophoblasts established in culture over 36 h post isolation was measured by the enzymatic colorimetric assay described in Chapter 3. Basal levels of total glycogen content were measured in trophoblasts grown in complete media at 5.5 mM glucose without further incubation. For other measurements, total glycogen content in the trophoblasts was measured following a further 2 h incubation in KRBH media containing from 1 to 35 mM glucose in the absence or presence of 0.25 mM NEFA. Total glycogen content increased minimally with increasing glucose concentrations in the media and was not affected by the presence of NEFA. Basal glycogen content was also similar to total glycogen content quantified after acute incubations in KRBH.

Two-way ANOVA: NEFA effect ns; glucose effect p=0.019; NEFA-glucose interaction ns. Bonferroni *post-hoc* test: ns. Data are means ± SEM of 4 independent experiments in which each point was the average of triplicate wells.

4.9 Discussion

The main aim of this research was to determine the fate of glucose flux in primary human trophoblasts exposed to increasing media glucose concentrations since studies have shown that total glucose uptake into placental tissue can increase as glucose supply concentrations rise to levels above 15 mM (165, 176), whereas glycolysis rates become maximal at much lower glucose supply concentrations of about 5 mM (200). This may be a consequence of placental glucose storage (total glucose utilisation minus lactate production from glucose and glucose oxidation) drastically rising at maternal glucose concentrations of $\geq$ 10 mM (165). In addition, the effects of 0.25 mM NEFA (palmitate and oleate) on glucose metabolism pathways, which have been extensively investigated in other tissues, were studied in primary human trophoblast cultures.

Results from this research showed that human trophoblasts, established in culture over 36 h post isolation and assessed using the labelled 2-deoxyglucose method over a 2 h period, were able to take up an increasing amount of glucose according to the glucose availability without evidence of saturation. Total glucose uptake presented a strong linear correlation with the media glucose concentration from 1 to 35 mM in both the presence and absence of NEFA. Glycolysis assessed by [5-^{3}H]-glucose metabolism, lactate release in the media quantified with an enzymatic colorimetric assay and glucose oxidation studied through [(U)-^{14}C]-glucose metabolism all reached a plateau at the relatively low media glucose concentration of 5 mM. Overall, NEFA did not affect these glucose metabolism pathways (total glucose uptake, glycolysis, lactate release into the media and glucose oxidation). Similarly to total glucose uptake, glucose flux into glycogen assessed by [(U)-^{14}C]-glucose accumulation as labelled glycogen linearly increased according to available glucose in the media. Moreover, glucose flux into glycogen was further enhanced in the presence of NEFA. On the other hand, total glycogen content quantified by an enzymatic colorimetric assay showed only a minimal trend to rise over a 2 h period according to the

glucose concentration in the media, with no demonstrable effect of the presence compared to the absence of NEFA. Palmitate oxidation, measured through [(U)-^{14}C]-palmitate metabolism, showed a trend of reduction at the supra-physiological media glucose concentration of 25 mM; whereas acid soluble product formation assessed in the same experiments was not affected by glucose.

4.9.1 Effects of increasing media glucose concentration on glucose metabolism pathways in primary human trophoblast cultures

4.9.1.1 Glucose uptake

Total glucose uptake rates in human trophoblasts obtained in this research are in accordance with previous publications which have shown that total glucose uptake in placental perfusion studies and experiments with trophoblast cultures is directly correlated with available glucose without saturation (176, 184, 192) or with saturation at supra-physiological glucose levels (165, 193, 194). Glucose is the main nutritional energy source to the fetus. The first step in the glucose flux from mother to the fetus is glucose uptake by trophoblasts which occurs mainly through GLUT1. Previous results have shown that GLUT1 is down-regulated when trophoblasts are cultured at high glucose concentrations for 24-96 h (184), but in the current experiments trophoblasts were cultured in the different glucose concentrations for 2 h only, which is not likely to be long enough to alter GLUT1 levels. Hahn *et al.* demonstrated that trophoblasts harvested from term placenta chronically exposed to high glucose concentration (25 mM glucose for ≥ 24 h) exhibited a decrease in GLUT1 mRNA by 50 % and a reduction in GLUT1 protein by 16 % in comparison with trophoblasts cultured at 5 mM (184). Glucose uptake by the experimental trophoblasts measured through the 3-O-[^{14}C]-methyl-D-glucose method was reduced by 25%, however only in circumstances when the cold glucose concentrations during measurements were increased to ≥ 20 mM (184). This effect was

caused by a reduction by 50% in the V_{max} for glucose uptake rather than a change in the K_m for glucose transport which was very high at 73 mM (184). As the V_{max} is determined by the number of transporters, the decrease in transport in response to sustained hyperglycaemia is consistent with a reduction in GLUT1 expression. Moreover, another study with primary human trophoblasts in co-culture with acellular amniotic membrane reported a half-saturation for trans-trophoblast D-glucose transport at 44 mM glucose (194). Studies with perfused cotyledons have also supported the hypothesis that the main determining factor for glucose uptake in the placenta is the substrate gradient and not GLUT1 concentration or activity. Glucose uptake increased linearly in two studies (r^2=0.74) (192) and (r^2=0.65) (176) with available glucose concentration up to 20-25 mM without suggestion of transport saturation. In agreement, maximum placental glucose uptake reported by Day *et al.* (192) was much higher than the predicted (theoretical) GLUT1 saturation, suggesting again that other factors regulate glucose uptake beyond GLUT1 transport. GLUT3, a high affinity glucose transporter expressed in cytotrophoblasts from term placentas (178), could maintain the glucose flux, even when GLUT1 is down-regulated. Thus, the placenta and trophoblast cells in culture, as investigated in this research, seem to have a high capacity for glucose uptake which is mostly determined by the available glucose concentration.

4.9.1.2 Glycolysis

Anaerobic glycolysis has been described as the main glucose utilisation pathway in the placenta (207). The placenta, however, seems to have a very limited ability to increase aerobic or anaerobic glycolysis rates in higher than physiological glucose concentrations. In the experiments of this thesis, glycolysis rates in primary human trophoblasts at 1 mM and 5 mM media glucose concentration were 83.3% and 95.6% of the maximum rates, respectively. These results coincide with previous data that showed that glycolysis rates were 90% of maximal at 4 mM glucose and maximum at 8 mM glucose in the culture

media (200). It is possible that the trophoblast's limited ability to increase glycolysis is due to a low activity of enzymes involved in glycolysis. With the exception of hexokinase and pyruvate kinase, liver enzymes are many times more active than placental enzymes (207). Thus, it is likely that excess glucose is not metabolised via glycolysis by human trophoblasts when the glucose supply to the cells is high. In accordance with minimal increases in glycolysis at elevated glucose concentrations in the media, lactate production in the current experiments did not increase for media glucose concentrations above 5 mM. This finding is similar to the results from past placental perfusion studies which report no increase in lactate production when maternal glucose is above 5.5 mM (165), or when the glucose supply was increased from 4 to 24 mM (176). Furthermore, in the latter study, there was no correlation between lactate production and maternal glucose (176). In the current work, the lactate production at 5 mM glucose represented about 69% of total glucose uptake, since 1 mol of glucose yields 2 mol of lactate. This proportion was similar to what was observed in another study with isolated trophoblasts from term placenta, in which 70% of glucose utilisation was converted to lactate (148). Our results also coincided with the lactate production rate of 68.7% of total glucose utilisation in placental slices (197), and to the fraction reported in placental perfusion studies. In these studies, lactate production per molecule of glucose was 69% of placental glucose utilisation at 5.6 mM maternal glucose concentration (165) and around 78% at 4 mM (176). Also, consistent with the results of this thesis, as glucose availability increased above 5 mM, the percentage of glucose uptake (trophoblast cultures of the current study) or percentage of glucose utilisation (placental perfusion studies), contributing to lactate production became less. For example, in the current study, at glucose concentrations in the media of 15 mM, only 37.5% of the glucose taken up by the isolated trophoblasts contributed to lactate production. In the placental perfusion studies, at the maternal glucose perfusate

concentrations of 16.9 mM (165) and 16 mM (176), respectively, 17% and about 45% of the glucose utilised by the placenta could be accounted for lactate production.

Of note, lactate production exceeded total glucose uptake at the media glucose concentration of 1 mM in this thesis, which is unlikely since the predominant source for lactate synthesis would have been glucose. Unknown, is the amount of glycogen breakdown that could have contributed to lactate production. Lactate production from amino acids was implausible because the only amino acid source in the incubating media in this research was BSA, which was used to bind and solubilise NEFA. It would have been inaccessible to metabolism. In addition, the absolute glycolysis rates were higher than the absolute total glucose uptake rates at media glucose concentrations of 1 and 5 mM. Furthermore, this measure was of glycolysis from the media glucose, as the glycogen stored within trophoblasts would have been unlabelled. Therefore, due to the lack of correlation between the percentage of glycolysis, lactate release and total glucose uptake, it is possible that total glucose uptake absolute rates obtained by 2-deoxyglucose method in this work were underestimated and/or the glycolysis absolute rates assessed by [5-^{3}H]-glucose were overestimated even though the trend according to media glucose seems to be reliable (see discussion below).

4.9.1.3 Glucose and palmitate oxidation

In the current studies, glucose oxidation as determined by the production of $^{14}CO_2$ from [(U)^{14}C]-glucose showed a plateau at 5 mM media glucose concentration, as for glycolysis. In accordance to these results, oxygen utilisation was shown to be limited in perfused placentas studies, without increments for maternal glucose rises from 3 to 53 mM (165). Also, studies in sheep have demonstrated that acute or chronic maternal hyperglycaemia increased utero-placental total glucose uptake, but did not alter the utero-placental oxygen consumption (289).

In order to directly compare the rates of trophoblast glucose and palmitate oxidation, both were performed at the same time within trophoblasts from the same placentas. The results of the current study showed a non-significant reduction of palmitate oxidation by 33% at the higher media glucose concentration (25 mM *vs* 5 mM). Previous experiments performed in human trophoblast cultures, conversely, did not show this trend, with palmitate oxidation rates unchanged across a range of media glucose concentrations from 0.5 to18 mM (200). On the other hand, the results of this thesis are similar to those of Visiedo *et al.* study with placental explants in which palmitate oxidation measured using the [9, 10 (*n*)-^{3}H]-palmitate metabolism method was significantly reduced by 20% in cultures exposed to high glucose levels (11 mM glucose *vs* 5 mM) incubated for 18 h (232). According to the latter study, the mechanism of palmitate oxidation inhibition by glucose was similar to that observed in other tissues, where high glucose concentrations induce increases in malonyl-CoA levels, which in turn inhibit CPT-1 activity and the long-chain NEFA transport into the mitochondria for oxidation (232). Incubation at 11 mM media glucose reduced the phosphorylation levels of acetyl-CoA carboxylase, the enzyme that converts acetyl-CoA into malonyl-CoA, by 25% and inhibited CPT-1 activity by 70%. (232). In this thesis research, however, glycolysis did not increase when cells were exposed to glucose concentrations higher than 5 mM during 2 h incubations. Thereupon, the assumption that malonyl-CoA was involved in palmitate oxidation reduction in this research cannot be made and other intermediates of glucose metabolism may play a role. Also, the results of Visiedo *el al.* study showed about 3-fold higher palmitate oxidation rates (at 5 mM glucose and 0.1 mM palmitate) (232) than the current research, which may be owing to methodological differences. Villous explants maintain placental tissue architecture and contain other cell types (i.e. endothelial cells, fibroblasts, macrophages) in addition to trophoblasts, which could increase fatty acid oxidation rates. Moreover, in the previous study (232), the incubations were performed for longer time

(18 h) than the current research and palmitate oxidation was assessed by [9, 10 (*n*)-^{3}H]-palmitate method, which may also lead to differences. Nevertheless, a study with cytotrophoblast cultures from term placentas (224) showed that palmitate oxidation performed with [9, 10 (*n*)-^{3}H]-palmitate method at 5.5 mM glucose had very similar rates to those found in this thesis (1.8 nmol palmitate/h/mg protein (224) *vs* 1.6 nmol palmitate/h/mg protein in this thesis).

Although fatty acids have been considered a minor nutritional source for placental metabolism (207), trophoblasts utilised a considerable amount of palmitate for energy production in this research. Since the oxidation of a 16-carbon palmitate molecule yields 108 ATP and a 6-carbon glucose only 32 ATP, trophoblasts are obtaining about 47% of oxidative energy from palmitate and 53% from glucose at 5 mM media glucose concentration; and about 30% of oxidative energy from palmitate and 70% from glucose at 25 mM media glucose concentration according to the current study. Hence, this suggests that fatty acid metabolism is an important energy source for the placenta. Indeed, the placenta expresses a range of enzymes that participate in fatty acid oxidation (290, 291) particularly within syncytio- and cytotrophoblasts. Some of these enzymes such as CPT-2 and VLCAD have even exhibited higher activity in the placenta than the liver (290). The finding of this research that fatty acids are a valuable nutritional source to trophoblasts would fit well with the known increased availability of NEFA in the maternal circulation from the second trimester of pregnancy, directly from adipose tissue lipolysis, but also from the increased circulating TG supply that can be hydrolysed by placental lipases (EL and LPL). A capacity for the placenta to be able to use NEFA for energy also makes sense owing to the many energy dependent processes the placenta is implicated. The placenta has to grow and develop rapidly. It is also responsible for the active transport of many substances to and from the fetus and it is very actively involved in the production and secretion of hormones, cytokines and adipokines, all of which demand high energy.

The rate of acid soluble product (ketone bodies, short-chain fatty acids and TCA cycle intermediates) production in trophoblast cultures did not change in the presence of the 5 mM compared to 25 mM glucose media concentration in this research. Of particular interest, however, is the finding that the acid soluble product accumulation from palmitate carbons was 2.5 times higher than CO_2 at 5 mM glucose, and 4.2 times higher at 25 mM. Unknown, is the percentage of ketone bodies in the acid soluble products compared to other metabolites such as acetate. Interesting, neonatal as opposed to adult pig hepatocytes are less able to produce ketone bodies and produce considerable quantities of acetate (292). Ketone bodies are synthesized from acetyl-CoA which does not enter the TCA cycle for further oxidation to CO_2. Thus, it may be that acetyl-CoA is being redirected to ketone bodies formation in the trophoblasts (refer to Chapter 1 for all reactions). These results suggest that trophoblast capacity to completely oxidise long-chain fatty acids is limited and that in the presence of fatty acids, the cells can shift NEFA from TCA cycle to acid soluble products which could be ketone bodies or other molecules. Of note, the expression of enzymes implicated in ketone body production by the placenta has been minimally investigated. On the other hand, it has been reported that the placenta contains enzymes implicated in ketone body metabolism such as β-hydroxybutyrate dehydrogenase, succinyl-CoA transferase and acetoacetyl-CoA thiolase (293). Furthermore, placental oxidation of β-hydroxybutyrate to CO_2, at least in rats, seems to be higher than oxidation in fetal brain or liver (294). Considering the substantial production of acid soluble products from human trophoblasts in this study, further investigation of fatty acid oxidation to products other than CO_2 are potentially very important.

4.9.1.4 Glycogen

Data from this research have shown that the human trophoblast can synthesize glycogen and the flux into this pathway is directly correlated with the available glucose in the media

in the absence of insulin. Recent research confirmed that cytotrophoblasts contain high levels of glycogen throughout pregnancy and that they express glycogen synthase and phosphorylase enzymes, which catalyse glycogen synthesis and breakdown, respectively (295). Also, it has been reported that term placenta trophoblasts express glycogenin, a protein essential to initiate glycogen synthesis (178). Besides, the results of this thesis are in agreement with earlier studies that have shown that the main regulating factor for placental glycogen formation is the available glucose levels and that placental glycogen is not highly regulated by insulin. In rats, placental glycogen was higher in diabetic mothers and was related to glucose and glucose 6-phosphate availability (296). Also, glycogen storage was independent of insulin regulation (297). In accordance to the findings of this study, abundant intracellular glycogen lakes were observed through transmission electron microscopy in primary human trophoblasts cultured for 24 h at 10 mM glucose concentration in the absence of insulin, whilst, no glycogen lakes were found when cells were cultured at 1 mM glucose for the same period (200). These results show that trophoblasts can store glucose as glycogen solely stimulated by high glucose concentration in the media (200). Indeed, there is evidence that glycogen synthase can be indirectly activated by high glucose levels as well as by glucose 6-phosphate (296). In addition, glucose can inhibit glycogen phosphorylase, thus contributing to glycogen storage by inhibiting glycogen breakdown (296).

In perfused placentas, placental glucose storage increased from 0-70% when maternal glucose levels rose from 4 to 53 mM (165). Although placental glycogen was not measured in that study, this dramatic glucose retention by the placenta suggests that glycogenesis may have increased (165). Another research study demonstrated that glycogen measured in placentas from T1DM mothers was increased and associated with a higher maternal-to-fetal glucose ratio in comparison with healthy mothers (209). Conversely, placental glycogen in women with GDM on insulin was not higher than that

of the control group, despite a maternal-to-fetal glucose ratio 40% higher than the control groups (209).

In the current research, total glycogen content measured with an enzymatic colorimetric assay increased minimally with rising media glucose concentration and this was not affected by the presence of NEFA. The difference between methods is that the metabolic tracer method only assesses newly formed glycogen less the newly formed glycogen that is catabolised within the 2 h incubation; whereas, the total glycogen content method takes into account the glycogen present at baseline and the total glycogen breakdown in the 2 h period. This total glycogen content results of this thesis are similar to the study of Schmon *et al*.(210), in which primary human trophoblasts cultured for 1 to 4 days after isolation did not change total glycogen content at 5.5, 17 or 28 mM glucose concentration, regardless of the presence of insulin (210). Interestingly, in this study glycogen content significantly increased for 2 h after changing the media. Also, the cells presented 50% higher glycogen content from 2 to 5 h after fresh media was added compared to that at the time of the change (210). Unknown from the study of Schmon *et al.* is the change in glycogen of the trophoblasts that may have been seen if the cells were incubated in glucose concentrations lower than 5.5 mM, as glycogen lakes observed using electron microscopy in another study were clearly reduced with incubation at 1 mM glucose (200). Comparing glycogen content (expressed as µg of glycogen/mg protein) measured in isolated trophoblasts cultured at 5 mM glucose in our study (45.7 ± 11.5) was lower than that from Hahn *et al.* (87.4 ± 16.4 µg/mg protein) (178), but higher than the results reported by Schmon *et al*. (17.7 ± 3.2 µg/mg protein) (210).

The discrepancies between acute glucose flux into glycogen and total glycogen content in response to increasing media glucose concentration add weight to the controversies about placental glycogen metabolism. Considering that total glycogen did not increase in trophoblast cultures at high glucose concentrations and was not responsive to insulin

(210), together with the finding that the greatest glycogen deposition in term placentas from mothers with well-controlled overt diabetes was found in fetal capillaries (endothelial cells and pericytes) (208), some authors have argued that placental cells other than trophoblasts are more responsible for glycogen accumulation in diabetic placentas. Moreover, factors other than maternal insulin and glucose may be responsible for glycogen accumulation in the placenta, including the possibility of fetal insulin (210). The report that the highest expression of glycogenin is in endothelial cells from term placentas supports this hypothesis (178). Nevertheless, experiments in rats with fetal insulin deficiency induced through intra-fetal streptozotocin administration refute this hypothesis. Placental glycogen was higher in diabetic pregnant rats than pregnant healthy rats independently of fetal hypoinsulinaemia or intra-fetal insulin administration (297). The activities of glycogen synthase, glycogen phosphorylase and the glycogen distribution in the placenta were also unchanged by induction of hypoinsulinaemic fetuses from both diabetic and control dams (297). However, fetal hypoinsulinaemia reduced fetal weight, hepatic size and glycogen content, which were restored by intra-fetal administration (297). Therefore, further studies are required to clarify the regulation of glycogen synthesis in the placenta.

4.9.2 NEFA effects on glucose metabolism pathways in primary human trophoblast cultures

Interactions between fatty acid and glucose metabolism have long been described in muscle and adipose tissue with particular regard to insulin resistance in T2DM (211). According to the Randle cycle hypothesis, glucose and fatty acid compete for their oxidation in muscle and the utilisation of one nutrient directly inhibits the use of the other. Fatty acids can affect glucose metabolism by decreasing glucose transport and hexokinase function, supressing phosphofructokinase-1 (a regulatory enzyme of glycolysis-refer to

Chapter 1) activity, and inhibiting pyruvate dehydrogenase, which catalyses the conversion of pyruvate into acetyl-CoA to be oxidised in the TCA cycle (212).

In this research, however, NEFA did not affect most glucose metabolism pathways. The absence of effects on glucose metabolism in trophoblasts observed in this thesis may be due to many factors: (i) NEFA concentration used during experiments (0.25 mM) could be too low to affect trophoblast metabolism, as is discussed in more details below; (ii) cells were exposed to NEFA for too short a period (2 h incubations) to observe NEFA effects, as longer exposure may be required to change gene and protein expression to affect glucose metabolism; (iii) it may be a consequence of the marked differences between glucose metabolism in trophoblasts and other cell types in which glucose metabolism has been shown to be affected by NEFA (e.g. myocytes and pancreatic β cells) such as the lack of insulin responsivity in trophoblasts and their abundant expression of GLUT1 and 3 (both insulin non-responsive), but not GLUT4 (191); (iv) it could be a consequence of the specific NEFA mixture used in this research, with the possibility that the palmitate and oleate mix used here may have quite different effects on glucose metabolism compared to a much more physiological NEFA mix; (v) the absence of L-carnitine during glucose metabolism experiments, as this could limit NEFA transport and oxidation into the mitochondria not allowing the catabolism of NEFA into oxidation products that could be important in mediating the effects of NEFA on glucose metabolism pathways, notably on glucose oxidation.

Palmitate and oleate were the selected NEFA in the current research because they are the commonest circulating NEFA (298) and the concentration of 0.25 mM was chosen because it represents a high physiological NEFA level in which toxicity would not be expected. The incubations were performed in 2 h to observe the acute effects on glucose metabolism since the placenta alters its metabolism almost immediately in response to changes in glucose supply (299).

Most literature regarding lipid effects on glucose transport and metabolism is based on glucose and NEFA interactions in insulin sensitive tissues such as skeletal muscle and adipocytes. The results emphasise the effects of saturated fatty acids in causing insulin resistance and mono and/or PUFAs having “protective” roles. To understand how different fatty acid types and doses, as well as the period of incubation in the presence of NEFA, may affect glucose metabolism in trophoblasts, studies performed in other tissues, in particular muscle, but also liver and adipose tissue, are discussed here.

In the current studies glucose uptake was not affected in the presence of 0.25 mM NEFA. Nonetheless, there are descriptions in other tissues of increase, decrease or maintenance of glucose uptake in the presence of oleate depending on its dose and insulin addition. Most studies only found significant palmitate effects on glucose uptake when it was at high concentration, for more than 4 h incubations or after insulin stimulation. A dose and time-response curve in rat muscle showed that exposure to palmitoleate, a monounsaturated (n-7) fatty acid, increased total glucose uptake measured through 2-deoxyglucose uptake from concentrations ≥ 0.25 mM with the maximum effect at 0.75 mM (300). This effect on total glucose uptake was observed only from 4 h of incubation with the maximum effect of 2.4-fold increase in total glucose uptake having been observed after 16 h (300). Incubations with oleate at 0.75 mM for 16 h also increased glucose uptake, however, exposure to palmitate at the same dose and duration neither affected glucose uptake alone or the rise promoted by palmitoleate (300). Nevertheless, pre-incubation with palmitate 0.75 mM inhibited total glucose uptake stimulated by insulin (300). Basal glucose uptake induced by palmitatoleate was not due to increased protein synthesis, but due to recruitment of GLUT1 and GLUT4 to the plasma membrane. Moreover, dissimilar to insulin action, which is fast and occurs in minutes, palmitoleate had a slow and sustained response (300). It is possible, therefore, that trophoblasts may have affected total glucose uptake and metabolism if exposed to NEFA at higher

concentrations or for longer time, even though trophoblast cells are not highly responsive to insulin as are muscle cells. Pre-incubation of human muscle cells with 0.6 mM oleate for 24 h had neither an effect on basal nor an effect on insulin-stimulated glucose uptake (301). On the other hand, incubations for 24 h with 0.6 mM eicosapentaenoic acid (EPA), a polyunsaturated (n-3) fatty acid, increased basal glucose uptake by 2.4-fold, which was further increased by insulin (301). In addition to a glucose uptake increment, the exposure to 0.6 mM EPA for 24 h led to an increase in GLUT1 mRNA expression of 2.5-fold, but no increase in GLUT4 mRNA (301). Thus, as EPA is an important dietary fatty acid during pregnancy, especially to the fetus nervous system tissue (302), it would be interesting to include this NEFA when addressing trophoblast metabolism. A study with 3T3-L1 adipocytes, a cell line, demonstrated that basal and insulin-stimulated glucose uptake rates were not affected after 4 h incubation with a high dose of palmitate (0.8 mM) (303). Moreover, a study with rat muscle strips reported that basal and insulin-mediated glucose uptake and phosphorylation (measured by the labelled 2-deoxyglucose method) was significantly reduced in cultures exposed to 2 mM palmitate only in incubations longer than 4 h (304). Conversely, insulin-mediated glucose uptake was not affected by a lower palmitate concentration (1 mM) in muscle strips incubated for the same duration (304). Interestingly, muscle strips also had reduced insulin-stimulated glucose uptake following 4 h incubation with 1 mM of oleate, but only at a high insulin concentrations (304).

Unlike previous published research in other organs and tissues, we did not find a significant effect of NEFA on glycolysis and lactate production in human trophoblast cultures. In renal proximal tubular cell cultures, palmitate (at 0.4 mM concentration for 24 h incubation) reduced both glycolysis and lactate release by 38% only when L-carnitine was added (305). On the other hand, palmitate at the same concentration for 96 h induced a significant decrease in glycolysis and lactate even without L-carnitine (305).

The decrease in glycolysis occurred in parallel with a similar reduction in total glucose uptake at both basolateral and apical cellular surfaces at 24 h, and the reduction at 96 h (without L-carnitine) was accompanied by a decrease in glucose uptake only from the basolateral surface (305). Hence, it is possible in the previous results in renal tubules that the shorter term (24 h) reduction in glycolysis and lactate production was due to a decline in the availability of glucose substrate in the presence of palmitate and L-carnitine; whilst, after 96 h other changes, such as inhibition of the expression of glycolytic enzymes, may have contributed to a reduction in the glycolysis rate (305). In rat hepatocytes incubated at 15 mM glucose concentration with insulin to mimic the post-prandial liver environment, exposure to palmitate or oleate (at 50 and 150 μM for at least 24 h) neither altered glycolysis measured by tritiated water production from [6-^{3}H]-glucose nor the accumulation of lactate and pyruvate (306). As discussed previously, products of lipid oxidation can affect glycolysis through inhibition of phosphofructokinase and pyruvate dehydrogenase. In accordance with our data, in rat placental slices glucose metabolism, including measures of total glucose uptake, as well as lactate and CO_2 formation, were not changed when incubated in the presence of 0.8 mM oleate for 1 h (207). In contrast, glycogen synthesis was increased by 0.8% (207). Also, the addition of citrate to placental cultures, a strong inhibitor of phosphofructokinase in muscle, did not inhibit total glucose uptake, lactate formation, glycogen synthesis or glucose oxidation (207).

Glucose oxidation can be inhibited in the presence of fatty acids, as has been shown in muscles (307). In the presence of lipids, fatty acid oxidation is promoted which leads to pyruvate dehydrogenase suppression in the mitochondria and, consequently, reduction of glucose oxidation (307). In the present research, however, glucose oxidation was affected by NEFA only at low glucose concentrations. Otherwise, NEFA had minimal effect on glucose oxidation, most likely owing to the reasons discussed above.

In the current study, NEFA increased the glucose flux into glycogen. *In vivo*, conditions such as prolonged physical exercise or poorly controlled diabetes can increase circulating NEFA and ketone bodies. NEFA concentrations are also increased after meals rich in fat (212). Consequently, glucose is not utilised for oxidation in these conditions and, at least in the heart, can be shifted to glycogenesis (212). Thus, it is possible that the first glucose metabolic pathways affected by NEFA in trophoblasts relate to glycogen storage (glycogenesis and possibly glycogenolysis), as the net rate of glycogen synthesis in the current studies, within 2 h incubations, was greater in the presence of fatty acids. Perhaps other pathways would be affected if the cells were incubated at the same NEFA concentration for longer periods. There are descriptions of both inhibition or stimulation of glycogen synthesis in the presence of NEFA in other tissues. In rat skeletal muscle cells, palmitoleate induced glucose flux into glycogen (300). This stimulation of glycogen influx, however, was less potent than that caused by insulin and did not seem to occur through the same classic molecular mechanism activated by insulin, i.e. phosphorylation of glycogen synthase kinase 3 and dephosphorylation of glycogen synthase (300). Conversely, in rat muscle palmitate decreased insulin-stimulated glycogen synthesis by 51%, with near maximum effect after 2 h at a 2 mM concentration or after 4 h at a 1 mM concentration (304). Interestingly, palmitate affected glycogen synthesis before inhibiting basal or insulin-stimulated glucose uptake (304). Oleate (at 1 mM concentration for 4 h) also decreased glycogen synthesis but only when cultures were in the presence of $\geq$ 300 μIU insulin/ml (304). Similarly, oleate (at 0.6 mM for 24 h) did not affect glycogen synthesis in human skeletal muscle cell cultures in the presence or absence of 100 nM insulin (17 μIU/ml) (301).

4.10 Limitations in the methods for the assessment of glucose metabolism

The main limitation in the interpretation of the results of this thesis chapter are the discrepancies between the absolute values of glucose metabolism in the various pathways using the different methods. This was particularly evident when comparing total glucose uptake with glycolysis rates. At the 1 mM media glucose concentration, glycolysis was between 2.7 (plus NEFA) and 3.7-fold (no NEFA) higher than total glucose uptake; at 5 mM media glucose concentration glycolysis was 1.6-fold higher than total glucose uptake; and at 15 mM total glucose uptake was between 1.2 (no NEFA) and 1.4-fold (plus NEFA) higher than glycolysis rates. It is clear therefore that the glycolysis rate was disproportionally high perhaps not reflecting the real absolute fractions of glucose partitioning into this pathway. Hence, results from different pathways assessed in this research cannot be directly compared in terms of absolute results and limitations of tracer/tracee methodology used in this research have to be considered.

At least in rats, 2-deoxyglucose is transferred across the placenta to the same extent as D-glucose (308). In this thesis research with isolated trophoblasts in culture, it is assumed that only phosphorylated 2-deoxyglucose remains intracellularly after media removal and cellular washes. It is possible that the total glucose uptake curve could be underestimated if trophoblasts are unable to phosphorylate all the 2-deoxyglucose taken up into the intracellular space or the phosphorylated 2-deoxyglucose is dephosphorylated at a significant rate depending on the presence of glucose 6-phosphatase or other less specific phosphatases. This could explain why the absolute values of the total glucose uptake curve are lower compared to some of the other pathways studied. The method used in this research does not discriminate between the accumulation of free and phosphorylated [(U)^{14}C]-2-deoxyglucose; thus the separation and purification of these compounds by

chromatography would be valuable. In isolated rat lungs perfused for 20 minutes, [(U)^{14}C]-2-deoxyglucose uptake was followed by accumulation not only of phosphorylated [(U)^{14}C]-2-deoxyglucose, but also of unphosphorylated [(U)^{14}C]-2-deoxyglucose, which was significantly higher than that of phosphorylated [(U)^{14}C]-2-deoxyglucose. (309). Unphosphorylated [(U)^{14}C]-2-deoxyglucose presented a kinetic curve similar to the total [(U)^{14}C]-2-deoxyglucose uptake curve (calculated as the sum of intracellular phosphorylated and unphosphorylated [(U)^{14}C]-2-deoxyglucose) (309). In that research, intracellular accumulation of unphosphorylated [(U)^{14}C]-2-deoxyglucose The authors of that paper (309) argued that in rat lungs [(U)^{14}C]-2-deoxyglucose intracellular transport may be higher than its phosphorylation owing to inhibition of hexokinase activity by a decrease in ATP levels in the tissue or by a [(U)^{14}C]-2-deoxyglucose 6-phosphate negative feed-back (309). Alternatively, the presence of enzymes with non-specific phosphatase activity in the lungs allows for the conversion of [(U)^{14}C]-2-deoxyglucose 6-phosphate into free [(U)^{14}C]-2-deoxyglucose (309). Total glucose uptake estimation by the [(U)^{14}C]-2-deoxyglucose method has been extensively studied in the brain. A study with rats showed that the rate of total glucose uptake in the brain using [(U)^{14}C]-2-deoxyglucose measures the rate of the hexokinase reaction, but not total glucose utilisation (310). In the brain, the rate constant for labelled 2-deoxyglucose phosphorylation was about 10%/minute, whereas the rate constant for dephosphorylation was about 3%/minute (310). In addition, the kinetics of D-glucose and 2-deoxyglucose were dissimilar (e.g. 2-deoxyglucose transport is 40% faster than D-glucose) and phosphorylation rates of each molecule can vary at extreme glucose conditions in the brain (310). Under low blood glucose arterial levels, transport through the blood-brain barrier would be optimised and higher than 2-deoxyglucose phosphorylation (310). In the presence of hyperglycaemia, glucose or 2-deoxyglucose proportional uptake would be limited by the blood-brain barrier to a greater extent than

hexose phosphorylation (311). Furthermore, glucose and 2-deoxyglucose metabolism was not found to be the same in different regions of the brain (312). Nonetheless, it may not be appropriate to extrapolate data derived from research in the brain, an organ highly complex, to much simpler cells such as cytotrophoblasts. Another hypothesis to explain the underestimation of glucose uptake measured in the current study at lower media glucose concentrations is that 2-deoxyglucose 6-phosphate may be dephosphorylated by phosphatases in the trophoblasts. The liver and kidney contain high concentrations of the endoplasmic reticulum glucose 6-phosphatase catalytic subunit-1 (G6PC1), which promotes glucose 6-phosphate hydrolysis for glucose production from the gluconeogenesis and glycogenolysis pathways (313). The placenta does not express G6PC1, but it expresses another glucose 6-phosphatase isoform (G6PC3), which is particularly found in the human brain, skeletal muscle and heart (313). G6PC3 showed a higher predilection for 2-deoxyglucose 6-phosphate as a substrate compared to glucose 6-phosphate (313). There are no data on specific G6PC3 expression and activity in human trophoblasts, since most literature has reported results from the whole placenta and not individual cellular groups. Thus, if there is G6PC3 expression in isolated human trophoblasts, the results from total glucose uptake measured in this research may be underestimated owing to 2-deoxyglucose 6-phosphate dephosphorylation by intracellular phosphatases. In addition, it is not known if the rate of dephosphorylation of 2-deoxyglucose 6-phosphate (if present) is homogenous through all glucose concentrations in all placental cellular groups.

In theory, the glycolysis tracer method used in the current research is based on ^{3}H losses from [5-^{3}H]-glucose into $^{3}H_2O$ mainly at the reaction catalysed by aldolase (284). In this reaction, fructose 1, 6-bisphosphate is cleaved into glyceraldehyde 3-phosphate and dihydroxyacetone-phosphate (refer to Chapter 1). If this reaction is not complete, $^{3}H_2O$ is produced at the enolase reaction, when 2-phosphoglycerate is dehydrated to

phosphoenolpyruvate (284). Nevertheless, results from a study which compared the glycolytic flux based on $^{3}H_2O$ synthesis from [5-^{3}H]-glucose metabolism with net glycolytic flux (net release of pyruvate plus lactate) and efflux of ^{14}C pyruvate plus ^{14}C lactate from ^{14}C labelled glucose in rat heart showed that the glycolysis rate based on the $^{3}H_2O$ release from [5-^{3}H]-glucose method was 260% higher than the other methods (314). In this study, the authors suggested that the non-oxidative branch of the pentose phosphate pathway was the major source of $^{3}H_2O$ via the reaction catalysed by the enzyme transaldolase (314), which is similar to the reaction catalysed by aldolase.

Another hypothesis to explain the overestimation of glycolysis rates measured by the [5-^{3}H]-glucose method is that a futile cycling between hexose and triose phosphate was present. However, this would depend on fructose 1,6-bisphosphatase activity, which was found to be very low in the human placenta (315).

Other potential limitations of the experiments of this chapter relate to possible osmotic pressure effects on cells incubated at the higher glucose concentrations, as these effects were not directly studied. It could be assessed using L-glucose, since the hexose transport system in the placenta, mainly via GLUT 1, is stereospecific for D-glucose and the rate of L-glucose transport in trophoblasts is only about 10% of the transport of D-glucose (184). However, cellular damage due to increased osmotic pressure in the media is unlikely to have occurred since, in some laboratories, trophoblasts are grown in regular DMEM that contains 25 mM glucose. In addition, no major cellular changes were observed during 2 h incubations at the media glucose concentration of 35 mM.

Finally, the results of this chapter all had high variability from placenta to placenta as is reflected in the standard error and standard deviations. This was especially true for glycolysis and lactate production. Although all trophoblast isolations were performed by the same researcher and the donor mothers were carefully selected under strict criteria, biological variations among primary cultures are common and may have occurred.

4.11 Conclusions

In conclusion, during acute exposure to high glucose media, human trophoblast take up increasing amounts of glucose that is not channelled to glycolytic and oxidative pathways. Conversely, glucose flux is diverted to non-oxidative metabolic pathways i.e. glycogen synthesis and perhaps the non-oxidative pentose phosphate pathway. In addition, glucose metabolism in human trophoblasts does not seem highly sensitive to NEFA action as demonstrated in other tissues.

Chapter 5

Results for metabolism and morphology studies in long-term primary trophoblast cultures

5.1 Metabolism studies

5.1.1 Introduction

The results of metabolism studies in primary human trophoblast short-term cultures were presented in Chapter 4. Since at this cellular differentiation stage (36 h) most cells were cytotrophoblasts, a new set of experiments were performed in primary human trophoblasts on day 5 of culture with complete DMEM supplemented with EGF (10 ng/ml) to induce syncytialisation (Figure 5.1). The rationale of these studies was to observe possible differences regarding glucose metabolism in a group of more differentiated cells with greater syncytialisation. Hence, key glucose and palmitate metabolism experiments were selected to be performed at physiological (5 mM) and high (25 mM) glucose concentrations in the presence or absence of NEFA (0.25 mM, palmitate: oleate ratio; 1:1). Only for glycolysis assessment, experiments at 1 mM media glucose concentration were also included to enable the analysis of a rate curve.

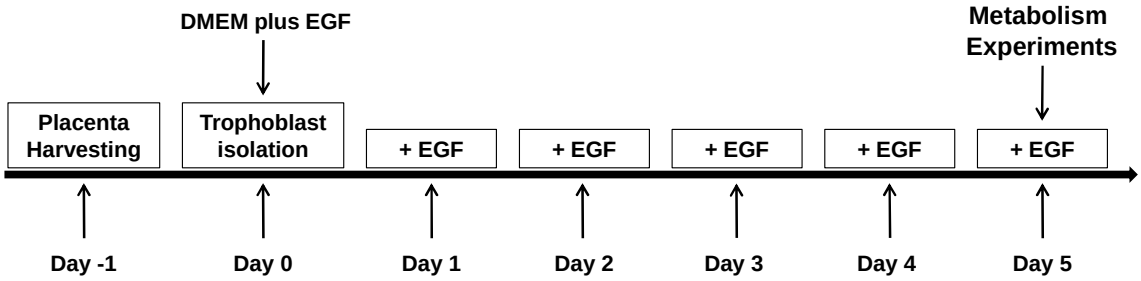

Figure 5.1. Experimental design scheme for metabolism studies in long-term primary human trophoblast cultures. Human placental villous tissue was harvested (day -1) and trophoblasts were isolated and seeded on the following day (day 0). Human trophoblast were established in culture over 5 days post isolation in complete DMEM (refer to Chapter 2 and Appendix 1 for culture details) at 5.5 mM glucose concentration supplemented with EGF (10 ng/ml) to induce syncytialisation. Long-term culture metabolism experiments were performed on day 5 after isolation when many cells are aggregated and fused into syncytiotrophoblasts, as was demonstrated in the results of Chapter 2.

DMEM: Dulbecco's Modified Eagle Medium; EGF: epidermal growth factor.

5.1.2 Results

5.1.2.1 Total glucose uptake

In primary human trophoblasts cultures established over 5 days post isolation in complete DMEM supplemented with EGF, the rate of glucose uptake as measured by the ^{14}C labelled 2-deoxyglucose 6-phosphate method during 2 h incubations, as previously described (Chapter 3), significantly increased with an increase in the media glucose concentration from 5 to 25 mM. Total glucose uptake in long-term trophoblast cultures was further increased in the presence of NEFA (Figure 5.2). The linear correlation between total glucose uptake and available glucose in the media was moderate in the absence of NEFA (r^2=0.58, p=0.027) and strong in the presence of NEFA (r^2=0.80, p=0.003).

Figure 5.2. Total glucose uptake by trophoblasts in long-term cultures increased with rising media glucose concentration and was higher in the presence of NEFA. Total glucose uptake in trophoblasts established in culture in the presence of EGF (10 ng/ml) over 5 days, as measured by the ^{14}C labelled 2-deoxyglucose 6-phosphate method during 2 h incubations (refer to Chapter 3), increased with an increase of the media cold glucose concentration from 5 to 25 mM. Total glucose uptake was further increased at the media glucose concentration of 25 mM glucose in the presence of 0.25 mM NEFA. Two-way ANOVA: NEFA effect p=0.049; glucose effect p=0.013, NEFA-glucose interaction p=0.038. Bonferroni *post-hoc* test: *25 mM glucose (no NEFA) *vs* 25 mM glucose (plus NEFA) p=0.022. Data are means ± SEM of 4 independent experiments in which each point was the average of triplicate wells.

5.1.2.2 Glycolysis

The rate of glucose utilisation via glycolysis by primary human trophoblasts cultures established over 5 days post isolation in the presence of EGF was measured by the [5-^{3}H]-glucose tracer method as described in Chapter 3. The glycolysis rate showed an increase with increasing media glucose concentrations according to the glucose main effect using ANOVA (Figure 5.3). However, with *post-hoc* testing, a significant increase in glycolysis rate was only demonstrated when the media glucose concentration was increased from 1 to 25 mM in the presence of NEFA. NEFA did not affect glycolysis in these experiments (Figure 5.3).

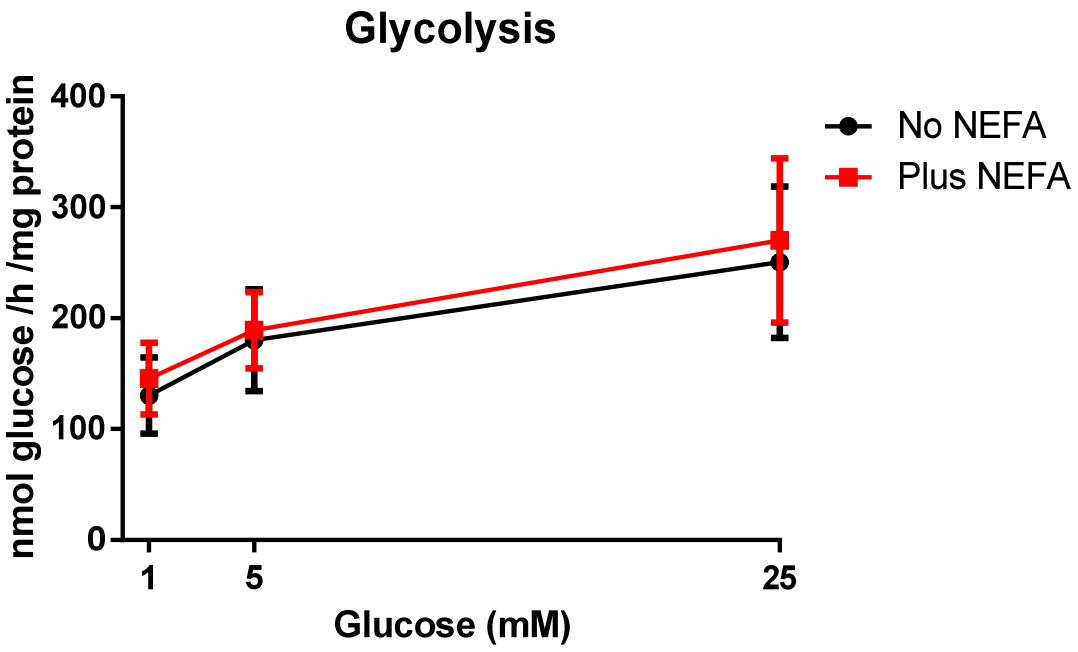

Figure 5.3. Glucose utilisation via the glycolysis pathway in long-term human trophoblast cultures increased with increasing glucose concentrations in the media. Glycolysis rate over 2 h was measured in trophoblasts cultured for 5 days in the presence of EGF using the [5-^{3}H]-glucose tracer method previously described (Chapter 3). Glycolysis rates were higher at increased glucose concentrations in the media, as assessed by the glucose main effect using ANOVA. However, in *post-hoc* assessment, a significant effect was only found for an increase in the media glucose concentration from 1 to 25 mM in the presence of NEFA. Overall, NEFA did not affect this metabolic pathway. Two-way ANOVA: NEFA effect ns; glucose effect p=0.006; NEFA-glucose interaction ns. Bonferroni *post-hoc* test: 1 mM *vs* 25 mM (plus NEFA) $p < 0.05$. Data are means ± SEM of 3 independent experiments in which each point was the average of triplicate wells.

5.1.2.3 Glucose oxidation

The glucose oxidation rate in primary human trophoblasts established in culture over 5 days after isolation in the presence of EGF was assessed through [(U)^{14}C]-glucose metabolism into ^{14}C labelled CO_2 as mentioned in Chapter 3. The glucose oxidation rate, in response to a rise in the media glucose concentration from 5 to 25 mM, increased according to the glucose main effect. However, in *post-hoc* testing this glucose effect was only significant for the increase found in the presence of NEFA (by 218.5%) (Figure 5.4).

Figure 5.4. Glucose oxidation rate in long-term human trophoblast cultures increased at the higher glucose concentration in the media. Glucose oxidation rates in human trophoblasts established in culture with EGF (10 ng/ml) over 5 days after isolation were measured by [(U)^{14}C]-glucose tracer metabolism into ^{14}C labelled CO_2 method as explained in Chapter 3. Glucose oxidation significantly increased with a rise in the media glucose from 5 to 25 mM as assessed by the main glucose effect using ANOVA. However, in *post-hoc* assessment, a significant effect was only found for an increase in the media glucose concentration from 5 to 25 mM in the presence of NEFA. Overall, NEFA did not affect this metabolism pathway.

Two-way ANOVA: NEFA effect ns; glucose effect p=0.007; NEFA-glucose interaction ns. Bonferroni *post-hoc* test: 5 mM glucose *vs* 25 mM glucose (plus NEFA) p=0.006. Data are means ± SEM of 6 independent experiments in which each value was the average of duplicate or triplicate T25 flasks.

5.1.2.4 Palmitate oxidation and acid soluble product formation

In primary human trophoblasts established in culture in the presence of EGF over 5 days post isolation, the rate of palmitate oxidation as measured during 2 h incubations by the [(U)^{14}C]-palmitate tracer metabolism into ^{14}C labelled CO_2 method (Chapter 3) showed a trend towards reduction with an increment of the cold glucose concentration in the media from 5 to 25 mM (Figure 5.5). The levels of acid soluble products from palmitate oxidation, as assessed by the method explained in Chapter 3, were similar in the presence of glucose concentrations in the media of 5 and 25 mM (Figure 5.6).

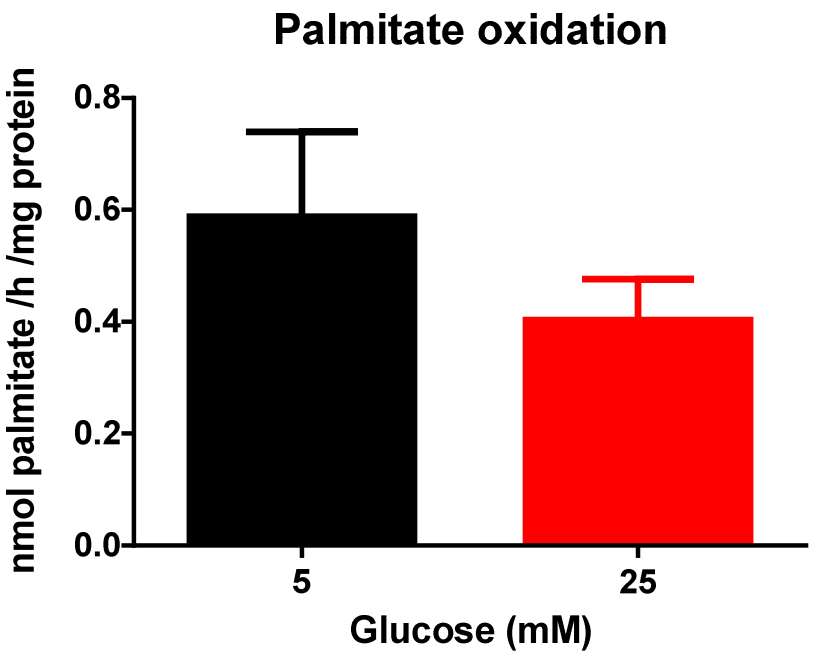

Figure 5.5. Palmitate oxidation in long-term human trophoblast cultures showed a trend towards reduction in the presence of the higher level of glucose in the media. Palmitate oxidation in human trophoblasts established in culture with EGF (10 ng/ml) over 5 days post isolation and measured by [(U)^{14}C]-palmitate tracer metabolism into ^{14}C labelled CO_2 method (described in Chapter 3) presented a downward trend at 25 mM glucose concentration in the media. Data are means ± SEM of 6 independent experiments in which each value was the average of duplicate or triplicate T25 flasks.

Figure 5.6. Acid soluble product synthesis during palmitate oxidation in long-term human trophoblast cultures were similar at low and high glucose concentrations in the media. Palmitate oxidation into acid soluble products in human trophoblasts established in culture with EGF over 5 days post isolation, as measured by [(U)^{14}C]-palmitate tracer metabolism into ^{14}C labelled acid soluble products method described in Chapter 3, showed similar values at 5 or 25 mM glucose concentrations in the media. Data are means ± SEM of 7 independent experiments in which each value was the average of duplicate or triplicate T25 flasks.

5.1.2.5 Glycogen synthesis with tracer

The flux of glucose into glycogen in primary human trophoblasts cultures established over 5 days post isolation in the presence of EGF, as measured by the [(U)^{14}C]-glucose tracer method previously explained in Chapter 3, increased by 142.4% in the absence of NEFA and by 252.3% in the presence of NEFA with an increment in the glucose concentration of the media from 5 to 25 mM. Although this increase in the glycogen synthesis rate was significant according to main glucose effect using ANOVA, it was not significant using Bonferroni *post-hoc* testing for the effects of glucose in the absence or presence of NEFA. Glucose flux into glycogen was not affected by the presence of 0.25 mM NEFA (Figure 5.7).

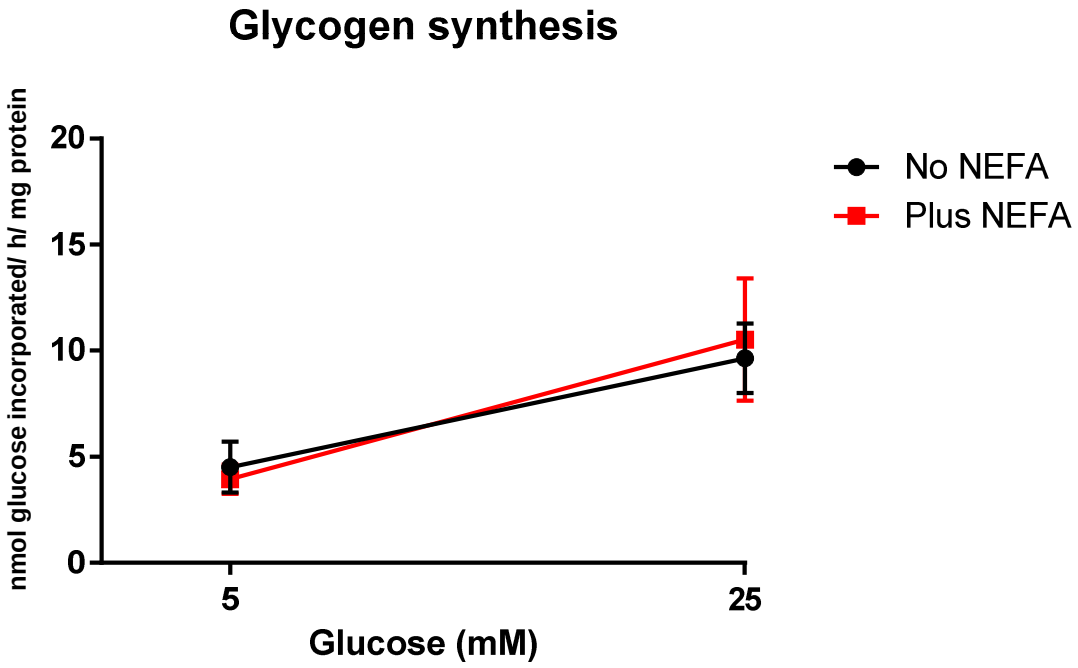

Figure 5.7. The acute glucose flux into glycogen synthesis in long-term primary human trophoblast cultures increased with an increase in the media glucose concentration. **The presence of NEFA did not affect this metabolic pathway.** The acute glucose flux into glycogen was measured in human trophoblasts established in culture supplemented with EGF over 5 days post isolation using the [(U)^{14}C]-glucose tracer method, as previously described (Chapter 3). Glycogen synthesis rates in the trophoblasts were significantly higher with incubation at 25 mM compared to 5 mM glucose according to the main glucose effect using ANOVA. However, with Bonferroni *post-hoc* testing, the effects of glucose, either in the presence or absence of NEFA, to increase glycogen synthesis was not significant. NEFA had no effects on glycogen synthesis rates.

Two-way ANOVA: NEFA effect ns; glucose effect p=0.017; NEFA-glucose interaction ns. Bonferroni *post-hoc* test: ns. Data are means ± SEM of 4 independent experiments in which each point was the average of triplicate wells.

5.2 Cellular morphology and triacylglycerol quantification in long-term primary human trophoblast cultures

5.2.1 Introduction

Primary human trophoblasts were established in culture in complete DMEM (at 5.5 mM glucose concentration) in the presence or absence of EGF (10 ng/ml) for 48 h after isolation. The media was change on day 2 to complete DMEM in the presence or absence of EGF and in the presence or absence of NEFA (0.1 mM, palmitate: oleate ratio; 1:1). For reagents and media preparation refer to Appendix 1. On the 5^{th} day of culture, trophoblasts were stained for Oil red O to observe EGF and/or NEFA effects on trophoblast morphological characteristics such as lipid droplet formation, cellular aggregation and syncytialisation (Figure 5.8). In addition, trophoblast intracellular TG content was quantified.

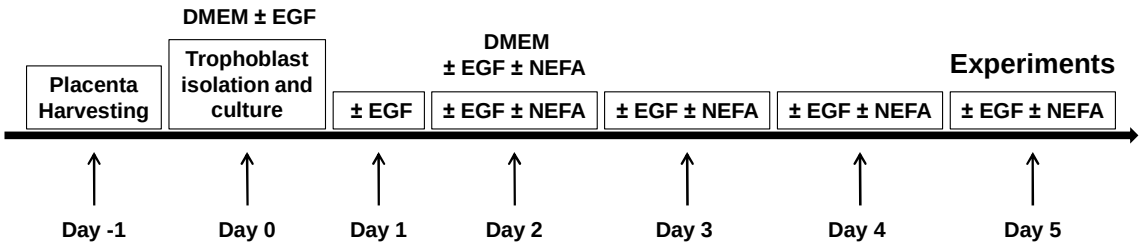

Figure 5.8. Experimental design scheme for morphology studies and TG quantification in long-term primary human trophoblast cultures. Human placental villous tissue was harvested (day -1) and trophoblasts were isolated and seeded on the following day (day 0). Trophoblasts were established in culture over 48 h in complete DMEM (at 5.5 mM glucose concentration) in the presence or absence of EGF (10 ng/ml). From this time point (day 2), trophoblasts were cultured in complete DMEM (at 5.5 mM glucose) in the presence or absence of NEFA (0.1 mM, palmitate: oleate ratio; 1:1) and in the presence or absence of EGF (10 ng/ml). On the 5th culture day, trophoblasts were stained for Oil red O and TG content was measured.

DMEM: Dulbecco's Modified Eagle Medium. EGF: epidermal growth factor; TG: triacylglycerol.

5.2.2 Results

5.2.2.1 Oil red O staining

Primary human trophoblast cultures were established in chamber slides over 48 h post isolation in complete DMEM (5.5 mM glucose) with or without EGF (10 ng/ml). From day 2 to 5 of culture, trophoblasts were grown in complete DMEM (5.5 mM glucose) in the presence or absence of EGF) and in the presence or absence of 0.1 mM NEFA. Trophoblasts were then stained for Oil red O according to the method described in Chapter 3. Slides stained for Oil red O were analysed by 2 independent viewers and scored according to Table 3.6 (refer to Chapter 3). Large and small lipid droplets formation was not significantly different in the conditions analysed (± EGF ± NEFA) (Figures 5.9 and 5.10). Cellular aggregation and syncytialisation increased in the presence of EGF in comparison with cultures in the absence of EGF. In cultures in the absence of EGF, the addition of NEFA did not change cellular aggregation, but resulted in a trend towards syncytialisation. In the presence of EGF, NEFA caused a trend towards cellular aggregation, but did not affect syncytialisation (Figure 5.11).

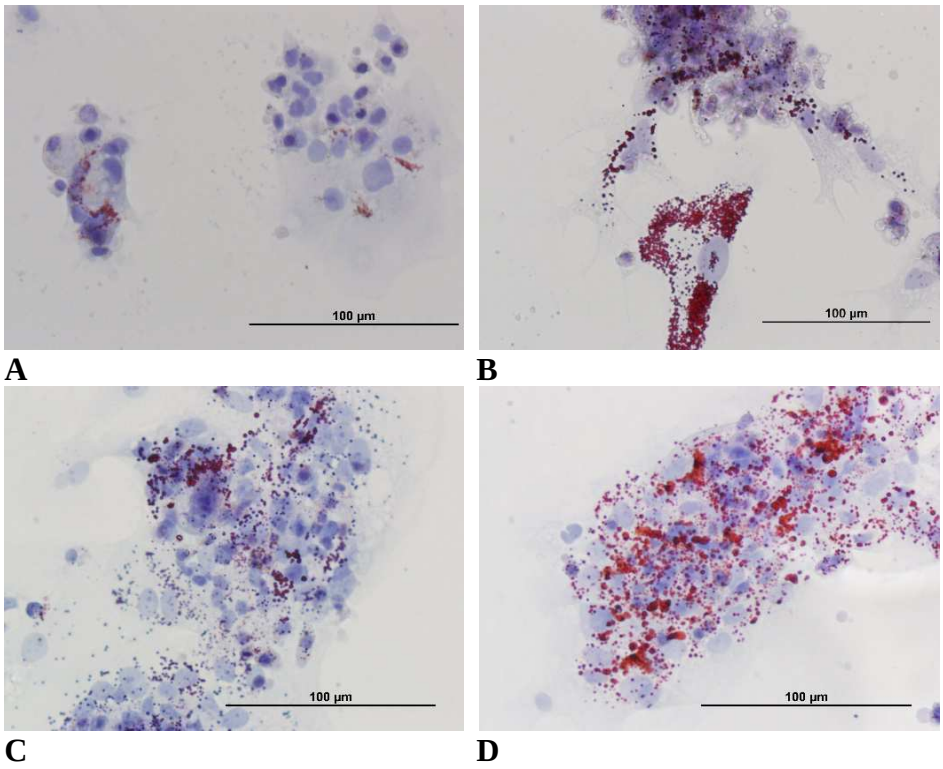

Figure 5.9. Representative photomicrographs of long-term primary human trophoblasts cultured in the presence or absence of EGF and in the presence or absence of NEFA stained for Oil red O. Primary human trophoblasts were cultured in chamber slides in complete DMEM (at 5.5 mM glucose concentration) with or without EGF (10 ng/ml) over 48 h post isolation (refer to Chapter 3). From day 2 to 5 of culture, trophoblasts were grown in the presence or absence NEFA (0.1 mM) and in the presence or absence of EGF. On day 5, slides were stained for Oil red O (red-staining for lipid droplets) and counterstained with haematoxylin (blue-staining for nuclei). A. Photomicrography of trophoblast culture in the absence of EGF and NEFA. B. Photomicrography of trophoblast culture in the absence of EGF and in the presence of NEFA. C. Photomicrography of trophoblast culture in the presence of EGF and in the absence of NEFA. D. Photomicrography of trophoblast culture in the presence of EGF and NEFA. Lipid droplet accumulation (small and large globules) was observed in all conditions (A-D).

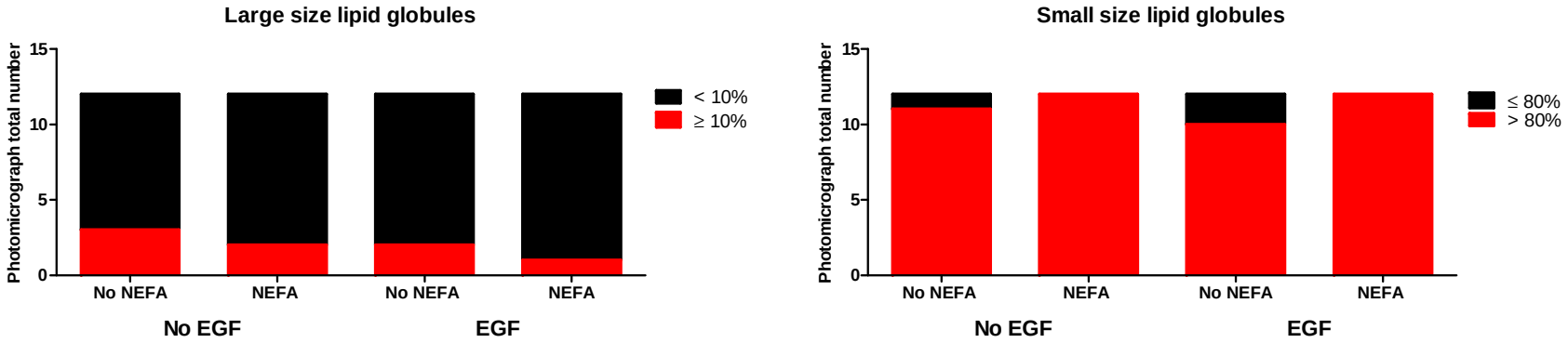

Figure 5.10. Lipid droplet formation was similar in long-term primary human trophoblast cultures stained for Oil red O in the presence or absence of NEFA and was not affected by EGF. Primary human trophoblast cultures were established in chamber slides over 48 h post isolation in complete DMEM (5.5 mM glucose) with or without EGF (10 ng/ml). From day 2 to 5 of culture, trophoblasts were cultured in complete DMEM (5.5 mM glucose) with or without 10 ng/ml of EGF in the presence or absence of 0.1 mM NEFA. On day 5 of culture, trophoblasts were stained for Oil red O according to the method described in Chapter 3. Slides stained for Oil red O were analysed by 2 independent viewers and scored for lipid droplet formation as described in Chapter 3 (Table 3.6). Lipid droplets were divided into small and large size. The accumulation of lipid droplets was similar for all 4 conditions studied for both small and large lipid droplets.
Data are the absolute number of photomicrographs scored in each category of 4 independent experiments in duplicates.

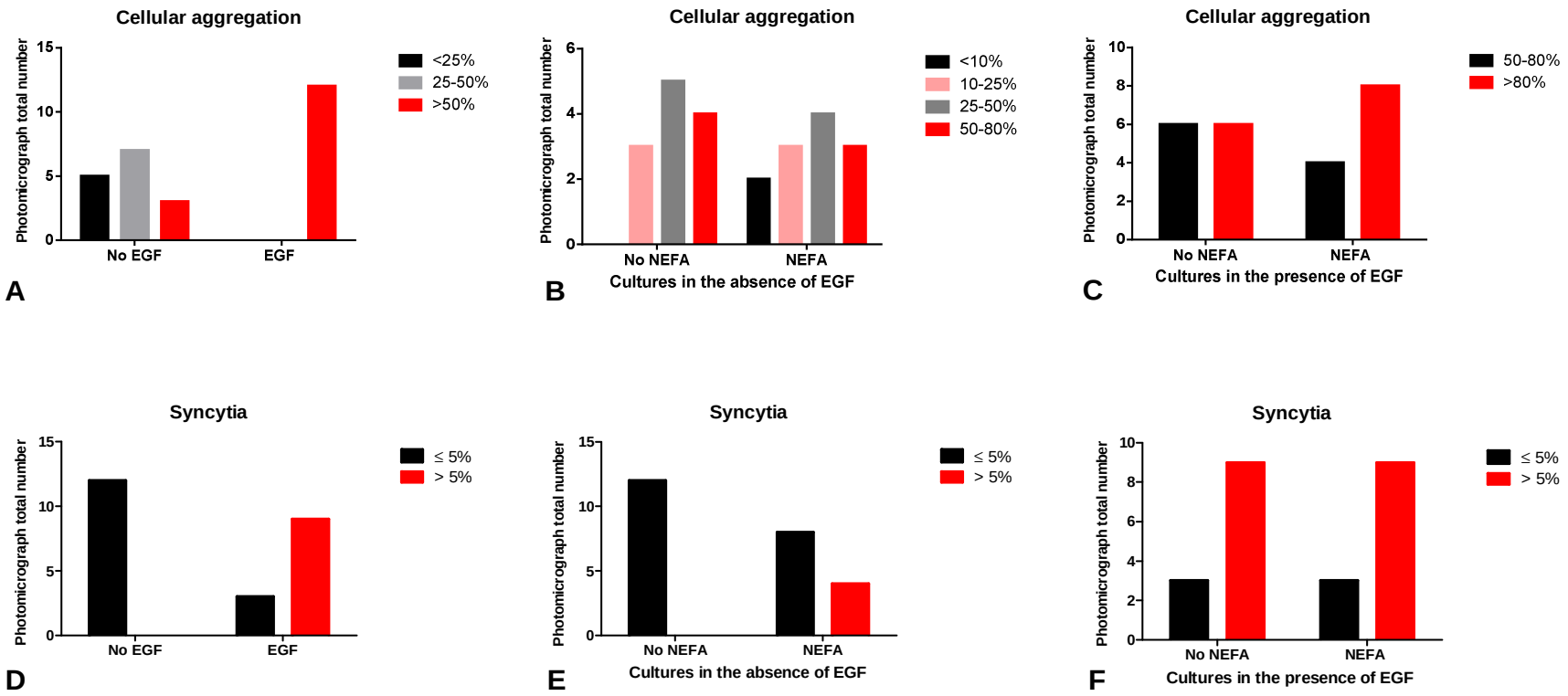

Figure 5.11. Long-term primary human trophoblast cultures stained for Oil red O showed increased syncytialisation in the presence of EGF, with less evident effects of NEFA. Primary human trophoblasts were cultured in chamber slides in complete DMEM (at 5.5 mM glucose concentration) with or without EGF (10 ng/ml) over 2 days post isolation. From day 2 to 5 of culture, trophoblasts were grown in the presence or absence NEFA (0.1 mM), and in the presence or absence of EGF. On day 5, slides were stained for Oil red O. A. EGF increased

cellular aggregation. B. In the absence of EGF, NEFA had no effect on cellular aggregation. C. In the presence of EGF, NEFA showed a trend towards increasing cellular aggregation. D. EGF induced syncytialisation. E. In the absence of EGF, NEFA showed a trend towards an increase of syncytialisation. F. In the presence of EGF, NEFA did not affect syncytialisation.

A. Chi-square for cellular aggregation (EGF effect) $p=0.0002$. B. Fisher's exact test for syncytia (EGF effect) $p=0.0003$. Data are the absolute number of photomicrographs scored in each category of 4 independent experiments in which at least 2 chambers with the same condition were scored.

5.2.2.2 Triacylglycerol quantification

Primary human trophoblast cultures were established in 6 well plates over 48 h post isolation in complete DMEM (5.5 mM glucose) in the presence or absence of EGF (10 ng/ml). For a further 3 days, trophoblasts were cultured in complete DMEM (5.5 mM glucose) with or without EGF in the presence or absence of NEFA (0.1 mM, palmitate: oleate ratio; 1:1). Trophoblasts were then collected and TG content of cells was analysed through an enzymatic colorimetric method as described in Chapter 3 to quantitatively assess the piece of information about lipid droplet formation obtained with Oil red O. TG content as measured by this method was similar in all conditions (Figure 5.12).

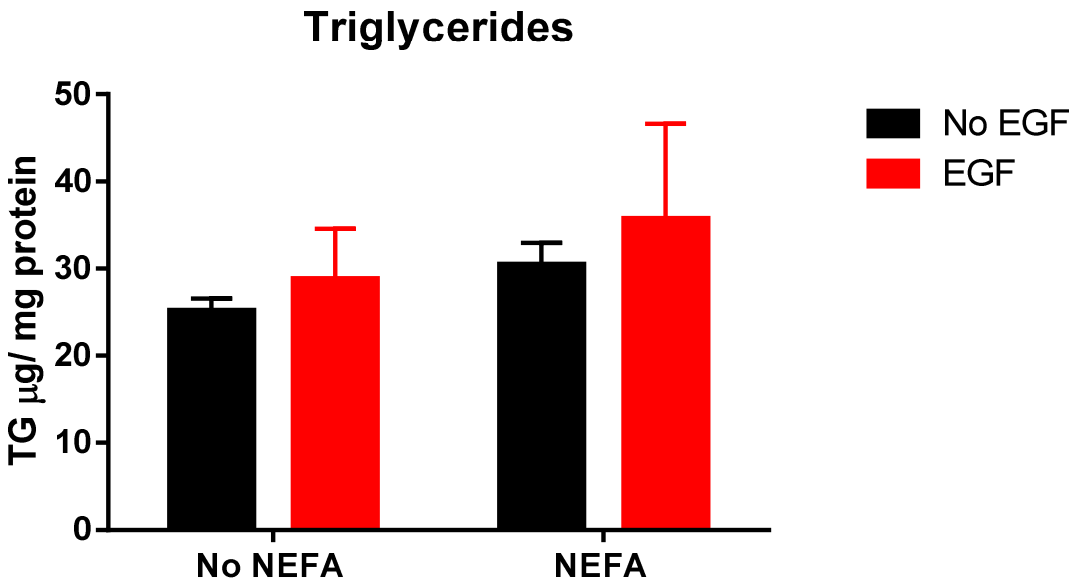

Figure 5.12. TG content was similar in long-term primary human trophoblasts in the presence or absence of EGF and in the presence or absence of NEFA. Primary human trophoblast cultures were established over 48 h post isolation in complete DMEM (5.5 mM glucose) with or without EGF (10 ng/ml). For a further 3 days, trophoblasts were cultured in complete DMEM (at 5.5 mM glucose) with or without EGF in the presence or absence of 0.1 mM NEFA. TG content of cells was quantified using the enzymatic colorimetric method as described in Chapter 3. There were no differences in the TG content between the conditions. Data are means ± SEM of 4 independent experiments in which each value was the average of triplicate wells.

5.3 Discussion

The main aim of the experiments performed in these longer-term primary human trophoblast cultures (5 days from the isolation day) was to investigate the glucose metabolism pathways following syncytialisation induced by EGF. The pathways analysed were similar to those of the short-term experiments (Chapter 4). In the majority of experiments, glucose metabolism was assessed at media glucose concentrations of 5 and 25 mM in 2 h incubations (except for glycolysis experiments in which 1 mM glucose concentration was also included). In addition, and as was performed in the short-term culture experiments, the acute effects of 0.25 mM NEFA (palmitate and oleate) on glucose metabolism was also studied.

Human trophoblasts established in culture over 5 days post isolation had higher glucose uptake rates at media glucose concentrations of 25 mM compared to 5 mM using the labelled 2-deoxyglucose metabolism method. Unexpectedly, total glucose uptake was significantly increased in the presence of NEFA. Glycolysis rates, assessed by [5-^{3}H]-glucose metabolism method, showed an increase with rising media glucose concentrations, but this was significant in *post-hoc* testing only for an increase in the media glucose concentration from 1 to 25 mM in the presence of NEFA. Similarly, glucose oxidation studied by the [(U)-^{14}C]-glucose metabolism method increased with an increment in the media glucose concentration from 5 to 25 mM, which again in *post-hoc* testing was only significant in the presence of NEFA. Palmitate oxidation measured by the [(U)-^{14}C]-palmitate metabolism method demonstrated a trend of reduction at 25 mM media glucose concentration, whilst acid soluble product formation assessed in the same experiments was not affected by glucose. Glucose flux into glycogen, measured by [(U)-^{14}C]-glucose accumulation as labelled glycogen method, increased with changes in the media glucose concentration from 5 to 25 mM according to ANOVA. However, non-

significant increases were seen for a glucose effect in the presence or absence of NEFA, when analysed with Bonferroni *post-hoc* testing. Of note, a limitation in *post-hoc* testing was the number of experiments. Overall, in the presence of high available glucose levels trophoblasts in long-term cultures showed increased total glucose uptake, glycolysis, glucose oxidation and glycogen synthesis. Moreover, NEFA did not affect most glucose pathways, only increasing total glucose uptake.

5.3.1 The effects of increasing the media glucose concentration on glucose metabolism pathways in primary human trophoblasts in long compared to short-term cultures

As for the short-term trophoblast cultures, the long-term cultures showed increased total glucose uptake when in the presence of greater media glucose concentrations. However, NEFA stimulated glucose uptake in long-term cultures and did not affect this pathway in short-term cultures. The reasons and mechanism by which NEFA stimulated glucose uptake in cultures richer in syncytiotrophoblasts are unclear. Making a parallel with the effects of palmitoleate on glucose uptake in rat muscle (300), as discussed in Chapter 4, oleate might lead to GLUT1 recruitment to the plasma membrane in syncytiotrophoblasts but not in cytotrophoblasts due to inherent differences between trophoblasts with distinct levels of differentiation.

Glycolysis rates in long-term trophoblast cultures showed an increase with increasing media glucose concentrations only significant in the presence of NEFA. This pattern was similar to that observed in short-term trophoblast cultures, in which the glycolysis rate was near maximum at 1 mM media glucose with a minimal rise with increments of the media glucose concentration above 1 mM to 15 mM, also only statistically significant in the presence of NEFA. Nonetheless, the percentage of increase of glycolysis rates from the lowest to the highest media glucose concentrations were higher for long-term

trophoblast cultures [83.8-113.9% (long-term cultures) *vs* 29.4-57.1% (short-term cultures)].

In the absence of NEFA, the glucose oxidation rate in long-term trophoblast cultures showed a non-significant increase of 48.4% when measured at the media glucose concentration of 25 compared to 5 mM. In the presence of NEFA, glucose oxidation by the more differentiated trophoblasts showed the same trend as for glycolysis, with a significant increase of 190.5%. Comparing the long-term to the short-term cultures, changes in the rates of glucose oxidation with increases in the media glucose concentrations from 5 to 25 mM glucose were between 1.4 and 2.1-fold higher. These dissimilarities between long and short-term cultures suggest that syncytiotrophoblasts and cytotrophoblasts may have different capabilities to metabolise glucose through glycolysis and oxidation. This may have implications in situations of chronic maternal hyperglycaemia as occurs in diabetic pregnancy.

Rates of palmitate oxidation to CO_2 in both the short and long-term trophoblast culture experiments trended down by about 30-33% at media glucose concentrations of 25 mM compared to 5 mM. However, unlike glucose oxidation, palmitate oxidation rates were about 2.7-fold lower in the long-term compared to the short-term trophoblast cultures. Palmitate metabolism into acid soluble products also was lower in the long compared to short-term culture experiments. These results suggest that glucose inhibits palmitate oxidation in a similar way in both long and short-term cultures, but lipids are utilised less for energy production in syncytiotrophoblasts compared to cytotrophoblasts. The only published study comparing the expression of enzymes involved in fatty acid oxidation in different placental cell types using immunostaining of placental sections suggested an increased quantity of MCAD, LCAD, VLCAD, SCHAD, LCHAD and LKAT in syncytiotrophoblasts compared to cytotrophoblasts (224). These results are at variance with our findings suggesting greater fatty acid oxidation capacity in cytotrophoblasts.

Considering that the activity of LCHAD, SCHAD, and LKAT in cultures of freshly isolated trophoblast from term placentas were 2 to 3 times higher than those in fresh placental tissue from term pregnancies (224), it is possible that increased fatty acid oxidation in cytotrophoblasts in culture may be a consequence of the isolation and culture process. Clearly though, the placenta has all the enzymes necessary for fatty acid oxidation and this pathway almost certainly contributes to the overall energy provisions for this tissue.

Glucose flux into glycogen rates in long-term trophoblast cultures at 5 mM media glucose concentration were between 1.9 (in the absence of NEFA) and 3-fold (in the presence of NEFA) lower than in short-term cultures. At 25 mM media glucose, these rates in long-term cultures were between 2.9 (in the absence of NEFA) and 3.6-fold (in the presence of NEFA) lower than in short-term cultures. These results suggest that there are major differences in glycogen synthesis capacity between cytotrophoblasts and syncytiotrophoblasts. Consistent with the results of the current thesis, glycogen content was about 3 times higher in cytotrophoblasts after 24 h of culture than in syncytiotrophoblasts after 96 h of culture in a previously reported study (316). The glycogen content of cytotrophoblasts peaked after 24 h of culture followed by intense glycogen hydrolysis without new glycogenesis prior to differentiation into syncytiotrophoblasts at 48 h (316). Based on the observations of their time course research, the authors of this paper suggested that glycogen hydrolysis is linked to syncytialisation. In addition, a recent study has shown that cytotrophoblasts present high levels of glycogen throughout pregnancy (from 6 weeks to term), in contrast with syncytiotrophoblasts, in which strong staining was not observed at any stage of pregnancy (295). Both these previous studies support the findings of the current research that glycogen synthesis is greater in cytotrophoblasts compared to syncytiotrophoblasts.

Overall, the results of our work indicate that cytotrophoblasts and sycytiotrophoblasts have important differences concerning glucose and lipid metabolism and how the cells deal with excess glucose supply. When exposed to high glucose media, syncytiotrophoblasts seem to utilise excess glucose for glycolysis and glucose oxidation, whereas cytotrophoblasts tend to divert excess glucose to glycogen synthesis. Furthermore, this research suggested that NEFA utilisation is less intense in syncytiotrophoblasts compared to cytotrophoblasts. Although not many works have investigated glucose and lipid metabolism in cytotrophoblast and syncytiotrophoblast cultures, there is other evidence that these cell groups metabolise nutrients in different ways. Moe *et al.* have suggested that the pentose phosphate pathway activity declines when cytotrophoblasts differentiate into syncytiotrophoblasts (148). Besides, changes in glucose metabolism seem to be necessary for the cellular fusion process. Bax *et al.* demonstrated that anaerobic glycolysis and glycogen hydrolysis suddenly increase while syncytia are being formed, with return to lower levels afterwards (316). Furthermore, impairment of BeWo cell line syncytialisation and differentiation induced by hypoxia were associated with up-regulation of glycolytic proteins (i.e. enolase and maleate dehydrogenase) together with up or down-regulation of proteins related to cytoskeletal formation, protein structure and degradation, signal transduction, oxidative stress regulation and cell mobility (317).

Also, there are hints in placental diseases, such as pre-eclampsia, that alterations in glucose metabolism may relate to the degree of syncytialisation, placental maturity and syncytial knots formation. For instance, the activity of phosphofructokinase was reduced by 32% in placentas from intrauterine growth restricted pregnancies (including mothers with pre-eclampsia, essential hypertension, diabetes and no medical conditions) (318). On the other hand, the expression of enzymes involved in glycolysis and the TCA cycle were upregulated in placentas from pregnancies with idiopathic intrauterine growth

restriction (319). Even though the placental pathological findings and maternal smoking status were not reported in this research (319), smoking is considered an important cause of intrauterine growth restriction (320) and has been associated with defective mitosis and differentiation of cytotrophoblasts (321). In addition to alterations related to intrauterine growth restriction, glycogen content was 10 times higher in villous syncytiotrophoblast microvesicles prepared from placentas affected by pre-eclampsia compared to placentas from age matched controls (322). Along with this rise in glycogen content, syncytiotrophoblast microvesicles from pre-eclampsia placentas had a 16 times higher glycogen synthase activity and a 3 times higher glycogen phosphorylase activity compared to control placentas (322). Interestingly, the same alterations were observed in syncytiotrophoblast microvesicles prepared from hydatidiform moles (322). Thus, the authors statement that glycogen accumulation is a sign of cellular immaturity (322) may be true in the case of pre-eclampsia, a disease marked by altered villous cytotrophoblast differentiation (323) leading to a dysfunctional syncytiotrophoblast layer.

Besides the metabolism studies, trophoblasts in long-term cultures were submitted to prolonged incubations (from day 2 to day 5 after the isolation) in the presence or absence of EGF and in the presence or absence of physiological levels of NEFA (0.1 mM) to investigate effects of both EGF and NEFA on lipid droplet formation and trophoblast morphology including syncytialisation. Unexpectedly, analysis of lipid droplet formation in cultures stained by Oil red O, a method which detects TG and cholesteryl esters (287), did not demonstrate differences between the various culture conditions. This suggests that trophoblasts in the presence of 0.1 mM NEFA did not increase TG synthesis, contrary to what was expected, and that lipid droplet formation was not influenced by syncytialisation. As Oil red O analysis only allows a qualitative analysis, total TG content of the cells were also performed and confirmed the results. One speculation is that the FBS batch used contained a significant source of NEFA. However, NEFA concentrations

in the FBS were tested using a NEFA colorimetric assay (described in Appendix 2) and were below the level of the method detection in all FBS batches. Earlier studies have shown increases in TG synthesis in trophoblasts and placenta explants exposed to fatty acids. Pathmaperuma *et al.* found an increase in TG synthesis in trophoblasts cultured for 24 h following increasing the media palmitate concentrations from 0.1 to 0.4 mM (200). Nevertheless, no control without palmitate was included, and the basal palmitate concentration was 0.1 mM (200), such that it is not possible to compare those findings with these of the current thesis. Scifres *et al*. demonstrated that primary human trophoblasts incubated for 24 h with 0.8 mM linoleic plus 0.4 mM oleate increased TG esterification by about 4 times in comparison with trophoblasts incubated with vehicle control (230). The concentrations of the NEFA mixes used in these previous studies were 2 (200) to 12-fold (230) greater than the concentration used in this thesis research, suggesting that the NEFA concentration may need to be at high physiological or supra-physiological levels to elicit effects on human trophoblasts even in prolonged incubations as performed in this thesis. Another difference between the studies is the duration of exposure to FBS with and without NEFA, which was much longer in the current study. It is possible that a steady state of lipid droplets is reached in both situations at the end, whilst, the rate of lipid droplet formation could have been different between the culture conditions.

On top of TG synthesis, morphology alterations were also analysed. In the absence of EGF, NEFA did not affect cellular aggregation of trophoblasts but it did lead to at least a trend for increased syncytialisation. Conversely, exposure to NEFA in the presence of EGF showed a trend of increasing cellular clumping without differences in syncytialisation. Previous findings have shown that incubations in the presence of 0.25 mM palmitate plus oleate for 48 h induced cellular aggregation and syncytialisation (200). Hence, it is possible that more robust results would be observed in this research if higher

NEFA concentrations were used. Notably, results of primary trophoblasts cultured with other lipid classes, e.g. oxysterols, have demonstrated opposite results with reductions in syncytialisation (234). Therefore, despite the results of this thesis on effects of NEFA on lipid accumulation in trophoblasts, it is highly likely that various lipid species do have an important role on trophoblast structure and function.

5.4 Limitations

The major limitation of these experiments is that, with exception of some glucose and palmitate oxidation experiments, long and short-term cultures did not contain trophoblasts isolated from the same placenta, which preclude a direct comparison of results owing to possible biological variation between the placentas. The ideal would be that all metabolism experiments could be performed in short and long-term cultures with trophoblasts from the same placenta.

Besides, syncytialisation was only analysed by cells stained in Oil red O, which is not an optimal stain for this purpose. E-cadherin immunofluorescence was performed in many experiments assessing cultures incubated from day 2 to day 5 post isolation under different conditions. Unfortunately, the quality of membrane staining was unsatisfactory for appropriate analysis. For this reason, these experiments have been excluded.

5.5 Conclusions

Data from this study suggest that glucose and lipid metabolism are different in human primary trophoblasts cultured for 36 h, when most are cytotrophoblasts, compared to 5 days, when most are syncytiotrophoblasts. This is particularly so when media glucose levels are elevated. Following longer-term culture with the induction of syncytialisation, glycolysis rates were generally higher, particularly at higher media glucose concentrations; whereas, fatty acid oxidation, acid soluble product formation and glucose flux into glycogen were generally lower. Glucose oxidation rates were similar in the

trophoblasts of the short and long-term cultures. Thus, synctiotrophoblasts may have a greater capacity to metabolise higher levels of glucose for energy production with less capacity for glycogen synthesis than cytotrophoblasts. In general, NEFA did not have a major effect on glucose metabolism pathways in either the short or long-term trophoblast cultures. However, the palmitate oxidation rate was generally lower in the longer-term cultured cells, suggesting that syncytiotrophoblasts may rely more on glucose for energy than lipid. Clearly though, lipid is a source of energy substrate for both cytotrophoblasts and syncytiotrophoblasts. In these experiments, there was a non-significant trend for palmitate oxidation to CO_2 to be reduced by high glucose concentrations, but palmitate metabolism into acid soluble products was not reduced by glucose. Of particular interest is the finding of relatively high amounts of palmitate being metabolised into acid soluble products compared to CO_2, such that this pathway is of significance in trophoblasts and warrants further investigation. These conclusions need to be considered within the context of the limitations of the studies, as described above, with confirmation in future studies in which a time course of assessment of trophoblast metabolism through the process of differentiation from cytotrophoblasts to syncytiotrophoblasts is undertaken.

Chapter 6

Summary of results and final conclusions

6.1 Summary of results

In order to understand the pathophysiology of elevated nutrient levels on placental function and adverse pregnancy outcomes in mothers with obesity and/or diabetes, it is important first to comprehend the normal physiology of placental nutrient metabolism. The primary aim of this thesis was to investigate the effects of high glucose and NEFA on the various pathways of glucose metabolism in primary human trophoblast cultures.

- **Chapter 2** demonstrated the establishment of a modified and optimised human trophoblast isolation protocol which was based on literature review and protocols from other laboratories. The harvesting technique, enzymatic digestion and culture conditions were the elements of the method that were most changed in the updated protocol. This protocol greatly increased the cell yield and trophoblast purity with almost no contamination with other placental cell groups. Minimal morphological alterations were observed in trophoblasts established in complete media with 10% FBS within 2 to 5 days post isolation. Significant syncytialisation was then noticed from the 3rd day after isolation with EGF supplementation.
- **Chapter 4** showed the results of metabolism experiments in human primary trophoblast short-term cultures in which the majority of cells were cytotrophoblasts.

  Total glucose uptake studies showed a high capacity of substrate transport without evidence of plateau at increasing glucose concentrations in the media from 1 to 35 mM. There was a strong correlation between the glucose uptake rate and glucose levels in the media. Glycolysis, lactate release into the supernatant and glucose oxidation were, however, limited with a maximal rate at a media glucose concentration of 1-5 mM. Glucose flux into glycogen (newly formed glycogen) was linearly increased with rising glucose levels, whereas total glycogen content (glycogen previously stored plus newly synthesised glycogen minus glycogen

hydrolysis) had a minimal increase. There was a trend for palmitate oxidation to CO_2 to be partially inhibited in the presence of high glucose levels. Conversely, the production of acid soluble products from palmitate metabolism was the same at physiological (5 mM) or high (25 mM) glucose concentrations. The acid soluble product accumulation from palmitate carbons was 2.5 times higher than CO_2 at 5 mM glucose, and 4.2 times higher at 25 mM. NEFA did not affect total glucose uptake, glycolysis, lactate release, glucose oxidation, nor total glycogen content. Glycogen synthesis, however, was further increased in the presence of NEFA.

- **Chapter 5** showed the key glucose metabolism pathway and fatty acid oxidation experiments performed in human trophoblasts cultured for 5 days in the presence of EGF in which many of the cells had differentiated into syncytiotrophoblasts. Overall, the activity of the pathways of glucose metabolism in these more differentiated trophoblasts were similar to the cytotrophoblast experiments of Chapter 4; nevertheless, not without some differences. The trophoblasts from the long-term cultures appeared to be able to increase glycolysis rates and glucose oxidation to some extent with increases in media glucose concentrations greater than 5 mM. This was not at all evident in the short-term cultured cells. Associated with this, there were lower overall rates of glycogen synthesis and fatty acid oxidation in the long-term cultured trophoblasts. In the results of this chapter, it was also shown that EGF significantly increased cellular aggregation and syncytialisation, but not lipid droplet formation as assessed by Oil red O staining. Using the same staining technique, NEFA (0.1 mM) also showed a trend towards increasing syncytialisation, but this was not evident in the presence of EGF. Interestingly, NEFA in these long-term experiments did not obviously increase lipid droplet formation. Lipid accumulation in cells was also assessed through the

measurement of cellular TG content, which was not different between the conditions (± EGF ± NEFA).

6.2 Discussion

Our results show that trophoblasts utilise mostly glucose for energy supply, which is well-established in previous literature, and that fatty acids are also substantially utilised for oxidative processes. In addition, the results indicate that syncytiotrophoblasts may be able to better utilise glucose at higher glucose concentrations than cytotrophoblasts as demonstrated by glycolysis and glucose oxidation rates. This is a new finding that still needs confirmation due to limitations in the current study as discussed below. Moreover, at elevated glucose concentrations, cytotrophoblasts have a high capacity for glycogen storage which is less evident in syncytiotrophoblasts. This result is supported by studies that have demonstrated reductions in glycogen throughout the syncytialisation process (316) and higher glycogen content in cytotrophoblasts in all stages of pregnancy (295). The finding of little change in total glycogen content over 2 h at different glucose concentrations seemed to be at variance with the glycogen synthesis rate results, but was in agreement with a previous study (210). This most probably reflects differences in what the two methods were measuring, i.e. the newly formed glycogen assessed with a radioactive tracer and the net total cellular glycogen content quantified using an enzymatic colorimetric assay.

Comparing the rates of the different glucose pathways, it was evident that glycolysis was significantly higher than the combination of lactate production and glucose oxidation to CO_2 by the TCA cycle. Interestingly, there is evidence that [5-^{3}H]-glucose metabolised by the pentose phosphate pathway in the heart can result in release of tritiated water and overestimation of glycolysis rates (314). The pentose phosphate pathway was not investigated in this thesis, but if it is active in the placenta, this could provide an

explanation for the glycolysis rates. The pentose phosphate pathway was previously assessed to be a minor pathway in human placental trophoblasts, but with substantial capacity (148). It only accounted for about 0.6% and 0.2% of the glucose metabolized by cells freshly isolated and cultured for 3 days, respectively (148). However, not evaluated were the effects of elevated glucose supply on this pathway in trophoblasts (148) The relevance of increased activity in fresh trophoblasts, as compared to trophoblasts following 3 days of culture is unknown, but it could be indicative of greater activity of this pathway in cytotrophoblasts compared to syncytiotrophoblasts.

The pentose phosphate pathway is of particular importance in cell proliferation and growth, as it is important for RNA and DNA synthesis as well as the provision of NADPH to the cell. Thus, if this pathway is more active when the supply of glucose is high, as occurs in diabetic pregnancy, it would support increased placental growth. In diabetes, especially without diagnosis or treatment, placental weights are very often increased with greater parenchymal volume due to a larger trophoblast layer as well as hypervascularisation of placental villi, among other pathological alterations (324). An increased placental size is also observed in obesity (325).

Increased oxidative stress has been reported in human diabetic placentas (326), but this is still controversial in placentas from obese mothers (327). In pregnant women with diabetes oxidative stress is promoted due to the combination of increased generation of reactive oxygen species and reduced antioxidant defences (328, 329). Vascular NADPH oxidase, which is expressed in human placental endothelial cells and syncytiotrophoblasts and is a source of reactive oxygen species (330), is activated in conditions of high oxidative stress, as occurs with hyperglycaemia and/or conditions causing high levels of pro-inflammatory cytokines (331). If increased glucose level results in enhanced pentose phosphate pathway activity, this would be able to replenish NADPH which would be depleted by high activity of this oxidase enzyme. Thereof, hyperglycaemia, via the

pentose phosphate pathway could support NADPH oxidase activity and reactive oxygen species production in the placenta.

Previous work showed that high glucose levels minimally affect trophoblast lipid metabolism causing decreased trophoblast lipid droplet formation without influencing fatty acid oxidation, lipolysis or fatty acid esterification (200). Here the results show that NEFA has little effect on glucose metabolism other than a mild effect of stimulating glycogen synthesis in cytotrophoblasts and total glucose uptake in syncytiotrophoblasts. Hence, high glucose and NEFA concentrations do not seem to act in synergy in human trophoblasts, at least in the assessed metabolic pathways in the current and previous studies (200), a finding that is dissimilar to what is observed in other human tissues.

The considerable NEFA oxidation, incomplete to acid soluble products and complete to CO_2, by trophoblasts found in this thesis is corroborated by preceding studies which have demonstrated the expression of a wide range of enzymes implicated in fatty acid oxidation in human trophoblasts (224, 290, 291). By comparing estimates of ATP production from glucose metabolism (combination of anaerobic and aerobic glycolysis) with that from lipid metabolism (combination of fatty acid oxidation to acid soluble products and CO_2) (Table 6.1), it is clear that NEFA metabolism has the potential to provide a significant proportion of the energy requirements of trophoblasts. From estimates of these current experiments, the proportion of ATP produced from fatty acids compared to glucose in syncytiotrophoblasts (19 % at 5 mM glucose) was less than for cytotrophoblasts (37% at 5 mM glucose) (Table 6.1.). Nonetheless, it contradicts the demonstration of higher expression of enzymes for lipid oxidation in syncytiotrophoblasts (224). Thus, further studies of this new finding from this thesis are necessary to elucidate these differences.

Table 6.1
Estimated ATP production for glucose and palmitate metabolism in short and long-term primary human trophoblast cultures[1]

	ATP production (nmol/h/mg protein) at 5 mM media glucose concentration[2]	
	Short-term cultures	Long-term cultures
ATP from glucose		
ATP from anaerobic glycolysis[3]	321	369
ATP from glucose metabolism to CO_2	197	139
Total ATP from glucose metabolism	*518*	*508*
ATP from NEFA		
ATP from FA β-oxidation to ASP	135	79
ATP from FA oxidation to CO_2	175	37
Total ATP from FA metabolism	*310*	*116*
Percentage ATP		
From glucose	63%	81%
From NEFA	37%	19%

[1]Calculations from glycolysis, glucose oxidation, fatty acid oxidation to CO_2 and acid soluble products (ASP) at 5 mM glucose in the presence of NEFA from short-term (Chapter 4) and long-term (Chapter 5) culture experiments.

[2]ATP calculation is based on the following (149):
Anaerobic glycolysis: 1 glucose molecule into pyruvate produces 2 ATP
Glucose metabolism to CO_2: 1 glucose molecule into CO_2 produces 32 ATP
Fatty acid (FA) β-oxidation to ASP[2] (assuming the production of acetoacetate from palmitate): produces 33 ATP
FA oxidation to CO_2: 1 palmitate molecule into CO_2 produces108 ATP

[3]Anaerobic metabolism of glucose was calculated as the total glycolysis rate minus the rate of glucose oxidation to CO_2.

Regardless the trophoblast culture age, palmitate oxidation in this research showed a downward trend in the presence of higher glucose concentration (5 *vs* 25 mM), which is in accordance with a previous study (232), but not with an earlier research performed by our group (200). This may be caused by methodological differences (e.g. the use of different tracers). The finding of no effect of glucose on fatty acid oxidation in isolated trophoblasts measured by [9, 10 (*n*)-^{3}H]-palmitic acid (200) may be reflected by a lack of suppression of acid soluble product synthesis in the presence of high glucose levels as demonstrated in the current work. This is because the [9, 10 (*n*)-^{3}H]-palmitic acid method cannot differentiate between metabolism to acid soluble products and CO_2.

The most novel finding of this thesis was that of the substantial accumulation of acid soluble products from NEFA by the trophoblasts, indicative of this being a significant metabolic pathway in placenta. To the best of our knowledge, no similar result has been published such that this warrants further investigation. A study with mitochondria isolated from murine muscle analysing the metabolomic profile in different palmitate concentrations showed that complete palmitate oxidation increased the levels of TCA intermediates (alpha-ketoglutaric acid, citric acid and malate), myristic acid (C14:0), octadecanol, inosine, β-hydroxybutyrate, lipid species (putrescine and 1-hexadecanol) and phthalic acid; whereas incomplete palmitate oxidation (acid soluble product synthesis) raised the concentrations of malate, eleidic acid, arachidonic acid, β-hydroxybutyrate, inosine, lactic and glycosylic acids (332). In this previous study, the incorporation of labelled palmitate carbons were about 2 to 4-fold higher in acid soluble products than in CO_2 (332), consistent with the findings of this thesis research in trophoblasts. Another finding of the murine muscle study was that, with increasing palmitate concentrations in the media, a linear increase in metabolism to acid soluble products was evident, while complete palmitate oxidation to CO_2 plateaued (332). Metabolomic analysis has been done in maternal biofluids, cord plasma (333) and in

human placentas mostly with focus on preeclampia (334), congenital malformations (335), small for gestational age, hypoxaemia among other complications (336). Studies of isolated cells or placental explants under diverse lipid or glucose concentrations are missing. Key to the future research is careful analysis of the nature of the acid soluble products (e.g. ketone bodies, short chain fatty acids or TCA cycle intermediates) produced by NEFA catabolism in trophoblasts.

Placental products of incomplete fatty acid oxidation such as ketone bodies could be utilised by the fetus, mother or the placenta itself. Hydroxybutyrate dehydrogenase activity, acetoacetyl-CoA thiolase and 3-oxoacid-CoA transferase activity, which are implicated in ketone bodies catabolism, have all been detected in early and term human placentas (337, 338). On top of that, it has been demonstrated that the mitochondria of human placenta can utilise acetoacetate at a rate of 0.8-1 nmol/min/mg protein (338). At least in rats, the placenta and fetal tissues such as the liver and brain, as well as the whole carcass, can oxidase β-hydroxybutyrate to CO_2 (236, 294). However, if ketone bodies do form a substantial proportion of the acid soluble products produced by trophoblasts, the fact that they were not oxidised to CO_2 is against ketone bodies oxidation being a substantial metabolic pathway of cytotrophoblasts and syncytiotrophoblasts. It is unknown to what extent acid soluble products can be utilised by other cells of the placenta, such as endothelial, immune or other mesenchymal cells, and by human fetal tissues. Besides energy production, acid soluble products may have other important actions in the placenta. For instance, short-chain fatty acids (e.g. acetate, propionate and butyrate) possess inflammatory modulation roles including inhibition of histone deacetylase (HDAC) and NF-kB activities, along with inhibition of cellular release of TNF-α and prostaglandin E2 (339). There is evidence that ketone bodies can also act as mediators of cellular signalling, including the suppression HDAC activity and indirect stimulation of histone acyltransferase activity, as well as the modulation of lipolysis and

cellular metabolic rates (340). Hence, placental acid soluble products may function as intermediates linking maternal nutrition, metabolism and inflammation, which may have consequences to the developing fetus. Whether the placental synthesis of acid soluble products is increased in pregnancies complicated by diabetes and obesity, and whether higher levels of these substances contribute to the pathophysiology of pregnancy complications are unclear. Even if a defined pathophysiological role for acid soluble products in pregnancy complications could not be established, they could still be used as biomarkers for the anticipation of adverse gestational outcomes in diabetic and obese gravidas (341).

The differences between trophoblasts cultured for short or long-term need to be interpreted with caution since we have not done a time course study of metabolism across the process of syncytialisation. Thus, those studies are needed for establishing more robust conclusions about differences in the rates of glycolysis, lipid oxidation, glycogen pathways in trophoblasts with diverse levels of syncytialisation. In addition to metabolism studies, the investigation of relevant gene expression at mRNA and protein levels together with enzyme activity measurements are worthy to better understand glucose and lipid metabolic pathways at the molecular level.

Our results show that trophoblasts have capacity to alter the partitioning of glucose metabolism through the various pathway options in the presence of excess glucose availability. In the short-term cultures, high media glucose stimulated glycogen synthesis that was further increased in the presence of NEFA. Therefore, this may be an adaptive mechanism that could occur in placentas from pregnancies complicated by diabetes and obesity. However, this extrapolation deserves prudence since the *in vivo* environment of pregnancy is much more complex than culture studies, with cross modulation between hormones, nutrients, cytokines and other factors between the mother and the feto-placental unit. Moreover, these metabolic findings may be altered in trophoblasts from

abnormal placentas, as previous studies have demonstrated differential expression of enzymes involved in glycogen turn-over in GDM placentas (205). Also, a reduction in glucose uptake, glucose utilisation and lactate release in GDM placentas was evident in perfusion studies (176, 198). The same may be true for alterations in fatty acid metabolism in placentas from diabetic and obese pregnancies, as many studies have shown alterations in genes and protein expression of lipid metabolism enzymes and transporters, particularly when GDM is combined with obesity (205, 218, 230, 231).

6.3 Future directions

- Placental production of acid soluble products from fatty acid metabolism may be a substantial metabolic pathway in this organ. Therefore, it is important to further verify the presence of this pathway, as well as quantitate the chemical components of the acid soluble products using metabolomic approaches.
- As the metabolism studies performed in long-term cultures were different from short-term cultures it would be valuable to complete the assessment of glucose and lipid metabolism pathways in time course studies with concomitant analysis of the syncytialisation.
- Among the glucose metabolism pathways, the study of the oxidative and non-oxidative branches of pentose phosphate pathway, is required in the short and long-term cultured trophoblasts at low and high glucose concentrations.
- In the current research, the effects of high levels of glucose and NEFA on glucose metabolism were studied in human trophoblasts isolated from placentas donated by healthy mothers without obesity or diabetes. Thus, we believe that our results express the normal metabolism of glucose and NEFA in human trophoblasts. Consequently, the study of glucose and lipid metabolic pathways in trophoblasts isolated from placentas of pregnancies affected by diabetes and/or obesity could

bring beneficial information about the trophoblast role in the pathogenesis of gestational complications associated with diabetes and obesity.

- To test the individual effects of saturated, monounsaturated and polyunsaturated NEFA, as well as other NEFA mixtures, on glucose metabolism pathways and morphology in trophoblasts with a dose and time-response curve would be worthwhile. The addition of carnitine to these experiments could be useful because long-chain fatty acids are unable to cross the mitochondrial membrane without adequate carnitine levels.
- In addition, the study of glucose and NEFA metabolism in endothelial cells is needed as, together with the trophoblasts, these cells form part of the critical interface between the maternal and fetal hormonal and metabolic milieus.
- A prospective study of gravidas of different BMI groups would also be valuable. Examining for associations between (i) maternal antenatal metabolic characteristics, (ii) placental development throughout pregnancy as assessed by ultrasound and post-delivery placental morphology and histology, (iii) trophoblast and endothelial cell glucose, lipid and amino acid metabolism, as well as metabolic gene expression, (iv) placental cytokine and adipokine production, (v) cord plasma nutrient levels, cytokines and adipokines, and (vi) maternal and fetal pregnancy outcomes, could help clarify the pathophysiological processes which link obesity/diabetes and adverse gestational outcomes.

6.4 Final conclusions

Human trophoblasts have high glucose and NEFA metabolism with adaptations to nutrient availability. Trophoblasts utilise a substantial amount of NEFA as fuel and produce a relatively large quantity of acid soluble products. Furthermore, the

characteristics of glucose and NEFA metabolism change according to the level of trophoblast differentiation from cytotrophoblast to syncytiotrophoblast.

Since the prevalence of gestational complications associated with obesity and diabetes is a current major burden, the study of nutrient metabolism in the placenta is highly relevant and more research is needed. Understanding the underlying pathophysiological mechanisms of these complications may contribute to the development of future therapies.

Appendix 1: Material, reagents and solutions

Material and reagents

Table 1

Reagents used in this research thesis, in alphabetic order, and their respective suppliers

Reagent	Supplier
Antibiotic and antimycotic solution (100X), 10,000 units/ml of penicillin, 10,000 µg/ml of streptomycin, and 25 µg/ml of amphotericin B	Invitrogen, Mulgrave, VIC, Australia
Calcium and magnesium free Hank's Balanced Salt Solution (HBSS)	Sigma, Castle Hill, NSW, Australia
Calcium and magnesium free phosphate buffered saline (PBS)	Sigma, Castle Hill, NSW, Australia
CD68 antibody clone KP1	DakoCytomation, Campbellfield, VIC, Australia
Cell conditioning 1 (CC1) reagent buffer pH 8-8.5	Ventana/Roche, Castle Hill, NSW, Australia
Cell lifter polyethylene	Corning, New York, NY, USA
Cell scraper	TPP, Trasadingen, Schaffhausen, Switzerland
Cell strainers, nylon mesh, 100 µm	Falcon BD Bioscience, Durham, NC, USA
Cheese cloth	Fisher Scientific, Scoresby, VIC, Australia
Connaught Medical Research Laboratories (CMRL) medium 1066, without L-glutamine	Sigma, Castle Hill, NSW, Australia
Cytokeratin antibody monoclonal-clone AE1/AE3	DakoCytomation, Campbellfield, VIC, Australia
Dade thrombin reagent 100 NIH unit/ml	Siemens Health Care, Marburg, Hesse, Germany
Dispase II, 5,000 caseinolytic units/100 ml bottle	BD Biosciences, Bedford, MA, USA
DNase 1 Type IV, from bovine pancreas, ≥ 2,000 KU/mg protein (for trophoblast isolation-protocol 1)	Sigma, Castle Hill, NSW, Australia

DNase 1 grade II, from bovine pancreas, ≥ 2,000 KU/mg protein (for trophoblast isolation-protocol 2)	Roche, Castle Hill, NSW, Australia
Dulbecco's Modified Eagle Medium (DMEM), Low Glucose (5.56 mM glucose), GlutaMAX ™ (3.97 mM L-alanyl-L-glutamine), sodium pyruvate (1 mM)	Invitrogen, Mulgrave, VIC, Australia
EDTA, BioUltra, anhydrous, ≥ 99% (titration)	Sigma, Castle Hill, NSW, Australia
Epidermal growth factor (EGF)	Invitrogen, Mulgrave, VIC, Australia
Fetal bovine serum, heat inactivated, US origin	Invitrogen, Mulgrave, VIC, Australia
Filter 0.22 µm–for solution sterilization	Millex GP, Carrigtwohill, Cork, IRL
HEPES (25 mM)	Sigma, Castle Hill, NSW, Australia
L-glutamine (99-100%)	Sigma, Castle Hill, NSW, Australia
Sodium chloride (NaCl)	Sigma, Castle Hill, NSW, Australia
Sodium bicarbonate ($NaHCO_3$)	Sigma, Castle Hill, NSW, Australia
Penicillin-Streptomycin-Neomycin (PSN), Antibiotic Mixture (100X), 5 mg/ml of penicillin, 5 mg/ml of streptomycin, and 10 mg/ml of neomycin	Invitrogen, Mulgrave, VIC, Australia
Percoll (for trophoblast isolation-protocol 1)	Sigma, Castle Hill, NSW, Australia
Percoll (for trophoblast isolation-protocol 2)	GE Healthcare Bio-Sciences AB, Uppsala, Sweden
Phosphate buffered saline (PBS) tablets	Medicago, Uppsala, Sweden
Protease 1	Ventana/Roche, Castle Hill, NSW, Australia
Rat tail collagen	Roche, Castle Hill, NSW, Australia
Trypsin 2.5% solution, from porcine pancreas (for trophoblast isolation-protocol 1)	Invitrogen, Mount Waverley, VIC, Australia
Trypsin type XII-S, from bovine pancreas, 1,32 x 10^6 BAEE unit/100 mg bottle (for trophoblast isolation-protocol 2)	Sigma, Castle Hill, NSW, Australia
0.4% Trypan blue	Sigma, Castle Hill, NSW, Australia
*ultra*View Multimer Ig	Ventana/Roche, Castle Hill, NSW, Australia
*ultra*View Universal DAB Detection Kit	Ventana/Roche, Castle Hill, NSW, Australia

Vimentin Pre-dilute antibody (V9)	Ventana/Roche, Castle Hill, NSW, Australia

KU: Kunitz units; BAEE: Na–benzoyl–L–arginine ethyl ester; DAB: 3, 3′-diaminobenzidine; HEPES: 4-(2-hydroxyethyl)-1-piperazineethanesulfonic acid; EDTA: ethylenediaminetetraacetic acid.

Solutions

0.22 μm filters were used for all sterile filtered solutions.

Trophoblast isolation-protocol 1 solutions

Sterile saline solution (0.9% NaCl)

9 g of NaCl was added in 1 l of Milli-Q water and autoclaved.

L-glutamine (100X, 205 mM)

200 ml of Milli-Q water was warmed up (37°C) and 6 g of L-glutamine was dissolved. The solution was sterile filtered, aliquoted in 5 ml and stored at -20°C.

$NaHCO_3$ (7.5%)

7.5 g of $NaHCO_3$ was dissolved in 100 ml of Milli-Q water. The solution was sterile filtered and kept at 4°C.

HEPES (1 M, pH 7.4)

23.83 g of HEPES was dissolved in Milli-Q water, the pH adjusted to 7.4 and the final volume made up to 100 ml. The solution was sterile filtered and kept at 4°C.

Calcium and magnesium free HBSS (1X) with HEPES (1 M, pH 7.4)

100 ml of calcium and magnesium free HBSS (10X) was mixed with 25 ml of HEPES (1 M, pH 7.4) and 875 ml of Milli-Q water. The solution was filtered and stored at 4°C.

Percoll (90%)

117 ml of Percoll was mixed with 13 ml of calcium and magnesium free HBSS (10X) and stored at 4°C.

NaOH (1 M)

1 ml of 50% NaOH was mixed in 9 ml of Milli-Q water. The solution was kept at room temperature.

Complete CMRL media

Table 2

Reagents added to complete CMRL media-trophoblast isolation-protocol 1

Reagent	**Volume (ml)**
CMRL 1066 medium-without L-glutamine	427.5
HEPES (1 M, pH 7.4)	12.5
PSN (100X)	5
L-glutamine (100X)	5
Fetal bovine serum	50
Total volume	500

Serum free CMRL media

Table 3

Serum free CMRL media reagents -trophoblast isolation-protocol 1

Reagent	**Volume (ml)**
CMRL 1066 medium-without L-glutamine	477.5
HEPES (1M, pH 7.4)	12.5
PSN (100X)	5
L-glutamine (100X)	5
Total volume	500

Digestion buffer

Reagents used for digestion buffer preparation (Table 4). The solution was prepared fresh on the experiment day, stored in a 1 l sterile glass bottle and kept at 37ºC until use.

Table 4

Digestion buffer-trophoblast isolation-protocol 1

Reagent	Volume (ml)
Calcium and magnesium free HBSS (10X)	70
$NaHCO_3$ (7.5%)	3.3
HEPES (1 M, pH 7.4)	17.5
Milli-Q water	532.2
Total volume	623

Enzyme digestion solution

Buffer and enzymes were distributed into two 500 ml Erlenmeyer flasks containing the placental harvested tissue (Table 5).

Table 5

Enzymatic digestion solution-trophoblast isolation-protocol 1

Reagent	1st digestion (ml)	2nd digestion (ml)	3rd digestion (ml)
Digestion buffer	134.1	89.7	67.275
Trypsin (2.5%)	15	10	7.5
DNase 1 (375 KU/15 ml)	0.9	0.3l	0.225
Total volume	150	100	75

KU: Kunitz units.

Percoll gradient

Percoll concentrations were prepared mixing 90% Percoll solution and calcium and magnesium free HBSS (1X) with HEPES (1 M, pH 7.4) in 50 ml Falcon tubes (Table 6). The concentrations were stored at 4°C. Gradients were prepared using a 5 ml pipette within 18 h of trophoblast isolation. 3 ml of each Percoll concentration was added, starting from 70 and going to 5% (Table 6). The layers were added at a constant and low speed. The gradient was not disturbed and kept at room temperature until use.

Table 6

Percoll concentrations for Percoll gradients-trophoblast isolation-protocol 1

Final Percoll (%)	Volume of 90% Percoll (ml)	Volume of HBSS (1X) with HEPES (ml)
70	15.6	4.4
65	14.4	5.6
60	13.3	6.7
55	12.2	7.8
50	11.1	8.9
45	10.0	10.0
40	8.9	11.1
35	7.8	12.2
30	6.7	13.3
25	5.6	14.4
20	4.4	15.6
15	3.3	16.7
10	2.2	17.8
5	1.1	18.9

Collagen-coated plates

10 mg of rat tail collagen was resuspended in 5 ml of sterile 0.2% acetic acid. The reconstituted collagen was distributed into plates according to the well surface (5 µl/cm^2). The solution was spread on the wells with a cell scraper and allowed to dry under sterile conditions. Plates were covered with aluminium foil and stored at 4°C no more than 15 days before use.

Trophoblast isolation-protocol 2 solutions

Calcium and magnesium free PBS

5 PBS tablets were dissolved in 1 l of Milli-Q water. The solution was autoclaved and stored at 4^{o}C.

L-glutamine (50 mM)

1.461 g of L-glutamine 99-100% was dissolved in 200 ml of warm Milli-Q water. The solution was filtered, aliquoted in 5 ml and stored at -20°C.

Calcium and magnesium free HBSS (10X) with HEPES (250 mM) pH 7.4

29.8 g of HEPES was dissolved in 500 ml of calcium and magnesium free HBSS (10X). The pH was adjusted to 7.4 with NaOH (1 M). The solution was filtered and stored at 4°C.

Complete DMEM

Table 7

Complete DMEM reagents-trophoblast isolation-protocol 2

Reagent	**Volume (ml)**
DMEM Low glucose (5.56 mM) GlutaMAX ™, pyruvate	430
HEPES (1 M, pH 7.4)	10
Antibiotic and antimycotic solution (100X)	5
L-glutamine (50 mM)	5
Fetal bovine serum	50
Total volume	500

For long-term cultures (> 3 days), epidermal growth factor (EGF) was added to complete media. EGF vial was briefly centrifuged and re-suspended in 1ml sterile PBS (stock concentration: 100 μg/ml). 50 μl was added to each 500 ml complete media (final dilution: 10 ng/ml) no more than 24 h before use.

Digestion Buffer–Dispase/HBSS/HEPES (DHH)

A total DHH volume of 500 ml was prepared for < 120 g of villous tissue to be digested and a total volume of 750 ml was prepared for > 120 g of villous tissue. 50 or 75 ml of calcium and magnesium free HBSS (10X) with HEPES (250 mM, pH 7.4) was mixed with Milli-Q water to make up 480 ml or 720 ml, respectively. The pH was adjusted to 7.4 with NaOH (1 M). 20 ml of dispase II (1,000 caseinolytic units) was added for a final

solution of 500 ml. 30 ml of dispase II (1,500 caseinolytic units) was added for a final solution of 750 ml. The solution was sterile filtered and stored at 37°C for same day use.

Percoll gradient

Percoll was mixed with calcium and magnesium free HBSS (1X) and HEPES (pH 7.4) to make different concentrations (Table 8). Tubes were capped and the solution mixed by inversion. Percoll (stock and gradients) was stored at 4°C and removed from the fridge before manipulation to equilibrate at room temperature. Percoll layering was prepared with a 5 ml pipette within 24 h of trophoblast isolation. The layering started adding 5 ml of each Percoll concentration from 60 to 20% (Table 8). 5% gradient was not added at this stage. Layers were added at a slow and constant speed. Gradient was not disturbed and kept at 4°C until use.

Table 8

Percoll concentrations for Percoll gradients-trophoblast isolation-protocol 2

Gradient (%)	Percoll (ml)	HBSS (1X) with HEPES (ml)
60	30	20
50	25	25
45	22.5	27.5
40	20	30
35	17.5	32.5
30	15	35
20	10	40
5	2.5	47.5

Erythrocyte lysis buffer (ELB)

ELB was prepared (Table 9), sterile filtered, distributed in 45 ml aliquots, sealed and stored at room temperature.

Table 9

Erythrocyte lysis buffer reagents-trophoblast isolation-protocol 2

Reagent	**Weight/volume**
NH_4Cl (50 mM)	1.34 g
$NaHCO_3$ (10 mM)	0.42 g
EDTA (0.1 mM)	0.0145 g
Milli-Q water	500 ml

Appendix 2: Material, reagents and solutions

Material and reagents

Table 1

Reagents used in this research thesis, in alphabetic order, and their respective suppliers

Reagent	Supplier
Amyloglucosidase, from Aspergillus niger lyophilized powder, 30-60 units/mg protein (biuret), ≤ 0.02% glucose	Sigma, Castle Hill, NSW, Australia
BCA protein assay kit acid-Pierce ™	Thermo Scientific, Rockford, IL, USA
Bovine serum albumin, fatty acid (BSA-FA free), ≥ 96%	Sigma, Castle Hill, NSW, Australia
D-Glucose	Sigma, Castle Hill, NSW, Australia
DMEM, no glucose no glutamine	Invitrogen, Mulgrave, VIC, Australia
Filters GF/B Glass Circles, 25 mm diameter	Whatman, Rydalmere, NSW, Australia
Glucose assay kit	Wako, Osaka, Japan
Glycogen from bovine liver Type IX	Sigma, Castle Hill, NSW, Australia
[5-^{3}H]-D-glucose	Perkin-Elmer Life Sciences, Waltham, MA, USA
HEPES powder	Sigma, Castle Hill, NSW, Australia
[5-^{3}H]-water	Perkin-Elmer Life Sciences, Waltham, MA, USA
Isopropanol	Ajax Finechem, Taren Point, NSW, Australia
KOH	Sigma, Castle Hill, NSW, Australia
Lactate Colorimetric Assay Kit II	BioVision, Milpitas, CA, USA
L-carnitine hydrochloride synthetic, ≥ 98%	Sigma, Castle Hill, NSW, Australia
Methanol	Selby-BioLab, Clayton, VIC, Australia
$NaHCO_3$	Sigma, Castle Hill, NSW, Australia
NEFA C (ACS-ACOD method) kit	Wako, Osaka, Japan
Nunc™ Lab-Tek™ II Chamber Slide™ System, culture area of 0.7 cm², 8 wells	Thermo Scientific, Scoresby, VIC , Australia
Perchloric acid (PCA), ACS reagent, 70%	Sigma, Castle Hill, NSW, Australia
PermaFluor Aqueous Mounting Medium	Thermo Scientific, Scoresby, VIC , Australia

PVC tubing-I.D. x O.D.: 3/16 x 5/16 inch	Thermo Fisher Nalgene, Scoresby, VIC, Australia
Read Safe cocktail (scintillation liquid)	Beckman Coulter, Fullerton, CA, USA
Rubber stoppers size 14.5, 7/16 LN	Thermo Fisher Nalgene, Scoresby, VIC, Australia
Scintillation vials	Super polyethylene vial, 20 ml, Perkin Elmer, Waltham, MA, USA
Sodium acetate	Sigma, Castle Hill, NSW, Australia
Sodium dodecyl sulphate (SDS)	Sigma, Castle Hill, NSW, Australia
Sodium oleate (C18:1)	Nu-chek-Prep, Elysian, MN, USA
Sodium palmitate (C16:0)	Nu-chek-Prep, Elysian, MN, USA
T25 culture flask, canted neck, slim type	IWAKI, Asahi techno glass, Shizuoka, Japan
Triglyceride Determination kit	Sigma, Castle Hill, NSW, Australia
Tris (hydroxymethyl) aminomethane	Sigma, Castle Hill, NSW, Australia
[(U) ^{14}C]-2-deoxy-D-glucose	Perkin-Elmer Life Sciences, Waltham, MA, USA
[(U)^{14}C]-D-glucose	Perkin-Elmer Life Sciences, Waltham, MA, USA
[(U)^{14}C]-palmitic acid	Perkin-Elmer Life Sciences, Waltham, MA, USA
Urea	Ajax Finechem, Auburn, NSW, Australia

HEPES: 4-(2-hydroxyethyl hydroxyethyl)-1-piperazineethanesulfonic acid. BCA: bicinchoninic acid.

Solutions

0.22 μm filters were used for all sterile filtered solutions.

HEPES (1 M, pH 7.4)

23.83 g of HEPES was dissolved in Milli-Q water, the pH adjusted to 7.4 and the final volume made up to 100 ml. The solution was sterile filtered and kept at 4°C.

$NaHCO_3$ 50X (100 mM)

0.84 g was dissolved in 100 ml of Milli-Q water. The solution was sterile filtered and kept at 4°C.

Glucose solution (1 M)

18.016 g of glucose was added to Milli-Q water to make up a 100 ml final solution. The solution was sterile filtered, aliquoted and kept at -20°C.

KOH (30%)

30 g of KOH was added to Milli-Q water to make up a 100 ml final solution. The solution was kept in a sealed glass bottle at room temperature.

KOH (0.5 M)

5.6 g KOH was dissolved in 200 ml of 95% ethanol. The solution was kept in a glass bottle at room temperature.

$MgSO_4$ (0.15 M)

11.07 g of $MgSO_4.7\ H_2O$ was added to 300 ml of Milli-Q water. The solution was kept in a glass bottle at room temperature.

Na_2SO_4 (6%)

6 g of Na_2SO_4 was added to Milli-Q water to make up a 100 ml final solution. The solution was kept in a glass bottle at room temperature.

L-carnitine (100 mM)

0.197 g of L-carnitine was diluted in 10 ml of Milli-Q water. The solution was sterile filtered, aliquoted in 20 µl into 0.5 ml sterile microtubes and stored at -20°C.

Na-Acetate buffer (0.5 M, pH 4.8)

21 g Na-acetate (anhydrous) was dissolved into 300 ml of Milli-Q water. The pH was adjusted to 4.8 with acetic acid and Milli-Q water added to make up a 500 ml final solution. Fresh solution was prepared for each experiment.

Amyloglucosidase solution (2 mg/ml)

This solution was freshly prepared in each experimental day. Amyloglucosidase was weighed and added to 0.5 M Na-acetate buffer (pH 4.8) to make up a 2 mg/ml final concentration. The final volume was calculated according to each assay.

5X Krebs-Ringer Bicarbonate (KRB) Buffer

5X KRB buffer was prepared in advance according to Table 2. Final solution was filtered and stored in a 500 ml sterile glass bottle at 4ºC until use.

Table 2

5X Krebs- Ringer Bicarbonate (KRB) Buffer

Reagent	**Weight/volume**
$CaCl_2$	0.55 g
NaCl	19.72 g
KCl	0.67 g
NaH_2PO_4	0.15 g
$MgCl_2$	0.25 g
Milli-Q water	Up to 500 ml
Total	500 ml

Krebs-Ringer Bicarbonate HEPES (KRBH)

KRBH was freshly prepared fresh in each experimental day. After mixing the reagents (Table 3), the pH was adjusted to 7.4 with NaOH (1 M) and the solution was kept inside a 5% CO_2 incubator at 37°C until use.

Table 3

Krebs-Ringer Bicarbonate HEPES (KRBH)

Reagent	**Volume (ml)**
$NaHCO_3$ (100 mM)	2
HEPES (1 M, pH 7.4)	1
KRB 5X	20
Milli-Q water	77
Total	100

NEFA stock preparation

Palmitate and oleate stocks were prepared according to method described by Roche *et al.* (342) with modifications. 5 g of BSA-FA free was resuspended in 100 ml of KRBH solution to obtain KRBH-5% BSA-FA free (wt/vol), and later sterile filtered. 70 ml was

taken for NEFA stock preparation and the remaining was kept at 4°C under sterile conditions. 200 mg of sodium palmitate was added to 30 ml of KRBH-5% BSA-FA free and 25 mg of sodium oleate was added to 40 ml of KRBH-5% BSA-FA free. Both solutions containing palmitate or oleate were gazed with nitrogen gas for a couple of minutes, sealed with parafilm M and incubated overnight on a rocker/shaker at 37°C. Following overnight incubation, NEFA-5% BSA solutions were filtered under sterile conditions. An aliquot of 200 µl was then taken for measurement of fatty acid concentration. Samples were serial diluted and measured using NEFA C kit according to manufacture instructions. The solution containing oleate and palmitate were adjusted to 4 mM concentration using KRBH-5% BSA. NEFA stocks were stored at -20°C in small aliquots to avoid repetitive thawing and freezing cycles. The stocks were used within 6 months of their preparation.

Complete DMEM with 1 mM glucose

Complete DMEM plus 1 mM glucose was prepared (Table 4) on the experimental day for pre-incubation of glycogen total content experiment (Chapter 3)

Table 4

Complete DMEM with 1 mM glucose

Reagent	**Volume**
HEPES 1 M (pH 7.4)	2 ml
L-glutamine (50 mM)	1 ml
Antibiotic and antimycotic solution (100X)	1 ml
Fetal bovine serum	10 ml
Glucose (1 M)	100 µl
DMEM, no glucose no glutamine	85.9 ml
Total	100 ml

Refer to Appendix 1 for reagent details.

Glucose and palmitate oxidation–material preparation

PVC tubing were cut into 3 cm length and filter papers were cut into 3 equal pieces. Then, one end of 3 cm of tubing piece was wrapped in parafilm without covering the lumen and the tubing was firmly fitted into the underside of the rubber stopper.

In order to improve $^{14}CO_2$ fixation, 150 µl of 5% KOH was applied on each filter paper which was later inserted into the tubing with tweezers in a position to let the tubing opening clear.

Protein lysis buffer

The reagents listed on Table 5 were one by one added to 80 ml of Milli-Q water. The pH was adjusted to 7.5 using NAOH (1 M). The final volume was finally completed to 100 ml and the solution was filtered and stored at room temperature.

Table 5

Protein lysis buffer

Reagent	**Weight/volume**
Urea	36.04 g
20% SDS (Sodium dodecyl sulphate)	10 ml
2 M TRIS base solution (pH 7.5)	3.13 ml
Milli-Q water	Up to 100 ml
Total	100 ml

Oil Red O stock solution

500 mg of Oil Red O dye powder was dissolved into 100 ml of isopropanol and allowed to stand overnight at room temperature.

Oil Red O working solution

Oil red O working solution was freshly prepared on the experimental day. 3 ml of Oil red O stock was mixed with 2 ml of diluted with ddH_2O [3:2 (vol/vol) ratio; Oil red O: ddH_2O]. The solution was allowed to stand for 10 minutes at room temperature and later filtered through a 0.22 µm filter into 50 ml Falcon tubes.

References

1. World Health Organizaton. Global Health Observatory (GHO) data [Access on 09/07/2015]. Available from: http://www.who.int/gho/ncd/risk_factors/obesity_text/en/.
2. Haslam DW, James WPT. Obesity. The Lancet. 2005; 366 (9492): 1197.
3. World Health Organization-Global Database on Body Mass Index. Web page update in 2011 [Access on 16/09/2011]. Available from: http://apps.who.int/bmi/index.jsp?introPage=intro_3.html
4. Cornier MA, Dabelea D, Hernandez TL, Lindstrom RC, Steig AJ, Stob NR, *et al.* The metabolic syndrome. Endocrine Reviews. 2008; 29 (7): 777.
5. Black RE, Victora CG, Walker SP, Bhutta ZA, Christian P, De Onis M, *et al.* Maternal and child undernutrition and overweight in low-income and middle-income countries. The Lancet. 2013; 382 (9890): 427.
6. McIntyre HD, Gibbons KS, Flenady VJ, Callaway LK. Overweight and obesity in Australian mothers: epidemic or endemic? The Medical Journal of Australia. 2012; 196 (3): 184.
7. Heslehurst N, Rankin J, Wilkinson J, Summerbell C. A nationally representative study of maternal obesity in England, UK: trends in incidence and demographic inequalities in 619323 births, 1989–2007. International Journal of Obesity. 2010; 34 (3): 420.
8. Australian Bureau of Statistics-National Health Survey: Updated Results, 2011-2012. Web page update in 2013 [Access on 06/01/15]. Available from: http://www.abs.gov.au/AUSSTATS/abs@.nsf/DetailsPage/4364.0.55.0032011-2012?OpenDocument.
9. Cundy Prof T, Ackermann E, Ryan EA. Gestational diabetes: New criteria may triple the prevalence but effect on outcomes is unclear. The British Medical Journal. 2014; 348.
10. Kim SY, Saraiva C, Curtis M, Wilson HG, Troyan J, England L, *et al.* Fraction of gestational diabetes mellitus attributable to overweight and obesity by race/ethnicity, California, 2007-2009. American Journal of Public Health. 2013; 103 (10): 65.
11. Chu SY, Callaghan WM, Kim SY, Schmid CH, Lau J, England LJ, *et al.* Maternal obesity and risk of gestational diabetes mellitus. Diabetes Care. 2007; 30 (8): 2070.
12. Gibson KS, Waters TP, Catalano PM. Maternal weight gain in women who develop gestational diabetes mellitus. Obstetrics & Gynecology. 2012; 119 (3): 560.
13. Morisset AS, Tchernof A, Dube MC, Veillette J, Weisnagel SJ, Robitaille J. Weight gain measures in women with gestational diabetes mellitus. Journal of Women's Health. 2011; 20 (3): 375.
14. Callaway LK, O'Callaghan M, McIntyre HD. Obesity and the hypertensive disorders of pregnancy obesity and hypertensive disorders. Hypertension in Pregnancy. 2009; 28 (4): 473.
15. Flenady V, Koopmans L, Middleton P, Froen JF, Smith GC, Gibbons K, *et al.* Major risk factors for stillbirth in high-income countries: a systematic review and meta-analysis. Lancet. 2011; 377 (9774): 1331.
16. Callaway LK, Prins JB, Chang AM, McIntyre HD. The prevalence and impact of overweight and obesity in an Australian obstetric population. The Medical Journal of Australia. 2006; 184 (2): 56.
17. Yogev Y, Catalano PM. Pregnancy and Obesity. Obstetrics and Gynecology Clinics of North America. 2009; 36 (2): 285.
18. Catalano PM, Tyzbir ED, Wolfe RR, Roman NM, Amini SB, Sims EAH. Longitudinal changes in basal hepatic glucose production and suppression during insulin

infusion in normal pregnant women. American Journal of Obstetrics and Gynecology. 1992; 167 (4, Part 1): 913.
19. Siegmund T, Rad NT, Ritterath C, Siebert G, Henrich W, Buhling KJ. Longitudinal changes in the continuous glucose profile measured by the CGMS® in healthy pregnant women and determination of cut-off values. European Journal of Obstetrics Gynecology and Reproductive Biology. 2008; 139 (1): 46.
20. Catalano PM, Tyzbir ED, Wolfe RR, Calles J, Roman NM, Amini SB, *et al.* Carbohydrate metabolism during pregnancy in control subjects and women with gestational diabetes. American Journal of Physiology-Endocrinology and Metabolism. 1993; 264 (1): 60.
21. Catalano PM, Tyzbir ED, Roman NM, Amini SB, Sims EAH. Longitudinal changes in insulin release and insulin resistance in nonobese pregnant women. American Journal of Obstetrics and Gynecology. 1991; 165 (6, Part 1): 1667.
22. Catalano PM, Drago NM, Amini SB. Longitudinal changes in pancreatic β-cell function and metabolic clearance rate of insulin in pregnant women with normal and abnormal glucose tolerance. Diabetes Care. 1998; 21 (3): 403.
23. Davison JM, Dunlop W. Renal hemodynamics and tubular function in normal human pregnancy. Kidney International. 1980; 18 (2): 152.
24. Di Cianni G, Miccoli R, Volpe L, Lencioni C, Del Prato S. Intermediate metabolism in normal pregnancy and in gestational diabetes. Diabetes/Metabolism Research and Reviews. 2003; 19 (4): 259.
25. McIntyre HD, Chang AM, Callaway LK, Cowley DM, Dyer AR, Radaelli T, *et al.* Hormonal and metabolic factors associated with variations in insulin sensitivity in human pregnancy. Diabetes Care. 2010; 33 (2): 356.
26. Buchanan TA, Metzger BE, Freinkel N, Bergman RN. Insulin sensitivity and B-cell responsiveness to glucose during late pregnancy in lean and moderately obese women with normal glucose tolerance or mild gestational diabetes. American Journal of Obstetrics and Gynecology. 1990; 162 (4): 1008.
27. Butte NF. Carbohydrate and lipid metabolism in pregnancy: normal compared with gestational diabetes mellitus. The American Journal of Clinical Nutrition. 2000; 71 (Suppl.): 1256.
28. Herrera E. Metabolic adaptations in pregnancy and their implications for the availability of substrates to the fetus. European Journal of Clinical Nutrition. 2000; 54 (Suppl. 1): 47.
29. Augustine RA, Ladyman SR, Grattan DR. From feeding one to feeding many: hormone-induced changes in bodyweight homeostasis during pregnancy. The Journal of Physiology. 2008; 586 (2): 387.
30. Catalano PM, Roman-Drago NM, Amini SB, Sims EA. Longitudinal changes in body composition and energy balance in lean women with normal and abnormal glucose tolerance during pregnancy. American Journal of Obstetrics and Gynecology. 1998; 179 (1): 156.
31. Li Y, He PP, Zhang DW, Zheng XL, Cayabyab FS, Yin WD, *et al.* Lipoprotein lipase: From gene to atherosclerosis. Atherosclerosis. 2014; 237 (2): 597.
32. Ramos M, Crespo-Solans M, Del Campo S, Cacho J, Herrera E. Fat accumulation in the rat during early pregnancy is modulated by enhanced insulin responsiveness. American Journal of Physiology-Endocrinology and Metabolism. 2003; 285 (2): 318.
33. Herrera E. Lipid metabolism in pregnancy and its consequences in the fetus and newborn. Endocrine. 2002; 19 (1): 43.
34. Choi SM, Tucker DF, Gross DN, Easton RM, DiPilato LM, Dean AS, *et al.* Insulin regulates adipocyte lipolysis via an Akt-independent signaling pathway. Molecular and Cellular Biology. 2010; 30 (21): 5009.

35. Belo L, Caslake M, Santos-Silva A, Castro EMB, Pereira-Leite L, Quintanilha A, *et al.* LDL size, total antioxidant status and oxidised LDL in normal human pregnancy: a longitudinal study. Atherosclerosis. 2004; 177 (2): 391.
36. Alvarez JJ, Montelongo A, Iglesias A, Lasuncion MA, Herrera E. Longitudinal study on lipoprotein profile, high density lipoprotein subclass, and postheparin lipases during gestation in women. Journal of Lipid Research. 1996; 37 (2): 299.
37. Brizzi P, Tonolo G, Esposito F, Puddu L, Dessole S, Maioli M, *et al.* Lipoprotein metabolism during normal pregnancy. American Journal of Obstetrics and Gynecology. 1999; 181 (2): 430.
38. Potter JM, Nestel PJ. The hyperlipidemia of pregnancy in normal and complicated pregnancies. American Journal of Obstetrics and Gynecology. 1979; 133 (2): 165.
39. Nolan CJ, Riley SF, Sheedy MT, Walstab JE, Beischer NA. Maternal serum triglyceride, glucose tolerance, and neonatal birth weight ratio in pregnancy. Diabetes Care. 1995; 18 (12): 1550.
40. McDonald-Gibson R, Young M, Hytten F. Changes in plasma non esterified fatty acids and serum glycerol in pregnancy. BJOG: An International Journal of Obstetrics and Gynaecology. 1975; 82 (6): 460.
41. Burt RL. Plasma nonesterified fatty acids in normal pregnancy and the puerperium. Obstetrics & Gynecology. 1960; 15: 460.
42. Benassayag C, Mignot T, Haourigui M, Civel C, Hassid J, Carbonne B, *et al.* High polyunsaturated fatty acid, thromboxane A2, and alpha-fetoprotein concentrations at the human feto-maternal interface. Journal of Lipid Research. 1997; 38 (2): 276.
43. Sivan E, Boden G. Free fatty acids, insulin resistance, and pregnancy. Current Diabetes Reports. 2003; 3 (4): 319.
44. Herrera E. Implications of dietary fatty acids during pregnancy on placental, fetal and postnatal development - A review. Placenta. 2002; 23 (Suppl. 1): 9.
45. McLachlan KA, O'Neal D, Jenkins A, Alford FP. Do adiponectin, TNF-α, leptin and CRP relate to insulin resistance in pregnancy? Studies in women with or without gestational diabetes, during and after pregnancy. Diabetes/Metabolism Research and Reviews. 2006; 22 (2): 131.
46. Hauguel-de Mouzon S, Guerre-Millo M. The placenta cytokine network and inflammatory signals. Placenta. 2006; 27 (8): 794.
47. Masuzaki H, Ogawa Y, Sagawa N, Hosoda K, Matsumoto T, Mise H, *et al.* Nonadipose tissue production of leptin: Leptin as a novel placenta- derived hormone in humans. Nature Medicine. 1997; 3 (9): 1029.
48. Lea RG, Howe D, Hannah LT, Bonneau O, Hunter L, Hoggard N. Placental leptin in normal, diabetic and fetal growth-retarded pregnancies. Molecular Human Reproduction. 2000; 6 (8): 763.
49. Linnemann K, Malek A, Sager R, Blum WF, Schneider H, Fusch C. Leptin production and release in the dually in vitro perfused human placenta. The Journal of CIinical Endocrinology and Metabolism. 2000; 85 (11): 4298.
50. Okereke NC, Huston-Presley L, Amini SB, Kalhan S, Catalano PM. Longitudinal changes in energy expenditure and body composition in obese women with normal and impaired glucose tolerance. American Journal of Physiology-Endocrinology and Metabolism. 2004; 287 (3): 472.
51. Haghiac M, Basu S, Presley L, Serre D, Catalano PM, Hauguel-De Mouzon S. Patterns of adiponectin expression in term pregnancy: Impact of obesity. The Journal of Clinical Endocrinology and Metabolism. 2014; 99 (9): 3427.
52. Catalano PM, Hoegh M, Minium J, Huston-Presley L, Bernard S, Kalhan S, *et al.* Adiponectin in human pregnancy: implications for regulation of glucose and lipid metabolism. Diabetologia. 2006; 49 (7): 1677.

53. Cortelazzi D, Corbetta S, Ronzoni S, Pelle F, Marconi A, Cozzi V, *et al.* Maternal and foetal resistin and adiponectin concentrations in normal and complicated pregnancies. Clinical Endocrinology. 2007; 66 (3): 447.
54. Nien JK, Mazaki-Tovi S, Romero R, Erez O, Kusanovic JP, Gotsch F, *et al.* Plasma adiponectin concentrations in non pregnant, normal pregnancy and overweight pregnant women. Journal of Perinatal Medicine. 2007; 35 (6): 522.
55. Fuglsang J, Skjærbæk C, Frystyk J, Flyvbjerg A, Ovesen P. A longitudinal study of serum adiponectin during normal pregnancy. BJOG: An International Journal of Obstetrics and Gynaecology. 2006; 113 (1): 110.
56. Chen D, Dong M, Fang Q, He J, Wang Z, Yang X. Alterations of serum resistin in normal pregnancy and pre-eclampsia. Clinical Science. 2005; 108 (1): 81.
57. Palik E, Baranyi E, Melczer Z, Audikovszky M, Szöcs A, Winkler G, *et al.* Elevated serum acylated (biologically active) ghrelin and resistin levels associate with pregnancy-induced weight gain and insulin resistance. Diabetes Research and Clinical Practice. 2007; 76 (3): 351.
58. Drolet R, Bélanger C, Fortier M, Huot C, Mailloux J, Légaré D, *et al.* Fat depot-specific impact of visceral obesity on adipocyte adiponectin release in women. Obesity. 2009; 17 (3): 424.
59. Norata GD, Ongari M, Garlaschelli K, Raselli S, Grigore L, Catapano AL. Plasma resistin levels correlate with determinants of the metabolic syndrome. European Journal of Endocrinology. 2007; 156 (2): 279.
60. Mazaki-Tovi S, Romero R, Vaisbuch E, Erez O, Mittal P, Chaiworapongsa T, *et al.* Maternal serum adiponectin multimers in gestational diabetes. Journal of Perinatal Medicine. 2009; 37 (6): 637.
61. Ranheim T, Haugen F, Staff AC, Braekke K, Harsem NK, Drevon CA. Adiponectin is reduced in gestational diabetes mellitus in normal weight women. Acta Obstetricia et Gynecologica Scandinavica. 2004; 83 (4): 341.
62. Megia A, Vendrell J, Gutierrez C, Sabaté M, Broch M, Fernández-Real J-M, *et al.* Insulin sensitivity and resistin levels in gestational diabetes mellitus and after parturition. European Journal of Endocrinology. 2008; 158 (2): 173.
63. Chen D, Fang Q, Chai Y, Wang H, Huang H, Dong M. Serum resistin in gestational diabetes mellitus and early postpartum. Clinical Endocrinology. 2007; 67 (2): 208.
64. Lappas M, Yee K, Permezel M, Rice GE. Release and regulation of leptin, resistin and adiponectin from human placenta, fetal membranes, and maternal adipose tissue and skeletal muscle from normal and gestational diabetes mellitus-complicated pregnancies. Journal of Endocrinology. 2005; 186 (3): 457.
65. Sacks G, Seyani L, Lavery S, Trew G. Maternal C-reactive protein levels are raised at 4 weeks gestation. Human Reproduction. 2004; 19 (4): 1025.
66. Kirwan JP, Hauguel-De Mouzon S, Lepercq J, Challier J-C, Huston-Presley L, Friedman JE, *et al.* TNF-α is a predictor of insulin resistance in human pregnancy. Diabetes. 2002; 51 (7): 2207.
67. Hotamisligil GS, Shargill NS, Spiegelman BM. Adipose expression of tumor necrosis factor-α: Direct role in obesity-linked insulin resistance. Science. 1993; 259 (5091): 87.
68. Hotamisligil GS, Arner P, Caro JF, Atkinson RL, Spiegelman BM. Increased adipose tissue expression of tumor necrosis factor-α in human obesity and insulin resistance. Journal of Clinical Investigation. 1995; 95 (5): 2409.
69. Loy SL, Kns S, Jm HJ. Increase in maternal adiposity and poor lipid profile is associated with oxidative stress markers during pregnancy. Preventive Medicine. 2013; 57 (Suppl.): 41.

70. Jarvie E, Hauguel-de-Mouzon S, Nelson SM, Sattar N, Catalano PM, Freeman DJ. Lipotoxicity in obese pregnancy and its potential role in adverse pregnancy outcome and obesity in the offspring. Clinical Science. 2010; 119 (3): 123.
71. Sivan E, Chen X, Homko CJ, Reece EA, Boden G. Longitudinal study of carbohydrate metabolism in healthy obese pregnant women. Diabetes Care. 1997; 20 (9): 1470.
72. Catalano PM, Huston L, Amini SB, Kalhan SC. Longitudinal changes in glucose metabolism during pregnancy in obese women with normal glucose tolerance and gestational diabetes mellitus. American Journal of Obstetrics and Gynecology. 1999; 180 (4): 903.
73. Xiang AH, Peters RK, Trigo E, Kjos SL, Lee WP, Buchanan TA. Multiple metabolic defects during late pregnancy in women at high risk for type 2 diabetes. Diabetes. 1999; 48 (4): 848.
74. Schaefer-Graf UM, Meitzner K, Ortega-Senovilla H, Graf K, Vetter K, Abou-Dakn M, *et al.* Differences in the implications of maternal lipids on fetal metabolism and growth between gestational diabetes mellitus and control pregnancies. Diabetic Medicine. 2011; 28 (9): 1053.
75. Qiu C, Rudra C, Austin M, Williams M. Association of gestational diabetes mellitus and low-density lipoprotein (LDL) particle size. Physiological Research. 2007; 56 (5): 571.
76. Sánchez-Vera I, Bonet B, Viana M, Quintanar A, Martín MD, Blanco P, *et al.* Changes in plasma lipids and increased low-density lipoprotein susceptibility to oxidation in pregnancies complicated by gestational diabetes: consequences of obesity. Metabolism. 2007; 56 (11): 1527.
77. Koukkou E, Watts GF, Lowy C. Serum lipid, lipoprotein and apolipoprotein changes in gestational diabetes mellitus: a cross-sectional and prospective study. Journal of Clinical Pathology. 1996; 49 (8): 634.
78. Weiss JL, Malone FD, Emig D, Ball RH, Nyberg DA, Comstock CH, *et al.* Obesity, obstetric complications and cesarean delivery rate–a population-based screening study. American Journal of Obstetrics and Gynecology. 2004; 190 (4): 1091.
79. Nanda S, Savvidou M, Syngelaki A, Akolekar R, Nicolaides KH. Prediction of gestational diabetes mellitus by maternal factors and biomarkers at 11 to 13 weeks. Prenatal Diagnosis. 2011; 31: 135.
80. Buchanan TA. Pancreatic B-cell defects in gestational diabetes: implications for the pathogenesis and prevention of type 2 diabetes. The Journal of Clinical Endocrinology and Metabolism. 2001; 86 (3): 989.
81. Homko C, Sivan E, Chen X, Reece E, Boden G. Insulin secretion during and after pregnancy in patients with gestational diabetes mellitus 1. The Journal of Clinical Endocrinology and Metabolism. 2001; 86 (2): 568.
82. HAPO Study Cooperative Research Group. Hyperglycaemia and adverse pregnancy outcome (HAPO) study: Associations with maternal body mass index. BJOG: An International Journal of Obstetrics and Gynaecology. 2010; 117 (5): 575.
83. Johansson S, Villamor E, Altman M, Bonamy AKE, Granath F, Cnattingius S. Maternal overweight and obesity in early pregnancy and risk of infant mortality: A Population based cohort study in Sweden. The British Medical Journal 2014; 349: g6572.
84. Steegers EAP, Von Dadelszen P, Duvekot JJ, Pijnenborg R. Pre-eclampsia. The Lancet. 2010; 376 (9741): 631.
85. Hyperglycemia and Adverse Pregnancy Outcome (HAPO) Study Cooperative Research Group. Hyperglycemia and Adverse Pregnancy Outcome (HAPO) study: preeclampsia. American Journal of Obstetrics and Gynecology. 2010; 202 (3): 255.

86. Berends AL, de Groot CJ, Sijbrands EJ, Sie MP, Benneheij SH, Pal R, *et al.* Shared constitutional risks for maternal vascular-related pregnancy complications and future cardiovascular disease. Hypertension. 2008; 51 (4): 1034.
87. Sebire NJ, Jolly M, Harris J, Wadsworth J, Joffe M, Beard R, *et al.* Maternal obesity and pregnancy outcome: a study of 287,213 pregnancies in London. International journal of obesity and related metabolic disorders: journal of the International Association for the Study of Obesity. 2001; 25 (8): 1175.
88. Mazouni C, Porcu G, Cohen-Solal E, Heckenroth H, Guidicelli B, Bonnier P, *et al.* Maternal and anthropomorphic risk factors for shoulder dystocia. Acta Obstetricia et Gynecologica Scandinavica. 2006; 85 (5): 567.
89. Li N, Liu E, Guo J, Pan L, Li B, Wang P, *et al.* Maternal prepregnancy body mass index and gestational weight gain on pregnancy outcomes. PLoS ONE. 2013; 8 (12): 82310.
90. Committee to Reexamine IOM Pregnancy Weight Guidelines Food and Nutrition Board and Board on Children, Youth, and Families. Weight gain during pregnancy: Reexamining the guidelines. Rasmussen K, Yaktine A, editors. National Academies Press; 2009: 2.
91. Johansson K, Cnattingius S, Näslund I, Roos N, Trolle Lagerros Y, Granath F, *et al.* Outcomes of pregnancy after bariatric surgery. The New England Journal of Medicine. 2015; 372 (9): 814.
92. Crowther CA, Hiller JE, Moss JR, McPhee AJ, Jeffries WS, Robinson JS. Effect of treatment of gestational diabetes mellitus on pregnancy outcomes. The New England Journal of Medicine. 2005; 352 (24): 2477.
93. Landon MB, Spong CY, Thom E, Carpenter MW, Ramin SM, Casey B, *et al.* A multicenter, randomized trial of treatment for mild gestational diabetes. The New England Journal of Medicine. 2009; 361 (14): 1339.
94. Metzger BE, Lowe LP, Dyer AR, Trimble ER, Chaovarindr U, Coustan DR, *et al.* Hyperglycemia and adverse pregnancy outcomes. The New England Journal of Medicine. 2008; 358 (19): 1991.
95. Schmidt MI, Duncan BB, Reichelt AJ, Branchtein L, Matos MC, e Forti AC, *et al.* Gestational diabetes mellitus diagnosed with a 2-h 75-g oral glucose tolerance test and adverse pregnancy outcomes. Diabetes Care. 2001; 24 (7): 1151.
96. Milne F, Redman C, Walker J, Baker P, Bradley J, Cooper C, *et al.* The pre-eclampsia community guideline (PRECOG): how to screen for and detect onset of pre-eclampsia in the community. The British Medical Journal. 2005; 330 (7491): 576.
97. Mathiesen ER, Ringholm L, Damm P. Pregnancy management of women with pregestational diabetes. Endocrinology and Metabolism Clinics of North America. 2011; 40 (4): 727.
98. Tennant PWG, Glinianaia SV, Bilous RW, Rankin J, Bell R. Pre-existing diabetes, maternal glycated haemoglobin, and the risks of fetal and infant death: A population-based study. Diabetologia. 2014; 57 (2): 285.
99. Wang Y, Zhao H, Li Y, Zhang J, Tan J, Liu Y. Relationship between recurrent miscarriage and insulin resistance. Gynecologic and Obstetric Investigation. 2011; 72 (4): 245.
100. Jovanovic L, Knopp RH, Kim H, Cefalu WT, Zhu X-D, Lee YJ, *et al.* Elevated pregnancy losses at high and low extremes of maternal glucose in early normal and diabetic pregnancy evidence for a protective adaptation in diabetes. Diabetes Care. 2005; 28 (5): 1113.
101. Ramsay JE, Ferrell WR, Crawford L, Wallace AM, Greer IA, Sattar N. Maternal obesity is associated with dysregulation of metabolic, vascular, and inflammatory pathways. The Journal of Clinical Endocrinology and Metabolism. 2002; 87 (9): 4231.

102. Magnussen EB, Vatten LJ, Lund-Nilsen TI, Salvesen KÅ, Smith GD, Romundstad PR. Prepregnancy cardiovascular risk factors as predictors of pre-eclampsia: population based cohort study. The British Medical Journal. 2007; 335 (7627): 978.
103. Gallos ID, Sivakumar K, Kilby MD, Coomarasamy A, Thangaratinam S, Vatish M. Pre-eclampsia is associated with, and preceded by, hypertriglyceridaemia: a meta-analysis. BJOG: An International Journal of Obstetrics and Gynaecology. 2013; 120 (11): 1321.
104. Sattar N, Bendomir A, Berry C, Shepherd J, Greer IA, Packard CJ. Lipoprotein subfraction concentrations in preeclampsia: pathogenic parallels to atherosclerosis. Obstetrics & Gynecology. 1997; 89 (3): 403.
105. Spracklen CN, Smith CJ, Saftlas AF, Robinson JG, Ryckman KK. Maternal hyperlipidemia and the risk of preeclampsia: a meta-analysis. American Journal of Epidemiology. 2014: 145.
106. Ness RB, Roberts JM. Heterogeneous causes constituting the single syndrome of preeclampsia: a hypothesis and its implications. American Journal of Obstetrics and Gynecology. 1996; 175 (5): 1365.
107. Lorentzen B, Henriksen T. Plasma lipids and vascular dysfunction in preeclampsia. Seminars in Reproductive Endocrinology. 1998; 16 (1): 33.
108. Gratacós E, Casals E, Gómez O, Llurba E, Mercader I, Cararach V, *et al.* Increased susceptibility to low density lipoprotein oxidation in women with a history of pre-eclampsia. BJOG: An International Journal of Obstetrics and Gynaecology. 2003; 110 (4): 400.
109. Wilson BJ, Watson MS, Prescott GJ, Sunderland S, Campbell DM, Hannaford P, *et al.* Hypertensive diseases of pregnancy and risk of hypertension and stroke in later life: results from cohort study. The British Medical Journal. 2003; 326 (7394): 845.
110. Smith GC, Pell JP, Walsh D. Pregnancy complications and maternal risk of ischaemic heart disease: a retrospective cohort study of 129 290 births. The Lancet. 2001; 357 (9273): 2002.
111. Bellamy L, Casas J-P, Hingorani AD, Williams DJ. Pre-eclampsia and risk of cardiovascular disease and cancer in later life: systematic review and meta-analysis. The British Medical Journal. 2007; 335 (7627): 974.
112. Kessous R, Shoham-Vardi I, Pariente G, Sergienko R, Sheiner E. Long-term maternal atherosclerotic morbidity in women with pre-eclampsia. Heart. 2015; 101 (6): 442.
113. Catov JM, Bodnar LM, Kip KE, Hubel C, Ness RB, Harger G, *et al.* Early pregnancy lipid concentrations and spontaneous preterm birth. American Journal of Obstetrics and Gynecology. 2007; 197 (6): 610.e1.
114. Catov JM, Ness RB, Wellons MF, Jacobs DR, Roberts JM, Gunderson EP. Prepregnancy lipids related to preterm birth risk: The coronary artery risk development in young adults study. The Journal of Clinical Endocrinology and Metabolism. 2010; 95 (8): 3711.
115. Alleman BW, Smith AR, Byers HM, Bedell B, Ryckman KK, Murray JC, *et al.* A proposed method to predict preterm birth using clinical data, standard maternal serum screening, and cholesterol. American Journal of Obstetrics and Gynecology. 2013; 208 (6): 385.
116. Catov JM, Bertolet M, Chen Y-F, Evans RW, Hubel CA. Nonesterified fatty acids and spontaneous preterm birth: A factor analysis for identification of risk patterns. American Journal of Epidemiology. 2014; 179 (10): 1208.
117. Chen X, Scholl TO. Association of elevated free fatty acids during late pregnancy with preterm delivery. Obstetrics & Gynecology. 2008; 112 (2, Part 1): 297.

118. Mudd LM, Holzman CB, Catov JM, Senagore PK, Evans RW. Maternal lipids at mid-pregnancy and the risk of preterm delivery. Acta Obstetricia et Gynecologica Scandinavica. 2012; 91 (6): 726.
119. Kitajima M, Oka S, Yasuhi I, Fukuda M, Rii Y, Ishimaru T. Maternal serum triglyceride at 24–32 weeks' gestation and newborn weight in nondiabetic women with positive diabetic screens. Obstetrics & Gynecology. 2001; 97 (5): 776.
120. Schaefer-Graf UM, Graf K, Kulbacka I, Kjos SL, Dudenhausen J, Vetter K, *et al.* Maternal lipids as strong determinants of fetal environment and growth in pregnancies with gestational diabetes mellitus. Diabetes Care. 2008; 31 (9): 1858.
121. Berneis KK, Krauss RM. Metabolic origins and clinical significance of LDL heterogeneity. Journal of Lipid Research. 2002; 43 (9): 1363.
122. Wang L, Gill R, Pedersen TL, Higgins LJ, Newman JW, Rutledge JC. Triglyceride-rich lipoprotein lipolysis releases neutral and oxidized FFAs that induce endothelial cell inflammation. Journal of Lipid Research. 2009; 50 (2): 204.
123. Hotamisligil GS. Role of endoplasmic reticulum stress and c-Jun NH2-terminal kinase pathways in inflammation and origin of obesity and diabetes. Diabetes. 2005; 54 (Suppl. 2): 73.
124. Itani SI, Ruderman NB, Schmieder F, Boden G. Lipid-induced insulin resistance in human muscle is associated with changes in diacylglycerol, protein kinase C, and IκB-α. Diabetes. 2002; 51 (7): 2005.
125. Boden G, She P, Mozzoli M, Cheung P, Gumireddy K, Reddy P, *et al.* Free fatty acids produce insulin resistance and activate the proinflammatory nuclear factor-κB pathway in rat liver. Diabetes. 2005; 54 (12): 3458.
126. Benítez S, Camacho M, Arcelus R, Vila L, Bancells C, Ordóñez-Llanos J, *et al.* Increased lysophosphatidylcholine and non-esterified fatty acid content in LDL induces chemokine release in endothelial cells: Relationship with electronegative LDL. Atherosclerosis. 2004; 177 (2): 299.
127. Bunn RC, Cockrell GE, Ou Y, Thrailkill KM, Lumpkin Jr CK, Fowlkes JL. Palmitate and insulin synergistically induce IL-6 expression in human monocytes. Cardiovascular Diabetology. 2010; 9: 73.
128. Barazzoni R, Zanetti M, Cappellari GG, Semolic A, Boschelle M, Codarin E, *et al.* Fatty acids acutely enhance insulin-induced oxidative stress and cause insulin resistance by increasing mitochondrial reactive oxygen species (ROS) generation and nuclear factor-κB inhibitor (IκB)-nuclear factor-κB (NFκB) activation in rat muscle, in the absence of mitochondrial dysfunction. Diabetologia. 2012; 55 (3): 773.
129. Kim C, Newton KM, Knopp RH. Gestational diabetes and the incidence of type 2 diabetes: A systematic review. Diabetes Care. 2002; 25 (10): 1862.
130. Lauenborg J, Hansen T, Jensen DM, Vestergaard H, Mølsted-Pedersen L, Hornnes P, *et al.* Increasing incidence of diabetes after gestational diabetes a long-term follow-up in a Danish population. Diabetes Care. 2004; 27 (5): 1194.
131. Lee AJ, Hiscock RJ, Wein P, Walker SP, Permezel M. Gestational diabetes mellitus: Clinical predictors and long-term risk of developing type 2 diabetes a retrospective cohort study using survival analysis. Diabetes Care. 2007; 30 (4): 878.
132. Bellamy L, Casas J-P, Hingorani AD, Williams D. Type 2 diabetes mellitus after gestational diabetes: A systematic review and meta-analysis. The Lancet. 2009; 373 (9677): 1773.
133. Pintaudi B, Lucisano G, Pellegrini F, D'Ettorre A, Lepore V, De Berardis G, *et al.* The long-term effects of stillbirth on women with and without gestational diabetes: a population-based cohort study. Diabetologia. 2015; 58 (1): 67.
134. Napoli C, D'armiento F, Mancini F, Postiglione A, Witztum J, Palumbo G, *et al.* Fatty streak formation occurs in human fetal aortas and is greatly enhanced by maternal hypercholesterolemia. Intimal accumulation of low density lipoprotein and its oxidation

precede monocyte recruitment into early atherosclerotic lesions. Journal of Clinical Investigation. 1997; 100 (11): 2680.
135. Whitaker RC. Predicting preschooler obesity at birth: the role of maternal obesity in early pregnancy. Pediatrics. 2004; 114 (1): 768.
136. Catalano PM, Farrell K, Thomas A, Huston-Presley L, Mencin P, de Mouzon SH, *et al.* Perinatal risk factors for childhood obesity and metabolic dysregulation. The American Journal of Clinical Nutrition. 2009; 90 (5): 1303.
137. Dabelea D, Mayer-Davis EJ, Lamichhane AP, D'Agostino RB, Liese AD, Vehik KS, *et al.* Association of intrauterine exposure to maternal diabetes and obesity with type 2 diabetes in youth the SEARCH case-control study. Diabetes Care. 2008; 31 (7): 1422.
138. Clausen TD, Mathiesen ER, Hansen T, Pedersen O, Jensen DM, Lauenborg J, *et al.* High prevalence of type 2 diabetes and pre-diabetes in adult offspring of women with gestational diabetes mellitus or type 1 diabetes the role of intrauterine hyperglycemia. Diabetes Care. 2008; 31 (2): 340.
139. Hochberg Ze, Feil R, Constancia M, Fraga M, Junien C, Carel J-C, *et al.* Child health, developmental plasticity, and epigenetic programming. Endocrine Reviews. 2010; 32 (2): 159.
140. Nolan CJ, Damm P, Prentki M. Type 2 diabetes across generations: from pathophysiology to prevention and management. The Lancet. 378 (9786): 169.
141. Wu JSR, Lever JE. Purification and reconstitution of a 75-kilodalton protein identified as a component of the renal sodium/glucose symporter. Biochemistry. 1987; 26 (19): 5958.
142. Peerce BE, Wright EM. Examination of the sodium-induced conformational change of the intestinal brush border sodium/glucose symporter using fluorescent probes. Biochemistry. 1987; 26 (14): 4272.
143. Augustin R, Carayannopoulos MO, Dowd LO, Phay JE, Moley JF, Moley KH. Identification and characterization of human glucose transporter-like protein-9 (GLUT9): Alternative splicing alters trafficking. Journal of Biological Chemistry. 2004; 279 (16): 16229.
144. Rogers S, Macheda ML, Docherty SE, Carty MD, Henderson MA, Soeller WC, *et al.* Identification of a novel glucose transporter-like protein-GLUT-12. American Journal of Physiology-Endocrinology and Metabolism. 2002; 282 (3): 733.
145. Mueckler M. Facilitative glucose transporters. European Journal of Biochemistry. 1994; 219 (3): 713.
146. Hahn T, Hartmann M, Blaschitz A, Skofitsch G, Graf R, Dohr G, *et al.* Localisation of the high affinity factilitative glucose transporter protein GLUT 1 in the placenta of human, marmoset monkey (Callithrix jacchus) and rat at different developmental stages. Cell and Tissue Research. 1995; 280 (1): 49.
147. Vander Heiden MG, Cantley LC, Thompson CB. Understanding the Warburg effect: the metabolic requirements of cell proliferation. Science. 2009; 324 (5930): 1029.
148. Moe AJ, Farmer DR, Nelson DM, Smith CH. Pentose phosphate pathway in cellular trophoblasts from full-term human placentas. American Journal of Physiology-Cell Physiology. 1991; 261 (6): 1042.
149. Nelson DL, Cox MM. Lehninger Principles of Biochemistry. 5th ed. New York, NYW. H. Freeman and Company-Macmillan; 2008: 528.
150. Boiteux A, Hess B. Design of Glycolysis. 1981; 293 (1063): 5.
151. Bellomo R. Bench-to-bedside review: lactate and the kidney. Critical Care. 2002; 6 (4): 322.
152. Przybytkowski E, Joly E, Nolan CJ, Hardy S, Francoeur AM, Langelier Y, *et al.* Upregulation of cellular triacylglycerol-free fatty acid cycling by oleate is associated with long-term serum-free survival of human breast cancer cells. Biochemistry and Cell Biology. 2007; 85 (3): 301.

153. Ruderman NB, Saha AK, Vavvas D, Witters LA. Malonyl-CoA, fuel sensing, and insulin resistance. American Journal of Physiology-Endocrinology and Metabolism. 1999; 276 (1, Part 1): 1.
154. Hers H. The control of glycogen metabolism in the liver. Annual Review of Biochemistry. 1976; 45 (1): 167.
155. Alonso M, Lomako J, Lomako W, Whelan W. A new look at the biogenesis of glycogen. The FASEB journal. 1995; 9 (12): 1126.
156. Kunau W-H, Dommes V, Schulz H. β-Oxidation of fatty acids in mitochondria, peroxisomes, and bacteria: A century of continued progress. Progress in Lipid Research. 1995; 34 (4): 267.
157. McGarry J, Foster D. Regulation of hepatic fatty acid oxidation and ketone body production. Annual Review of Biochemistry. 1980; 49 (1): 395.
158. Rampersad R, Cervar-Zivkovic M, Nelson DM. The Placenta: From Development to Disease. Kay H, Nelson M, Wang Y, editors. John Wiley & Sons; 2011: 17.
159. Benirschke K. Remarkable placenta. Clinical Anatomy. 1998; 11 (3): 194.
160. Huppertz B. The anatomy of the normal placenta. Journal of Clinical Pathology. 2008; 61 (12): 1296.
161. Espinoza J, Romero R, Yeon MK, Kusanovic JP, Hassan S, Erez O, *et al.* Normal and abnormal transformation of the spiral arteries during pregnancy. Journal of Perinatal Medicine. 2006; 34 (6): 447.
162. Burton GJ, Sibley CP, Jauniaux ER. Obstetrics: normal and problem pregnancies. Gabbe SG, Niebyl JR, Galan HL, Jauniaux ER, Landon MB, Simpson JL, *et al.*, editors. Copyright Elsevier Health Sciences; 2012: 3.
163. Carter AM, Enders AC. Comparative aspects of trophoblast development and placentation. Reproductive Biology and Endocrinology. 2004; 2 (1): 46.
164. Illsley NP. Glucose transporters in the human placenta. Placenta. 2000; 21 (1): 14.
165. Hauguel S, Desmaizieres V, Challier J. Glucose uptake, utilization, and transfer by the human placenta as functions of maternal glucose concentration. Pediatric Research. 1986; 20 (3): 269.
166. Desoye G, Gauster M, Wadsack C. Placental transport in pregnancy pathologies. The American Journal of Clinical Nutrition. 2011; 94 (6): 1896.
167. Gil-Sánchez A, Demmelmair H, Parrilla J, Koletzko B, Larqué E. Mechanisms involved in the selective transfer of long chain polyunsaturated fatty acids to the fetus. Frontiers in Genetics. 2011; 2.
168. Battaglia FC, Regnault TRH. Placental transport and metabolism of amino acids. Placenta. 2001; 22 (2–3): 145.
169. Desoye G, Van Poppel M. The feto-placental dialogue and diabesity. Best Practice and Research: Clinical Obstetrics and Gynaecology. 2015; 29 (1): 15.
170. Hiden U, Maier A, Bilban M, Ghaffari-Tabrizi N, Wadsack C, Lang I, *et al.* Insulin control of placental gene expression shifts from mother to foetus over the course of pregnancy. Diabetologia. 2006; 49 (1): 123.
171. Catalano PM, Hauguel-De Mouzon S. Is it time to revisit the Pedersen hypothesis in the face of the obesity epidemic? American Journal of Obstetrics and Gynecology. 2011; 204 (6): 479.
172. Murphy VE, Smith R, Giles WB, Clifton VL. Endocrine regulation of human fetal growth: The role of the mother, placenta, and fetus. Endocrine Reviews. 2006; 27 (2): 141.
173. Kalhan S, Parimi P. Gluconeogenesis in the fetus and neonate. Seminars in Perinatology. 2000; 24 (2): 94.
174. Baumann MU, Deborde S, Illsley NP. Placental glucose transfer and fetal growth. Endocrine. 2002; 19 (1): 13.

175. Johnson LW, Smith CH. Monosaccharide transport across microvillous membrane of human placenta. The American Journal of Physiology. 1980; 238 (5): 160.
176. Osmond DT, Nolan CJ, King RG, Brennecke SP, Gude NM. Effects of gestational diabetes on human placental glucose uptake, transfer, and utilisation. Diabetologia. 2000; 43 (5): 576.
177. Carstensen M, Leichtweiss HP, Molsen G, Schroeder H. Evidence for a specific transport of D hexoses across the human term placenta in vitro. Archiv fur Gynakologie. 1977; 222 (3): 187.
178. Hahn D, Blaschitz A, Korgun ET, Lang I, Desoye G, Skofitsch G, *et al.* From maternal glucose to fetal glycogen: Expression of key regulators in the human placenta. Molecular Human Reproduction. 2001; 7 (12): 1173.
179. Ericsson A, Hamark B, Powell T, Jansson T. Glucose transporter isoform 4 is expressed in the syncytiotrophoblast of first trimester human placenta. Human Reproduction. 2005; 20 (2): 521.
180. Dawson PA, Mychaleckyj JC, Fossey SC, Mihic SJ, Craddock AL, Bowden DW. Sequence and functional analysis of GLUT10: A glucose transporter in the type 2 diabetes-linked region of chromosome 20q12-13.1. Molecular Genetics and Metabolism. 2001; 74 (1-2): 186.
181. Scheepers A, Schmidt S, Manolescu A, Cheeseman CI, Bell A, Zahn C, *et al.* Characterization of the human SLC2A11 (GLUT11) gene: Alternative promoter usage, function, expression, and subcellular distribution of three isoforms, and lack of mouse orthologue. Molecular Membrane Biology. 2005; 22 (4): 339.
182. Desoye G, Shafrir E. The human placenta in diabetic pregnancy. Diabetes Reviews. 1996; 4 (1): 70.
183. Ebeling P, Koistinen HA, Koivisto VA. Insulin-independent glucose transport regulates insulin sensitivity. FEBS letters. 1998; 436 (3): 301.
184. Hahn T, Barth S, Weiss U, Mosgoeller W, Desoye G. Sustained hyperglycemia in vitro down-regulates the GLUT1 glucose transport system of cultured human term placental trophoblast: A mechanism to protect fetal development? FASEB Journal. 1998; 12 (12): 1221.
185. Illsley N, Sellers M, Wright R. Glycaemic regulation of glucose transporter expression and activity in the human placenta. Placenta. 1998; 19 (7): 517.
186. Hahn T, Hahn D, Blaschitz A, Korgun ET, Desoye G, Dohr G. Hyperglycaemia-induced subcellular redistribution of GLUT1 glucose transporters in cultured human term placental trophoblast cells. Diabetologia. 2000; 43 (2): 173.
187. Jansson T, Wennergren M, Illsley NP. Glucose transporter protein expression in human placenta throughout gestation and in intrauterine growth retardation. The Journal of Clinical Endocrinology and Metabolism. 1993; 77 (6): 1554.
188. Barrosa L, Yudilevich D, Jarvis SM, Beaumont N, Baldwin S. Quantitation and immunolocalization of glucose transporters in the human placenta. Placenta. 1995; 16 (7): 623.
189. Johnson LW, Smith CH. Glucose transport across the basal plasma membrane of human placental syncytiotrophoblast. Biochimica et Biophysica Acta (BBA)-Biomembranes. 1985; 815 (1): 44.
190. Korgun ET, Celik-Ozenci C, Seval Y, Desoye G, Demir R. Do glucose transporters have other roles in addition to placental glucose transport during early pregnancy? Histochemistry and Cell Biology. 2005; 123 (6): 621.
191. Xing A, Challier J, Lepercq J, Cauzac M, Charron M, Girard J, *et al.* Unexpected expression of glucose transporter 4 in villous stromal cells of human placenta The Journal of Clinical Endocrinology and Metabolism. 1998; 83 (11): 4097.
192. Day PE, Cleal JK, Lofthouse EM, Hanson MA, Lewis RM. What factors determine placental glucose transfer kinetics? Placenta. 2013; 34 (10): 953.

193. Rice PA, Rourke JE, Nesbitt Jr REL. In vitro perfusion studies of the human placenta. IV. Some characteristics of the glucose transport system in the human placenta. Gynecologic Investigation. 1976; 7 (4): 213.
194. Bullen BE, Bloxam DL, Ryder TA, Mobberley MA, Bax CM. Two-sided culture of human placental trophoblast. Morphology, immunocytochemistry and permeability properties. Placenta. 1990; 11 (5): 431.
195. Hauguel S, Challier JC, Cedard L, Olive G. Metabolism of the human placenta perfused in vitro: Glucose transfer and utilization, O_2 consumption, lactate and ammonia production. Pediatric Research. 1983; 17 (9): 729.
196. Holzman IR, Philipps AF, Battaglia FC. Glucose metabolism, lactate, and ammonia production by the human placenta in vitro. Pediatric Research. 1979; 13 (2): 117.
197. Sakurai T, Takagi H, Hosoya N. Metabolic pathways of glucose in human placenta. Changes with gestation and with added 17β-estradiol. American Journal of Obstetrics and Gynecology. 1969; 105 (7): 1044.
198. Osmond DTD, King RG, Brennecke SP, Gude NM. Placental glucose transport and utilisation is altered at term in insulin-treated, gestational-diabetic patients. Diabetologia. 2001; 44 (9): 1133.
199. Diamant YZ, Kissilevitz R, Shafrir E. Changes in activity of enzymes related to glycolysis, gluconeogenesis and lipogenesis in placentae from diabetic women. Placenta. 1984; 5 (1): 55.
200. Pathmaperuma AN, Mana P, Cheung SN, Kugathas K, Josiah A, Koina ME, *et al.* Fatty acids alter glycerolipid metabolism and induce lipid droplet formation, syncytialisation and cytokine production in human trophoblasts with minimal glucose effect or interaction. Placenta. 2010; 31 (3): 230.
201. Özer N, Aksoy Y, Ögüs IH. Kinetic properties of human placental glucose-6-phosphate dehydrogenase. The International Journal of Biochemistry and Cell Biology. 2001; 33 (3): 221.
202. Ginsburg J, Jeacock MK. Pathways of glucose metabolism in human placental tissue. Biochimica et Biophysica Acta (BBA)-General Subjects. 1964; 90 (1): 166.
203. Leonce J, Brockton N, Robinson S, Venkatesan S, Bannister P, Raman V, *et al.* Glucose production in the human placenta. Placenta. 2006; 27 (Suppl.): 103.
204. Huang K-P, Robinson JC. Purification and properties of the glucose-6-phosphate-dependent form of human placental glycogen synthase. Archives of Biochemistry and Biophysics. 1976; 175 (2): 583.
205. Radaelli T, Lepercq J, Varastehpour A, Basu S, Catalano PM, Hauguel-De Mouzon S. Differential regulation of genes for fetoplacental lipid pathways in pregnancy with gestational and type 1 diabetes mellitus. American Journal of Obstetrics and Gynecology. 2009; 201 (2): 209.
206. Tsoi SC, Cale JM, Bird IM, Kay HH. cDNA microarray analysis of the gene expression profiles in human placenta: Up-regulation of the transcript encoding muscle subunit of glycogen phosphorylase in preeclampsia. Journal of the Society for Gynecologic Investigation. 2003; 10 (8): 496.
207. Desoye G, Shafrir E. Placental metabolism and its regulation in health and diabetes. Molecular Aspects of Medicine. 1994; 15 (6): 505.
208. Jones CJP, Desoye G. Glycogen distribution in the capillaries of the placental villus in normal, overt and gestational diabetic pregnancy. Placenta. 1993; 14 (5): 505.
209. Desoye G, Hofmann HH, Weiss PA. Insulin binding to trophoblast plasma membranes and placental glycogen content in well-controlled gestational diabetic women treated with diet or insulin, in well-controlled overt diabetic patients and in healthy control subjects. Diabetologia. 1992; 35 (1): 45.

210. Schmon B, Hartmann M, Jones CJ, Desoye G. Insulin and glucose do not affect the glycogen content in isolated and cultured trophoblast cells of human term placenta. The Journal of Clinical Endocrinology and Metabolism. 1991; 73 (4): 888.
211. Randle P, Garland P, Hales C, Newsholme E. The glucose fatty-acid cycle its role in insulin sensitivity and the metabolic disturbances of diabetes mellitus. The Lancet. 1963; 281 (7285): 785.
212. Hue L, Taegtmeyer H. The Randle cycle revisited: a new head for an old hat. American Journal of Physiology-Endocrinology and Metabolism. 2009; 297 (3): 578.
213. Gil-Sánchez A, Koletzko B, Larqué E. Current understanding of placental fatty acid transport. Current Opinion in Clinical Nutrition and Metabolic Care. 2012; 15 (3): 265.
214. Gauster M, Hiden U, Blaschitz A, Frank S, Lang U, Alvino G, *et al.* Dysregulation of placental endothelial lipase and lipoprotein lipase in intrauterine growth-restricted pregnancies. The Journal of Clinical Endocrinology and Metabolism. 2007; 92 (6): 2256.
215. McCoy MG, Sun G-S, Marchadier D, Maugeais C, Glick JM, Rader DJ. Characterization of the lipolytic activity of endothelial lipase. Journal of Lipid Research. 2002; 43 (6): 921.
216. Larqué E, Demmelmair H, Gil-Sánchez A, Prieto-Sánchez MT, Blanco JE, Pagán A, *et al.* Placental transfer of fatty acids and fetal implications. American Journal of Clinical Nutrition. 2011; 94 (6): 1908.
217. Haggarty P. Placental regulation of fatty acid delivery and its effect on fetal growth-A review. Placenta. 2002; 23 (Suppl. 1): 28.
218. Barrett HL, Kubala MH, Scholz Romero K, Denny KJ, Woodruff TM, McIntyre HD, *et al.* Placental lipases in pregnancies complicated by gestational diabetes mellitus (GDM). PLoS ONE. 2014; 9 (8): 104826.
219. Bildirici I, Roh C-R, Schaiff WT, Lewkowski BM, Nelson DM, Sadovsky Y. The lipid droplet-associated protein adipophilin is expressed in human trophoblasts and is regulated by peroxisomal proliferator-activated receptor-γ/Retinoid X Receptor. The Journal of Clinical Endocrinology and Metabolism. 2003; 88 (12): 6056.
220. Hiden U, Desoye G. The placenta in a diabetic pregnancy. Journal fur Reproduktionsmedizin und Endokrinologie. 2010; 7 (1): 27.
221. Herrera E, Ortega-Senovilla H. Disturbances in lipid metabolism in diabetic pregnancy Are these the cause of the problem? Best Practice & Research Clinical Endocrinology & Metabolism. 2010; 24 (4): 515.
222. Aye ILMH, Waddell BJ, Mark PJ, Keelan JA. Placental ABCA1 and ABCG1 transporters efflux cholesterol and protect trophoblasts from oxysterol induced toxicity. Biochimica et Biophysica Acta (BBA)-Molecular and Cell Biology of Lipids. 2010; 1801 (9): 1013.
223. Dubé E, Ethier-Chiasson M, Lafond J. Modulation of cholesterol transport by insulin-treated gestational diabetes mellitus in human full-term placenta. Biology of Reproduction. 2013; 88 (1): 16.
224. Shekhawat P, Bennett MJ, Sadovsky Y, Nelson DM, Rakheja D, Strauss AW. Human placenta metabolizes fatty acids: implications for fetal fatty acid oxidation disorders and maternal liver diseases. American Journal of Physiology-Endocrinology and Metabolism. 2003; 284 (6): 1098.
225. Dunlop M, Court JM. Lipogenesis in developing human adipose tissue. Early Human Development. 1978; 2 (2): 123.
226. Berghaus T, Demmelmair H, Koletzko B. Fatty acid composition of lipid classes in maternal and cord plasma at birth. European Journal of Pediatrics. 1998; 157 (9): 763.
227. Das UN. Essential fatty acids: biochemistry, physiology and pathology. Biotechnology Journal. 2006; 1 (4): 420.

228. Gil-Sánchez A, Larqué E, Demmelmair H, Acien MI, Faber FL, Parrilla JJ, *et al.* Maternal-fetal in vivo transfer of [^{13}C] docosahexaenoic and other fatty acids across the human placenta 12 h after maternal oral intake. The American Journal of Clinical Nutrition. 2010; 92 (1): 115.
229. Lager S, Jansson N, Olsson AL, Wennergren M, Jansson T, Powell TL. Effect of IL-6 and TNF-α on fatty acid uptake in cultured human primary trophoblast cells. Placenta. 2011; 32 (2): 121.
230. Scifres CM, Chen B, Nelson DM, Sadovsky Y. Fatty acid binding protein 4 regulates intracellular lipid accumulation in human trophoblasts. Journal of Clinical Endocrinology and Metabolism. 2011; 96 (7): 1083.
231. Gauster M, Hiden U, van Poppel M, Frank S, Wadsack C, Hauguel-de Mouzon S, *et al.* Dysregulation of placental endothelial lipase in obese women with gestational diabetes mellitus. Diabetes. 2011; 60 (10): 2457.
232. Visiedo F, Bugatto F, Sánchez V, Cózar-Castellano I, Bartha JL, Perdomo G. High glucose levels reduce fatty acid oxidation and increase triglyceride accumulation in human placenta. American Journal of Physiology-Endocrinology and Metabolism. 2013; 305 (2): 205.
233. Ethier-Chiasson M, Duchesne A, Forest J-C, Giguere Y, Masse A, Mounier C, *et al.* Influence of maternal lipid profile on placental protein expression of LDLr and SR-BI. Biochemical and Biophysical Research Communications. 2007; 359 (1): 8.
234. Aye IL, Waddell BJ, Mark PJ, Keelan JA. Oxysterols inhibit differentiation and fusion of term primary trophoblasts by activating liver X receptors. Placenta. 2011; 32 (2): 183.
235. Herrera E, Amusquivar E, Lopez-Soldado I, Ortega H. Maternal lipid metabolism and placental lipid transfer. Hormone Research in Paediatrics. 2006; 65 (Suppl. 3): 59.
236. Shambaugh Iii GE, Koehler RR, Yokoo H. Fetal fuels III: Ketone utilization by fetal hepatocyte. American Journal of Physiology Endocrinology Metabolism and Gastrointestinal Physiology. 1978; 4 (3): 330.
237. de la Torre SRA, Serrano MA, Medina JM. Carrier-mediated β-D-hydroxybutyrate transport in brush-border membrane vesicles from rat placenta. Pediatric Research. 1992; 32 (3): 317.
238. Visiedo F, Bugatto F, Carrasco-Fernández C, Sáez-Benito A, Mateos R, Cózar-Castellano I, *et al.* Hepatocyte growth factor is elevated in amniotic fluid from obese women and regulates placental glucose and fatty acid metabolism. Placenta. 2015; 36 (4): 381.
239. Cleal JK, Lewis RM. The mechanisms and regulation of placental amino acid transport to the human foetus. Journal of Neuroendocrinology. 2008; 20 (4): 419.
240. Larqué E, Ruiz-Palacios M, Koletzko B. Placental regulation of fetal nutrient supply. Current Opinion in Clinical Nutrition and Metabolic Care. 2013; 16 (3): 292.
241. Johnson LW, Smith CH. Neutral amino acid transport systems of microvillous membrane of human placenta. American Journal of Physiology-Cell Physiology. 1988; 254 (6): 773.
242. Hoeltzli SD, Smith CH. Alanine transport systems in isolated basal plasma membrane of human placenta. American Journal of Physiology-Cell Physiology. 1989; 256 (3): 630.
243. Kudo Y, Boyd C. Characterization of amino acid transport systems in human placental basal membrane vesicles. Biochimica et Biophysica Acta-Biomembranes. 1990; 1021 (2): 169.
244. Cleal J, Glazier J, Ntani G, Crozier S, Day P, Harvey N, *et al.* Facilitated transporters mediate net efflux of amino acids to the fetus across the basal membrane of the placental syncytiotrophoblast. The Journal of Physiology. 2011; 589 (4): 987.

245. Aiko Y, Askew DJ, Aramaki S, Myoga M, Tomonaga C, Hachisuga T, *et al.* Differential levels of amino acid transporters System L and ASCT2, and the mTOR protein in placenta of preeclampsia and IUGR. BMC Pregnancy and Childbirth. 2014; 14 (1): 181
246. Norberg S, Powell TL, Jansson T. Intrauterine Growth Restriction Is Associated with a Reduced Activity of Placental Taurine Transporters. Pediatric Research. 1998; 44 (2): 233.
247. Roos S, Powell TL, Jansson T. Human placental taurine transporter in uncomplicated and IUGR pregnancies: cellular localization, protein expression, and regulation. American Journal of Physiology 2004; 287 (4): 886.
248. Ayuk P, Theophanous D, D'Souza S, Sibley C, Glazier J. L-arginine transport by the microvillous plasma membrane of the syncytiotrophoblast from human placenta in relation to nitric oxide production: effects of gestation, preeclampsia, and intrauterine growth restriction. The Journal of Clinical Endocrinology and Metabolism. 2002; 87 (2): 747.
249. Cariappa R, Heath-Monnig E, Smith CH. Isoforms of amino acid transporters in placental syncytiotrophoblast: Plasma membrane localization and potential role in maternal/fetal transport. Placenta. 2003; 24 (7): 713.
250. Cleal JK, Brownbill P, Godfrey KM, Jackson JM, Jackson AA, Sibley CP, *et al.* Modification of fetal plasma amino acid composition by placental amino acid exchangers in vitro. The Journal of Physiology. 2007; 582 (2): 871.
251. Philipps A, Holzman I, Teng C, Battaglia F. Tissue concentrations of free amino acids in term human placentas. American Journal of Obstetrics and Gynecology. 1978; 131 (8): 881.
252. Roos S, Powell T, Jansson T. Placental mTOR links maternal nutrient availability to fetal growth. Biochemical Society Transactions. 2009; 37 (1): 295.
253. Galan HL, Marconi AM, Paolini CL, Cheung A, Battaglia FC. The transplacental transport of essential amino acids in uncomplicated human pregnancies. American Journal of Obstetrics and Gynecology. 2009; 200 (1): 91.
254. Jozwik M, Teng C, Wilkening RB, Meschia G, Battaglia FC. Reciprocal inhibition of umbilical uptake within groups of amino acids. American Journal of Physiology-Endocrinology and Metabolism. 2004; 286 (3): 376.
255. Glazier JD, Cetin I, Perugino G, Ronzoni S, Grey AM, Mahendran D, *et al.* Association between the activity of the system A amino acid transporter in the microvillous plasma membrane of the human placenta and severity of fetal compromise in intrauterine growth restriction. Pediatric Research. 1997; 42 (4): 514.
256. Cetin I, Corbetta C, Sereni LP, Marconi AM, Bozzetti P, Pardi G, *et al.* Umbilical amino acid concentrations in normal and growth-retarded fetuses sampled in utero by cordocentesis. American Journal of Obstetrics and Gynecology. 1990; 162 (1): 253.
257. Cetin I, de Santis MSN, Taricco E, Radaelli T, Teng C, Ronzoni S, *et al.* Maternal and fetal amino acid concentrations in normal pregnancies and in pregnancies with gestational diabetes mellitus. American Journal of Obstetrics and Gynecology. 2005; 192 (2): 610.
258. Jansson N, Rosario FJ, Gaccioli F, Lager S, Jones HN, Roos S, *et al.* Activation of placental mTOR signaling and amino acid transporters in obese women giving birth to large babies. Journal of Clinical Endocrinology and Metabolism. 2013; 98 (1): 105.
259. Jansson T, Ekstrand Y, Björn C, Wennergren M, Powell TL. Alterations in the activity of placental amino acid transporters in pregnancies complicated by diabetes. Diabetes. 2002; 51 (7): 2214.
260. Kuruvilla AG, D'Souza SW, Glazier JD, Mahendran D, Maresh MJ, Sibley CP. Altered activity of the system A amino acid transporter in microvillous membrane

vesicles from placentas of macrosomic babies born to diabetic women. The Journal of Clinical Investigation. 1994; 94 (2): 689.
261. Ditchfield AM, Desforges M, Mills TA, Glazier JD, Wareing M, Mynett K, *et al.* Maternal obesity is associated with a reduction in placental taurine transporter activity. International Journal of Obesity. 2015; 39 (4): 557.
262. von Versen-Höynck F, Rajakumar A, Parrott MS, Powers RW. Leptin Affects System A Amino Acid Transport Activity in the Human Placenta: Evidence for STAT3 Dependent Mechanisms. Placenta. 2009; 30 (4): 361.
263. Farley DM, Choi J, Dudley DJ, Li C, Jenkins SL, Myatt L, *et al.* Placental amino acid transport and placental leptin resistance in pregnancies complicated by maternal obesity. Placenta. 2010; 31 (8): 718.
264. Jones HN, Jansson T, Powell TL. Full-length adiponectin attenuates insulin signaling and inhibits insulin-stimulated amino acid transport in human primary trophoblast cells. Diabetes. 2010; 59 (5): 1161.
265. Jones HN, Jansson T, Powell TL. IL-6 stimulates system A amino acid transporter activity in trophoblast cells through STAT3 and increased expression of SNAT2. American Journal of Physiology-Cell Physiology. 2009; 297 (5): 1228.
266. Constância M, Hemberger M, Hughes J, Dean W, Ferguson-Smith A, Fundele R, *et al.* Placental-specific IGF-II is a major modulator of placental and fetal growth. Nature. 2002; 417 (6892): 945.
267. Nelson DM, Johnson RD, Smith SD, Anteby EY, Sadovsky Y. Hypoxia limits differentiation and up-regulates expression and activity of prostaglandin H synthase 2 in cultured trophoblast from term human placenta. American Journal of Obstetrics and Gynecology. 1999; 180 (4): 896.
268. Kliman HJ, Nestler JE, Sermasi E, Sanger JM, Strauss JF, 3rd. Purification, characterization, and in vitro differentiation of cytotrophoblasts from human term placentae. Endocrinology. 1986; 118 (4): 1567.
269. Di Santo S, Sager R, Andres AC, Guller S, Schneider H. Dual in vitro perfusion of an isolated cotyledon as a model to study the implication of changes in the third trimester placenta on preeclampsia. Placenta. 2007; 28 (Suppl.): 23.
270. Di Santo S, Malek A, Sager A, Andres AC, Schneider H. Trophoblast viability in perfused term placental tissue and explant cultures limited to 7-24 hours. Placenta. 2003; 24 (8-9): 882.
271. Miller RK, Genbacev O, Turner MA, Aplin JD, Caniggia I, Huppertz B. Human placental explants in culture: Approaches and assessments. Placenta. 2005; 26 (6): 439.
272. Huppertz B, Borges M. Cell Fusion. Methods in Molecular Biology. Chen EH, editor. Humana Press; 2008: 135.
273. Huppertz B, Gauster M. Cell Fusion in Health and Disease. Advances in Experimental Medicine and Biology. Dittmar T, Zänker KS, editors. Springer Netherlands; 2011: 81.
274. Morrish DW, Dakour J, Li H, Xiao J, Miller R, Sherburne R, *et al.* In vitro cultured human term cytotrophoblast: a model for normal primary epithelial cells demonstrating a spontaneous differentiation programme that requires EGF for extensive development of syncytium. Placenta. 1997; 18 (7): 577.
275. Whitley GS. Placenta and Trophoblast: Methods and Protocols. Methods in Molecular Medicine. Soares MJ, Hunt JS, editors. Humana Press Inc; 2006: 219.
276. Frank HG, Genbacev O, Blaschitz A, Chen CP, Clarson L, Evain-Brion D, *et al.* Cell culture models of human trophoblast-primary culture of trophoblast-a workshop report. Placenta. 2000; 21 (Suppl. A): 120.
277. Travis SF, Morrison AD, Clements Jr RS, Winegrad AI, Oski FA. Metabolic alterations in the human erythrocyte produced by increases in glucose concentration. The role of the polyol pathway. Journal of Clinical Investigation. 1971; 50 (10): 2104.

278. Rennie MJ. An introduction to the use of tracers in nutrition and metabolism. Proceedings of the Nutrition Society. 1999; 58 (04): 935.
279. Cobelli C, Foster D, Toffolo G. Tracer kinetics in biomedical research: From data to model. Kluwer Academic Publishers; 2001: 1.
280. Vella A, Rizza RA. Application of isotopic techniques using constant specific activity or enrichment to the study of carbohydrate metabolism. Diabetes. 2009; 58 (10): 2168.
281. Miller JH, Mullin JM, McAvoy E, Kleinzeller A. Polarity of transport of 2-deoxy-D-glucose and D-glucose by cultured renal epithelia (LLC-PK1). Biochimica et Biophysica Acta (BBA)-Biomembranes. 1992; 1110 (2): 209.
282. Shah S, Zhao H, Low S, McArdle H, Hundal H. Characterization of glucose transport and glucose transporters in the human choriocarcinoma cell line, BeWo. Placenta. 1999; 20 (8): 651.
283. Barash V, Riskin A, Shafrir E, Waddell ID, Burchell A. Kinetic and immunologic evidence for the absence of glucose-6-phosphatase in early human chorionic villi and term placenta. Biochimica et Biophysica Acta (BBA)-General Subjects. 1991; 1073 (1): 161.
284. Neely J, Denton R, England P, Randle P. The effects of increased heart work on the tricarboxylate cycle and its interactions with glycolysis in the perfused rat heart. Biochemistry Journal. 1972; 128: 147.
285. Goda SK, Al-Feel W, Akhtar M. Mechanism of the formation of the two epimeric diamino-hexose rings of neomycin B. Journal of the Chemical Society, Perkin Transactions 1. 1986: 1383.
286. Walaas O, Walaas E. Effect of epinephrine on rat diaphragm. The Journal of Biological Chemistry. 1950; 187 (2): 769.
287. Ramirez-Zacarias J, Castro-Munozledo F, Kuri-Harcuch W. Quantitation of adipose conversion and triglycerides by staining intracytoplasmic lipids with Oil red O. Histochemistry. 1992; 97 (6): 493.
288. Salmon D, Flatt J. Effect of dietary fat content on the incidence of obesity among ad libitum fed mice. International Journal of Obesity. 1984; 9 (6): 443.
289. Aldoretta P, Carver T, Hay W. Ovine uteroplacental glucose and oxygen metabolism in relation to chronic changes in maternal and fetal glucose concentrations. Placenta. 1994; 15 (7): 753.
290. Oey N, Den Boer M, Ruiter J, Wanders R, Duran M, Waterham H, *et al.* High activity of fatty acid oxidation enzymes in human placenta: Implications for fetal-maternal disease. Journal of Inherited Metabolic Disease. 2003; 26 (4): 385.
291. Oey NA, van Vlies N, Wijburg FA, Wanders RJA, Attie-Bitach T, Vaz FM. L-carnitine is synthesized in the human fetal-placental unit: Potential roles in placental and fetal metabolism. Placenta. 2006; 27 (8): 841.
292. Lin X, Shim K, Odle J. Carnitine palmitoyltransferase I control of acetogenesis, the major pathway of fatty acid β-oxidation in liver of neonatal swine. American Journal of Physiology-Regulatory, Integrative and Comparative Physiology. 2010; 298 (5): 1435.
293. Zolnierowicz S, Scislowski PWD, Swierczynski J, Zelewski L. Acetoacetate utilization by human placental mitochondria. Placenta. 1984; 5 (3): 271.
294. Shambaugh GE, Mrozak SC, Freinkel N. Fetal fuels. I. Utilization of ketones by isolated tissues at various stages of maturation and maternal nutrition during late gestation. Metabolism. 1977; 26 (6): 623.
295. Jones CJP, Choudhury RH, Aplin JD. Tracking nutrient transfer at the human maternofetal interface from 4 weeks to term. Placenta. 2015; 36 (4): 372.
296. Barash V, Gutman A, Shafrir E. Mechanism of placental glycogen deposition in diabetes in the rat. Diabetologia. 1983; 24 (1): 63.

297. Barash V, Gutman A, Shafrir E. Fetal diabetes in rats and its effect on placental glycogen. Diabetologia. 1985; 28 (4): 244.
298. Kangani CO, Kelley DE, DeLany JP. New method for GC/FID and GC–C-IRMS analysis of plasma free fatty acid concentration and isotopic enrichment. Journal of Chromatography B. 2008; 873 (1): 95.
299. Hay W, Sparks JW, Wilkening RB, Battaglia FC, Meschia G. Fetal glucose uptake and utilization as functions of maternal glucose concentration. American Journal of Physiology-Endocrinology And Metabolism. 1984; 246 (3): 237.
300. Dimopoulos N, Watson M, Sakamoto K, Hundal HS. Differential effects of palmitate and palmitoleate on insulin action and glucose utilization in rat L6 skeletal muscle cells. Biochemical Journal. 2006; 399 (3): 473.
301. Aas V, Rokling-Andersen MH, Kase ET, Thoresen GH, Rustan AC. Eicosapentaenoic acid (20:5 n-3) increases fatty acid and glucose uptake in cultured human skeletal muscle cells. Journal of Lipid Research. 2006; 47 (2): 366.
302. Lunn J, Theobald HE. The health effects of dietary unsaturated fatty acids. Nutrition Bulletin. 2006; 31 (3): 178.
303. Nugent C, Prins JB, Whitehead JP, Wentworth JM, Chatterjee VKK, O'Rahilly S. Arachidonic acid stimulates glucose uptake in 3T3-L1 adipocytes by increasing GLUT1 and GLUT4 levels at the plasma membrane: Evidence for involvement of lipoxygenase metabolites and peroxisome proliferator-activated receptor γ. Journal of Biological Chemistry. 2001; 276 (12): 9149.
304. Thompson AL, Megan Y-C, Kraegen EW, Cooney GJ. Effects of individual fatty acids on glucose uptake and glycogen synthesis in soleus muscle in vitro. American Journal of Physiology-Endocrinology and Metabolism. 2000; 279 (3): 577.
305. Bolon C, Gauthier C, Simonnet H. Glycolysis inhibition by palmitate in renal cells cultured in a two-chamber system. American Journal of Physiology-Cell Physiology. 1997; 273 (5): 1732.
306. Swagell CD, Morris CP, Henly DC. Effect of fatty acids, glucose, and insulin on hepatic glucose uptake and glycolysis. Nutrition. 2006; 22 (6): 672.
307. Dulloo AG, Gubler M, Montani J-P, Seydoux J, Solinas G. Substrate cycling between de novo lipogenesis and lipid oxidation: a thermogenic mechanism against skeletal muscle lipotoxicity and glucolipotoxicity. International Journal of Obesity. 2004; 28: 29.
308. Thomas CR, Lowy C. Placental transfer and uptake of 2-deoxyglucose in control and diabetic rats. Metabolism. 1992; 41 (11): 1199.
309. Fricke RF, Longmore WJ. Effects of insulin and diabetes on 2-deoxy-D-glucose uptake by the isolated perfused rat lung. Journal of Biological Chemistry. 1979; 254 (12): 5092.
310. Huang MT, Veech RL. Metabolic fluxes between [^{14}C] 2-deoxy-D-glucose and [^{14}C] 2-deoxy-D-glucose-6-phosphate in brain in vivo. Journal of Neurochemistry. 1985; 44 (2): 567.
311. Pardridge WM, Crane PD, Mietus LJ, Oldendorf WH. Kinetics of regional blood–brain barrier transport and brain phosphorylation of glucose and 2-deoxyglucose in the barbiturate–anesthetized rat. Journal of Neurochemistry. 1982; 38 (2): 560.
312. Schmidt K, Mies G, Sokoloff L. Model of kinetic behavior of deoxyglucose in heterogeneous tissues in brain: a reinterpretation of the significance of parameters fitted to homogeneous tissue models. Journal of Cerebral Blood Flow & Metabolism. 1991; 11 (1): 10.
313. Guionie O, Clottes E, Stafford K, Burchell A. Identification and characterisation of a new human glucose-6-phosphatase isoform. FEBS Letters. 2003; 551 (1–3): 159.

314. Goodwin GW, Cohen DM, Taegtmeyer H. [5-^{3}H] glucose overestimates glycolytic flux in isolated working rat heart: role of the pentose phosphate pathway. American Journal of Physiology-Endocrinology and Metabolism. 2001; 280 (3): 502.
315. Papamarcaki T, Tsolas O. Demonstration of fructose 1,6-bisphosphatase in human term placenta. Experientia. 1991; 47 (1): 67.
316. Bax BE, Bloxam DL. Energy metabolism and glycolysis in human placental trophoblast cells during differentiation. Biochimica et Biophysica Acta (BBA) - Bioenergetics. 1997; 1319 (2–3): 283.
317. Hu R, Jin H, Zhou S, Yang P, Li X. Proteomic analysis of hypoxia-induced responses in the syncytialization of human placental cell line BeWo. Placenta. 2007; 28 (5): 399.
318. Magnusson AL, Powell T, Wennergren M, Jansson T. Glucose Metabolism in the Human Preterm and Term Placenta of IUGR Fetuses. Placenta. 2004; 25 (4): 337.
319. Lee MH, Jeon YJ, Lee SM, Park MH, Jung SC, Kim YJ. Placental gene expression is related to glucose metabolism and fetal cord blood levels of insulin and insulin-like growth factors in intrauterine growth restriction. Early Human Development. 2010; 86 (1): 45.
320. Murphy DJ, Dunney C, Mullally A, Adnan N, Deane R. Population-Based Study of Smoking Behaviour throughout Pregnancy and Adverse Perinatal Outcomes. International Journal of Environmental Research and Public Health. 2013; 10 (9): 3855.
321. Zdravkovic T, Genbacev O, McMaster MT, Fisher SJ. The adverse effects of maternal smoking on the human placenta: A review. Placenta. 2005; 26 (Suppl.): 81.
322. Arkwright PD, Rademacher TW, Dwek RA, Redman CWG. Pre-eclampsia is associated with an increase in trophoblast glycogen content and glycogen synthase activity, similar to that found in hydatidiform moles. Journal of Clinical Investigation. 1993; 91 (6): 2744.
323. Huppertz B. Placental origins of preeclampsia challenging the current hypothesis. Hypertension. 2008; 51 (4): 970.
324. Huynh J, Dawson D, Roberts D, Bentley-Lewis R. A systematic review of placental pathology in maternal diabetes mellitus. Placenta. 2015; 36 (2): 101.
325. Huang L, Liu J, Feng L, Chen Y, Zhang J, Wang W. Maternal prepregnancy obesity is associated with higher risk of placental pathological lesions. Placenta. 2014; 35 (8): 563.
326. Lyall F, Glbson JL, Greer IA, Brockman DE, Eis ALW, Myatt L. Increased nitrotyrosine in the diabetic placenta: Evidence for oxidative stress. Diabetes Care. 1998; 21 (10): 1753.
327. Roberts VHJ, Smith J, McLea SA, Heizer AB, Richardson JL, Myatt L. Effect of Increasing maternal body mass index on oxidative and nitrative stress in the human placenta. Placenta. 2009; 30 (2): 169.
328. Shang M, Zhao J, Yang L, Lin L. Oxidative stress and antioxidant status in women with gestational diabetes mellitus diagnosed by IADPSG criteria. Diabetes Research and Clinical Practice. 2015; 109 (2): 404.
329. Boyle KE, Newsom SA, Janssen RC, Lappas M, Friedman JE. Skeletal muscle MnSOD, mitochondrial complex II, and SIRT3 enzyme activities are decreased in maternal obesity during human pregnancy and gestational diabetes mellitus. Journal of Clinical Endocrinology and Metabolism. 2013; 98 (10): 1601.
330. Cui XL, Brockman D, Campos B, Myatt L. Expression of NADPH oxidase isoform 1 (Nox1) in human placenta: involvement in preeclampsia. Placenta. 2006; 27 (4–5): 422.
331. Gao L, Mann GE. Vascular NAD(P)H oxidase activation in diabetes: a double-edged sword in redox signalling. Cardiovascular Research. 2009; 82 (1): 9.

332. Seifert EL, Fiehn O, Bezaire V, Bickel DR, Wohlgemuth G, Adams SH, *et al.* Long-chain fatty acid combustion rate is associated with unique metabolite profiles in skeletal muscle mitochondria. PLoS ONE. 2010; 5 (3): 9834.
333. Dessì A, Marincola FC, Fanos V. Metabolomics and the great obstetrical syndromes-GDM, PET, and IUGR. Best Practice and Research: Clinical Obstetrics and Gynaecology. 2015; 29 (2): 156.
334. Dunn WB, Brown M, Worton SA, Davies K, Jones RL, Kell DB, *et al.* The metabolome of human placental tissue: Investigation of first trimester tissue and changes related to preeclampsia in late pregnancy. Metabolomics. 2012; 8 (4): 579.
335. Chi Y, Pei L, Chen G, Song X, Zhao A, Chen T, *et al.* Metabonomic profiling of human placentas reveals different metabolic patterns among subtypes of neural tube defects. Journal of Proteome Research. 2014; 13 (2): 934.
336. Fanos V, Atzori L, Makarenko K, Melis GB, Ferrazzi E. Metabolomics application in maternal-fetal medicine. BioMed Research International. 2013; 2013: 1.
337. Żołnierowicz S, Świerczyński J, Żelewski L. β-Hydroxybutyrate dehydrogenase activity in human placenta. Placenta. 1984; 5 (2): 183.
338. Żołnierowicz S, Ścisłowski PWD, Świerczyński J, Żelewski L. Acetoacetate utilization by human placental mitochondria. Placenta. 1984; 5 (3): 271.
339. Vinolo MAR, Rodrigues HG, Nachbar RT, Curi R. Regulation of inflammation by short chain fatty acids. Nutrients. 2011; 3 (10): 858.
340. Newman JC, Verdin E. Ketone bodies as signaling metabolites. Trends in Endocrinology and Metabolism. 2014; 25 (1): 42.
341. Heazell AEP, Bernatavicius G, Warrander L, Brown MC, Dunn WB. A metabolomic approach identifies differences in maternal serum in third trimester pregnancies that end in poor perinatal outcome. Reproductive Sciences. 2012; 19 (8): 863.
342. Roche E, Buteau J, Aniento I, Reig JA, Soria B, Prentki M. Palmitate and oleate induce the immediate-early response genes c-fos and nur-77 in the pancreatic beta-cell line INS-1. Diabetes. 1999; 48 (10): 2007.